ERDC/GSL TR-15-10

Geotechnical and Structures Laboratory

US Army Corps
of Engineers®
Engineer Research and
Development Center

ERDC
INNOVATIVE SOLUTIONS
for a safer, better world

Evaluation of Precast Portland Cement Concrete Panels for Airfield Pavement Repairs

Lucy P. Priddy

May 2015

The US Army Engineer Research and Development Center (ERDC) solves the nation's toughest engineering and environmental challenges. ERDC develops innovative solutions in civil and military engineering, geospatial sciences, water resources, and environmental sciences for the Army, the Department of Defense, civilian agencies, and our nation's public good. Find out more at www.erdc.usace.army.mil.

To search for other technical reports published by ERDC, visit the ERDC online library at http://acwc.sdp.sirsi.net/client/default.

ERDC/GSL TR-15-10
May 2015

Evaluation of Precast Portland Cement Concrete Panels for Airfield Pavement Repairs

Lucy P. Priddy

Geotechnical and Structures Laboratory
U.S. Army Engineer Research and Development Center
3909 Halls Ferry Road
Vicksburg, MS 39180-6199

Final report

Prepared for Headquarters, Air Force Civil Engineer Center
Tyndall Air Force Base, FL 32403-5319

Abstract

During the period November 2011 through August 2013, research was conducted to develop a precast panel repair system suitable for airfield pavement repairs. This investigation included the selection and refinement of a precast panel system, fabrication of precast panels, timed repair activities, and accelerated pavement testing. Simulated C-17 traffic was applied to three repair surfaces of various sizes to determine whether the precast panel repairs were suitable for emergency or contingency airfield operations. This report presents the description of the process for selection and modification of a precast system, results of accelerated pavement testing including the passes-to-failure, surface deterioration, load transfer efficiencies, deflections, stress-strain measurements during trafficking, and three-dimensional finite element analyses. Results indicated that the repairs were capable of supporting anticipated contingency pass levels defined by the U.S. Air Force, but the precast panel system's dowel diameter should be increased to reduce stresses, decrease foreign object damage potential, and improve repair performance. Finally, the precast repair technology was compared to other expedient repair techniques in terms of repair speed, performance, and cost. Compared to other methods, the precast panel repair alternative provided similar return-to-service timelines and traffic performance at a slightly higher cost. Modifications to the system design and placement procedures are also recommended to improve the field performance of the panels.

Contents

Figures and Tables

Figures

Tables

Preface

This report presents the doctoral dissertation of the author entitled *Evaluation of Precast Portland Cement Concrete Panels for Airfield Pavement Repairs*, submitted in partial fulfillment of the requirements for her doctoral degree at Virginia Polytechnic Institute and State University, Blacksburg, VA. The study description and results presented in the dissertation were conducted for the U.S. Air Force Civil Engineer Center (AFCEC) under the project title "Evaluation of Precast Panel Technologies." The Technical Monitor was Dr. Craig Rutland, AFCEC.

The work was performed by the Airfields and Pavements Branch (GMA) of the Engineering Systems and Materials Division (GM), U.S. Army Engineer Research and Development Center, Geotechnical and Structures Laboratory (ERDC-GSL). At the time of publication, Dr. Gary L. Anderton was Chief, CEERD-GMA; Dr. Larry N. Lynch was Chief, CEERD-GM; and Dr. David A. Horner, CEERD-GVT, was the Technical Director for Force Projection and Maneuver Support. The Deputy Director of ERDC-GSL was Dr. William P. Grogan, and the Director was Dr. David W. Pittman.

LTC John T. Tucker III was the Acting Commander of ERDC, and Dr. Jeffery P. Holland was the Director.

Unit Conversion Factors

Multiply	By	To Obtain
cubic feet	0.02831685	cubic meters
cubic inches	1.6387064 E-05	cubic meters
cubic yards	0.7645549	cubic meters
degrees Fahrenheit	(F-32)/1.8	degrees Celsius
feet	0.3048	meters
gallons (U.S. liquid)	3.785412 E-03	cubic meters
Inches	0.0254	meters
pounds (force)	4.448222	newtons
pounds (force) per foot	14.59390	newtons per meter
pounds (force) per inch	175.1268	newtons per meter
pounds (force) per square foot	47.88026	pascals
pounds (force) per square inch	6.894757	kilopascals
square feet	0.09290304	square meters
square inches	6.4516 E-04	square meters
tons (force)	8,896.443	newtons

1 Introduction

Ever decreasing construction timelines for repair of operating facilities necessitate rapid, or expedient, repair techniques for Portland cement concrete (PCC) airfield and highway pavements. These repair timeframes are often as short as 4 to 6 hr, regardless of repair size or pavement use. PCC repair methods using conventional PCC, high early-strength concrete, and proprietary cementitious rapid-setting repair materials are the most broadly practiced repair methods. Traditional cast-in-place repairs using conventional PCC require longer closure periods than high-early strength concretes or rapid-setting repair materials because of conventional PCC's slower strength gain. While both proprietary rapid-setting repair materials and high early-strength concrete have been used successfully for both partial- and full-slab replacements within the objective repair timeframe, these materials are expensive and can be difficult to mix in large batches due to their flash-setting potential. Additionally, high early-strength concrete may not be as durable as traditional PCC and may require closure periods of 8 to 12 hr to gain sufficient strength prior to reopening to traffic.

The application of precast concrete panel technologies to pavements may eliminate some of the issues associated with the use of traditional cast-in-place concrete for conducting pavement repairs. Panels can be precast on site in anticipation of repair activities using conventional PCC that is allowed to cure to its ultimate strength and stockpiled for future use, or panels can be ordered from a precasting facility and delivered to the repair site when needed. Furthermore, precast panels can be placed within a narrow construction/repair window, and a number of commercial and generic systems can be placed either alone as single-panel repairs or in combination with other panels to complete larger, multiple-panel repairs. Additional benefits gained from using precast technology include improved repair quality due to the controlled fabrication process, reduced pavement closure times, and improved potential for long-lasting repairs. Because of these benefits, the precast panel repair technique has gained interest in the highway sector in recent years.

Despite these benefits and numerous recent research and development efforts for highway applications, few recent investigations for the application of this technology for airfield pavements have been conducted.

Research was required to determine if precast panel technology was suitable for expedient airfield pavement repairs.

This report documents a comprehensive experimental and numerical modeling study centered on a full-scale precast PCC pavement test section built in Vicksburg, MS. A single precast PCC panel system developed for airfield use was evaluated as an expedient repair method to gain a general understanding of precast panel's behavior and performance under simulated aircraft traffic. A complementary finite element modeling study of precast panel repairs was used to extrapolate field and laboratory experimental results to understand the mode of failure for the panels and to develop recommendations for improving the precast panel design and the repair procedure for airfield pavement repairs.

1.1 Problem statement

Ensuring safe and dependable flight operations on airfields requires that pavements be repaired quickly with the highest quality and most durable materials available. Precast panel technologies have been evaluated as a pavement repair method by a number of researchers for more than 50 years; however, a standard repair method has not been identified for either highway or airfield pavements. Furthermore, while recent focused efforts to improve the design and placement of precast panels in the U.S. for highway repairs have been documented, no reports on similar efforts to improve the design and placement of airfield panels are available. Only a limited number of airfield pavement precast technology applications are described in the literature.

Simply adopting a highway precast panel system for airfield repairs would not take into account the differences in structure and loading between airfield and highway pavements. Even though airfield pavements are subjected to fewer traffic passes than highway pavements, they are exposed to significantly higher tire pressures and loadings from more complex gear configurations. The various available repair systems require careful review to determine their suitability for airfield repair applications.

A versatile precast panel repair system is needed that is compatible with heavy aircraft loadings. Any proposed system must be tested under realistic aircraft traffic for the intended application to evaluate its performance, including pass-to-failure rates and failure modes for various repair configurations. In addition to performance, other aspects of the

precast panel repair method must be compared to currently accepted expedient repair methods to understand what benefit the repair technique offers in terms of cost and time. Finally, recommendations for improving the precast panel system should be made based upon full-scale field testing results and data obtained through finite element modeling to improve the panel design while limiting the cost and burden associated with additional full-scale field testing.

1.2 Objectives

The main objectives of this investigation are (1) to determine feasibility of using precast panels for conducting expedient pavement repairs in airfield pavements and (2) to develop a numerical model to understand the mechanical properties of a precast panel repair in response to simulated static aircraft loads in order to help refine the panel system design without additional costly field testing.

Additional objectives of this research are

- To identify, develop, or refine the design of an existing precast panel system suitable for use in conducting single- and multiple-panel airfield repairs,
- To determine pass-to-failure rates and failure modes for single- and multiple-panel repairs under simulated aircraft trafficking,
- To determine the mechanical responses of the panel repairs subjected to aircraft loadings and to make design recommendations to improve the repair performance,
- To determine the benefit of using the precast panel repair technique compared to using other expedient repair technologies, and
- To make recommendations to reduce repair timelines.

1.3 Research approach

Figure 1.1 shows the tasks completed in order to achieve the overall objectives of the investigation. The tasks are further detailed in the following text.

1. **Literature review**. In order to acquire a deeper knowledge of the past and present advances in precast panel technologies, an extensive literature review was conducted. The review suggests that while numerous precast panel investigations have been conducted for more than 50 years, limited

documentation is available for airfield applications, and these documents provide minimal information regarding the panel performance and successful design approaches. Despite the lack of robust information for airfield use, both recent advances in highway applications and limited commercial and military airfield feasibility studies indicate that precast panels may be suitable for airfield applications.

Figure 1.1. Research approach schematic.

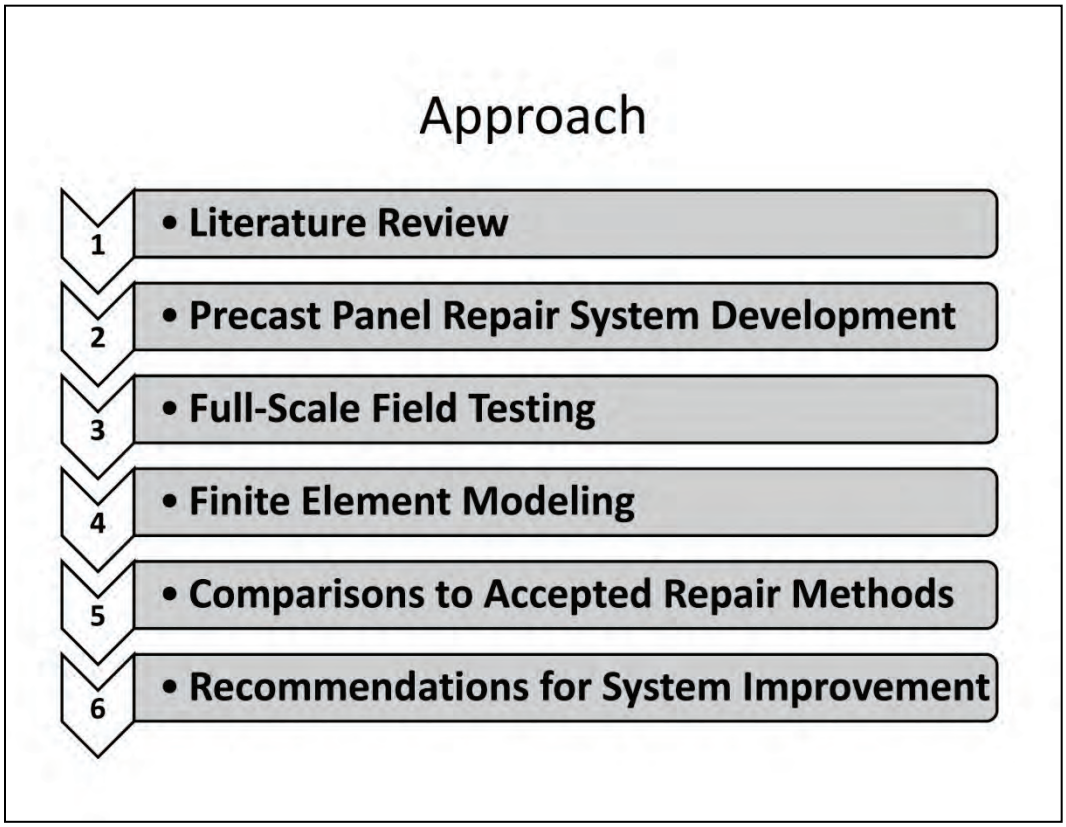

2. **Precast panel repair system development**. A single precast panel system was identified in the literature review and was refined to develop panel designs and formwork used to fabricate precast panels on site for full-scale field testing. The report provides design drawings and procedures for fabricating and installing precast panels for repair purposes.
3. **Full-scale field testing**. Following the development of precast panel designs and field fabrication of panels, a full-scale pavement test section was designed and constructed to simulate an airfield runway. Three panel repairs of various sizes were conducted, and each repair task was timed. Completed repairs were trafficked using simulated C-17 aircraft traffic. Performance data— including visual inspection of the pavement condition, sublayer and surface instrumentation, and nondestructive testing data—

were collected during trafficking. Through field testing, the mode of failure and the pass-to-failure rates for the panel repairs were determined.

4. **Finite element modeling**. A three-dimensional finite element model of the transverse, doweled repair joint was developed and validated using instrumentation and nondestructive testing data collected during full-scale field testing. Stresses generated in the model under static loadings were determined and compared to both theoretical calculations and field measurements. The model was used to develop recommendations for modifying the panel design to improve field performance.
5. **Comparison to accepted repair methods**. The performance, cost, and timing data collected for the precast panel repairs were compared to data collected for currently accepted expedient PCC airfield pavement repair methods. Comparisons were made to determine the suitability of the precast panel repair system for airfield use and to make recommendations for the various repair methods for different airfield operational scenarios.
6. **Recommendations for system improvement**. This document presents recommendations for modifying the panel design to improve the in-place performance of the repairs and to improve the panel repair process. Recommendations are based upon analyses of field and finite element modeling data.

1.4 Report organization

This report presents the doctoral dissertation of the author and follows a manuscript format, which includes a collection of papers; each manuscript is used as an individual chapter. Because the chapters are written as self-contained documents, some repetition will occur among the introductory and background sections for the different chapters. Permissions to include these papers in this report were granted by each publishing entity. Because unit requirements varied among the various publishing entities, unit conversion factors are presented in the forward material of this report.

Chapter 1 – *Introduction*: The general contents of the report, the problem statement, the research objectives, and the research approach are presented here.

Chapter 2 – Review of Precast Portland Cement Concrete Panel Technologies for Use in Expedient Portland Cement Concrete Airfield Pavement Repair: This paper presents the current state of knowledge regarding precast PCC panels for pavement applications and identifies

relevant precast technologies considered for further investigation. The paper compares modern precast panel systems to identify a single precast panel system for optimization. Recommendations for modifying the selected airfield precast panel system are also provided. This chapter was presented at the 92nd annual meeting of the Transportation Research Board held 13-17 January 2013 in Washington, DC and published in its proceedings (Priddy et al. 2013a).

Chapter 3 –*Full-Scale Field Testing of Precast Portland Cement (PCC) Panel Airfield Pavement Repairs*: This paper presents the evaluation of the modified precast panel repair system identified in Chapter 2 and discusses the full-scale test section construction and the accelerated pavement testing of three different sized panel repairs. The development and general design of the precast panel system, the panel fabrication process, and the general repair processes are described in this paper. The paper also explains the traffic testing procedures and discusses the performance of the panels under simulated C-17 aircraft traffic, including pass-to-failure rates, deflections, distresses, and instrumentation responses. Research findings indicate that the precast panels are suitable for supporting at least 5,000 and as many as 10,000 C-17 passes. This chapter was published in the March 2014 edition of the *International Journal of Pavement Engineering* (Priddy et al. 2014b).

Chapter 4 – *Load Transfer Characteristics of Precast Portland Cement Concrete Panels for Airfield Pavement Repairs:* This paper explores the general load transfer characteristics of the various panel joints involved in the panel repairs using nondestructive data collected during the full-scale field testing described in Chapter 3. The data are analyzed to calculate load transfer efficiency, or joint efficiency, of the panels' joints. The analysis shows that the load transfer characteristics such as load transfer efficiency cannot be used to predict the performance of the joints undergoing trafficking due to current panel installation procedures. The analysis also suggests that the failure of the joints may be caused by inadequate load transfer at the doweled joints and possibly the panel installation practice of sealing the joints. One recommendation of this paper is to conduct finite element analyses to understand the stresses generated in the doweled repair joint under aircraft loads. This chapter was published in the proceedings of the Transportation Research Board 93rd Annual Meeting held 12-16 January 2014 in Washington, DC and was accepted for publication in the *Transportation Research Record* (Priddy et al. 2014a).

Chapter 5 –*Three-Dimensional Finite Element Modeling of Precast Concrete Panel Joints:* This paper presents the findings of a study to quantify the stresses generated in the precast panel repair joint under aircraft loads by using finite element modeling. The paper describes the development and validation of a three-dimensional finite element model for the transverse doweled joint between the precast panel and the parent slab. The model is validated using nondestructive testing and instrumentation data collected during field testing described in Chapter 3. The stresses generated in the concrete surrounding the dowels under various load configurations are presented. Using the critical load situation, additional models are constructed to determine whether stresses in the concrete surrounding the dowels could be reduced by increasing the dowel diameter. Based on the modeling results, recommendations to redesign the panels by using larger diameter dowels and other methods are presented. This paper was submitted to the American Society of Civil Engineers (ASCE) *Journal of Transportation Engineering* in March 2014.

Chapter 6 –*Development of Expedient Military Concrete Airfield Pavement Repairs*: This paper presents a more detailed comparison of the precast panel repair method to other expedient airfield repair techniques than that presented in Chapter 3. The paper compares all currently accepted repair techniques, summarizes their developments, and provides results of their performances under simulated and actual aircraft operations. The results of more than 100 pavement repairs are analyzed to develop recommendations as to the suitability of each technique for different military operational scenarios. Results presented in this paper show that many expedient repair techniques, including precast panels, can be used to support many more passes than previously required for expedient repairs while still being completed in the expedient repair timeframe of 4 to 6 hr. Analyses indicate that the precast panel repair method is suitable for all military repair operational scenarios and may be suitable for permanent airfield pavement repairs. This chapter was published in May 2013 in the journal *Magazine of Concrete Research*, Special Issue: *Military Concrete*.

Chapter 7 – *Findings, Conclusions, and Recommendations for Future Research:* This chapter summarizes the key findings and conclusions and provides recommendations for future research on precast panels for airfield pavement repairs.

Appendix A – *Extended Literature Review:* This appendix provides additional details of the review of the literature. Portions of this appendix were included in Bly et al. (2013).

Appendix B – *Precast Panel Construction:* This appendix provides additional details of the steps required to fabricate precast panels and provides schematics of the panel designs. Portions of this appendix were included in Bly et al. (2013).

Appendix C – *Test section Construction and Precast Panel Placement Procedures:* This appendix provides additional details of the design and construction of the test section and procedures used to conduct each repair. Field measurements, laboratory specimen data, and timing data are also included in this appendix.

Appendix D – *Accelerated Pavement Testing:* This appendix provides additional details of the accelerated pavement testing including load cart and traffic operation procedures, repair failure criteria, and data collection procedures. This appendix also contains detailed surface deterioration results for each repair with increasing traffic applications, settlement, and faulting measurements, and additional details of the nondestructive testing. Portions of this appendix were included in Priddy et al. (2013b).

Appendix E – *Finite Element Modeling:* This appendix provides additional schematics, calculations, and data from the finite element modeling efforts.

1.5 Significance

The main scientific contributions are represented by providing a comprehensive analysis of precast panel technology for airfield pavement repair applications. Very few precast panel investigations have focused on airfield repair applications; and only limited design, installation, and performance data are available in the literature. Real data were analyzed from a full-scale airfield test section constructed specifically to determine the precast panel repair life under complex, heavy aircraft loadings. These data were used to develop a three-dimensional finite element model that provides a means for improving precast panel design and analyses, and the methodology used can be applied to evaluate additional panel design configurations.

The main engineering contributions of this research include the identification and development of a precast panel repair system and repair procedure for use on airfield pavements. Use of this repair technique can return an airfield to service within 4 to 10 hr, depending on repair size. This repair technique shows potential for application at both military and civilian airfields to reduce the time runways and taxiways are removed from service. In addition, this report presents a summary of current expedient airfield pavement repair methods and their performances under simulated and actual aircraft traffic. Comparisons regarding performance, repair speed, and cost are used to determine probable applications for each repair type. Expedient repairs are important to reduce airfield closure times to ensure that airfields maintain their operational tempos, do not have increased user costs caused by takeoff/landing delays, reduce passenger frustration, and ensure prompt delivery of goods and services.

2 Review of Precast Portland Cement Concrete Panel Technologies for Use in Expedient Portland Cement Concrete Airfield Pavement Repairs

L.P. Priddy[1], P.G. Bly[2], and G.W. Flintsch[3]

Published in *Proceedings of the 92nd Annual Meeting of the Transportation Research Board*, January 2013, Washington, DC. Reprinted by permission of the publisher (Transportation Research Board), August 2014. TRB does not endorse any product, method, practice, or policy presented.

Abstract: Currently, there is a resurgent interest in the use of precast Portland cement concrete (PCC) technologies for pavement construction and repairs. Precast PCC slabs or panels using conventional materials have been utilized at irregular intervals for the last 50 or more years and can offer similar reductions in field installation time as cast-in-place PCC using rapid strength gaining materials. This paper documents the history of precast pavement panels around the world for airfield and highway pavements for both repair and new construction work. This information will be used to assist in the development of a methodology for use in rapid full-depth airfield repairs, ranging from temporary patches to permanent replacement slabs for rehabilitation. Specific challenges related to military airfield pavement repairs using precast PCC panels are also presented for optimization of a repair panel system for emergency airfield repairs.

[1]Research Civil Engineer, U.S. Army Engineer Research and Development Center, Vicksburg, MS 39180. Email:lucy.p.priddy@usace.army.mil.
[2]Research Civil Engineer, U.S. Army Engineer Research and Development Center, Vicksburg, MS 39180. Email:peter.g.bly@usace.army.mil.
[3] Director, Center for Sustainable Transportation Infrastructure, Virginia Tech Transportation Institute and Professor, The Charles Via, Jr., Department of Civil and Environmental Engineering, Virginia Tech, Blacksburg, VA 24061. Email: flintsch@vt.edu.

2.1 Background

Airfield repair personnel require expedient methods for conducting full-depth repairs in damaged Portland cement concrete (PCC) airfield pavements. Damaged areas must be replaced quickly to restore flight operations in the shortest times possible. Damage requiring a full-depth repair can result from either traditional pavement distresses (i.e., from repeated traffic or overloading by heavy traffic, as-built construction errors, and environmental conditions) or from explosive blasts. Typical PCC pavement damage, including blowups from thermal expansion, shattered slabs, corner breaks, durability cracking, deep spalling (past mid-depth), punch-outs, deteriorating patches, and utility cuts have the potential to damage aircraft, even if these distresses are moderately severe (UFC 2001a). Damage from explosive blasts may include deep spalls, craters, or camouflets. In some situations, damaged airfields may contain both traditional and explosive distresses. Regardless of the cause of damage or the repair environment, these distresses are normally repaired by full-depth patches that require the removal and replacement of the damaged PCC with repair to sublayers performed as needed.

The most broadly used materials for repairs to PCC pavements are conventional PCC, high early-strength concrete, and proprietary rapid-setting repair materials (Williams et al. 2011, 2012). Current military guidance for conducting full-slab replacement and full-depth repairs in PCC airfield pavements suggests using conventional PCC (UFC 2001a). Generally, conventional PCC provides the best results when conducting permanent repairs in PCC airfield areas because the replaced material has similar mechanical properties to that of the adjacent pavement. Disadvantages of using conventional cast-in-place PCC include the long curing duration required to gain sufficient strength to open to traffic and the inability to place the material in all weather conditions. Both of these situations conflict with airfield operations, particularly in wartime scenarios (Ashtiani et al. 2011; Priddy and Rushing 2012). Over the past several years, the performance of proprietary rapid-setting rigid repair materials has improved, and their use is acceptable for a wide range of repair procedures including emergency, temporary, and permanent airfield repairs (Hammons and Saeed 2010; Priddy 2011).

Proprietary rapid-setting repair materials have been successfully used for partial- and full-slab replacements for airfield repairs; however, these materials are expensive and can be a logistical burden to transport to

remote locations (Priddy and Jersey 2009). Military repair teams may have limited quantities of these materials; thus, these costly materials may be applied only to smaller repair areas or the most critical airfield repairs. Numerous products appropriate for military airfield repairs have been identified and certified for various categories and sizes (Priddy 2011; Priddy and Rushing 2012).

High early-strength concretes have gained acceptance in the commercial and military airfield repair communities in recent years. The combination of high cement content and the use of accelerating admixtures results in repairs that can be reopened to traffic within 4 to 8 hr. High early-strength concretes may be more costly compared to traditional PCC, but are usually significantly less expensive than proprietary rapid-setting repair materials. In addition to cost, durability is a concern due to the high cement contents required (Williams et al. 2011).

A promising alternative repair method is the use of precast PCC panels for full-depth patches. This repair method has been explored for both highway and airfield repair as early as the 1930s. A recent resurgence in precast panel repair research indicates that this technology may be applied beyond highway pavements. One main advantage to using precast PCC panels is that the panels may provide a higher quality patch, since the panels can be prepared with traditional PCC and constructed in a controlled environment with fewer time limitations than those encountered during narrow construction windows on highly trafficked airfield pavements. Hasty patching, regardless of material or construction practice used, may result in a poor quality patch. Precast panels can be fabricated in a controlled manner with less demanding environmental constraints that allow for good standard concreting practices to be followed. Panels made can be reserved and stored off-site for later use when needed. Another advantage is that using conventional PCC with local materials may be more economical than using expensive proprietary materials for cast-in-place repairs (Hossain et al. 2006). Both of these advantages require further exploration to understand the requirements of time installation and cost to use this repair technology compared to current expedient and permanent repair methods already used for airfields.

2.2 Research objective

The paper presents the first step in a comprehensive study to understand the current state of practice in the U.S. and in the world in using precast

PCC panels for airfield pavement repairs. The intent was to gain a better understanding of current best practices and design methods to apply for precast panel repairs in military airfields, particularly those in remote environments. Information pertaining to precast concrete panel systems was gathered to select a system for expedient airfield repairs in remote locations. The paper briefly presents relevant precast pavement experiences in the U.S. and in the world that were reviewed to understand the history and challenges in precast panel fabrication and placement. The methods available (or best applicable) for the expedient pavement airfield repairs were determined, and unique challenges to applying a selected method for the repair situation are also presented.

2.3 Precast slab experiences

Precast construction of PCC elements such as concrete columns, beams, piles, highway barriers, and railroad ties are used extensively in construction industries (Rollings and Chou 1981; FHWA 2007). Off-site fabrication and storage of these elements benefit the user by reducing job site congestion and providing a controlled manufacturing process that results in increased quality and minimized costs (Rollings and Chou 1981). The use of precast concrete slabs in conventional road and airfield pavements for either new construction or repair is not a recent innovation; several precast pavement studies have been conducted over the past 50 to 80 years. Researchers report that one reason widespread pavement use has lagged behind other precast elements is that precast panels used to repair a pavement require more effort to place and require level bedding materials than other precast construction elements when installed. Careful grading of bedding materials is required to provide full contact of the slabs with the underlying base, but the process can be time consuming and requires experienced field crews and heavy or specialized equipment (Rollings and Chou 1981; Kohler et al. 2009). Placement of precast panels generally requires the use of a crane, which in turn requires additional experienced operators and equipment on the jobsite compared with traditional PCC placement. As a result, this repair method was not necessarily applicable to emergency or contingency repair efforts where experienced crews or heavy equipment were not available.

Another reason that precast pavement repairs have lagged behind other repair techniques, according to literature, is the lack of consistent, documented design and construction techniques for using precast panels (Tayabji et al. 2013). While proprietary and non-proprietary panels exist

and have been explored in recent years, there has been a hesitancy to use them on an extensive basis due to the lack of documentation for their success, particularly for airfields. Finally, the use of panels may be more expensive compared to other repair or construction techniques due to the need for heavy construction equipment, proprietary systems, and specially trained crews.

A review of literature revealed numerous instances of the use of precast PCC slabs for a variety of single- and multiple-panel repairs as well as for rapid pavement construction in North America, Europe, the former Soviet Union, and Asia as early as the 1930s. Use of precast panels was primarily for airfield construction in the former Soviet Union as early as the 1930s and in Europe from 1947 through 1958 (Rollings and Chou 1981). Infrequent studies were conducted in the U.S. from 1970 to 2000; however, there has been a resurgence of investigations of this technology in the past 10 years (FHWA 2007; Tayabji et al. 2009). Until recently, countries studied the precast PCC panel systems periodically for "technical feasibility" (Tayabji et al. 2009) with the exception of the former Soviet Union, which used these systems extensively. In recent years, additional countries including Japan, the Netherlands, France, and Indonesia have used precast PCC slabs for roadway, highway, and in some cases, airfield applications. A summary of early precast panel use in U.S. and foreign projects (Rollings and Chou 1981) and more recent applications are documented (Brabston 1984; FHWA 2007; Kohler et al. 2007; Tayabji et al. 2009, 2013). The following sections summarize early and current uses of precast panels in the U.S. and other countries for pavement repairs and/or construction.

2.3.1 Early experiences

2.3.1.1 Soviet Union

Perhaps the earliest instance of PCC precast panel construction for airfields was in the former Soviet Union during the early 1930s (Rollings and Chou 1981; Brabston 1984). Rollings and Chou (1981) report that the panels were useful for "construction in regions where swelling or settlement caused construction problems, where rapid construction was required, where pavements could be overlaid by panels to strengthen the pavement, or in below freezing applications." Airfield precast panels were slightly over 6 ft wide and varied in length from 13 to 20 ft with a length-to-width ratio of 2 to 3. In addition to airfield construction, the Soviet Union also used precast PCC panels extensively for road construction. By the 1980s, the Soviet

Union had a sophisticated precast concrete industry for both airfield and road construction (Rollings and Chou 1981).

2.3.1.2 Europe

Additional airfield construction was conducted in Europe from the late 1940s through the late 1950s. The first precast, prestressed concrete slabs in airfield construction took place at Orly Airport in Paris, France, in 1947 (Rollings and Chou 1981; Brabston 1984). The slabs were 3.3 ft wide, 3.3 ft long, and 6.3 in. thick. Another instance is reported to have taken place in London in 1949. Additional pavement construction with precast, prestressed slabs occurred in 1956 at Finningley, England, and in 1958 at Melsbroek, Belgium. The slabs at Finningley were 9 ft wide, 30 ft long, and 6 in. thick; and the slabs used at Melsbroek were 4.1 ft wide, 39 ft long, and 3 in. thick. Emergency airfield repairs of simulated munitions blasts using precast concrete slabs were conducted in Germany in the 1980s. The slabs were 6.6 ft wide, 6.6 ft long, and 4.7 to 5.9 in. thick. No application of test traffic was reported (Brabston 1984).

2.3.1.3 Japan

Precast concrete panels designed for DC-8 aircraft traffic were constructed and tested in Japan prior to 1981 (Brabston 1984). These panels were 3.2 ft long, 7.5 ft wide, and 7.9 in. thick. Other reported instances of precast panel use in Japan were precast concrete panels used in the 1970s for container yards and airports (Kohler et al. 2007). Panels were also used for roadway pavements in Japan after 1991. Panels for road repairs were 3.3 ft by 6.6 ft, 6.6 ft by 6.6 ft and 9.8 ft by 6.6 ft, and were approximately 5.9 in. thick. No load transfer devices were used between these panels.

2.3.1.4 U.S.

A review of the literature reveals several repair efforts in the U.S. using precast panel technologies for highway repairs during the 1960s and 1970s. Additional panel studies were conducted in the 1970s and 1980s for airfield repair applications. Table 2.1 presents a summary of the U.S. experiences with precast panels for both highway and airfield repairs from the 1960s through the 1980s, as reported in the literature. The table shows a great variety of panel designs, seating methods, load transfer mechanisms, and reinforcement type among the reported efforts.

Table 2.1. Early U.S. highway and airfield repair efforts using precast panels.

Time Period	Location	Pavement Type	Dimensions	Comments	References
1960s	South Dakota	Highway	6 ft wide, 24 ft long, and 4.5 in. thick	Panels were overlaid with 1.5 to 3.5 in. of AC. Panels were prestressed.	Rollings and Chou 1981
1970s	Michigan	Highway	6 to 12 ft wide, 10 to 11 ft long, and 8 or 9 in. thick	Doweled and undoweled panels	Simonsen 1971; Simonsen 1972; Rollings and Chou 1981
	New York	Highway	12 to 13 ft wide, 20 to 30 ft long, and 9 in. thick	Pretensioned precast panels	Overacker 1974
	Florida	Highway	12 ft wide, 20 ft long, and 8 in. thick	Panels raised into place using slab jacking. Used to conduct interstate repairs.	Grimsley and Morris 1975
	California	Freeway	11.4 ft wide,12.3 to 17.4 ft long, and 8 in. thick	Grout bedding and grout-filled joints	Prefab Pavement 1974
	Virginia	Highway	1 to 2 ft wide, 1 to 3 ft long, and 2 in. thick	Conducted 68 partial depth patches using precast panels seated on epoxy grout	Creech 1975
	South Dakota	Highway	Unknown	Partial-depth precast panels	Rollings and Chou 1981
	New York	Airfield	12 ft wide, 30 ft long, and 9 in. thick		Overacker 1974
1980s	Wisconsin	Highway	6 ft wide, 6 ft long, and 8.5 in. thick	Panels were placed on 0.5 in. of mortar grout.	Sharma 1990
	California	Airfield	Customized	116 panels were replaced, and each panel was custom built to the slab requiring replacement. The panels were overlaid with 8 in. of AC.	Rollings and Chou 1981; Brabston 1984
	Florida	Airfield	6 ft wide, 6 ft long, and 8 to 12 in. thick	Placed on grade and bonded with polymer concrete and/ or covered with polymer concrete	Brabston 1984
	Mississippi	Airfield		Predicted repair times for continuous repairs of bomb craters 20 to 50 ft wide, 20 to 50 ft long, and 6 to 8 in. thick	Brabston 1984

2.3.2 Recent U.S. experiences

2.3.2.1 Testing of 'Soviet-style' slabs

The U.S. encountered precast panel airfield pavements in former Soviet Union-occupied countries during recent military operations in Afghanistan and Iraq. Research was conducted in the U.S. to understand the load-carrying capacity of the panels to predict damage caused by U.S. aircraft (Tingle et al. 2007). A precast panel runway using "Soviet-style" prestressed, precast slabs was constructed in 2007-2008. Panels were connected by welding deformed rebar near the corners of each slab. During this time, another study was conducted to understand the Soviet precast panel manufacturing and design process to determine whether the technology could be applied for U.S. efforts (Sapozhnikov and Rollings 2007). To date, only preliminary information is available on the field testing effort.

2.3.2.2 Commercial airfield investigations

During the early 2000s, investigations were conducted at Dulles International Airport in Washington, DC (Farrington et al. 2003) and at La Guardia International Airport in New York City (Chen et al. 2003). In 2001, precast panels were used for repairs conducted at Dulles International Airport. Panel sizes utilized included 12.5-ft by 12.5-ft and 6.5-ft by 10-ft panels to repair damaged slabs on two taxiways. The repairs utilized the Uretek Method, described later in this paper of foam injection for leveling and fiberglass ties for load transfer restoration. The repairs conducted at La Guardia were conducted in test sections on Taxiway D-D, using two types of precast panels, including 16-in.-thick conventionally reinforced panels and 12-in.-thick pretensioned precast panels. Both types of panels had dimensions of 12.5 ft by 25 ft and each was used to construct 100-ft by 50-ft test sections. Panels included male-female connections to establish load transfer using grouted dowel receptacles formed in the surface of a panel. Two unique aspects of the panel installation were the use of setting bolts to minimize surface elevation differences and the use of a fast-setting cement bedding grout. As of 2007, these sections were performing satisfactorily, but no information has been published regarding their long-term performance (Olidis et al. 2009).

2.3.3 Highway repairs

In addition to the study of Soviet-style precast panels, numerous other studies have been conducted in the U.S. in recent years, but the major focus

has been for highway repairs. A published summary of precast panel initiatives since 1995 has resulted in a resurgence of interest and investigations into precast panels for highway repairs (Tayabji et al. 2009); a brief summary is provided here.

In the late 1990s, the FHWA sponsored research at the Michigan DOT to investigate the use of precast PCC panel systems for full-depth PCC repairs. This work led to the "Michigan" Method of precast slab repair, discussed later in this paper. This method is one of the major repair methods available today for highway repairs using precast PCC panels (Buch et al. 2003; Tayabji et al. 2009). More recent activities include AASHTO-promoted technology transfer of precast PCC repair and construction activities including precast panel design, fabrication, and repair installation specifications during 2006 to 2008 (Tayabji et al. 2009). In addition to the FHWA and AASHTO efforts, precast panel technology investigations have been conducted since 2000 by numerous agencies including Caltrans, Illinois Tollway Authority, Iowa DOT, New Jersey DOT, New Jersey Turnpike, New York State DOT, and the New York State Thruway Authority among others. Other users reported include Colorado, Delaware, Florida, Hawaii, Indiana, Michigan, Minnesota, Missouri, Texas, and Virginia (Davis 2006; Tayabji et al. 2009).

2.3.4 Strategic Highway Research Program 2 (SHRP 2)

From 2008 through 2012, SHRP2 Project R05-Modular Pavement Technology focused almost exclusively on precast panel technologies to develop and evaluate the use of modular pavement systems. As part of this research, various precast panel systems in the U.S. and abroad were investigated. Results (Tayabji et al. 2013) indicate that as long as the panels were installed with care, including adequate bedding material and dowel alignment during installation, they have the potential to provide long-term service for pavement repairs of 15 to 20 years for highway applications. This projected long-term service life on highway pavements makes the use of precast panels for airfield repairs more promising.

2.3.5 Common precast panel systems in the U.S.

Currently, the most commonly used methods of precast panel repairs in the U.S. are the Fort Miller Super-Slab Method, the Michigan Method, and the Uretek Method or some variation of these three methods. Additional commercial systems have been developed recently including the Kwik Slab

System (Kwik Slab 2011) and the Roman Road System® by the Roman Stone Construction Company (Roman Stone Construction 2012). The main differences between repair methods are the base support, panel size, and spacing and number of dowels. The following sections present a summary of each method and recent experiences with each method.

2.3.5.1 Fort Miller Super-Slab Method

Since 2002, the Fort Miller Super-Slab® Method has been used by several agencies in the U.S. with the most use occurring in New York, New Jersey, and California (Thomas 2008; Tayabji et al. 2013). The method consists of placing factory-fabricated slabs on a carefully graded aggregate bedding material. Standard sizes can be produced; however, individual panels fabricated to fit the exact area (or warped to fill volume) to be replaced can be made. Panels are tied together through dowel receptacles that are manufactured in the bottom of the slabs to tie to existing or retrofitted dowels in the adjacent slabs (parent slabs). The dowel receptacles are grouted after placement with rapid-setting cementitious grout to provide slab interlock and allow load transfer using predrilled or manufactured grout holes. The panels also have grout holes that allow a bedding grout to be pumped under a slab through precast channels on the underside of the slab to fill voids and level the panels (Fort Miller 2003). If precast panels are connected, then dowel bars are cast on one side of the precast panel with dowel receptacles precast in the other side.

2.3.5.2 Michigan Method

In 2003, the Michigan Method was used to install 21 precast panels for a full-depth patching effort along two interstates in Michigan. The panels were typically 12 ft long, 12 ft wide, and 10 in. thick with three 1.5-in.-diam dowel bars cast into the precast panel wheel paths to provide load transfer across the joints (Buch et al. 2003). This method uses precast panels that are seated on a layer of flowable fill or alternatively leveled in place using high-density polyurethane foam injected through preformed or drilled holes. Dowel bars cast into the panels are connected to the surrounding pavement through dowel slots that are saw cut and excavated using a jackhammer. After the dowel slots or receptacles are prepared, the panels are lowered into place, leveled, and then the dowel slots are filled with a rapid-setting grout. The final step in the process is to seal the joints. Time-consuming repair activities include the preparation of the dowel slots, the saw cutting, demolition, and removal of the existing PCC, and the

adjustment of the panel elevation with respect to the surrounding slabs (Buch et al. 2003).

2.3.5.3 Uretek Method

Uretek USA, Inc., developed a repair method in the late 1990s for raising in-place slabs. The method requires the injection of high-density polyurethane foam through holes drilled through the PCC surface into the sublayers to lift settled slabs to the elevation of the surrounding pavement. Recently, this method has also been applied for precast panel leveling using both the Michigan Method and the Air Force Method that will be described in a following section. For precast panels, the foam injection method is combined with surface-mounted fiberglass ties to restore load transfer in jointed concrete pavements. In this repair method, with little or no bedding preparation, a precast panel is lowered into the area where damaged pavement has been removed. The slab is then leveled by injecting the foam under the slab. Injection ports are either preplaced during panel construction or drilled after slab seating. Once the slabs are leveled, then the ties are used to provide load transfer between the precast panel and the surrounding pavement (Tayabji et al. 2009; Ashtiani et al. 2011). The ties are inserted and grouted into slots that extend from the existing slab to the precast panel or precast panel to precast panel.

The U.S. Air Force evaluated the Uretek Method without the fiberglass ties for leveling precast panels in 2007. Results of the study indicated that the Uretek Method provided better load transfer between single-panel repairs and the surrounding pavement than poured flowable fill seating preparations. However, the researchers did not recommend this procedure for expedient airfield repair applications due to the precision and training that would be required to properly use the foam injection system (Ashtiani et al. 2011).

2.3.5.4 Kwik Slab System

The Kwik Slab System is a newer precast panel repair system developed and marketed in Hawaii and Singapore. The system relies on the placement of precast panels that are connected using steel couplers precast in one or more panel ends. The couplers are then grouted with a high-strength grout. The panels are lifted into place using polyurethane injection, through plastic leveling shims, or grout leveling pads (Kwik Slab 2011).

2.3.5.5 Roman Road System®

The Roman Road System® is a newer precast panel repair system that was developed by the Roman Stone Construction Company in 2009. Panels are placed into the prepared repair area then lifted into place using injected polyurethane foam in the same manner as the Uretek or Michigan seating methods. The load transfer is provided by saw cutting through both the parent PCC and the precast panel and installing load transfer devices following the leveling of the panel. Dowels are placed in locations of expected truck traffic, similar to the Michigan Method. The panels are typically thinner than the existing pavement by 1 in. (Roman Stone Construction 2012; Tayabji et al. 2013).

2.3.5.6 Air Force method

Recently, the U.S. Air Force developed a method of airfield pavement repair using single precast panels. The panels were designed such that deployed personnel could assemble prefabricated forms in the field and cast and stockpile panels on site for future use. Precast panels were prepared on site using specially designed forms made by the Air Force. The precast panels were 9 ft 10.5 in. long, 9 ft 10.5 in. wide, and 11 in. thick. Load transfer was provided by ten 1.0-in.-diam, 22-in.-long dowels precast into the slabs on both sides of the panel in the direction of traffic. Similar to the Michigan Method, dowel slots were saw cut and prepared in the surrounding PCC as dowel receptacles. Following the placement of each panel, the dowel slots were filled with rapid-setting proprietary repair material.

In the study conducted by the Air Force, two single-panel repairs were conducted using foam injection for leveling, and a third single panel was seated on a layer of flowable fill backfill. Each repair was trafficked using an F-15E load cart for 1,508 passes. Load transfer was monitored for each repair before, during, and after trafficking (Ashtiani et al. 2011). Although the foam-injected repairs provided better load transfer compared to the third repair, the flowable fill backfill provided sufficient support for the design traffic and was deemed suitable for contingency (emergency) repairs (Ashtiani et al. 2011). Currently, the U.S. Air Force Research Laboratory (AFRL) and the U.S. Army Engineer Research and Development Center (ERDC) are working together to refine the panel design and repair process so that single- and multiple-panel repairs can be conducted.

2.3.6 Recent international experiences

In addition to the recent U.S. experiences, a resurgence of precast panel research has occurred around the world. Recent worldwide experiences with precast panels have also been reported (Kohler et al. 2007). Several pilot studies were conducted in the Netherlands during the period 2004 to 2006 as part of a "Roads to the Future" contest by the Dutch Ministry of Transport. One precast panel concept investigated included ModieSlab. ModieSlab is a modular pavement structure where precast concrete panels are used to construct pavements that rest on concrete piles or are embedded into the existing pavement. A pilot study and an accelerated pavement testing study were conducted using ModieSlab (among other technologies). In the pilot study, the ModieSlabs were constructed on a motorway in the Netherlands, and the study reported problems such as smoothness, raveling, and polished aggregate (Houben et al. 2004a, b).

A study was also conducted in France using hexagonal-shaped panels (similar to the early Soviet precast airfield slabs) placed over a granular bedding material (Kohler et al. 2007). This precast panel research was part of an ongoing Removable Urban Pavements research project coordinated by the Laboratoire Central des Ponts et Chaussees. This study focused on new road construction methods using modular precast concrete elements in which small hexagonal panels were connected to form a pavement surface that could be quickly removed and replaced when damaged. A modular road design allows repair teams to make repairs to the sublayers by removing the panels. Once sublayer repairs are complete, the panels may be reused or only the damaged panels replaced, potentially reducing costs of repaving the entire pavement section (Removable Urban Pavement 2010). Each slab was 8 in. thick and had an equivalent diameter of 5 ft.

2.3.7 Candidate repair methods for airfield repairs

The literature reviewed revealed numerous investigations in recent years that show promise for widespread acceptance or use of precast panels for highway or roadway repair applications. Despite the amount of research applied to the topic of pavement repair, a single repair method or system has not been established in the U.S. or worldwide. As part of this research, the current methods of precast panel repairs were reviewed to select a single repair method that could be applied in current or modified form for contingency (emergency) airfield repairs anticipated in remote locations. In these locations, repair teams would not necessarily have access to proprietary

repair materials or high-early strength concrete for making cast-in-place repairs. Figure 2.1 presents several precast panels described in the literature. Differences in the size of panels and number and spacing of dowels can be seen in this figure. Methods presented outside the U.S. were eliminated from consideration due to the lack of performance and design information available.

For repairs on permanent civilian or military airfields, commercial or generic systems could be used to prepare panels for placement; however, for contingency repairs in remote locations, the needs of both situations must be considered to create an optimal system. Remote locations will most likely not be within suitable transport distance from precasting facilities with well-established routes. Panel fabrication would be required on-site from locally available materials to decrease production and transport costs and ensure the panels would arrive without damage. Quick, efficient, and correct installation by available personnel who may not be completely familiar with this construction concept demands a system that requires limited training to operate and utilizes basic supplies and equipment a typical operator can use with little experience. For this reason, most commercial systems discussed in the literature are not applicable to this specific set of conditions. Commercial systems may be best applied for non-emergency repairs in which repair window and transportation constraints are less stringent. Further investigation into the applicability of commercial systems intended for traditional airfield repairs utilized in non-emergency airfield repairs is recommended.

Other systems presented in the literature rely on prestressing panels before installation. Due to the nature of contingency repairs, these systems are also not applicable for contingency repairs, because they require additional equipment and training that will not necessarily be available for troops tasked with repair in remote environments. Post-tensioning considerations would be the most difficult to implement for quick, small repairs, since multiple slabs are typically tied together, and significant work is required to complete post-tensioning efforts after the panel is placed on grade. By eliminating prestressed panels, several previously used systems were excluded from further consideration.

Figure 2.1. (a) Soviet Style precast slab placement (Tingle et al. 2007), (b) Super-Slab® installation (Thomas 2008), (c) Michigan Method slab installation (Buch et al. 2003), (d) Roman Road slab installation (Roman Stone Construction 2012), (e) Kwik Slab precast panel (Kwik Slab 2011), and (f) Air Force Method panel (Ashtiani et al. 2011).

(a)

(b)

(c)

(d)

(e)

(f)

The use of injected polyurethane foam has been investigated for multiple repair methods including the U.S. Air Force Method, Uretek Method, Michigan Method (injection method), Kwik Slab System, and Roman Road System. The injection of foam requires highly trained personnel to prevent cracking of the panels, excessive lifting, and damage to surrounding pavements (Priddy et al. 2010a).

While this process worked well in previous field investigations for precast panel leveling, it would be best applied for non-contingency environments. This step in the repair process also requires additional equipment and materials that may be difficult to maintain and store in remote locations. Due to the risk of failing to install the panels properly and equipment demands on an installation and personnel, methods that rely on injected-foam leveling are not recommended for contingency airfield pavement repairs using precast slabs.

Backfilling options that remain include compacted aggregate and flowable fill. Compacted aggregate backfill is used in the Fort Miller Method, which requires either a lightweight laser screed or customized spreading equipment to place the base and provide the correct cross-section shape. Heavy equipment is a necessity for this backfilling option, due to the area covered, quantities installed, and the acceptable tolerances required; however, using heavy equipment for small repair areas may be difficult and may damage the existing pavement. Additionally, previous studies conducted by the ERDC regarding different strategies for airfield repairs have shown repairs with aggregate bases take considerably more time to construct than those with flowable fill and foam, therefore reducing the attractiveness of this option (Priddy 2009).

After eliminating repair methods for the various reasons stated above, only the Michigan Method and Air Force Method using flowable fill bedding remained for further examination. Both options are similar in terms of ease of fabrication and use of commonly available materials. The Air Force Method was designed for single-panel repairs only, and the panels could not be connected to repair larger areas. The dimensions and doweling of both systems are also different, but this is not surprising since the panels were designed for different pavement applications. The Michigan Method size is suited for a replacement of a typical single highway lane slab (12 ft wide) with dowels only in the wheel path, whereas the Air Force Method is suited for a partial airfield slab replacement with an area of roughly 10 ft

by 10 ft with dowels spaced at regular intervals across the panel. The lack of dowels and vehicle traffic-sized slabs make implementation of the Michigan Method very difficult for airfield use, therefore leaving the Air Force Method as the most applicable for contingency airfield repairs.

2.4 Comparison of precast panel repairs to traditional full-depth airfield repairs

In selecting a method to repair a damaged airfield pavement, one must consider the repair speed, cost, and performance. For contingency repairs, faster repair speeds and longer lasting repairs may come at a higher cost compared to traditional PCC repairs that require longer curing durations. Because of this, the speed, cost, and performance of precast panel repairs reported in the literature were compared to other repair methods.

2.4.1 Speed

Complete timing data for precast airfield repairs was only available for the Air Force Method. For the Air Force Method using flowable fill bedding material, a total repair time was reported to be 4 hr; however, this did not include curing of dowel-slot material (Ashtiani et al. 2011). A realistic return to service time for the Air Force Method repairs would be 6 hr including a minimum 2-hr cure for a typical rapid-setting grout. Repairs conducted at Dulles International Airport took place over six nights with 7-hr work windows. The work was staged over several nights, and total time per repair was not reported (Farrington et al. 2003). At LaGuardia Airport, test section timing data indicated that construction could be completed within a 36-hr timeframe (Chen et al. 2003).

Because of the lack of airfield repair timing data, highway work was also reviewed for additional information. Highway repairs using precast slabs may be installed in a single night (8-hr work window) or in two or more days when the repair process is completed in phases to minimize traffic disruptions (Buch et al. 2003; FHWA 2007; Tayabji et al. 2009). An FHWA study reported total precast panel repair times for several repairs in Michigan and Colorado of less than 4 hr, but these reported times did not include dowel-slot material curing or joint sealing in the total repair time (FHWA 2007). Considering these reported times, the Air Force Method is similar to those reported in the literature for highway repairs. If precast panels are selected for airfield repair work, filling the dowel is an essential work task that must be completed before reopening. Due to the

loads and tire pressures aircraft have compared to automobiles, significant care must be taken to minimize damage to aircraft tires. High-speed movements over multiple unfilled dowel slots, such as those required for the Air Force panels, is not recommended. Traffic traversing precast repairs with open dowel slots may be more appropriate for road repairs.

In comparing the Air Force Method with rapid-setting repair techniques, the Air Force Method requires more time than a cast-in-place rapid-setting material repair. ERDC testing has shown these repairs can be completed in less than 4 hr from identification of damage to reopening to traffic (Priddy 2009). Recent ERDC testing revealed slightly longer curing durations for non-proprietary rapid-setting or high-early strength PCC repairs. For these repairs, 4 to 10 hr was required prior to reopening to traffic (Williams et al. 2011).

2.4.2 Cost

The Air Force Method panels cost approximately $2,500 (2011) each or $25/ft^2 including the panel, rapid-setting grout, joint sealant, miscellaneous disposable materials, and flowable fill bedding materials. This cost does not include forms, labor, or equipment costs. The Minnesota DOT (2005) reported the lowest bid cost $9,040 per panel using the Fort Miller Method or $63/ft^2. This is over 250% more costly than the Air Force Method; however, it is unknown how the MnDOT value was developed. Precast panel costs have decreased significantly since this project and range from $27 to 56/ft^2 (Tayabji et al. 2013).

While the Air Force Method appears to be similar in cost to current precast systems, its cost compared to cast-in-place methods for emergency repairs may not. The average cost for an emergency repair using proprietary rapid-setting repair materials in 2011 was $440/yd^3 to $500/yd^3, depending on repair material utilized, and $140/yd^3 to $200/yd^3 for high-early strength PCC based on Vicksburg, MS, PCC vendor pricing. For comparison purposes, the cost of a conventional airfield PCC mixture was $125/yd^3. Based on a full-depth (11-in. panel plus 9 in. of flowable fill) PCC pavement repair, the maximum depth the Air Force Method will replace, prices for these three cast-in-place repair methods (proprietary rapid-setting PCC, high-early strength PCC, and conventional PCC) are $24/ft^2 to $28/ft^2, $8/ft^2 to $11/ft^2, and $7/ft^2, respectively. The precast panel repair cost ($25/ft^2) is similar to proprietary rapid-setting repair materials but has a sizable cost difference to high-early strength or conventional PCC. This cost

difference comes from the additional materials needed to construct the panel so that it can be lifted into place, accounting for approximately 67% of the total panel cost.

2.4.3 Performance

The only recent performance data of the use of precast panels for airfield repair are from the Soviet style construction project and the Air Force Method research. The Soviet style panels were intended for airfield construction or pavement overlays. Simulated traffic testing with F-15E (35,000-lb single wheel load at 325 psi) and C-17 traffic (6 wheels with 38,500-lb tire load at 141 psi each) revealed the most cracking around joints and corners (Tingle et al. 2007). The Air Force Method field testing resulted in the three panels being trafficked but not failing after 1,508 applications of F-15E traffic (Ashtiani et al. 2011). The overall surface condition of the panels and surrounding pavement following traffic was good, with minor spalling noted in the dowel grout near the joints.

Another reported performance of precast panels included accelerated pavement testing in California indicating a repair life of 25 to 37 years for highway traffic for sections constructed using Fort Miller slabs (Kohler et al. 2009). This life expectancy was based upon traffic data conducted with both simulated truck and aircraft loadings. The test section trafficked with simulated aircraft loading withstood more than 1,500,000 load applications (approximately 34,000-lb single-wheel load at 209 psi). Corner breaks, spalling, and cracking were noted at failure.

2.5 Optimization of selected precast panel method

The Air Force Method has a few drawbacks that require system modification or verification of specific design elements before implementation. Additional research will be required to thoroughly review the selected method's precast panel design, fabrication methods, and field placement techniques to optimize critical items for a future field placement study:

- The panels were developed for installing a single panel into an existing damaged slab for repairs. Repairs not requiring replacement of an entire slab could be made using these panels; however, the current panel design does not allow for tying multiple panels together for full-slab replacements.

- A review of typical airfield pavement slab sizes is required for selecting the appropriate panel size. A single set of panel dimensions will be selected to standardize prefabricated, reusable formwork, and construction methods. This design is very stringent and limits panel optimization at the project level from its "one size fits all" mentality; however, the system will reduce storage, transport, and lifting challenges that can arise from multiple-sized panels. This option eliminates the need to design sturdy, reusable formwork that is flexible enough to allow casting multiple different panel dimensions. Formwork designed for this task may not be cost effective for a few small jobs.
- The reinforcement design needed should be sufficient for all phases of the panel's lifecycle and follow typical structural concrete design guidance. The panels should be capable of being lifted, transported, and stockpiled without damage.
- Lifting capabilities at remote locations are variable and are a design challenge. The dimensions of the panels and large, removed mass sections of damaged pavement must allow for safe and efficient operation. Airfield pavements are generally thicker than roadway pavements since the loading per pass is significantly higher for aircraft. If lifting capabilities are limited, then thicker panels will require smaller panel dimensions for installation. Integrating a minimum crane size available at typical installations should be considered.
- Streamlining the work tasks required by personnel to fabricate panels and install them into a pavement is required to ensure panel quality and performance. Adapting existing, or using common, commercially available equipment and disposable supplies is needed as well to limit the training or learning curve required for personnel with little construction-related background knowledge and operation in various work environments.
- Techniques for prompt demolition of the damaged existing pavement should be explored since this is expected to be the most time-consuming work task. Current methodologies focus on breaking the pavement into smaller, manageable pieces or removing intact slabs. Removal of intact slabs shows the most promise for efficiency, speed, and mitigation of existing pavement damage.
- Specifications for selecting flowable fill material and its expeditious placement as bedding material are needed. Strength requirements should revolve around preventing damage of this material under the various aircraft loads expected.

- The timing data reported for each individual work task used for installing the panels should be assessed to ascertain inefficient tasks. Modifications to the equipment or procedures should be used to reduce the overall installation time for minimal airfield downtime.
- The major failure modes precast panels experience under aircraft traffic require identification. Modifications to the materials used and panel design should be made to mitigate potential sources of foreign object debris damage and tire hazards.
- The finalized precast system should be compared against other commonly used repair methods and the results analyzed.

2.6 Summary and conclusions

There has been resurgence in the use and study of precast PCC panels for highway and airfield construction in recent years. The majority of research in the U.S. has focused on highway applications. This paper summarizes worldwide experiences using precast PCC panels for pavement repairs. For more than 50 years, various procedures have been developed and investigated around the world, and these procedures are still evolving as more experience is gained. The advantages of using precast pavement technology include better quality concrete repairs through use of precision fabrication and reduced delay in reopening a pavement to traffic. The main disadvantages of precast panel repairs include panel size restrictions due to lifting capabilities in the field, seating and leveling issues, and the uncertainty of the long-term performance of the current systems.

Based on the current methods and systems available, the Air Force Method of precast panel repair was selected for further investigation for military contingency airfield repairs. Flowable fill was selected for the bedding material due to the cost, equipment, and operational concerns. Modifications will be required to tailor the system to best construct panels on-site, increase installation rates, determine the most efficient supplies and materials for use, and expand the system to allow for larger repairs with multiple panels. An analysis of the modified system is underway to compare this method to other accepted repair methods to assist with making cost efficient and justified decisions when conducting pavement repairs. Continued research is required to refine the current processes. Performance testing of single- and multiple-panel repairs under simulated aircraft loads is required to understand the life of the repairs under aircraft traffic.

2.7 Future research

The next step in this research effort is to optimize and investigate the field performance of the selected Air Force Method of making precast panel repairs. Optimization will focus on determining the most efficient panel dimensions based on projected slab sizes, reinforcement needs, and lifting considerations. A standard listing of disposable supplies and small equipment needed to perform rapid airfield repair of PCC pavements with precast panels will be developed, along with guidance to construct and install the panels. Supplies and small equipment recommended will encompass all aspects of the precast pavement job, from construction and storage of panels on the project site using local materials to the installation of the cured panels.

Once all initial modifications are made, a full-scale field investigation will be conducted using the optimized system to evaluate the performance of partial- and full-slab replacements using precast panels in a PCC test section constructed at the ERDC. Panels will be trafficked to failure under simulated, accelerated C-17 aircraft loads. Data regarding the repaired pavement's surface deterioration and mechanical properties will be collected during trafficking. In addition to performance, the required installation work tasks will be timed to assist with identifying equipment and manpower requirements needed to complete repairs in less than 6 hr. Results of the field investigations will be used to make further improvements to the panel design, construction, and installation tasks. Additional field testing will be required to verify and finalize the panel design, construction, and installation procedures.

2.8 Acknowledgments

Information described and presented herein, unless otherwise noted, was obtained from research sponsored by the U.S. Air Force Civil Engineer Center and performed at the U.S. Army Engineer Research and Development Center. Permission to publish this information was granted by the Director, Geotechnical and Structures Laboratory.

3 Full-Scale Field Testing of Precast Portland Cement (PCC) Panel Airfield Pavement Repairs

L.P. Priddy[1], P.G. Bly[2], C.J. Jackson[3], and G.W. Flintsch[4]

Reprinted by permission of Taylor & Francis, Ltd, http://www.tandfonline.com), August 2014. Citation: Priddy, L.P., Bly, P.G., Jackson, C.J., and Flintsch, G.W. (2014). Full-Scale Field Testing of Precast Portland Cement (PCC) Panel Airfield Pavement Repairs, *International Journal of Pavement Engineering*, 15(09-10), 840–853, Taylor & Francis Ltd, http://www.tandfonline.com.

Abstract: A series of various sized Portland cement concrete (PCC) airfield repairs was performed using precast panels. The repairs received simulated C-17 aircraft traffic, and each repair was trafficked to failure. A heavy weight deflectometer (HWD) was used to measure the panels' response to loading with increasing traffic applications. The results of traffic testing were used to evaluate the suitability of the precast panel repair technique for rapidly repairing PCC airfield pavements. Test results showed that the repair system was capable of supporting at least 5,000 passes and possibly as many as 10,000 passes of C-17 traffic. Compared to other rapid airfield repair methods, the precast panel repair alternative may provide similar return-to-service timelines and traffic performance at a slightly higher cost. Modifications to the system design and placement procedures are recommended to improve the field performance of the panels.

[1]Research Civil Engineer, U.S. Army Engineer Research and Development Center, Vicksburg, MS 39180. Email:lucy.p.priddy@usace.army.mil.
[2]Research Civil Engineer, U.S. Army Engineer Research and Development Center, Vicksburg, MS 39180. Email:peter.g.bly@usace.army.mil.
[3] Research Civil Engineer, Applied Research Associates, Tyndall Air Force Base, FL. Email: Christopher.Jackson.ctr@tyndall.af.mil.
[4] Director, Center for Sustainable Transportation Infrastructure, Virginia Tech Transportation Institute and Professor, The Charles Via, Jr., Department of Civil and Environmental Engineering, Virginia Tech, Blacksburg, VA 24061. Email: flintsch@vt.edu.

3.1 Introduction

Ever decreasing construction timelines drive the need for rapid, or expedient, repair techniques for both highway and airfield Portland cement concrete (PCC) pavements. While traditional PCC remains the recommended repair material for PCC military airfield repairs, the curing durations with this material require long pavement closures (UFC 2001a). To complete repairs within current allotted timeframes as short as 4 to 6 hr, rapid-setting, cementitious repair materials or high-early strength concretes are typically used after gaining acceptance by the airfield and highway pavement communities.

Another repair technique gaining interest over the past 10 years in the highway sector is the use of precast PCC slabs or panels; and numerous systems, both generic and commercial, to make such repairs have been developed and investigated. Recent syntheses of panel systems have been conducted by Olidis et al. (2009), Tayabji et al. (2013), and Bly et al. (2013). These documents reveal several benefits to using precast panels for repairing pavements, including improved repair quality due to the controlled fabrication process, reduced pavement closure times, and improved potential for long-lasting repairs. Some drawbacks to precast panel repairs include potentially higher costs compared to other repair methods, specialized and heavy-equipment needs, surface roughness concerns, lack of fabrication and installation guidance, and lack of documentation of panel performance, particularly for airfield usage. Research is required to determine if precast panel systems are suitable for rapid airfield pavement repairs, and whether the potential drawbacks or limitations reported in the literature can be overcome through improved repair guidance.

3.1.1 Research objective

The objective of this study was to determine the feasibility of using precast panel repair technology to conduct rapid airfield pavement repairs within a 4- to 6-hr time frame and to determine whether the panels could support minimum pass levels of 3,700[1] passes of C-17 aircraft traffic prior to failing. Repairs meeting this pass criterion would be suitable for temporary repairs, and repairs supporting more than 5,000 passes would potentially be suitable for permanent pavement repairs.

[1]This threshold has been reduced to 3,000 passes since the publication of this paper.

3.1.2 Methodology

The experimental program consisted of developing and testing a precast panel repair system for conducting rapid repairs in a PCC airfield pavement. Three full-depth repairs of various sizes were made in a pavement test section at the U.S. Army Engineer Research and Development Center (ERDC) in Vicksburg, MS. Following placement, each repair was trafficked to failure under simulated C-17 aircraft traffic. During trafficking, pavement response data from instrumentation were recorded. Following predetermined traffic intervals, nondestructive tests were conducted using a heavy weight deflectometer (HWD), and the results and physical damage to the repairs were observed and noted. Trafficking was continued until passes-to-failure rates were determined. The speed, cost, and performance of the precast repair method were then compared to other rapid repair methods to determine the feasibility of using this repair method as opposed to other methods currently adopted.

3.2 Precast panel system development

In 2011, a joint research effort between the U.S. Army ERDC and U.S. Air Force Research Laboratory (AFRL) was initiated by the U.S. Air Force (USAF) to determine the suitability of precast panels for rapid airfield pavement repairs. Following a review of available literature on the subject, a precast panel design developed by the AFRL in 2007 was selected as the most applicable to the operational constraints (Bly et al. 2013). A system was desired that would allow similarly sized panels to be fabricated using local materials and stockpiled on-site for emergency use. To minimize training and specialized equipment needs, the system required common, commercially available tools and equipment to facilitate the construction and installation of panels at any location worldwide.

Details of the original AFRL precast panel development are provided by Ashtiani et al. (2010). This precast panel design was intended to replace approximately 3-m by 3-m slabs, and results of simulated F-15E trafficking indicated that the panels were suitable for aircraft traffic. This research also identified rapid-setting, non-excavatable flowable fill as a suitable seating material for the precast panels. While the study provided documentation related to the performance of a precast panel under aircraft traffic, it focused on small, full-slab replacements. The use of panels to repair typical airfield pavement slabs with larger dimensions was not investigated. Furthermore, the original system's panel could not be

connected to another panel for larger repairs. Thus, the research team worked to redesign the technology so that it could be used for a variety of slab sizes, could be connected with other precast panels for multiple-panel repairs, and could be used by both F-15 and C-17 aircraft.

The redesign of the precast panel system began with the selection of the panel dimensions that would provide panels that were small enough to be lifted and placed using the worst-case (minimum) lifting capacity available to a repair team in a deployed location: 13,600 kg. While custom-fit panels would be the ideal for repair efforts, a single precast panel size was selected to reduce storage and transportation problems that could arise from the use of different sized panels and to eliminate the need to design and construct numerous panel forms. The approximate size of the original AFRL panel (3 m by 3 m) was determined by the Air Force to be versatile for a variety of PCC slabs that might be encountered. A panel thickness (28 cm) was selected based on these dimensions and the minimum lifting capabilities. While the panels were expected to be thinner than some in-place slabs, the panels were expected to support the minimum 3,700 passes of C-17 traffic, with more than 5,000 passes predicted for a 28-cm slab using airfield pavement design methodology (UFC 2001b).

Once the general dimensions were selected, the reinforcement of the panels was then designed. The panels were minimally reinforced to reduce potential damage during lifting and storage of the panels, not to reduce the panel thickness. The main reinforcement was at the bottom of the panel and was comprised of a 305-mm grid of 9.5-mm-diam, Grade 420 reinforcement bars placed 38 mm from the bottom of the panel. Additional reinforcement was provided on all sides of panels with two layers of 16-mm-diam, Grade 420 reinforcement bars placed 57 mm from the bottom of the panel and 14 cm from the top of the panels. Each panel required approximately 2.7 m^3 of airfield quality PCC with a minimum 35 MPa compressive strength at 28 days. The concrete and steel reinforcement material properties used in design calculations were selected as typical for military airfield pavement construction. Using these properties, the structural capacity of the panel was determined and compared to the load cases generated during lifting, transport, and storage in accordance to ACI 318 (ACI 2011) procedures for precast concrete, as these load cases can be more damaging than during in-place service. Crane rigging equipment was selected following manufacturer's information and standard lifting practices. Details of the design process may be found in Bly et al. (2013).

Once the general design was complete, it was slightly modified to generate two panel types, a standard panel and a terminal panel, which were required to enable both single-panel repairs and multiple-panel repairs. The panel types are shown in Figure 3.1. Both panel types had a plan area slightly smaller than 3 m by 3 m to allow 9.5-mm-wide joints for the single-panel repair and 13-mm-wide joints around each panel for the multiple-panel repairs. These joint widths were within the minimum width requirement for joint sealant for construction joints in concrete pavements, based on military criteria (UFC 2001b).

Figure 3.1. Panel schematics.

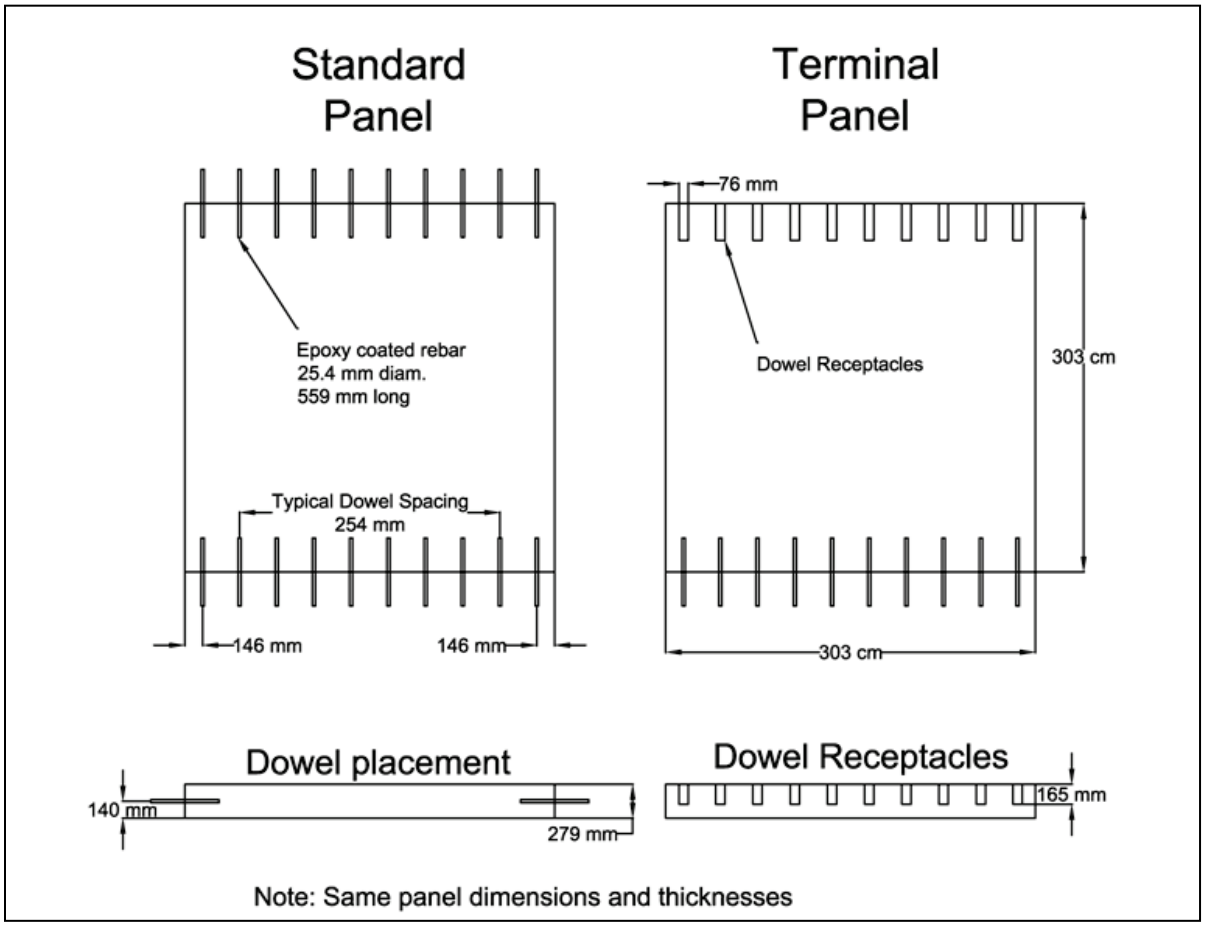

The standard panel had integrated mid-depth load transfer dowels on both transverse edges. The dowels were 25 mm in diameter, 560 mm long, and epoxy coated as specified for military airfield pavements of this thickness (UFC 2001b). The terminal panel included integral mid-depth load transfer dowels on one transverse edge, while the other transverse edge had cast-in-place dowel slots (from the top of the panel) for connecting multiple panels together to facilitate larger repairs.

The precast panels were fabricated by engineering technicians in a concrete surfaced, open-ended aircraft hangar prior to field testing. Reusable steel formwork was used to cast all panels. Detailed formwork design and fabrication information is provided in Bly et al. (2013). After placement of the reinforcement bar, slot casting formwork (terminal panels only), and dowels, the concrete was placed, consolidated, and screeded. After leveling the surface, round head lifting and transport anchors were installed while the concrete was still plastic. The panels were then textured with a fine broom finish, and curing compound was applied. Forms were removed after three days of curing, and the construction process was repeated until all required panels were made. Panels were allowed to cure at their casting location for at least 28 days before lifting.

3.3 Full-scale field testing

3.3.1 Test section description

A full-scale PCC test section, shown in Figure 3.2, was constructed at the ERDC during July 2011. The test section was constructed with a 1% longitudinal slope and a 0.5% cross slope for drainage and to minimize cut-and-fill requirements. The existing pavement was designed to accommodate 50,000 passes of simulated C-17 traffic under military airfield design guidance (UFC 2001b). The section consisted of 355 mm of airfield quality PCC over a 152-mm compacted well-graded limestone base, over compacted sandy, low-plasticity clay. Measured PCC material strengths of field-cured specimens revealed the PCC had an average 28-day unconfined compressive strength of 50 MPa and flexural strength of 6.5 MPa. Slab dimensions were 6.1 m by 6.1 m, representative of airfield pavement slab sizes. Tests performed on the compacted base revealed an effective modulus of subgrade reaction of 75 kPa/mm.

3.3.2 Rapid repair procedures

Following 28 days of curing for the PCC test section, three repair areas were marked as shown in Figure 3.2. Repair 1 (Panel 1) simulated a partial-slab replacement along two joints with a single panel. This repair surface area was 3 m by 3 m. Repair 2 (Panels 2 and 3) simulated a half-slab replacement along a joint requiring two panels to repair a surface area of 3.0 m by 6.1 m. Repair 3 simulated a full-slab replacement requiring four panels (Panels 4, 5, 6, and 7) to repair a surface area of 6.1 m by 6.1 m. All repairs were conducted during October and November 2011 by a team of

12 personnel, representative of a small military repair team. The times required to accomplish repair tasks were also recorded during the repair process.

Figure 3.2. Repair layout and traffic pattern.

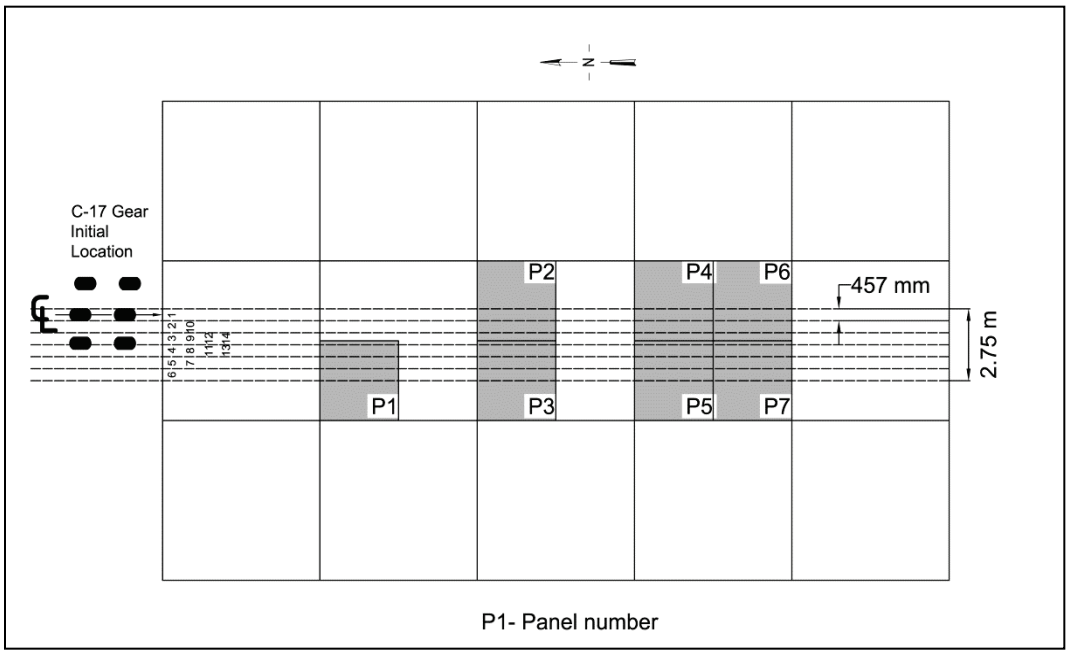

The general repair process is shown in Figure 3.3. The three repair areas were prepared by first marking the repair area boundaries. Following marking, saw cutting of the perimeter of the repair and dowel slots was conducted using a walk-behind concrete floor saw. A series of progressively larger blades was utilized to saw cut the pavement full depth. For this investigation, in lieu of breaking the pavement out and excavating the designated repair area, the saw-cut PCC to be replaced was lifted using commercially available concrete expansion anchors installed in accordance with manufacturer-recommended instructions. The expansion anchors were attached to commercial rigging equipment sized for the lifts, and the cut slab pieces were removed using a mobile crane.

Following pavement removal, the dowel-slot areas were prepared in the existing pavement. Parallel saw cuts for the slots, approximately 75 mm apart, were made during saw-cutting operations. A 10-kg demolition hammer was then used to remove the material between the parallel cuts to make prism-shaped slots spaced at 300 mm on center. Simultaneously, steel bridge plates were attached to the panels to support their weight after placement and to ensure a flush panel installation to the surrounding

Figure 3.3. (a) Saw cutting perimeter, (b) installing lifting eyes, (c) lifting pavement, (d) preparing dowel slots, (e) prepared repair area, (f) screeding flowable fill, (g) lowering panel with bridge plates, and (h) sealing dowel slots.

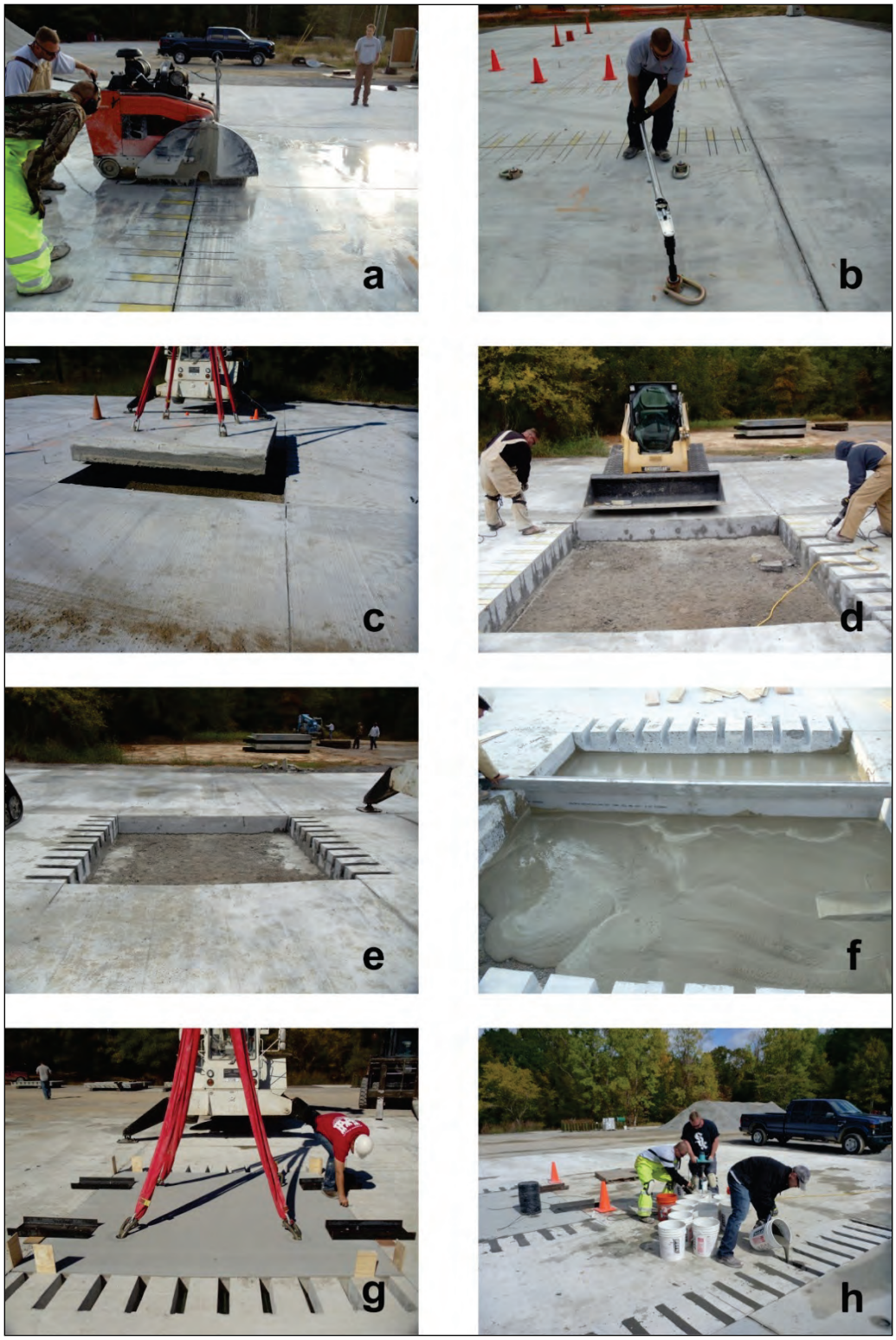

pavement. Each plate was secured to the panel using two 13-mm-diam wedge anchors (per plate) that were installed following manufacturer's guidance. Bridge plates were removed once the bedding material gained sufficient bearing capacity. Figure 3.4 shows a layout of the test section, including the location of bridge plates and lifting points for the panels. Detailed information regarding the design and installation of the bridge plates is provided by Bly et al. (2013).

After the dowel slots were prepared, a thin layer of non-excavatable, rapid-setting flowable fill was placed directly on top of the base course to provide seating material for the panels and to fill the difference in thickness (75 mm) between the repair panels and the parent slabs. No problems were encountered with flowability of the flowable fill due to the slope of the test section. The flowable fill was overfilled approximately 3 mm to help ensure adequate contact between it and the panel. The flowable fill was screeded several times using a simple aluminum screed designed to allow the flowable fill to be leveled within the repair void. The rapid-setting flowable fill was a locally available material capable of attaining a compressive strength of 0.6 MPa within 2 hr of placement and an ultimate compressive strength exceeding 1.4 MPa. The fill was prepared and delivered by a local concrete plant using standard PCC transit trucks. Descriptions of the fill, screed, and the determination of minimum strength for traffic opening are detailed in Bly et al. (2013).

Segregation and high fluidity were noticed during the placement of the flowable fill for Repair 1 (single-panel repair), indicating that the material delivered was not the specified rapid-setting, nonexcavatable fill. Thus, the vendor was contacted to ensure that the specified material was delivered for the remaining repairs. Because of time constraints, the fill was not removed and replaced for the first repair. No segregation was noted for the remaining flowable fill; however, no samples could be obtained for quality assurance testing due to manpower and timing issues.

Immediately following the placement of flowable fill, the precast panel was lowered via a mobile crane into the repair void. Wooden shims were used to center the panel, and a vibratory compactor with a gross vehicle weight of 6,908 kg and a drum weight of 3,908 kg was used to level the panels to the correct surface elevation of the surrounding pavement as needed. To prevent damage to the surface of the panels, sheets of plywood were laid over the surface; no cracking of the panels was noticed after leveling.

Figure 3.4. Bridge plate layout and lifting eye locations.

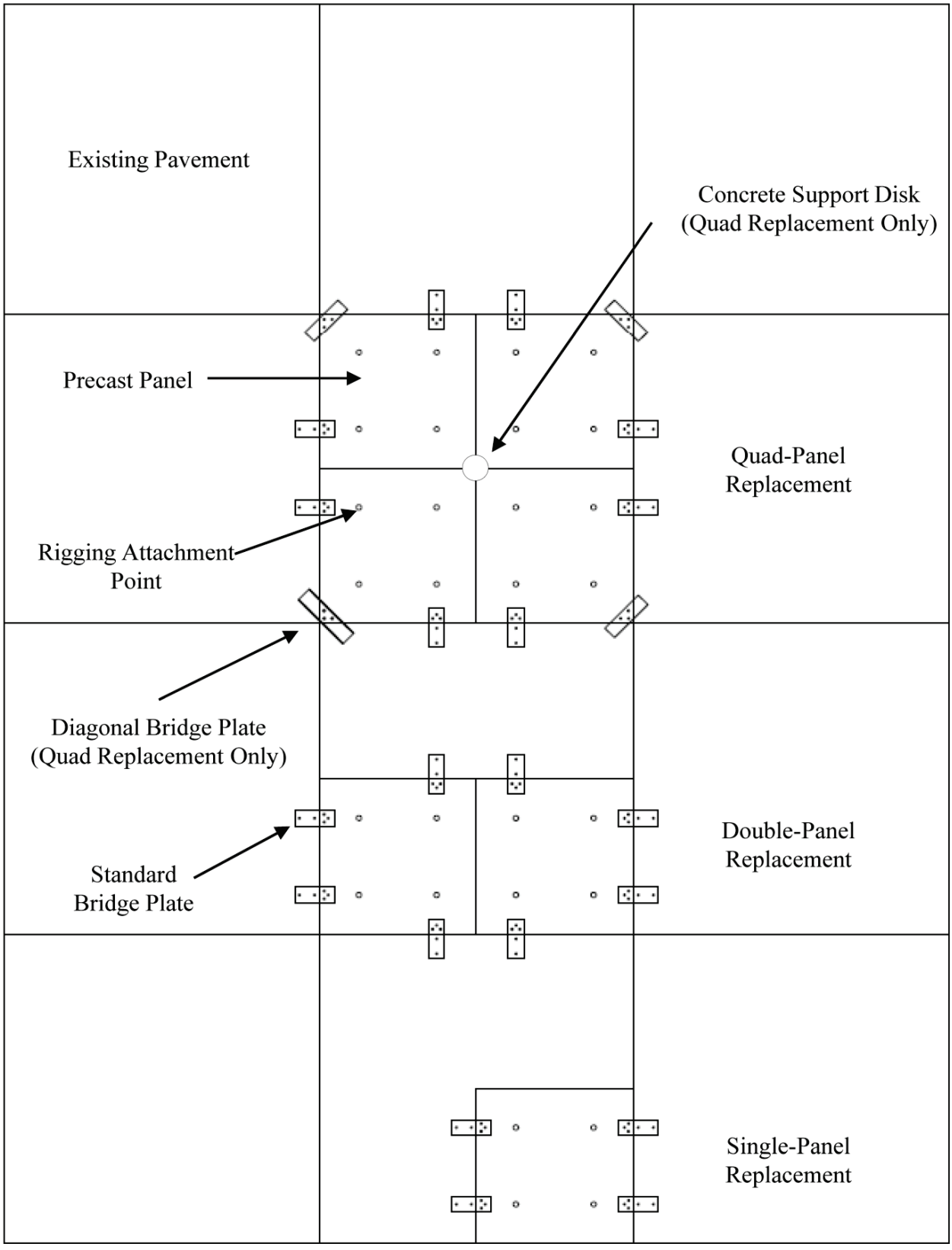

During this step, the flowable fill was pressed into the joints and dowel-slot areas. To simulate likely military installation practices, no attempts were made to remove the flowable fill from the joints, but the material was removed from the dowel slots. The dowel slots were then filled with a proprietary, rapid-setting grout capable of attaining a compressive strength of at least 21 MPa within 3 hr of placement. In keeping with the expedient nature of the repairs, no attempts were made to prevent the grout from escaping the slots, and it was allowed to completely fill the joints. After the grout cured, the temporary bridge plates were removed, the grout-filled joints were shallowly saw cut to accommodate a joint sealant material, and the joints were sealed.

The quad-panel repair required slight modifications for implementation due to its larger area. A 75-mm-thick, 600-mm-diam concrete pedestal was placed into the center of the repair area (as shown in Figure 3.4) to support the interior corners of the four panels to prevent the panels from tilting inwards while the flowable fill was gaining strength. Once the pedestal was in place, the flowable fill was placed in approximately one-half of the repair area, and a terminal panel was lowered into place in one corner. Then a standard panel was placed, allowing the load transfer dowels to be aligned in the slots of the terminal panel and the parent slab. Once these were in place, the process was repeated, and the remaining repair activities including leveling, grouting, curing, and joint sealing were completed.

3.3.3 Instrumentation

During the construction of the test section, the prepared subgrade was instrumented with ten 23-cm-diam earth pressure cells (EPCs). The EPCs were located beneath each precast panel, beneath the parent PCC as a reference, and in the corners of selected panels to monitor the vertical stress distributed to the subgrade under loading. Following the placement and curing of the surface PCC and the installation of all precast panels, 20 surface strain gauges were placed on selected PCC parent slabs and on the surface of all precast panels. Eight strain gauges were also mounted on the sides of two repair panels (Repair 3 – Panels 5 and 6). During trafficking, the EPC data were collected at a rate of 1 kHz; strain gauge data were collected at a rate of 5 kHz.

3.3.4 Traffic testing procedures

As mentioned previously, to be considered appropriate for temporary pavement repairs by the U.S. Air Force, the repairs had to be capable of sustaining at least 3,700 passes of C-17 traffic before failure. To be suitable for permanent repairs, the repairs had to be capable of supporting at least 5,000 passes of the same aircraft. The load cart used for trafficking matched the geometry and loading of one side of the main gear of a C-17, or a full set of six tires, each inflated to 0.98 MPa and supporting 20,300 kg. For each repair, a simulated normally distributed C-17 traffic pattern was applied in a 2.75-m-wide traffic lane, as shown in Figure 3.2. During trafficking, the centerline (CL) of the load cart traveled first south then north (one pass each direction) in each lane (numbered 1-14) until the pattern, consisting of 28 passes (maximum of 25 coverages), was completed. The pattern simulated the channelized traffic distribution patterns, or wander width, typically seen when a C-17 aircraft taxis to and from an active runway. The repair surfaces were periodically inspected for damage during trafficking; however, maintenance was not performed during traffic testing.

Repair failure was expected to occur due to the surface deterioration from overloading the pavement (load-related distresses), loss of base support under the panels (resulting in settlement), or from lack of load transfer at the joints (resulting in spalling, faulting, or settlement). Visual inspections were performed at selected traffic intervals to identify specific distresses associated with high foreign object debris (FOD) potential such as cracking and spalling. Cracking was considered minor until spalled material accumulated or the repair panel was divided into four or more pieces by intersecting cracks (shattered) with cracks exhibiting high-severity spalling or crack widths exceeded 25 mm. When distresses posed high FOD potential or tire hazards were identified, the repair was considered to have failed.

3.4 Results

Data collected during trafficking included periodic visual assessments of surface condition to identify distresses, HWD measurements, instrumentation readings, and pavement faulting/settlement measurements. These tests were also conducted after repair failure.

3.4.1 Surface condition

During trafficking, panels were monitored for any changes in surface condition following traditional PCC pavement distress inspection procedures. Each of the three repairs withstood different amounts of traffic before failing. Repair 1 withstood 5,600 passes before it failed due to shattering of both the parent slab and the precast panel, resulting in high-severity spalling on the doweled transverse panel joints. The parent slab split and cracked into numerous pieces with cracks extending from the corners of the saw cuts for the precast panel repair and from the corners of the dowel slots. Repair 2 was trafficked for 10,000 passes prior to failure due to high-severity spalling of the transverse panel joints and dowel slots in the parent slabs. Similar cracking in the parent slab to that seen in Repair 1 was also noted, with cracks extending from the longitudinal joint between the two panels, essentially separating the slab into four pieces. Repair 3 received 7,100 passes prior to failing due to a high-severity joint spalling along the south transverse edge of the repair. In both the repair panels and the dowel slots in the parent PCC slabs seen in the other repairs, similar spalling was noted.

Distresses were minor until approximately 2,800 passes had been applied. After that point, spalling along the corners and joints increased in severity. Distresses common to all three repairs included spalling and hairline cracking within the panels, dowel-slot cracking and spalling, and cracking in the parent slabs between the dowel slots (shown in Figure 3.5). The joint deterioration led to the failure of all three repairs. This indicated that the repairs were not transferring load efficiently. The extensive cracking and spalling in and around Repair 1 also indicated that the flowable fill may not have been capable of supporting the C-17 loads. Overcutting saw kerfs into the parent slabs also resulted in uncontrolled cracks progressing from partial saw cuts in the surrounding parent slabs. To control cracking in the parent slabs for long-term use, extending the saw cuts the remaining distance to the joint may be necessary.

3.4.2 HWD testing

The HWD was used to obtain deflection basins for the repairs at predetermined traffic intervals. Deflection measurements were taken in the center of the repair panel, along the joints, and in selected corners of the panels. Center and corner deflections measured at the maximum load level at the first sensor were normalized to an applied force of 22,680 kg and are

presented in Figure 3.6. The highest deflections were recorded for Panel 1 of Repair 1 and for Panels 4, 5, and 7 of Repair 3. These figures show the general trend that, as traffic applications increased, the deflections also increased for all repairs and adjacent pavement (parent PCC). These figures also show that lower deflections were recorded for Panels 2 and 3 of Repair 2 and that they were slightly less than parent slab deflections.

Deflection measurements conducted at the joints were used to determine the load transfer efficiency (LTE) under traffic and were taken on both the longitudinal and transverse joints between the precast panels and the surrounding PCC slabs. The ratios of the deflections measured between the unloaded and loaded slabs were calculated as a percentage. As with the center and corner panel tests, the deflections measured at the maximum drop load were used. In general, as traffic levels increased, the LTE

Figure 3.5. Repair failure details: (a) Repair 1, Panel 1: high-severity corner break/spall and shattered parent slab; (b) Repair 2: diagonal cracking in parent slab between Repairs 1 and 2 and cracking and spalling of Panel 2 due to the parent slab deterioration; (c) close-up of the cracking and deterioration in the parent slab and dowel slots and corner of Panel 2; (d) Repair 3, Panels 6 and 7: high-severity spalling in corner of Panels 6, 7, and the parent slabs south of the repair.

Figure 3.6. (a) Center and (b) corner deflections for selected panels.

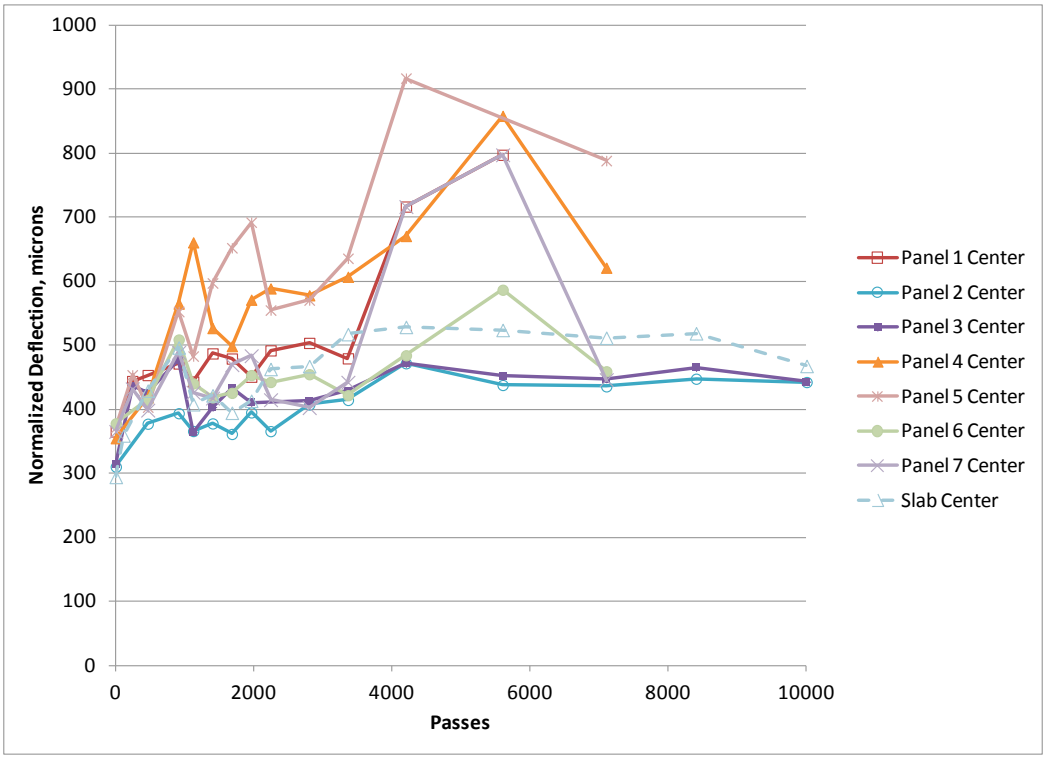

(a)

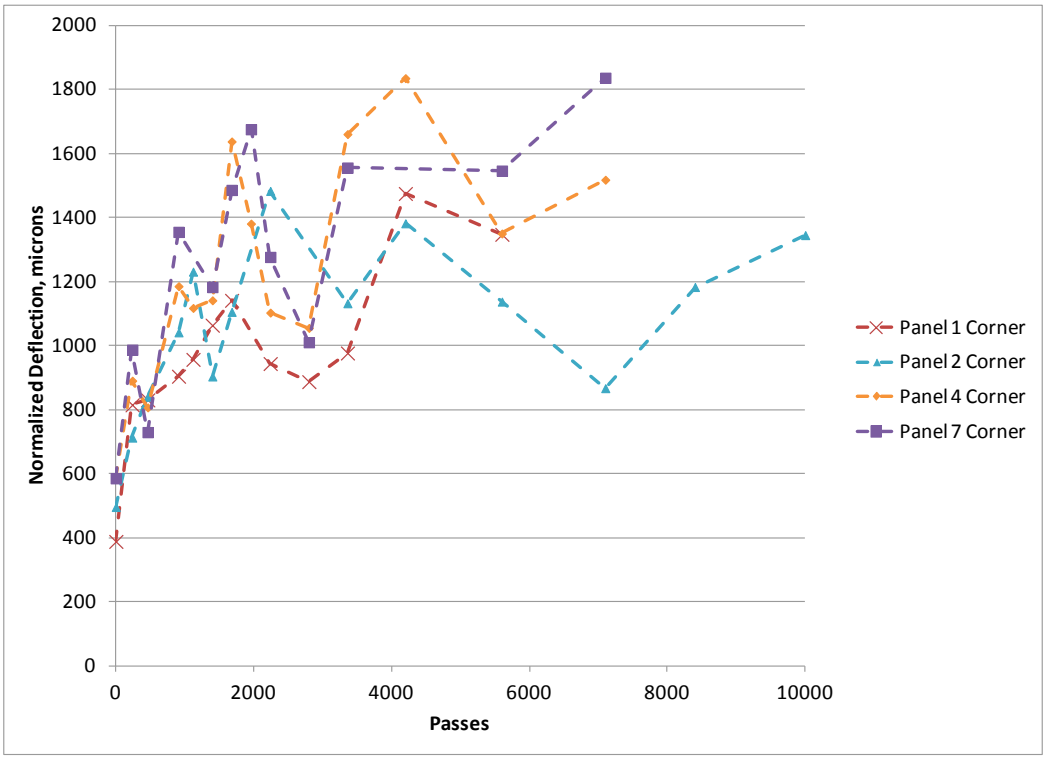

(b)

decreased with higher LTE values for the doweled, transverse panel joints than for the undoweled, longitudinal joints. Poorer LTE was also measured between the panels of Repairs 2 and 3 along the centerline joint (east joint of Repair 2 , Panel 2 and west joints of Repair 3, Panels 4 and 6), where the panels were not doweled together. Values for initial and final LTE are presented in Figure 3.7(a).

For highway pavements, transverse joints are required to have an LTE of 70%, and Ashtiani et al. (2010) considered the same minimum LTE for transverse joint acceptability for airfield precast panel repairs. In looking at Figure 3.7(a), after installation, all transverse joints (N-S joints) had LTEs well above this minimum. The high LTE values did not translate to good physical condition of the transverse joints; the physical damage at the joints suggest that the load was not being transferred efficiently.

Differential deflection, the absolute difference in deflection between the loaded and unloaded slab, provided a better indicator of the performance of the joints. Increases in differential deflection can indicate dowel bar and/or surrounding concrete deterioration near the joint such as that seen in the precast panels' transverse doweled joints. Crushing of the dowel grout creates voids around the bars, resulting in decreased load transfer and subsequent joint spalling, as seen in the field tests. It has been suggested that differential deflections in excess of 127 μm indicate potential joint deterioration for highway pavements (Embacher and Snyder 1999). The calculated differential deflections for the precast panel joints before and after failure are shown in Figure 3.7(b).

In looking at Figure 3.7(b), after installation, most of the transverse doweled joints (N-S joints) had differential deflections below the recommended maximum of 127 μm— including those in Repair 1, Repair 2, and all panels in Repair 3 with the exception of Panel 4. In general, the differential deflections increased with increasing pass levels as illustrated in Figure 3.7(c).

The deflections most likely increased due to breakdown of the dowel grout and crushing of the concrete near the joint, causing voids. The spalling of the concrete at the joints might have also been accelerated by the dowel grout in the joints that did not allow sufficient space for thermal expansion of the parent PCC and panels. Dowels that are too small or weak grout around the dowels could also cause high stress concentrations surrounding the dowels.

Figure 3.7. (a) Initial and final LTE, (b) initial and final differential deflections, and (c) differential deflections with traffic for Repairs 1 and 2.

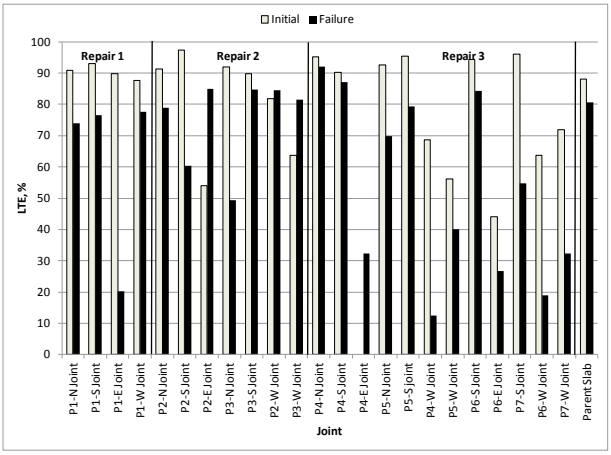

(a)

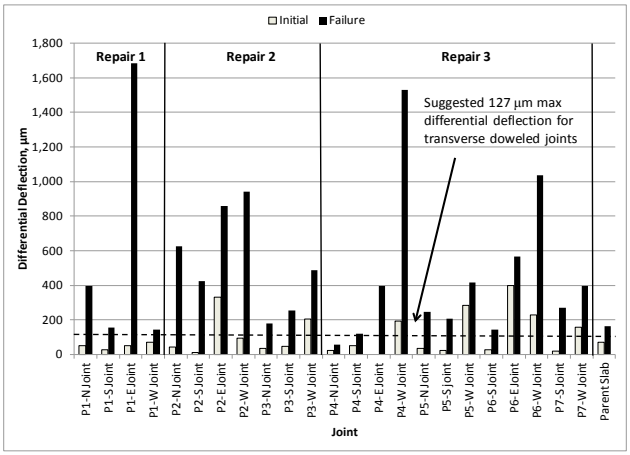

(b)

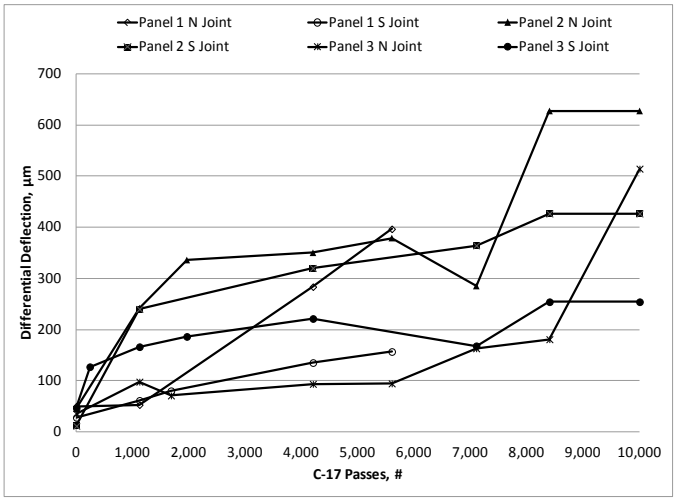

(c)

While the LTE did decrease with traffic, it was not an effective measure of the joint performance because the high LTE values at failure did not indicate that the load transfer provided by the dowels was compromised. The high LTE values at failure were most likely attributed to the contact of the panels with the surrounding pavement due to thermal expansion and the grout within the joints. Additional tests are recommended to aid in the development of an improved doweled joint design and better placement procedures that might increase the life of the repair panels. Additional testing should include increasing the dowel diameter and/or length, selecting an alternative dowel grout, and preventing the flow of dowel grout into the joints. Additional tests for determining LTE thresholds for acceptable precast panel performance are also recommended after the panel design and placement procedure have been optimized.

3.4.3 Settlement and faulting

In addition to monitoring surface distresses, researchers also recorded elevation measurements during trafficking. Any settlement or faulting was measured using a 3-m straight edge and hand ruler across the joints at every edge of the panels. These measurements are important because large differences in elevation can place tremendous stresses on landing gear. For this investigation, the maximum allowable elevation difference was 76 mm. While this elevation difference may seem excessive or dangerous compared to those allowed for civilian airfield or highway vehicle operations, this maximum difference is based on probable aircraft tire tolerances for the C-17. Despite the loss of load transfer, no faulting or settlement was observed during trafficking. The maximum elevation difference measured throughout trafficking was 9.5 mm, and the average difference was only 2.4 mm, far below the criterion. Elevation measurements also indicated the concrete pedestal was able to resist downward tilting of the corners of the quad-panel repair during installation.

3.4.4 Instrumentation

EPC and strain gauge data collected during trafficking were used to determine stresses and strains in the repairs as a function of traffic. Despite care in installation, the instrumentation was damaged due to abrasion from traffic loading and environmental elements. Several of the installed gauges and EPCs (under Panels 1, 2, 3, and 7) were damaged prior to and during the first few load cart passes.

The available instrumentation data indicated that the maximum vertical stress measured in the subgrade under the panels was in the corner of Repair 1, Panel 1 and Repair 2, Panel 2 with the maximum stress measured being approximately 0.09 MPa for Panel 1 and 0.07 MPa for Panel 2. The vertical stress measurements under the centers of Panels 4, 5, and 6 of Repair 3 were lower, with measurements not higher than 0.06 MPa. Overall, the stress measurements for each trafficking interval remained relatively constant, as shown in Figure 3.8. During trafficking, the average center panel stress was 0.03 MPa, and the average corner panel stress was 0.07 MPa. The average measured stresses were compared to calculated stresses for a PCC slab to determine whether the panels exhibited similar behavior to traditional PCC. The measured average center panel vertical stress measurement was similar to that calculated using fundamental PCC theory (0.05 MPa), linear elastic analysis (0.06 MPa), and two-dimensional finite element model software (ISLAB2000) (0.03 MPa). The measured vertical stress under a parent slab was also compared to the panels. Compared to the average vertical stress measured under the parent slab (0.02 MPa), the center panel stress measurements were similar to traditional PCC. The average corner stress measurement of 0.07 MPa was higher than that calculated using ISLAB2000 (0.04 MPa), and the corner stresses were in general much higher than the center stresses. The higher corner stress measurements indicate that either differences in the foundation support beneath the panels or inadequate load transfer occurred. EPC measurements indicated that the peak corner stresses occurred in Panel 1 after approximately 1,500 passes, and the measurements for Panel 1 were consistently higher than those recorded for Panel 2 in the double-panel repair. The corner in which the stresses were measured for Panel 1 was the corner that deteriorated rapidly under traffic. Cores taken following completion of testing indicated that the flowable fill was firmly bonded underneath the corners and in the center of the traffic lanes for the double- and quad-panel repairs; however, the cores taken from Panel 1 indicated that the flowable fill was not bonded to the panel.

Additional analyses are recommended because of the failure of Panel 1's corner and the fact that only two corners were tested. The higher deflections in the corner are also likely to be the result of poor load transfer indicated by the high differential deflections discussed earlier. Overall, the stresses did not increase significantly between installation and failure, indicating that the panels were able to carry the majority of the load without distributing additional stress to the subgrade as the panels

deteriorated. Since the measured responses to loading are similar to those determined by current PCC pavement models, current PCC design methodology could potentially be applied for precast panel structural design to select panel thickness based on projected traffic.

Figure 3.8. Vertical stress measurements using EPCs.

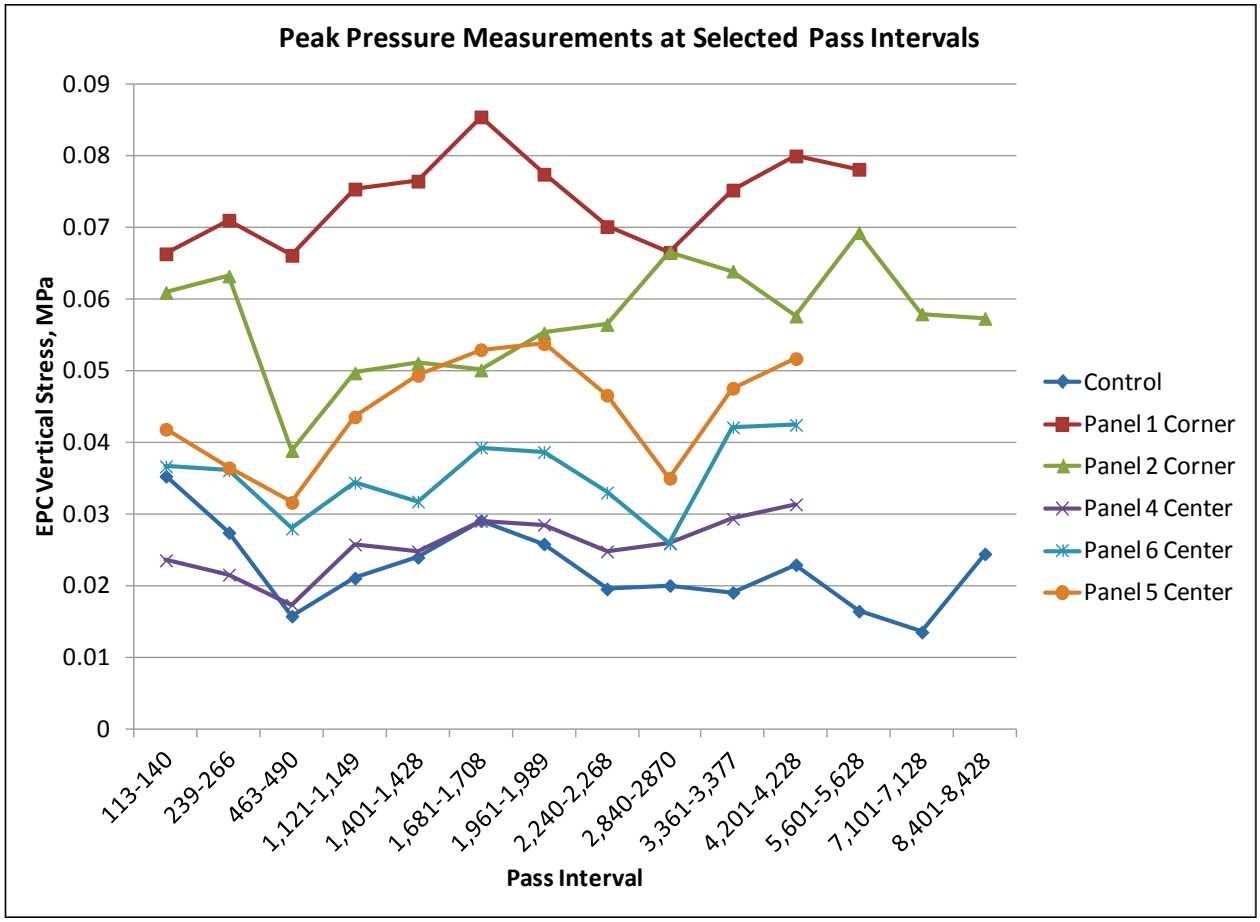

As mentioned previously, a PCC pavement of the same thickness and foundation support as the panel repair was predicted to withstand at least 5,000 passes of the C-17 following military PCC pavement evaluation procedures. The same general design process presented in the "Precast panel system development" section could be applied to develop other precast panel sizes, taking into account both the available lifting capacity at an airfield and the anticipated traffic levels to determine the panel dimensions. The remaining design steps follow general precast concrete practices to prevent the panels from being damaged during lifting, transport, and storage. This preliminary design process for selecting thickness requires additional field testing for validation.

Data from only a few of the strain gauges mounted on the panels' surfaces were collected due to damage under load cart testing. The peak strain measurements for passes 1 through 5 are provided in Figure 3.9. The average initial strain measurement on the panel side of the joint was 3.5E-4. Compared to the strain predicted using ISLAB2000, the predicted strain ($1.66 \cdot 10^{-4}$) was less than the measured strain. For the PCC side of the joint, the average measured strain was $-2.6 \cdot 10^{-4}$ compared to $-1.47 \cdot 10^{-4}$ (predicted). In comparing the predicted and measured values, in general, the model under-predicted the measured strains. The model may not be capable of accounting for differences in the thicknesses of the panel and the surrounding slab and for the differences in base material composition. Further analyses using three-dimensional finite element software are recommended.

Figure 3.9. Surface strain peak measurements, passes 1 through 5.

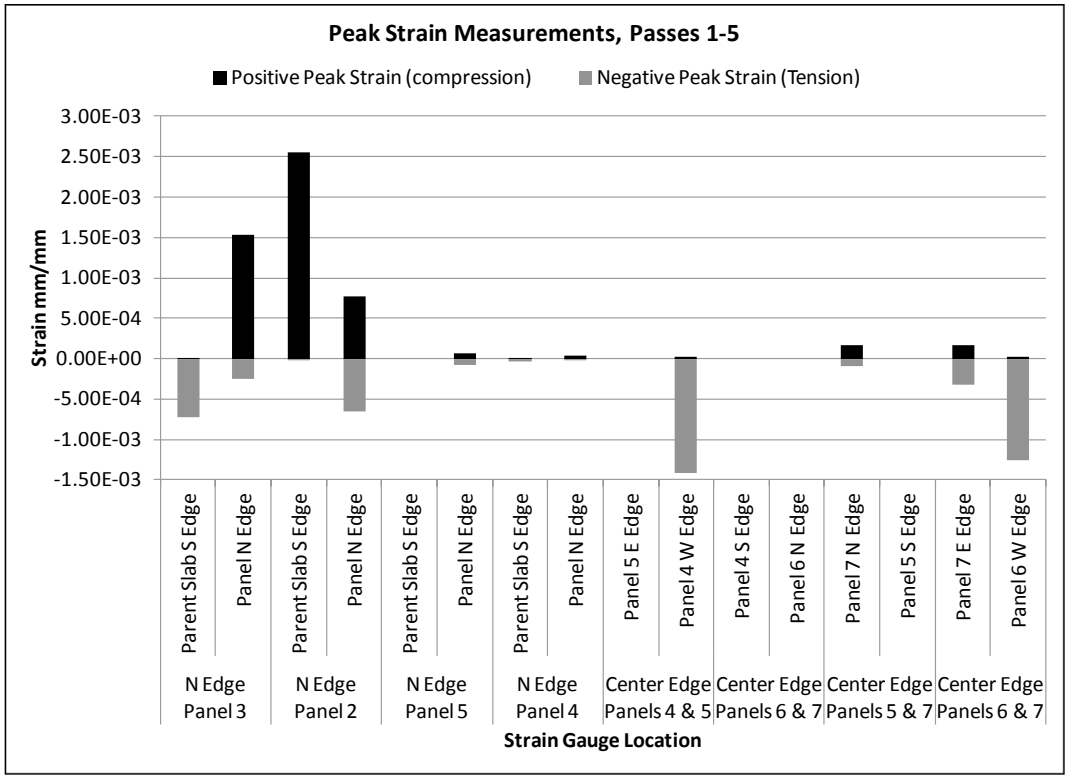

3.5 Benefits of precast panels relative to other repair methods previously tested

The precast panel repair method was compared to previously tested rapid repair techniques developed by the U.S. military forces (Army, Navy, and Air Force) to conduct repairs up to full- and multiple-slab replacements

within a 4- to 6-hr window, as dictated by a return-to-service requirement. These repair techniques relied on using proprietary rapid-setting cementitious repair materials over compacted aggregate, expanding polyurethane foam, injected-foam backfill, or rapid-setting flowable fill. For comparison purposes each repair type was examined in terms of its performance, completion time, and cost. This was accomplished by extracting data from more than 100 airfield repairs that had been conducted during the past several years. Time data were recorded for each task associated with more than 50 of these repairs. Additional details of the repair procedures are provided by Priddy et al. (2007b; 2008; 2010a, b), Priddy and Newman (2010), and Priddy (2011).

Completion time data were reviewed to determine the average time required to complete each required repair task. Tasks included repair area preparation (including distressed area removal), placement of backfill (base) material, and placement of the wearing surface (rapid-setting cap or panel) including curing time. Table 3.1 presents the average repair time and the average total repair volume for each repair type. Table 3.2 presents a breakdown of times required for each precast panel task.

Because the repair sizes and material volumes varied between repairs, the times required to complete a small repair the size of the single-panel repair (3.0 m by 3.0 m by 355 mm) were estimated for each repair type. This included a 254-mm rapid-setting cap over 102 mm of foam or aggregate backfill or a 279-mm-thick precast panel over 76 mm of flowable fill. Average task rates for the rapid-setting repairs were calculated for each repair type by dividing the time to complete each repair task by the volume prepared (removed or placed) as recorded during field testing (e.g., backfill rate = m^3/hr). The average task rates were then used to estimate the total repair times for each repair type reported in Table 3.3 for the same-sized repair. The time for the precast panel repair was based on the total repair time for a single-panel repair.

The performance of the repairs reported in Table 3.3 was based upon average performance per repair type under simulated C-17 traffic. After 5,000 passes, the rapid-setting repairs over compacted aggregate and rapid-setting flowable fill did not fail, and trafficking was discontinued, so the true life of the repairs is unknown.

Table 3.1. Comparison of the precast panel method to other repair types.

Repair Type	No. Repairs	Average Total Repair Volume, m^3	Repair Area Preparation, hr	Backfilling, hr	Capping, hr	Total, hr
Rapid-Setting Cap/ Compacted Aggregate	3	8.2	1.3	1.2	2.7	5.2
Rapid-Setting Cap/Poured Foam	19	5.9	0.6	0.5	2.9	4
Rapid-Setting Cap/Injected Foam	8	5.8	1.2	0.2	2.4	3.8
Rapid-Setting Cap/Rapid-Setting Flowable Fill	20	4.1	0.7	0.2	2.4	3.3
Precast Panel/Rapid-Setting Flowable Fill	3	7.7	3.1	0.31	3.7	7.1[a]

[a] Times based on average of three different sized repairs. See Table 3.2 for individual timings.

Table 3.2. Precast panel installation timeline.

Task	Timing, min[a]		
	Single-panel Repair	Double-panel Repair	Quad-panel Repair
Mark perimeter of distressed slab	10	15	20
Saw-cutting operations	15	35	60
Dowel-slot cutting	25	50	50
Anchor drilling and installation	20	40	80
Attach crane rigging hardware	0[b]	0[b]	5
Lift distressed section	5	10	20
Dowel-slot excavation (existing PCC slab)	30	60	60
Flowable fill placement	10	20	25
Precast panel placement	5	10	30
Compaction (if needed)	5	10	20
Removal of flowable fill from dowel slots	5	5	10
Placement of joint and dowel sealant	30	55	90
Dowel-slot finishing	5	10	20
Curing	120	120	120
Total repair time, min	285	440	610
Total repair time, hr	4.75	7.33	10.17

[a] Times rounded to the nearest 5-min interval.

[b] Task required less than 1 min to complete.

Table 3.3. Comparison of the precast panel method to other repairs.

Repair Type	Repair Detail	Passes to Failure, #	Time to Complete Repair, hr	Estimated Material Cost, U.S. $
Rapid-Setting Cap/Aggregate	250 mm cap 102 mm compacted aggregate	5,000+	3.5	$1,380
Rapid-Setting Cap/ Foam	254 mm cap 102 mm foam	1,000	3.2	$6,055
Rapid-Setting Cap/ Injected Foam	254 mm cap debris	1,000	3.8	$6,020
Rapid-Setting Cap/Flowable Fill	254 mm cap 102 mm flowable fill	5,000+	3.4	$1,865
Precast Panel/ Flowable Fill	279 mm panel 76 mm flowable fill	5,000+	4.8[a]	$2,500
Traditional PCC (full-depth)	356 mm PCC	5,000+	28 days	$555

[a] Based on time to complete a single-panel repair.

Costs reported in Table 3.3 were based on the materials required to conduct a 3.0-m by 3.0-m by 355-m repair. Material costs were based on 2011 to 2012 pricing for materials. No costs were included for labor or equipment for any repair, as these are not a contributing decision factor for a military pavement repair team. Labor and equipment costs will increase the cost of the repair significantly (as high as twice the material costs alone) for non-military repairs. As can be seen in Table 3.3, the least expensive repair was the traditional cast-in-place PCC; however, rapid return to traffic was not possible with this method.

Combining cost, performance, and speed, the precast slab was the third-best option of those considered for rapid repair, following the rapid-setting cap over either compacted aggregate or rapid-setting flowable fill. Based upon performance and timing, this method may provide an additional repair technique suitable for temporary or permanent pavement repair of military airfields.

Additional analyses should be conducted to determine whether costs can be reduced through minor changes such as using a less expensive repair material for filling the dowel slots. The cost of the precast panels could also be reduced if panels were prepared in a factory, benefiting from bulk material discounts, as the cost of precast panel technology has declined steadily in recent years (Tayabji et al. 2013). Additional field tests are also recommended to determine whether the performance of the panels can be

improved by making changes to the design of the doweled joint and preventing the excess grout for the dowels from entering into the joints.

Finally, additional field trials can also help to determine whether efficiencies may be obtained in performance of the individual precast repair tasks. For the reported effort, repair tasks were divided over several days, and the times required for each repair task were summed for each repair. Efficiencies in time may be gained in working from beginning to end on a single repair and through work task and personnel assignment refinements. Additionally, while the crew was experienced in general pavement construction and repair, crew members were not experienced in precast panel placement, and more experience with the process could improve repair timelines. Until such tests are completed and refinements made, only single-panel repairs may be capable of being completed within the targeted 4- to 6-hr time frame with double- and quad-panel repairs typically requiring 8 to 10 hr to complete.

3.6 Summary and conclusions

Three full-depth repairs were constructed using a newly developed precast panel system, and the performance of the repairs under simulated aircraft traffic was evaluated. Repairs required removal and replacement of a 355-mm-thick PCC pavement with rapid-setting flowable fill and precast PCC panels. The performance, cost, and time of the repair method were compared to data from historical tests on other repair materials and procedures. The following conclusions were reached from the results of the testing:

- The precast panel repair system met the temporary repair requirement of withstanding at least 3,700 passes prior to failure. All the repairs were capable of withstanding at least 5,000 passes, as predicted, using traditional PCC design methodologies, thereby meeting the requirement for permanent repairs. The double-panel repair withstood 10,000 passes prior to failing.
- Only the single-panel repair may be conducted in less than 6 hr; larger repairs may require 8 to 10 hr to complete.
- Repairs failed primarily due to cracking and spalling along the transverse edges of the panels. Cracking and spalling occurred in both the repair panel and the parent slab, including the PCC sections between the dowel slots. The presence of dowel-slot grout and flowable fill within the joints surrounding the panels most likely contributed to the failure of the transverse joints.

- Cracking in the surrounding parent slabs was due to overcutting during the preparation of the repair areas for lift-out of the damaged pavement. To control cracking in the parent slabs for long-term use, extending the saw cuts the remaining distance to the joint in the parent slab may be necessary.
- The precast panel repair method shows potential application for airfield PCC repairs where rapid-setting materials or other repair methods are not available.
- Further optimization of the panel design and installation techniques can improve upon the performance and timing data presented in this paper. Additional timed trials of multiple repairs (timed from start to finish) are required to validate that this repair procedure can be accomplished within the target repair window.

3.7 Recommendations

Further research into the most efficient doweling requirement and installation procedure is recommended to reduce costs, improve performance, and reduce installation timing. Based on the distresses identified in and around the dowel slots, further investigation into the load transfer mechanisms and load transfer characteristics of the precast panels is recommended. Some items to explore include increasing the dowel diameter and length and selecting alternative dowel grouts. Trials conducted without dowel-slot grout in the joints are recommended to determine appropriate LTE and differential deflection thresholds for the joints. Additionally, the support system beneath the quad-panel repair requires further investigation, as it changes the support stiffness beneath the interior corners of the repair. Finally, a further program of field tests is proposed to improve the panel design and constructability. Experiences gained from the reported and future work will be used to improve precast panel design procedures, including panel fabrication and placement methods for conducting airfield pavement repairs.

3.8 Acknowledgements

The tests described and the resulting data presented herein, unless otherwise noted, were obtained from research sponsored by the U.S. Air Force Civil Engineer Center and performed at the U.S. Army Engineer Research and Development Center. Permission to publish this information was granted by the Director, Geotechnical and Structures Laboratory.

4 Load Transfer Characteristics of Precast Portland Cement Concrete Panels for Airfield Pavement Repairs

L.P. Priddy[1], D.W. Pittman[2], and G.W. Flintsch[3]

Reprinted by permission of TRB, August 2014. Citation: Priddy, L.P., Pittman, D.W., and Flintsch, G.W. (2014). Load Transfer Characteristics of Precast Portland Cement Concrete Panels for Airfield Pavement Repairs, *Transportation Research Record* (in press), TRB of the National Academies. TRB does not endorse any product, method, practice, or policy presented.

Abstract: Portland cement concrete (PCC) pavement repair technologies using precast PCC panels have been investigated for decades and recently have gained acceptance and increased use in the U.S. for highway pavements but only limited use for airfields. The recent field testing of a new airfield precast panel repair system indicated that precast panels were suitable for expedient airfield pavement repairs, withstanding between 5,000 and 10,000 passes of C-17 aircraft traffic. Failure of the panels was due to spalling of the transverse doweled joints. The purpose of this paper is to discuss the load transfer effectiveness, or load transfer efficiencies (LTE), of the panel repairs. A heavy weight deflectometer (HWD) was used to collect deflection data before, during, and after trafficking to calculate precast panel LTE based on deflections (LTE_δ) or stress (LT). The LTE values were then evaluated to determine whether current measures of effectiveness were suitable for precast panel repairs. Based on the results of this investigation, few of the joints provided the current military airfield design assumption of 25% LT, but the majority of the transverse joints exceeded the proposed LTE_δ threshold of 70% even after failure of the transverse joints. It was recommended that additional field tests be conducted without the use of rapid-setting grout in the joints prior to making recommendations on thresholds.

[1]Research Civil Engineer, U.S. Army Engineer Research and Development Center, Vicksburg, MS 39180. Email:lucy.p.priddy@usace.army.mil.
[2]Director, Geotechnical and Structures Laboratory, U.S. Army Engineer Research and Development Center, Vicksburg, MS 39180. Email:david.w.pittman@usace.army.mil.
[3] Director, Center for Sustainable Transportation Infrastructure, Virginia Tech Transportation Institute and Professor, The Charles Via, Jr., Department of Civil and Environmental Engineering, Virginia Tech, Blacksburg, VA 24061. Email: flintsch@vt.edu.

4.1 Introduction

Both the identification and validation of expedient portland cement concrete (PCC) repair technologies, including precast PCC panels, have been the focus of the pavements research community for decades. Because the panel is fully cured and has gained full strength prior to its use, this repaired surface may be trafficked immediately, thus eliminating the need for long curing durations required for conventional PCC repairs. Several syntheses of precast panel technologies investigated over the past 50 years have recently been prepared (Olidis et al. 2009; Tayabji et al. 2013; Priddy et al. 2013a) and show that various precast panel technologies are suitable for both highway and airfield repair applications.

While the majority of precast panel research in the U.S. has focused on highway repair applications, precast technology has also been applied to airfield repairs. Since 2000, U.S. investigations have been conducted at La Guardia International Airport, New York, NY, and Dulles International Airport, Washington, DC. Summaries of these and additional airfield applications are documented (Olidis et al. 2009; Bly et al. 2013) and are not repeated here. In 2007, the U.S. Air Force developed a system for airfield precast panel repairs intended for use in deployed, contingency military operational environments where conventional pavement repairs using traditional PCC could not be accomplished to meet expedient repair requirements of 4 to 6 hr (Ashtiani et al. 2010). In 2011, this system was redesigned to allow for either single- or multiple-panel repairs, and experiments were conducted to determine the suitability of the panels for expedient airfield applications. The primary driver for the field experiments replicated construction techniques and repetitive aircraft loading that would be experienced in a military contingency environment. The results indicated that the trafficking of the panels could commence 4 to 10 hr from the initiation of repair activities, depending on repair size; and the pavement repairs could support between 5,000 and 10,000 passes of C-17 gear load traffic before failure and may be suitable for contingency repair scenarios (Priddy et al. 2013b). Failures of the pavement repairs were due to severe spalling and cracking of the transverse doweled joints. During field testing, data were collected to determine what benefit the doweled joints provided for load transfer between the panel and the parent PCC.

The specific objectives of this study were as follows:

- Evaluate the joint efficiency/load transfer efficiency of joints in precast panel repairs using nondestructive testing techniques,
- Analyze the load transfer characteristics of the joints from these data, and
- Ascertain whether load transfer efficiency or other thresholds could be determined from the performance of the precast concrete panel repairs.

4.2 Description of the precast panel test section

In August 2011, a 120-ft-long and 60-ft-wide PCC test section was designed and constructed at the U.S. Army Engineer Research and Development Center in Vicksburg, MS, to support 50,000 passes of a C-17 aircraft. Individual slab dimensions were 20 ft by 20 ft by 14 in. The PCC was constructed on a 6-in.-thick, well-graded limestone base over a sandy, low-plasticity clay subgrade. The PCC had an average 28-day compressive strength of 7,240 lb/in.^{2} and an average flexural strength of 940 lb/in.^{2} Plate-bearing tests conducted on top of the limestone base indicated an effective modulus of subgrade reaction, k, of 276 lb/in.^{2}/in.

Concurrently, precast PCC panels were fabricated with an average 28-day compressive strength of 5,710 lb/in.^{2} The PCC panels had individual approximate dimensions of 10 ft by 10 ft by 11 in., each weighing approximately 14,000 lb. The panel thickness and dimensions were limited by the lifting equipment that would be available on military installations. The standard panel was designed to be used alone for single-panel repairs or in combination with other panels to complete multiple-panel repairs. The terminal panel was designed for use with the standard panel to connect panels to complete a larger repair. Each panel was reinforced minimally to reduce the occurrence of cracking during lifting and storage of the panels, not to reduce the panel thickness for traffic loading purposes. Schematics of the panels are provided in Figure 4.1; detailed design and fabrication information can be found in the literature (Bly et al. 2013).

After constructing the panels and the test section, three repairs were made in November 2011, including a single-panel repair replacing one-quarter of a slab, a double-panel repair replacing one-half of a slab, and a quadruple-panel repair replacing a full slab. The general process is presented herein; detailed descriptions may be found in the Bly et al. (2013) report. The

repaired areas were prepared by saw cutting the parent PCC slabs using a walk-behind concrete saw; additional saw cuts were then made perpendicular to the transverse joints to establish the vertical edges of the dowel slots. Each saw-cut slot was 3 in. wide and approximately 6.5 in. deep. The parent PCC was removed in 10-ft by 10-ft sections by installing concrete expansion anchors for lifting eyes and removing the saw-cut sections with a mobile crane. Jackhammers were then used to remove the concrete between dowel-slot cuts. Following this step, approximately 3 in. of non-excavatable, rapid-setting flowable fill was placed directly on top of the base course to provide a seating material for the panels and to fill the difference in thickness between the PCC slab and the panels. The panels were then seated upon the flowable fill and were prevented from sinking into the fill by using temporary steel bridge plates anchored to the top surface of the panels.

Figure 4.1. Precast panel schematics.

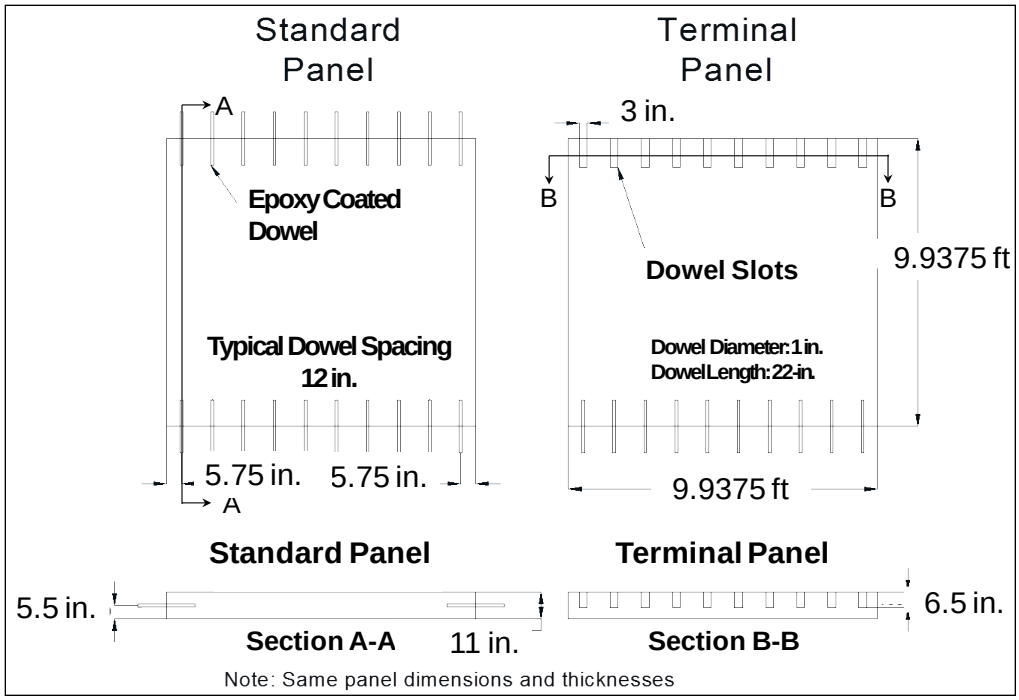

During installation of the panels, the flowable fill was pressed into the joints surrounding the panels up to the level of the dowel slots. Any flowable fill that entered the dowel slots was removed; however, to simulate likely field installation practices, no attempts were made to remove the flowable fill in the joints, which were approximately 0.375 to 0.5 in. wide. The dowel slots were then filled with a proprietary, rapid-setting grout capable of achieving at least 3,000 psi compressive strength within

3 hr of placement with a maximum compressive strength of 5,000 psi. In keeping with the expedient nature of the repair and to simulate likely repair practices, no attempt was made to prevent the grout from escaping the slots, and it was allowed to completely fill the joints. After the grout cured, the temporary bridge plates were removed, the dowel-filled joints were shallowly saw cut to accommodate a joint sealant material, and the joints were sealed. Figure 4.2 highlights the general steps required in the repair process.

4.3 Accelerated pavement testing

4.3.1 Description of trafficking procedure

The precast panels were trafficked in May 2012 with a multi-wheel load cart simulating a C-17 aircraft landing gear (Figure 4.3a). The delay between placement and testing was due to availability of the C-17 load cart. The ambient temperatures during placement were 56 to 70°F (November 2011). When trafficking commenced, the ambient temperatures were 62 to 87°F (May 2012). The load cart configuration represented one-half of a fully loaded C-17 gear, as shown in Figure 4.3b. The gear was composed of 50-in.-diam, 21-in.-wide, 20-ply tires with tire pressures of approximately 144 psi. Traffic loads were applied in a normally distributed pattern, as shown in Figure 4.3c. During trafficking, the centerline (CL) of the load cart traveled down and back (two passes) in each lane (numbered 1-14) until the pattern consisting of 28 passes (25 coverages) was completed. Patterns were repeated until repairs failed.

The panels were considered failed when any of the following distresses were manifested in the panels: (1) joint or corner spalls deeper than 3 in. or wider than 15 in., (2) shattered slabs with high-severity cracks, (3) settlement and/or faulting of the panels or slabs in excess of 3 in., or (4) any distress posing high tire damage potential or high foreign object damage (FOD) potential. These failure criteria may seem excessive or dangerous compared to those used for civilian airfield operations; however, they are based on probable aircraft tire tolerances for the C-17 operating in a contingency environment.

Figure 4.2. Repair procedure: (a) saw cutting the repair area and dowel slots, (b) installing lifting eyes to concrete expansion anchors, (c) removing parent PCC, (d) preparing dowel slots, (e) prepared repair area, (f) screeding flowable fill bedding material, (g) lowering panel into repair area, and (h) sealing dowel slots with rapid-setting grout.

Figure 4.3. (a) C-17 load cart, (b) gear configuration, and (c) C-17 traffic pattern.

(a)

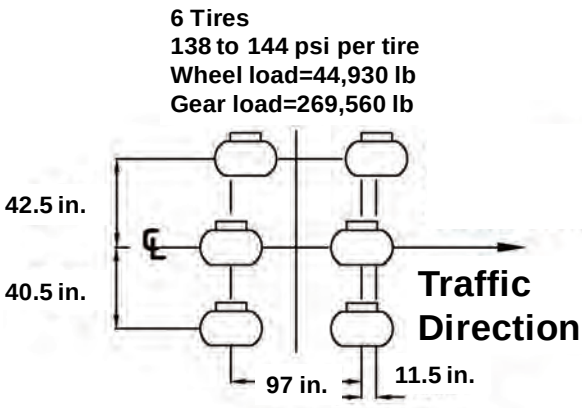

(b)

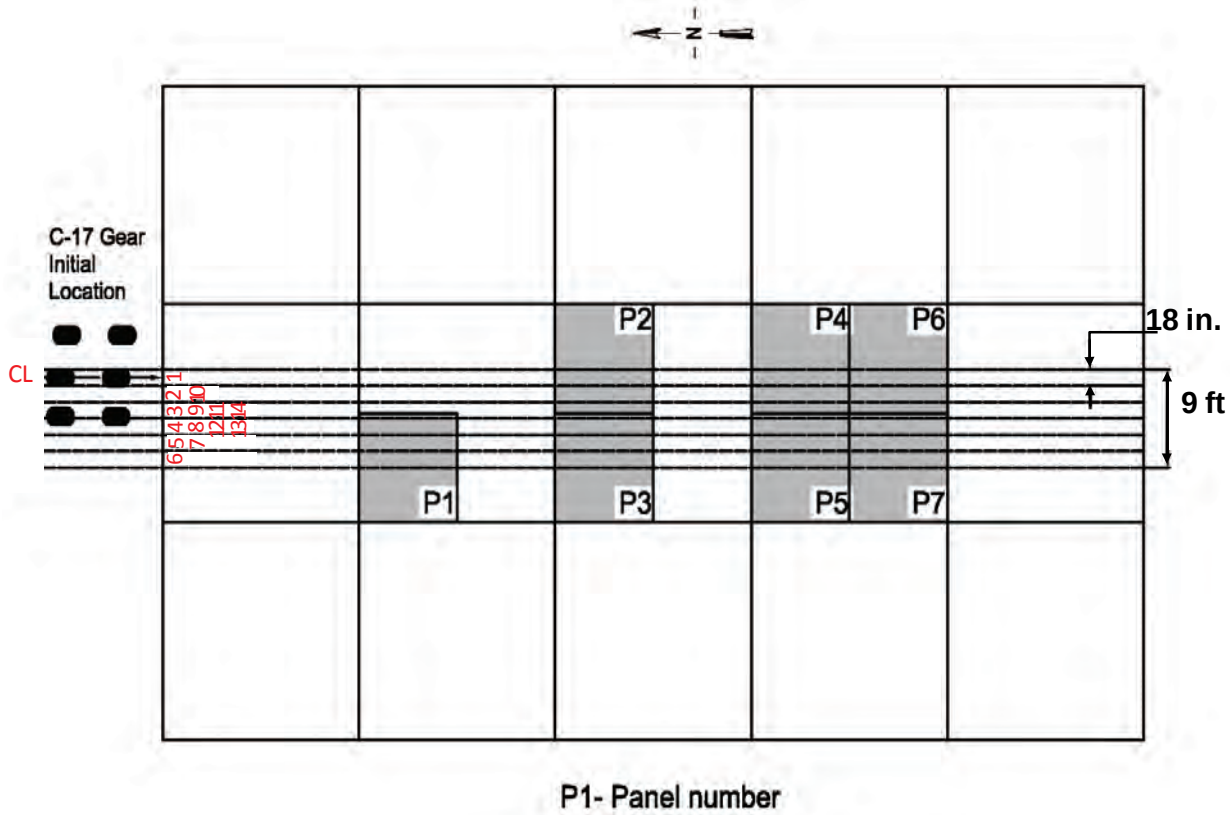

P1- Panel number

(c)

4.3.2 Results of traffic testing

The single-panel repair, double-panel repair, and quadruple-panel repair supported 5,600, 10,000 and 7,100 passes, respectively, prior to failing. Additional details of the traffic testing results are provided in the literature (Priddy et al. 2013b). The transverse joints of all three repairs deteriorated rapidly after approximately 2,000 passes on both the panel and parent slab sides of the joints, as shown in Figure 4.4, while the interior portions of most of the panels remained in relatively good condition with only low-severity or hairline cracks. Spalling most likely was the result of a combination of high traffic loads, stresses caused by dowel bending, and restriction of the slabs caused by the incompressible grout within the joints. The results of the trafficking suggested that the performance of the transverse joint between the panel and the parent PCC should be investigated further to understand the behavior of these joints under loading and to improve the design of the repair system and the load transfer mechanisms in order to increase the life of the pavement repair.

Figure 4.4. Examples of deterioration of transverse joints: (a) Panel 1 N joint, (b) Panel 2 S joint, (c) Panels 2 and 3 N joints, and (d) Panels 6 and 7 S joints.

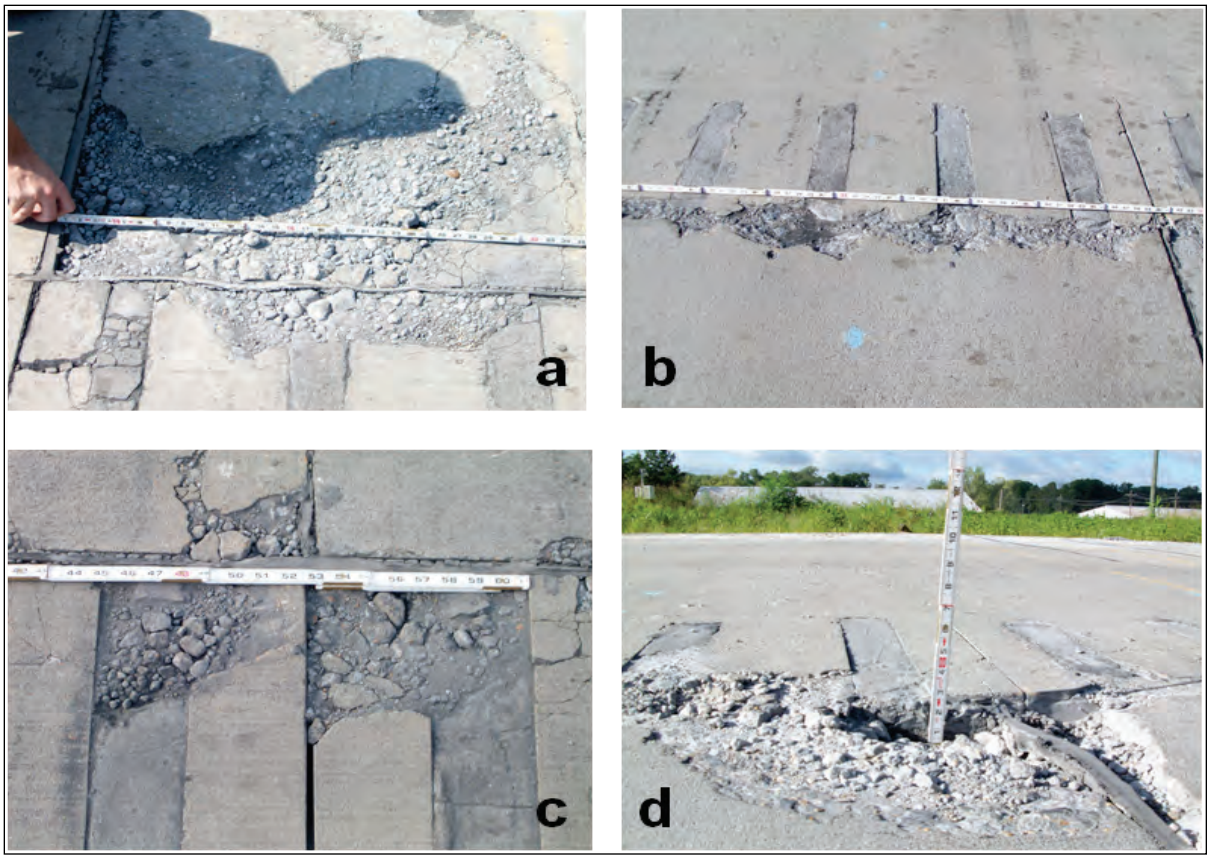

4.4 Measurement of load transfer

4.4.1 Load transfer mechanisms

Ideally, when a load passes over a PCC joint, the slabs on either side of a joint will deflect in unison because of load transfer. However, both sides do not typically deflect equally due to the width of the joint opening, performance of the load transfer devices (dowels), differences in slab thicknesses, and uniformity of support provided by the base. Failure to properly achieve adequate load transfer at the joints can result in a shortened repair life; if the repair joints cannot transfer load, then higher stresses will be generated under the loaded slab (or panel) edges and corners, resulting in distresses such as faulting, corner breaks, mid-slab cracking, and spalling along the joint. To evaluate the effectiveness of load transfer at a joint, the load transfer efficiency (LTE), sometimes referred to as the joint efficiency, is determined from direct measurements of the slabs' vertical movement during loading and has been investigated by many researchers over the years (Colley and Humphrey 1967; Ioannides and Korovesis 1990, 1992; Frabizzio and Buch 1999; Guo 2003; Swati et al. 2009; Ashish et al. 2011; AASHTO 1993).

To evaluate the performance of the joints during the trafficking portion of this study, the LTEs of four different precast panel joint types were tested using a heavy weight deflectometer (HWD):

- Doweled transverse joints between a parent slab and a repair panel (doweled slab-to-panel),
- Doweled transverse joint between connected repair panels (doweled panel-to-panel),
- Undoweled longitudinal joints between a repair panel and a parent slab (undoweled slab-to-panel), and
- Undoweled longitudinal joint between repair panels (undoweled panel-to-panel).

For the doweled slab-to-panel joints, the load transfer was provided by dowels precast in the panels on the transverse joints. For the longitudinal joints, minimal load transfer was expected because no dowel bars were used and both the panel and the parent slab had smooth faces. However, direct contact of the panels with themselves or with the parent slab caused by closure of the joint due to higher ambient temperatures would result in higher LTE values than would have been measured if the panels had been

tested immediately after placement. Additional means of load transfer might also have been provided by the presence of rapid-setting grout and flowable fill in the joints and/or from the foundation support.

4.4.2 Load transfer efficiency (LTE)

LTE expresses the degree of load transferred from the loaded slab to the unloaded slab and can be estimated in terms of transferred stresses (LT), strains (LTE_{ε}), or deflections (LTE_{δ}). Most often it is measured in the field using deflections obtained from a joint load test using an HWD (for airfield pavements) to determine the LTE_{δ}. The HWD uses heavy weights dropped onto a padded, 11.8-in.-diam plate to measure the pavement's response (deflections) to an applied vertical dynamic load (up to 50,000 lb). In the joint load test, the HWD load is applied at one side of a joint close to the edge of a slab (or panel), and the deflections are measured on both sides of the joint by seven geophones located at a spacing of 12 in. For this study, HWD tests were conducted on both the longitudinal and transverse joints of precast panel repairs before trafficking, during trafficking at selected pass levels, and after failure using the testing layout shown in Figure 4.5. The HWD was also used to conduct center slab and panel tests (also shown in Figure 4.5). The joint testing regime was limited to one side of the joint due to a short trafficking window caused by the testing schedule. The level of HWD testing conducted in this study was less than what might be expected for a robust load transfer study. However, a primary driver for this study was replicating a realistic contingency environment, including expedient repair and repetitive loading by aircraft that precluded an extensive set of data collection.

The minimum LTE_{δ} threshold suggested for precast panel performance for transverse joints in highway pavements is 70% (Tayabji et al. 2013), and this threshold has also been suggested for airfield precast panel repairs (Ashtiani et al. 2010). Currently there is no LTE_{δ} threshold for precast panel longitudinal joints. For regular airfield PCC pavements, there is no LTE_{δ} threshold for any joint; however, the load transfer assumption used for design purposes is stress-based (LT) and assumes that 25% of an applied load is transferred across a joint for all joint types, with the exception of butt and thickened joints (UFC 2001c). For this reason, both deflection-based (LTE_{δ}) and stress-based (LT) load transfer were analyzed.

Figure 4.5. Location of HWD tests.

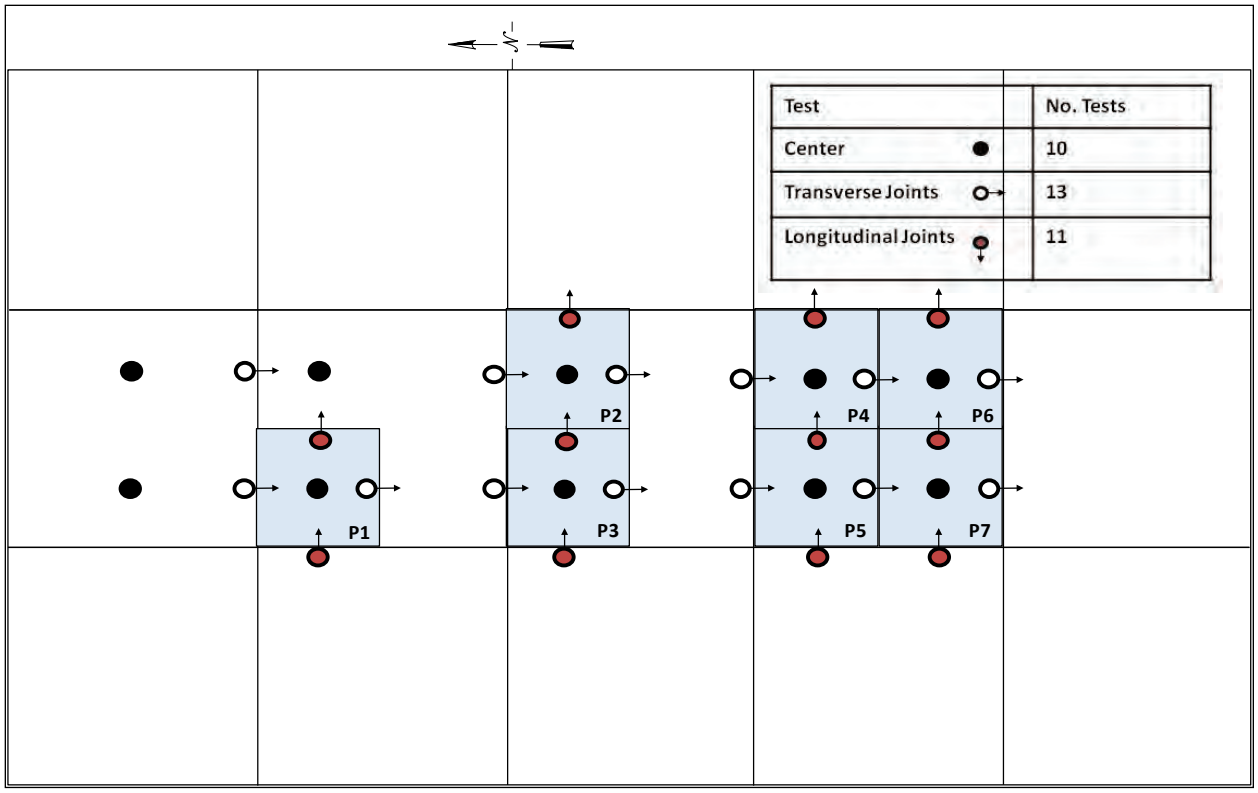

4.5 Analyses of load transfer test data

4.5.1 Determination of deflection-based load transfer efficiency (LTE_δ)

The LTE_δ for the panel joints was calculated using Equation 4.1 (Ioannides and Korovesis 1990) at various intervals during trafficking. Typical deflections and mean values for the various joints just prior to trafficking are presented in Table 4.1. The LTE_δ relationship is usually used for slabs of equal thickness. As mentioned previously, testing was conducted with the load plate on only one side of each joint; thus, comparisons between the transfer of load across the same joint from thicker to thinner pavement (and vice versa) could not be made. Therefore, no corrections for differences in pavement thickness were applied for the calculations. Very low differential deflections ($\delta_l - \delta_u$) and high initial LTE_δ calculations are shown in Table 4.1 for the doweled joints, indicating good load transfer prior to trafficking. As might be expected, higher differential deflections and lower initial LTE_δ calculations were found for the undoweled joints.

$$LTE_\delta = \delta_u / \delta_l \times 100 \quad (4.1)$$

where:

δ_u = deflection of the unloaded side of the joint
δ_l = deflection of the loaded side of the joint

Table 4.1. Summary of initial deflection and LTE_δ results.

	Before Trafficking: 0 passes			
	LTE_δ	δ_l	δ_u	$\delta_l - \delta_u$
Joint Type	%	mils	mils	mils
Transverse Doweled Joint, Panel to Panel				
Mean	93	18.9	17.5	1.4
Max	95	18.2	17.4	0.8
Min	90	19.5	17.6	1.9
No. Tests	2			
Transverse Doweled Joint, Panel to Slab				
Mean	94	16.2	15.3	0.9
Max	97	15.2	14.7	0.5
Min	90	16.4	14.7	1.7
No. Tests	5			
Transverse Doweled Joint, Slab to Panel				
Mean	92	18.4	17	1.4
Max	95	18	17.2	0.8
Min	91	20.4	18.5	1.9
No. Tests	5			
Longitudinal Undoweled Joint, Panel to Panel				
Mean	71	21	14.9	6.1
Max	82	18.5	15.2	3.3
Min	64	22.5	14.3	8.2
No. Tests	3			
Longitudinal Undoweled Joint, Panel to Slab				
Mean	71	20.7	14.7	6
Max	95	18.2	17.3	0.9
Min	44	25.5	11.2	14.3
No. Tests	4			
Longitudinal Undoweled Joint, Slab to Panel				
Mean	70	21.2	14.8	6.4
Max	88	20.9	18.3	2.6
Min	56	23.7	13.3	10.4
No. of Tests	4			

4.5.2 Influence of pavement temperature on LTE_{δ}

To limit the influence of temperature on the LTE_{δ} as suggested by other researchers (Foxworthy 1985; Korovesis 1990; Frabizzio and Buch 1999; UFC 2001c), measurements were made in the morning when temperatures were lowest. Higher pavement temperatures typically result in higher LTE_{δ} due to increased frictional resistance between the PCC faces caused by both the downward turning of the slab edges and thermal expansion of the slabs, forcing the joint opening to decrease or close altogether. To measure the effect of temperature on the LTE_{δ} of the precast panel joints, HWD data was collected the same day with an average surface temperature increase of 16°F for the double-panel repair shown in Figure 4.6. The measurements were taken after 8,400 passes and after 10,000 passes when the repair was considered failed due to spalling along the transverse joints.

Figure 4.6. Effect of pavement temperature on load transfer efficiency of panels.

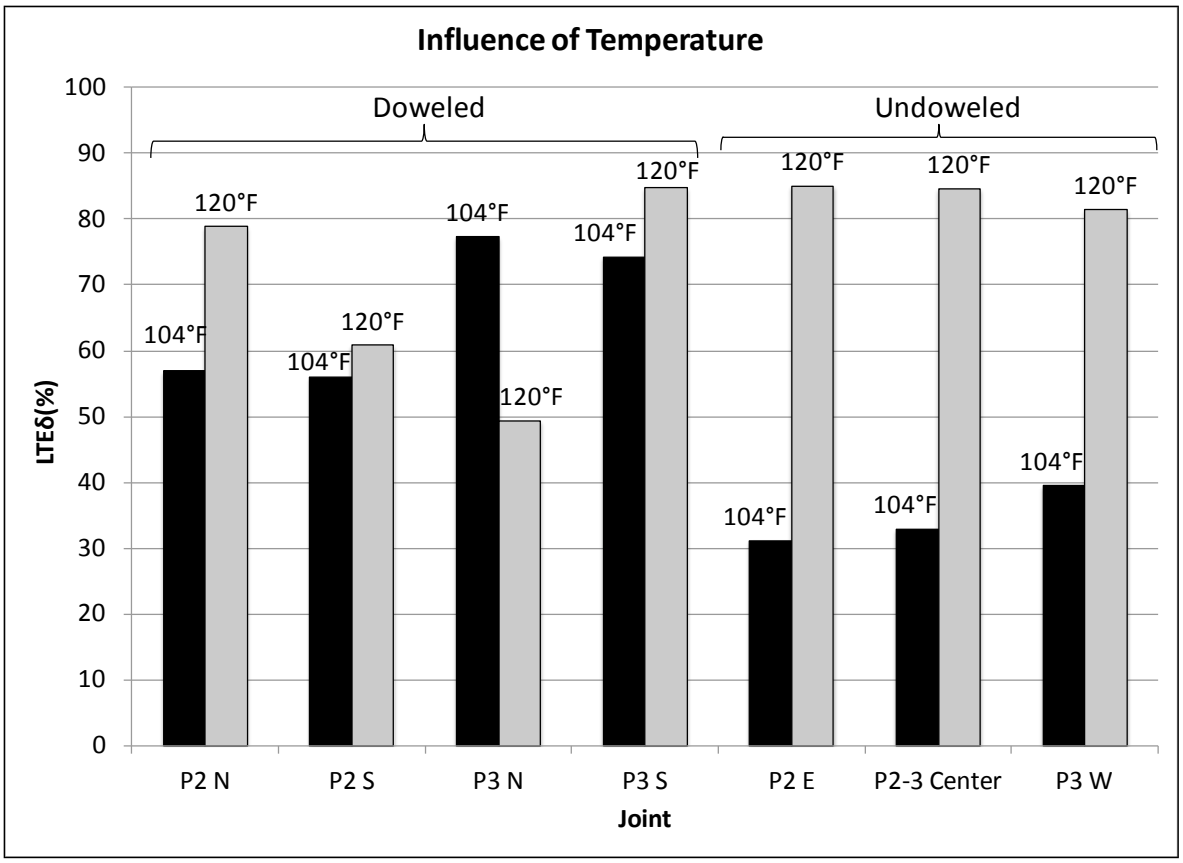

Two important observations can be made from the data. First, the 16°F increase in temperature resulted in the LTE_{δ} increasing by an average 92%. The most dramatic increase in LTE_{δ} due to the temperature change was seen at the undoweled longitudinal joints, which increased an average

146%, while the transverse doweled joints increased only 37%. This difference in performance of the doweled versus undoweled joints is not unexpected, as the LTE_{δ} of undoweled joints depends upon the joint (crack) width, which can open dramatically with small decreases in pavement temperature, thereby reducing contact at the vertical interface. The doweled joints provide more latitude for joint movement while still providing load transfer via the stiffness and shear strength of the dowel itself. Second, regardless of joint type (doweled or undoweled), the LTE_{δ} data at high temperatures were tightly grouped around an average value of 82%,with a range of only 6 percentage points for all joint types. Conversely, at the lower temperature, while the average LTE_{δ} dropped about 35 percentage points for all joint types, the range of LTE_{δ} values for all joints was 43 percentage points. Interestingly, while the doweled joints had an overall average LTE_{δ} of 47% at the lower temperature with a range of 25 percentage points, the undoweled joints had an overall average LTE_{δ} of 34% but a range of only 9 percentage points. The lower variance in LTE_{δ} values at the lower temperatures for undoweled joints versus doweled joints is expected, as the load transfer of undoweled joints tends to zero with lower pavement temperatures. The variance also would tend to zero.

4.5.3 Calculation of stress-based load transfer (*LT*)

The stress-based load transfer (*LT*) was also calculated for each joint, a process requiring multiple steps. First, a normalized area (*AREA*) was calculated using center-panel test data, providing characteristic deflection basins for each panel or slab taken at the same intervals as the joint tests. *AREA* was calculated using Equation 4.2 (Hoffman and Thompson 1981). The next step was to calculate the LTE_{δ} for each joint test. The radius of relative stiffness for the slabs and panels, or *l*, was then computed with the midpanel HWD deflection data using the relationship between *l* and *AREA* presented in Equation 4.3 (Kim 2001). The values of *l* were similar to those computed using PCC theory. The next step was to normalize *l* using the radius (a) of the HWD load plate (a = 5.9 in.) to form the *a*/*l* ratio.

$$AREA = \frac{S}{2D_0}[D_0 + 2(D_1 + D_2 + \ldots + D_{n-1}) + D_n] \tag{4.2}$$

where:

$AREA$ = normalized deflection area (in.)

S = spacing between sensors
D_i = deflection at sensor i = 1, 2, 3, etc. (in.)
n = number of sensors used in the calculation, less one.

$$l = 0.0007(AREA)^3 - 0.0566(AREA)^2 + 2.2285(AREA) - 14.792 \quad (4.3)$$

where:

$AREA$ = normalized deflection area (in.)

The a/l ratios were calculated for each pass interval using the appropriate l based on the loaded pavement (parent PCC or panel) for all joints. Using the LTE_δ values, the average LT was determined by using a set of curves relating LTE_δ to LT as a function of the a/l ratios through interpolation of the original results (Ioannides and Korovesis 1990; Hammons et al. 1995; Hammons and Ioannides 1997). Figure 4.7 shows the relationship between LTE_δ and LT for the pavements in this study for a range of a/l ratios.

Figure 4.7. Relationship between LT and LTE_δ for the precast panel repairs.

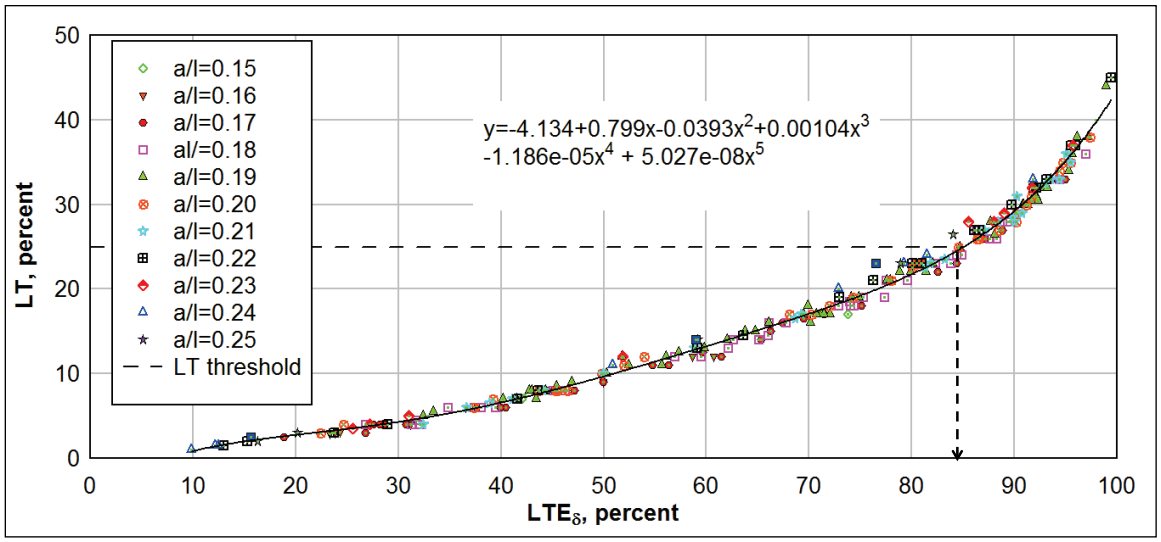

4.6 Results

A summary of the load transfer values for each joint type and the deflections of the loaded and unloaded slabs with increasing passes of C-17 traffic is presented in Table 4.2 and illustrated in Figure 4.8a (LTE_δ) and b (LT). Several observations can be made from these data.

Table 4.2. Summary of deflections, LTE_δ, and LT results.

Joint Type	Before Trafficking: 0 Passes					After 5,600 Passes					After 8,400 Passes				
	δ_l	δ_u	δ_l-δ_u	LTE_δ	LT	δ_l	δ_u	δ_l-δ_u	LTE_δ	LT	δ_l	δ_u	δ_l-δ_u	LTE_δ	LT
	mils	mils	mils	%	%	mils	mils	mils	%	%	mils	mils	mils	%	%
Transverse Doweled Joint, Panel to Panel															
Mean	18.9	17.5	1.4	93	33	41.1	34.4	6.7	83	25	39.1	31.9	7.2	82[a]	25[a]
Max	18.2	17.4	0.8	95	35	40.9	34.4	6.5	84	27	41	34.4	6.6	84[a]	27[a]
Min	19.5	17.6	1.9	90	31	41.2	33.5	7.7	81	24	37.2	29.5	7.7	79[a]	23[a]
Tests	2					2					2[a]				
Transverse Doweled Joint, Panel to Slab															
Mean	16.2	15.3	0.9	94	36	33	22	11	67	19	38.6	26	12.6	68	15
Max	15.2	14.7	0.5	97	39	24.8	19	5.8	77	23	36.4	27.1	9.3	74	18
Min	16.4	14.7	1.7	90	33	42.4	25	17.4	59	14	40.8	24.8	16	61	12
Tests	5					5					2				
Transverse Doweled Joint, Slab to Panel															
Mean	18.4	17	1.4	92	31	39.1	29.1	10	75	20	39.9	25.3	14.6	64	16
Max	18	17.2	0.8	95	34	32.2	28.4	3.8	88	26	37.2	29.4	7.8	79	19
Min	20.4	18.5	1.9	91	30	48.7	30.5	18.2	63	14	42.7	21.1	21.6	50	12
Tests	5					5					2				
Longitudinal Undoweled Joint, Panel to Panel															
Mean	21	14.9	6.1	71	18	76.6	14.5	62.1	25	4	69.6	13.6	56	20[b]	3[b]
Max	18.5	15.2	3.3	82	23	40.1	20.1	20	50	9	53.4	17	36.4	32[b]	5[b]
Min	22.5	14.3	8.2	64	15	110.4	10.9	99.5	10	1	92.1	11.5	80.6	12[b]	2[b]
Tests	3					3					3[b]				
Longitudinal Undoweled Joint, Panel to Slab															
Mean	20.7	14.7	6	71	22	38.6	15.6	23	40	6	28.4	9.2	19.2	31	4
Max	18.2	17.3	0.9	95	36	38.6	15.6	23	40	6	28.4	9.2	19.2	31	4
Min	25.5	11.2	14.3	44	8	38.6	15.6	23	40	6	28.4	9.2	19.2	31	4
Tests	4					1					1				
Longitudinal Undoweled Joint, Slab to Panel															
Mean	21.2	14.8	6.4	70	18	27.3	15.3	12	57	11	31.5	13.5	18	41	6
Max	20.9	18.3	2.6	88	28	24	18.6	5.4	78	21	31.5	13.5	18	41	6
Min	23.7	13.3	10.4	56	12	29.8	11.1	18.7	37	6	31.5	13.5	18	41	6
Tests	4					5					1				

[a] Average Repair 3 data after 7,100 passes (Repair 3 failed prior to 8,400 passes).

[b] Average Repair 2 and Repair 3 data after 7,100 passes (Repair 3 failed prior to 8,400 passes).

Figure 4.8. (a) LTE_{δ} and (b) LT results of precast pavement repair joints with increasing traffic.

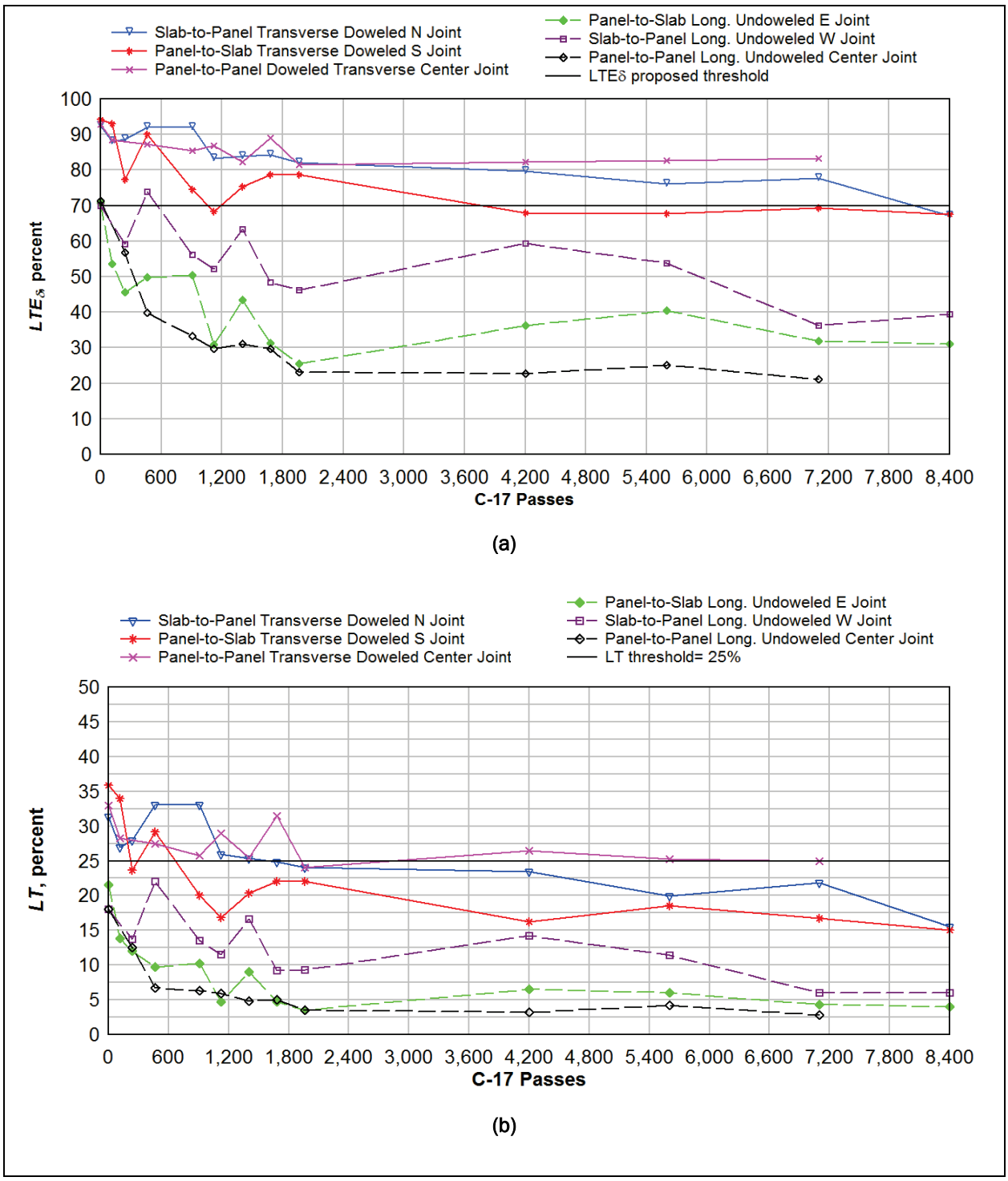

First, as traffic load repetitions increased, the load transfer of all the joint types decreased, as might be expected for regular jointed PCC pavements. Initially, all the undoweled joints had a mean LTE_{δ} of close to 71% and mean values of LT between 18 and 22% prior to the application of traffic.

This was likely due to the bonding of the panel to surrounding pavement (or adjacent panel) caused by the flowable fill and rapid-setting grout within the joints. This bond would be weakened by traffic applications and thermal movements of the slabs and panels, resulting in reduced load transfer for all joints. For the undoweled joints, the mean LTE_δ dropped to 20 to 41%, and the mean LT dropped to 3 to 6% after 8,400 passes. Similarly, the doweled joints' mean LTE_δ dropped from close to 93% to 64 to 82% after 8,400 passes, with a corresponding drop in LT from a mean close to 33% to 15 to 25%.

Second, as might be expected, the undoweled joints exhibited much lower load transfer characteristics than the doweled joints for all levels of trafficking. The difference in LTE_δ between doweled and undoweled joints increased with increased levels of trafficking but remained about the same in terms of LT (approximately 15%). One explanation for the relative stability of the difference in LT values for doweled versus undoweled joints versus the divergence in average values of LTE_δ for doweled versus undoweled joints for lower values of LTE_δ could be the relationship between LTE_δ and LT for given values of a/l. For larger values of LTE_δ, relatively small changes in LTE_δ result in relatively large changes in LT, and for smaller values of LTE_δ, the same change in LT corresponds to large changes in LTE_δ.

Finally, apparent differences were seen in the load transfer performance of the joints. The panel-to-slab connection, where the panel represents the loaded side of a load transfer test, exhibited the highest LT values for transverse doweled joints (36% LT) and longitudinal undoweled joints (22% LT) before trafficking began, followed by the panel-to-panel joints (33% and 18%, respectively) and slab-to-panel joints (31% and 18%, respectively). The LTE_δ values followed a similar pattern, with the exception that the longitudinal undoweled joints all exhibited LTE_δ values in a relatively tight grouping of 70% to 71%. This order of performance changed after traffic loading was applied. After 5,600 passes, the panel-to-panel connection was the superior performer for the transverse doweled joints (LT of 25%, LTE_δ of 83%) while the slab-to-panel connection performed best in the longitudinal undoweled joints (LT of 11%, LTE_δ of 57%). This pattern held true at the 8,400 pass level as well.

Table 4.2 shows that initially the differential deflections between the loaded and the unloaded sides of the joint for the doweled connections are

low (approximately 1 to 2 mils). After 5,600 passes, the mean difference increased to 7 to 11 mils, with the panel-to-panel doweled joint having the lowest mean deflection difference; and after 8,400 passes, the panel-to-panel doweled joint had a mean deflection difference of approximately 7 mils, compared to 13 and 15 for the other doweled joints. Differential deflections should be further investigated to determine threshold values that indicate compromised load transfer. Based on the failure of the doweled joints, a threshold of 5 mils may be appropriate for the transverse joints.

Overall, the best performing joint over the life of the test section was the transverse doweled panel-to-panel connection, which was the only joint that met or exceeded the 25% *LT* design assumption and 70% LTE_δ threshold proposed at the beginning of the study. Additionally, this joint had the lowest mean differential deflections throughout testing. None of the other joint types met or exceeded either criterion after 5,600 passes, although the panel-to-slab and slab-to-panel transverse doweled joints came close to matching the 70% LTE_δ threshold after 8,400 passes, at 69% and 67% LTE_δ, respectively. Specific discussions of the load transfer performance of various joints are provided in the following sections.

4.6.1 LTE_δ performance for east and west longitudinal undoweled joints

Differences were expected between the east (E) and west (W) undoweled longitudinal joints. As shown in Figure 4.3c, no traffic testing was conducted along the W joints and only the E joint of Panel 1. The data presented in Figure 4.8a show that the W joints exhibited higher LTE_δ than the E joints. During trafficking, the LTE_δ decreased for both the E and W joints. The E joint LTE_δ decreased rapidly after its initially high LTE_δ of 70%. As mentioned previously, this was most likely attributed to the bond caused by the flowable fill and dowel grout in the joints. Although the W joints did not directly receive traffic, the rocking of the panels under traffic and thermal effects might have broken the bond between the panels and the material in the joints, causing the LTE_δ to decrease despite not being trafficked directly.

4.6.2 LTE_δ performance for north and south transverse doweled joints

As can be seen in Figure 4.8a, both the north (N) and south (S) joints provided similar LTE_δ with initial values of 92 and 94%, respectively. As trafficking progressed, the LTE_δ of the S joints deteriorated more rapidly than

that of the N joints. At first glance, this suggests that the load is more efficiently transferred from the PCC slab to the panel than from the panel to the PCC slab. On average, none of the N and S transverse doweled joint LTE_δ values were below the proposed transverse LTE_δ threshold of 70%.

This good LTE_δ performance did not translate to good physical condition of the joint, however. In fact, the physical damage at these joints suggest that the load was not being transferred efficiently. The grout material in the joints might have also contributed to the failure of the joints by not allowing the panels and PCC slabs sufficient space to expand and contract properly during daily heating and cooling cycles, which in turn can cause damaging stress concentrations at the joints.

4.6.3 LTE_δ performance of the panel-to-panel transverse doweled and longitudinal undoweled joints

The transverse doweled panel-to-panel joints provided similar, if not slightly better, LTE_δ compared to the N and S slab-to-panel/panel-to-slab joints. The longitudinal undoweled joints between the panels (for the double- and quadruple-panel repairs) provided the lowest LTE_δ of any of the joints examined. For both of these cases, the center of the traffic lane was along this joint. Despite the low LTE_δ values, the condition of these joints remained relatively good during trafficking, with only minor spalling and cracking. This indicates that the current design for multiple-panel repairs, which does not require the use of dowels along the longitudinal panel-to-panel joints, may be adequate if traffic is applied only in the longitudinal direction.

4.6.4 Summary of the load transfer (*LT*) performance of the joints

Figure 4.8b presents the average load transfer for each panel joint with increasing pass levels. Similar trends between the LT and LTE_δ for the various joint types were experienced with increasing traffic. As can be seen in the figure, the LT values for the transverse joints were initially greater than 25% but dropped after approximately 500 to 1,000 passes for the panels. As mentioned before, the panel-to-panel joints were the only joints that provided approximately 25% LT after 2,000 passes.

From Figure 4.7, if the LT threshold is held at 25%, the corresponding LTE_δ is approximately 85% for the range of a/l values encountered in this study. A threshold of 85% is much higher than the proposed minimum

threshold of 70% for transverse joints. From Figure 4.8a, for an LTE_{δ} threshold of 85%, the S transverse doweled joints would have been considered unacceptable after approximately 250 passes, and the N and C transverse doweled joints would have been unacceptable after approximately 1,750 passes. This number of passes until failure is much lower than that allowed for a dominant mode of failure of the panels from mid-slab cracking; however, this level of passes does correspond with the occurrence and increase in severity of spalls on the transverse doweled joints as detailed in Priddy et al. (2013b). A threshold of 85% may be too high, particularly since these panels were intended for temporary repairs, and it is likely that the material in the joints contributed to the joint spalling as opposed to a loss in load transfer effectiveness.

As shown in Figure 4.8b, it is apparent that none of the longitudinal undoweled or transverse doweled joints, with the exception of the panel-to-panel transverse joints, met the 25% *LT* criteria for the full extent of trafficking. Two of the transverse doweled joints, the N and S slab-to-panel joints, exceeded the 25% load transfer requirement for 1,500 and 600 passes, respectively. None of the longitudinal undoweled joints met the 25% threshold, but these joints also received little damage under traffic, perhaps because the gear load never crossed perpendicular to the joint and, in some cases, never touched the longitudinal joint directly. Because these joints did not suffer from distress and because these joints experienced limited trafficking, no recommendation for establishing a load transfer efficiency criterion for longitudinal joints is made.

4.7 Conclusions and recommendations

This investigation evaluated the load transfer characteristics of precast PCC panel joints using nondestructive testing techniques to understand the mechanisms of load transfer for the repairs. The following conclusions can be made:

- The precast panels transfer loads similarly to jointed cast-in-place PCC, with higher load transfer values for the doweled joints than for the undoweled joints, and load transfer measurements decreased with increasing traffic.
- Differences in thickness between the slabs and the panels likely influence the load transfer efficiencies, with joints formed by two slabs or two panels of the same thickness performing the best in this study.

- Slab temperature considerably influences the load transfer characteristics, especially for the undoweled joints.
- The dowel-slot grout in the joints may have contributed to higher initial load transfer values.
- The dowel-slot grout in the joints may have contributed to spalling and failure of the joints by not allowing free thermal expansion.
- The majority of the transverse doweled joints met the proposed minimum LTE_{δ} threshold criterion (70%) at failure despite extensive spalling and cracking. No recommendations are made for establishing or adopting an LTE_{δ} threshold, due to the use of dowel grout in the joints.
- The undoweled longitudinal joints exhibit low LTE_{δ} characteristics; despite low LTE_{δ} values, the center longitudinal joints between multiple-panel repairs performed well under traffic compared to the transverse joints, indicating that if traffic is applied only in the longitudinal direction, the current design with no dowels in the longitudinal direction may be adequate.
- Because not all undoweled joints were trafficked, no recommendations for establishing a minimum LTE_{δ} criterion for undoweled longitudinal joints can be made at this time.
- The minimum LT threshold criterion (25%) is not met by the majority of the joints with the exception of the N and panel-to-panel transverse doweled joints.
- A minimum LT value of 25% corresponds to an LTE_{δ} of about 85% for a reasonable range of a/l values, which may be too stringent compared to the 70% threshold proposed.
- Finally, LTE_{δ} does not provide a good measure of joint performance for the panel repairs. The use of differential deflections may be more appropriate, and a threshold of 5 mils may be appropriate for doweled transverse joints.

Additional field testing is recommended to compare the performance of precast panels with and without the dowel-slot grout within the joints. Methods of preventing the dowel grout from entering the joints, such as using foam or other inserts to prevent grout from escaping the dowel slot, should be applied. These results may help to establish minimum load transfer and differential deflection threshold values for the joint types and to determine if the absence of the grout in the joints reduces spalling. Additional testing should also be conducted to determine whether correction factors are required for determining the load transfer between different slab thicknesses. Finite element analyses are also recommended

to help estimate the stresses in and around the slabs, panels, and joints due to the unique precast panel joints and differences in panel and slab thicknesses. Reducing the stresses through refined panel and joint design or improved placement methods could also improve the life and performance of the precast panel repairs.

4.8 Acknowledgments

Information described and presented herein, unless otherwise noted, was obtained from research sponsored by the U.S. Air Force Civil Engineer Center and performed at the U.S. Army Engineer Research and Development Center. Permission to publish this information was granted by the Director, Geotechnical and Structures Laboratory.

5 Three-Dimensional Finite Element Modeling of Precast Concrete Panel Joints

L.P. Priddy[1], J.D. Doyle[2], G.W. Flintsch[3], D.W. Pittman[4], and G.L. Anderton[5]

This paper was submitted to ASCE *Journal of Transportation Engineering* (March 2014).

Abstract: This paper examines the mechanical response of precast panel repair joints under static aircraft loadings using the finite element method. Three-dimensional finite element models were developed using the ABAQUS software code, and their results were compared to and validated against results of full-scale field tests and theoretical calculations. Unlike previous modeling efforts for precast slabs and dowel retrofitting studies, all parts of the repair joint were modeled, including the dowels, dowel-slot material, parent concrete, precast slab, and sublayers. Results show that high stress concentrations occur in the dowel-slot material and that the current panel design can be improved by modifying the dowel diameter.

1 Research Civil Engineer, U.S. Army Engineer Research and Development Center, Vicksburg, MS 39180. Email:lucy.p.priddy@usace.army.mil.

2 Research Civil Engineer, U.S. Army Engineer Research and Development Center, Vicksburg, MS 39180. Email: jesse.d.doyle@usace.army.mil@usace.army.mil.

3 Director, Center for Sustainable Transportation Infrastructure, Virginia Tech Transportation Institute and Professor, The Charles Via, Jr., Department of Civil and Environmental Engineering, Virginia Tech, Blacksburg, VA 24061. Email: flintsch@vt.edu.

4 Director, Geotechnical and Structures Laboratory, U.S. Army Engineer Research and Development Center, Vicksburg, MS 39180. Email:david.w.pittman@usace.army.mil.

5 Research Supervisory Engineer, U.S. Army Engineer Research and Development Center, Vicksburg, MS 39180. Email:gary.l.anderton@usace.army.mil.

5.1 Background

For more than 50 years, precast concrete technologies have been investigated to develop alternative repair methods to cast-in-place Portland cement concrete (PCC) for expediently repairing concrete pavements. Recent syntheses are available in the literature (Olidis et al. 2009; Bly et al. 2013; Tayabji et al. 2013; Priddy et al. 2013a). The main advantage of precast pavement technology is that PCC panels can be constructed and cured prior to placement, alleviating the need for long closure periods to allow for curing of cast-in-place materials. The "place and use" advantage of precast elements has led to precast technology acceptance by the transportation community for bridge construction, traffic barriers, railroad ties, etc. However, only recently has the highway sector accepted this technology for precast pavement repair/construction techniques (Tayabji et al. 2013). While few precast pavement applications for airfields are reported in the literature, successful implementations by the highway industry and results of recent airfield investigations indicate that this technology is also suitable for airfield repairs (Olidis et al. 2009; Bly et al. 2013; Priddy et al. 2013a).

5.2 Research objective

This paper presents the results of an investigation of a doweled precast panel repair joint using three-dimensional finite element analysis software and static analyses of aircraft traffic. Test data collected during field trials and theoretical calculations are used to validate the model. The model is then used to determine mechanical responses of the precast panel repair joint under static aircraft loads with the intent to better understand the complex stress interactions within the doweled repair joints and to provide recommendations to improve the design and performance of panel repairs for airfield pavements.

5.3 Summary of previous work

Several phases of research were conducted to investigate the suitability of precast panel technology for conducting expedient airfield pavement repairs. The ultimate objective was to develop an expedient, temporary, precast panel repair technique for the U.S. military that was capable of supporting an objective of 5,000 C-17 aircraft traffic applications until permanent repairs could be conducted. For reference, typical military

airfields are designed to support between 50,000 and 100,000 C-17 passes, depending on their mission.

The initial research phase identified a single-panel repair precast system described by Ashtiani et al. (2010) capable of supporting F-15 aircraft for further evaluation. In the second research phase, this precast system was redesigned to accommodate both single- and multiple-panel repairs and to support C-17 traffic (Bly et al. 2013). The final repair method required establishing load transfer on the transverse joints between the panel and the repaired slab (parent slab) using saw-cut dowel slots 76 mm wide, 305 mm long, and 165 mm deep in the parent PCC (shown in Figure 5.1) that were filled with rapid-setting grout following panel placement (similar to dowel retrofitting). No load transfer devices were installed in the longitudinal direction, based on field and analytical results of the earlier panel system tests (Ashtiani et al. 2010). The third research phase included full-scale field testing of single- and multi-panel repairs in an airfield PCC test section. Mechanical properties, including deflections and stresses, were measured during this phase to compare to finite element modeling (FEM) results. Results of simulated traffic testing indicated that the panel repairs were capable of supporting at least 5,000 and as many as 10,000 passes of a C-17 aircraft and easily met the objective pass level of 5,000 passes. Additional details of traffic testing are available (Priddy et al. 2013b, 2014b).

The main failure mode was deterioration of the transverse doweled joints, as shown in Figure 5.1. During the first 2,000 passes, cracks were noted in the grout material within the dowel slots closest to the panel's edge, followed by spalling in the parent PCC between the dowel slots. With repeated traffic applications, the cracks within the dowel grout progressed, and the surface material crushed, causing accumulation of spalled material. Additionally, as trafficking continued, cracks formed between the dowel slots in the parent PCC, leading to additional spalling at the joint. Spalled material was generally confined a distance less than 100 mm from the joint, and some spalling along the entire joint on both sides was also noted; however, the major spalling occurred in the dowel grout and PCC between dowel slots. The failure at these joints was most likely due to excessive dowel bearing stresses generated in the dowel-slot material and to the expedient installation procedure of filling the joints with rapid-setting cementitious grout. This practice likely contributed to the failure of the repairs by introducing incompressible material within the joint (Priddy et al. 2013b; 2014a, b).

Figure 5.1. Deterioration of transverse joints.

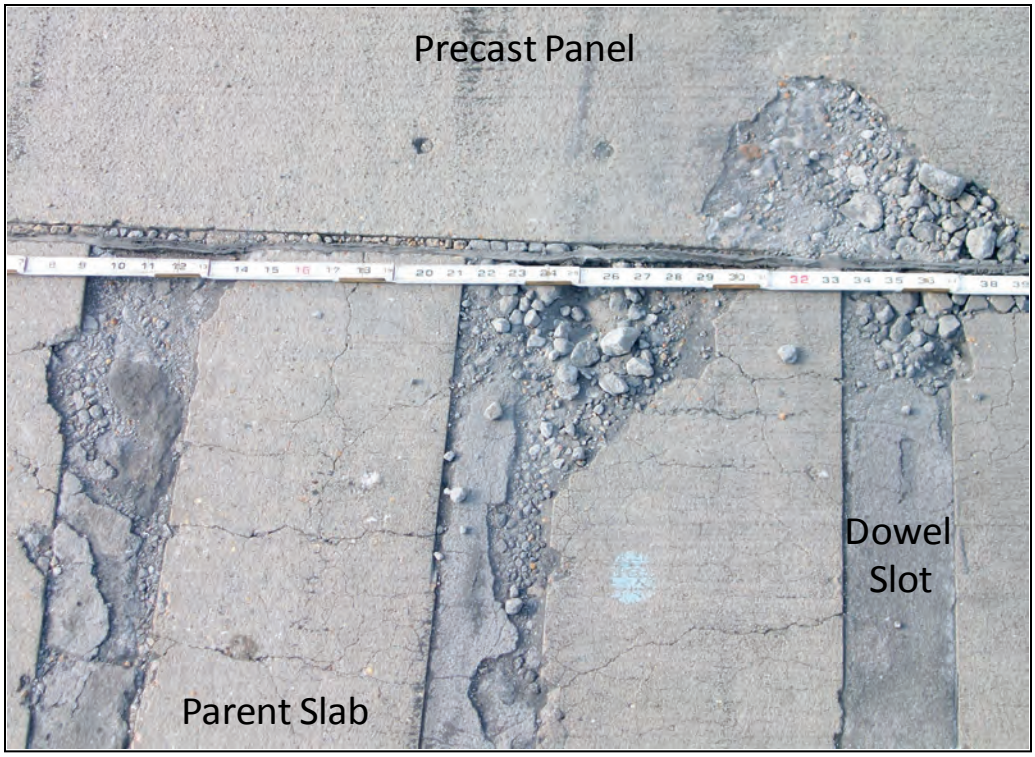

5.4 Literature review

The literature reveals only a limited number of FEM studies of precast panels for pavement applications and dowel retrofit modeling efforts. Some basic FEM efforts were conducted in the 1980s and 1990s for a U.K. precast panel design using a finite element package PAFEC (Bull 1986; Bull and Singh 1990; Bull and Woodford 1997). The models considered the effect of load on a single precast panel without load transfer dowels. Two other precast pavement panel investigations by Hachiya et al. (2001) and Ashtiani et al. (2010) focused on airfield applications. Hachiya et al. (2001) used three-dimensional (3-D) FEM software to model special load transfer mechanisms in a Japanese precast panel system; however, the precise software package used was not specified and did not explore partially retrofitted dowels. Ashtiani et al. (2010) investigated a single-panel repair as a full-slab replacement using ISLAB2000. However, the dowel slots were not modeled as individual components, and the panels were assumed to be directly doweled to the parent PCC. Ashtiani et al. (2010) assumed that the dowel slot would not interfere with the load transfer and that any differences in material properties between the dowel-slot repair material and the parent slab were minimal. This approach was also applied in dowel retrofit modeling efforts for

establishing load transfer across cracks and faulted joints (Hiller and Buch 2004) using ISLAB2000. The investigators also assumed that no differences existed between the dowel slots and the parent PCC.

Despite limited reports of precast panel and dowel retrofitting investigations, the literature reveals many studies using FEM techniques for PCC pavements (Tabatabaie-Raissi 1978; Huang 1985; Guo et al. 1995; Hammons and Ioannides 1997; Davids et al. 1998; Bhatti et al. 1998; Kim and Hjelmstad 2003). A number of software programs, including PCC-specific FEM programs such as ISLAB2000 and general-purpose FEM software such as ABAQUS, were used for pavement modeling. Bayrak and Ceylan (2008) provide a review of the limitations and benefits of numerous programs used for PCC FEMs. Researchers also applied a variety of PCC joint modeling approaches, including Timoshenko beam elements connected to plate elements (through elastic springs), 3-D continuum solid elements for both dowels and concrete slabs with frictional contact interfaces, and solid elements with embedded beam elements. Riad (2001), Kim and Hjelmstad (2003), and Wadkar (2011) discuss the benefits and limitations to these approaches. Of these approaches, Kim and Hjelmstad (2003) reports that using 3-D continuum solid elements for concrete and dowels and frictional contact interactions provides more detailed stress distributions at the dowel-concrete interface than simplifying the connections using spring elements provides. The biggest drawback to this approach is that it requires a fine mesh for the dowel and surrounding concrete, necessitating a large computational effort. The use of supercomputing resources reduces the burden of large problem size.

5.5 Modeling of the precast panel-parent slab joint

Based on the review of the literature, ABAQUS (version 6.11-1) (Simulia 2011a) was selected for this study due to its widespread use for modeling PCC pavements and its built-in concrete damage models (Brill 1998; Hammons 1998; Kim and Hjelmstad 2003; Lee et al. 2004; Liu et al. 2007; Prabhu et al. 2009; Caliendo and Parisi 2010). Only the repair joint was modeled, because traditional PCC theory has shown that the edge and corner loadings are the most critical for design purposes. Each physical part in the repair with dimensions shown in Table 5.1 corresponds to a separate part in the FEM, and separate parts were used for the rapid-setting grout-filled slots and the dowels (Figure 5.2). Three-dimensional-reduced integration elements (C3D8R) were used for the model based upon successful application in doweled PCC pavement investigations (Cook 1995; Prabhu et al. 2009).

Table 5.1. Model dimensions.

Part	No. Parts	Length, mm	Width, mm	Thickness, mm	Element Size, mm
Parent PCC	1	3048	3048	355.6	25.4[a] 101.6[b]
Precast Panel	1	3048	3048	279.4	25.4[a] 101.6[b]
Dowels	10	558.8	25.4[c]	n/a	5.1
Dowel Grout	10	304.8	76.2	165.1	15.24
Flowable Fill	1	3048	3048	76.2	152.4
Base	1	6105.5	3048	152.4	304.8
Subgrade	1	6105.5	3048	1828.8	457.2
Joint (air gap)	n/a	n/a	9.5	n/a	n/a

[a] Doweled region.
[b] Non-doweled region.
[c] Diameter of dowel.

Figure 5.2. Plan view of model.

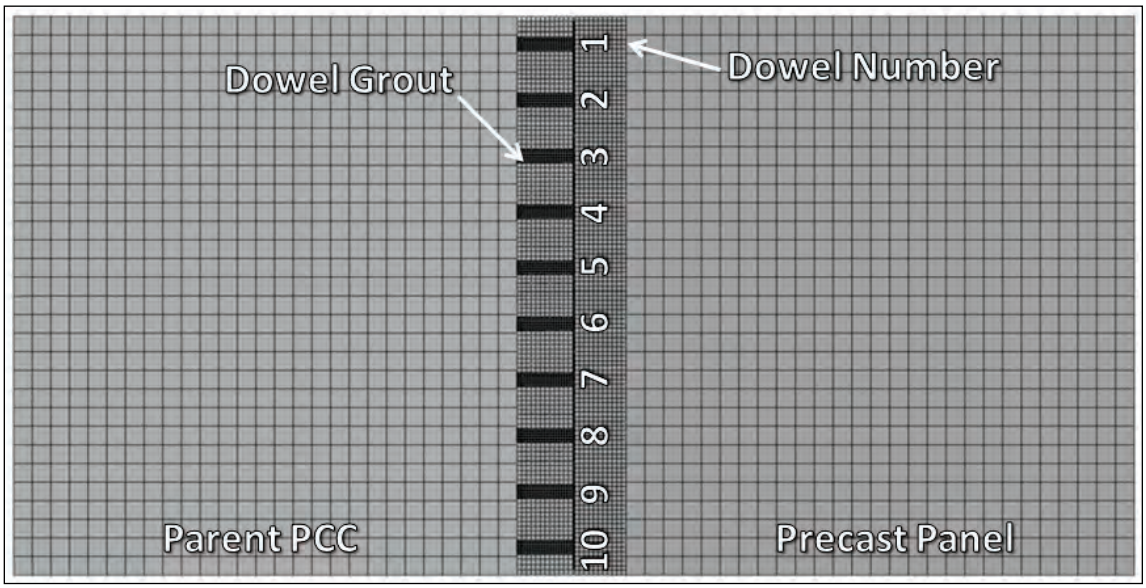

In the FEM, the parent slab section consists of the PCC slab over an aggregate base on top of the subgrade to simulate the structure in field testing. The precast panel section consists of the precast panel over cementitious flowable fill, over the aggregate base, and on top of the subgrade. A 9.5-mm-wide joint is placed between the panel and the parent slab to simulate the field joint width. At this joint width and due to the smooth faces of the panel and slab, aggregate interlock does not contribute signifi-

cantly to transferring load at the transverse joint. A finer mesh is assigned to the doweled portions of the pavement sections, as the response of the dowel-concrete interfaces at the joint is of highest interest. Larger meshes are assigned to the other portions of the model as shown in Table 5.1.

5.5.1 Material properties and interactions

Elastic material behavior input parameters were assigned for all model parts. ABAQUS's concrete damaged plasticity model (Lubliner et al. 1989; Lee and Fenves 1998) was also used for the concrete parts. This model uses stress-strain relationships to correlate parameters for concrete damage in both tension and compression (Simulia 2011b). In this investigation, the compressive stress-strain curves for the concrete materials used were based on laboratory response data from specimens collected during construction of the test section and panels and historical laboratory tests on the dowel grout material. Tensile stress (σ_{t0}) values were obtained from compressive laboratory test data using the direct tensile strength relationship $\sigma_{t0} = 1.7 (f_{c0})^{2/3}$. These and other input parameters for this model are provided in Table 5.2 and are based on field measurements, ABAQUS defaults (Simulia 2011b), and input parameters reported by other researchers (Khazanovich et al. 2009; Tyau 2009). As shown in Table 5.2, the strength of the parent PCC was higher than that of the dowel grout and panel PCC.

Table 5.2. Model input parameters.

Material Property	Parent Slab	Panel	Dowel Grout	Steel Dowel	Base	Flowable Fill	Subgrade
Mass density, kg/m^3	2.32E+03	2.32E+03	1.84E+03	7.80E+03	2.00E+03	1.91E+03	1.84E+03
Young's modulus, *E*, MPa	33 440	33 440	22 063	199 948	379	276	145
Poisson's ratio, v	0.2	0.2	0.2	0.3	0.4	0.2	0.4
Ultimate stress, σ_{cu}, MPa	49.9	39.4	34.5				
Failure stress, σ_{t0}, MPa	4.4	3.7	3.4				
Dilation angle, ψ	30	30	30				
Flow potential eccentricity, *m*	0.1	0.1	0.1				
Initial biaxial/uniaxial ratio, σ_{b0}/σ_{c0}	1.16	1.16	1.16				
Ratio of the second stress invariant on the tensile to compressive meridian, K_c	0.667	0.667	0.667				
Viscosity parameter, μ	0	0	0				
Fracture energy, G_F	0.67	0.67	0.67				

Note: Blanks indicate that the value was not required as input.

The contact interactions between the different materials were modeled using surface-to-surface contact and frictional behavior. A friction coefficient of 1 was assigned for the interaction between the portion of the dowel embedded in the grout and for the grout interaction with the parent PCC. The greased dowel portion within the precast panel was assigned a friction coefficient of 0.076 (Buch et al. 2007). For the panel-flowable fill interaction, a friction coefficient of 1 was used, based on cores taken after the completion of traffic testing that showed the flowable fill bonded to the precast panel. For the remaining sublayer interactions, a friction coefficient of 0.35 was used.

5.5.2 Loading

A gravity load was applied first to the entire model, then two different static load types were simulated. The main load type simulated the static loads from the C-17 load cart used during field testing. A uniform pressure of 1 MPa was applied to six elliptical tire imprints with areas of 1613 cm^2 and widths of 356 mm. The other load type was a static 222.4-kN heavy weight deflectometer (HWD) load modeled by applying a uniform pressure distribution of 3.2 MPa over the surface of a 300-mm-diam contact area. This load was applied at the edge of the precast panel joint.

In this study, six load cases (Cases 1-6) (Figure 5.3) were examined to determine the most critical loading condition at the joint and to replicate locations of the gear during traffic testing on both sides of the joint. Load Case 7 was used for model verification purposes of center loading discussed in the next section. As shown in the figure, several load cases had tires outside the modeled area. In the field case, these tires would rest on adjacent slabs or panels. Because the adjacent slabs were not tied or doweled and the joint width was 9.5 to 12.7 mm, it was assumed that minimal load transfer would occur at the longitudinal joint. This assumption was confirmed by field test measurements that showed load transfer (stress-based LT) of only 1 to 6% (Priddy et al. 2014a).

5.6 FEM results

5.6.1 Model validation

To validate the FEM, several steps were conducted, including comparison of mechanical responses from the FEM to data collected during field testing and through theoretical calculations using PCC theory. First, the

Figure 5.3. Load cases.

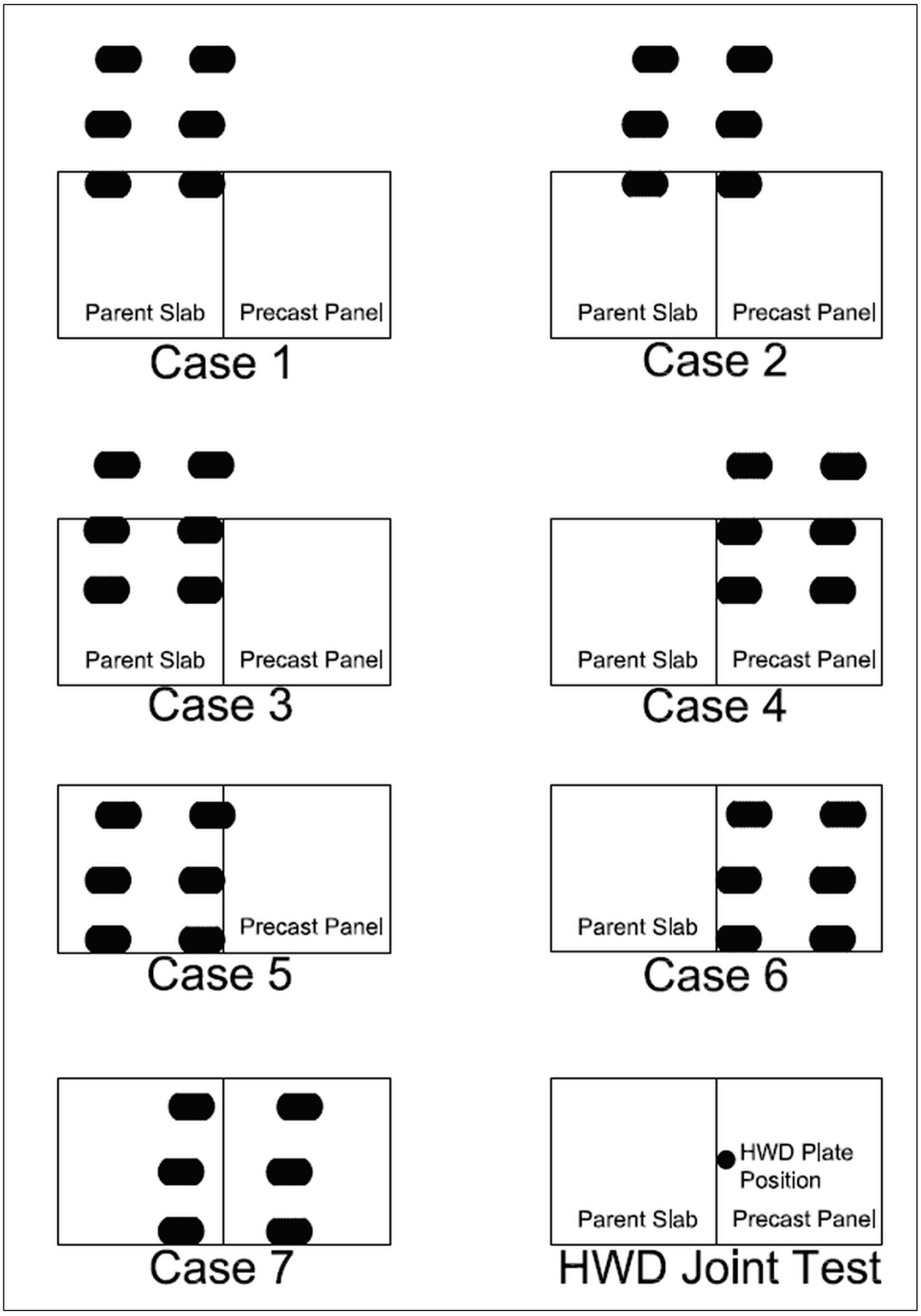

mechanical responses of the FEM and field HWD joint load tests were compared. The joint load test deflection measurements on each side of the joint were used to calculate the load transfer efficiency (LTE) of the repair

joint. In both scenarios, the HWD load (approximately 222.4 kN) was applied to the precast panel side of the joint positioned approximately 152.4 mm from the edge, as shown in Figure 5.3. The average HWD-measured deflections on the panel (D_0) and the parent slab (D_1) from field testing are presented in Table 5.3. As shown in this table, the FEM-predicted deflections do not compare well with the HWD-measured deflections ascertained before trafficking. This difference is not surprising, as in the field the panel was initially bonded to the parent slab by the provision of an additional means of load transfer beyond that of the dowels only: the rapid-setting grout within the joints. For comparison purposes, the LTE of the joint was computed using the equation $LTE(\%) = D_1/D_0 \times 100$. The field condition joint had an LTE of 94%, much higher than that predicted by the model (72%). The model, however, assumed that the joint width was maintained with no contact between the panel and the parent PCC surface. HWD measurements recorded after additional traffic applications compared to the FEM (Table 5.3) indicated that the grout bond would have broken after approximately 1,000 passes. Deflections measured after 910 and 1,120 passes more closely matched the model and the calculated LTE. Additional modeling efforts were conducted to allow contact between the panel and the parent slab (no joint spacing) with various friction coefficients. These modeling efforts could not replicate the bonded field condition, and the data are not shown for brevity. Thus, the original joint width of 9.5 mm was used for the remainder of the modeling efforts.

Table 5.3. Comparison of measured and predicted joint deflections.

	HWD Meas. (Ave.)		HWD Meas. LTE	FEM Pred. (static case)		FEM Pred. LTE	% Error Pred. v. Meas.		Calc.[a] (Theory)		Calc. LTE
	Defl., microns			Defl., microns			%		Defl., microns		
Passes	Panel	Parent Slab	%	Panel	Parent Slab	%	Panel	Parent Slab	Panel	Parent Slab	%
0	460	432	94				37	20			
910	684	529	77				7	0.2			
1,120	781	514	66	732	528	72	7	3	610	430	70
1,960	882	611	70				21	16			
4,200	932	623	67				27	18			
8,400	1136	650	57				55	23			

Note: precast panel = loaded slab, D_0; parent slab = unloaded slab, D_1; measured on south joints of panel repair during joint load tests.

[a] Calculated using Westergaard's edge deflection equation.

Second, to determine the deflection that might be experienced without the bond, the free edge deflections according to Westergaard (Huang 2004) were also computed for both the panel and the parent PCC slab using the material properties listed in Table 5.2 and a modulus of subgrade of reaction of 75 MN/m^3 measured during field testing (Bly et al. 2013) assuming that half of the load would be transferred to the other slab, half the load was used for the theoretical calculations of deflection. While results of theoretical calculations for deflection were lower than those predicted by the model, the calculated and FEM-predicted LTE values are comparable (approximately 70%).

Finally, the mechanical responses from the panel under the assumed critical corner (Load Case 4) and center loading conditions (Load Case 7) were compared to average peak measurements from earth pressure cells (EPCs) installed in the subgrade of the test section under select panels (positioned in the corners and centers of panels) after 112 passes of load cart traffic. Priddy et al. (2013b) provides details of the EPC placement and measurements. The average EPC-measured (66 kPa) and FEM-predicted stress (57 kPa) values for panel corner loading compare reasonably well. The measured and predicted center stress values also compare well with values of 35 and 33 kPa, respectively. Any differences in measured versus estimated stresses could be related to minor differences in the material properties in the model compared to the as-constructed test section or to differences related to contributions of the confining surrounding pavement not represented by the joint model in this study. Based on these validations, the model is determined to adequately represent the behavior of the precast panel joint in the unbonded condition.

5.6.2 Determination of critical and effective dowels

Following validation, Load Cases 1 through 6 were explored to determine the most critical load-case scenario for the precast panel transverse joint. The critical load case is the loading scenario that causes the highest compressive stress in the concrete materials around the dowels at the face of the joint. This corresponds to the load case whose dowel carries the highest portion of the shear load (critical dowel). For comparison purposes, theoretical calculations of shear stress for the critical dowel were computed. Theoretical behavior of dowels generally assumes that when a dowel is loaded, some of the load is carried by adjacent dowels within a certain distance away from the load, with the shear forces carried by the dowels decreasing inversely with increasing distance from the load. The

distance at which the dowels no longer carry the load is generally assumed to be between 1.0*l* and 1.8*l* from the load location, where *l* is the radius of relative stiffness of the pavement. Dowels within this distance carry a portion of the load and are considered "effective dowels." The determination of the number of effective dowels is used to calculate the shear force on the critical dowel. Equation 5.1 is used to calculate *l* (Huang 2004).

$$l = \left[\frac{E_c h^3}{12k(1-\nu^2)} \right]^{0.25} \tag{5.1}$$

In Equation 5.1, E_c is the modulus of elasticity for concrete (33.4 GPa), *h* is the slab thickness, *k* is the modulus of foundation support (75 MN/m^3) from field measurements, and *v* is the Poisson's ratio of concrete (0.2) from laboratory investigations. For the panel, *l* is computed to be 960 mm, and for the slab, *l* is computed to be 1150 mm; differences are due to the differing thicknesses of the panel and parent slab.

If the joint is 100% efficient in transferring the wheel loads, the panel will carry only half the load; thus, the load applied at the critical dowel is divided in half. This amount is then divided by the number of critical dowels to determine the shear force carried by the critical dowel. Pavement design typically assumes that 40 to 50% of the design load (total shear load) is transferred from the loaded side of a joint to the unloaded side through the dowel. For the calculations, 45% was assumed along with an initial effective distance of 1.8*l*.

The calculated and FEM-predicted shear forces for the critical dowel and number of active dowels for each edge load case are presented in Table 5.4. The number of active dowels from each load case was determined by assuming that if the dowel carries more than 5% of the total gear load, it is an active dowel. The FEM-predicted number of effective dowels agrees reasonably well with the calculated numbers. The assumption of 1.8*l* provides calculated values of shear force similar to those predicted in the model. By varying the effective distance from 1.0*l* to 1.8*l*, it was determined that a distance of 1.5*l* resulted in values closer to those predicted in the model. Also, the load transferred by the critical dowels based on FEM-predicted shear forces (LT=unloaded/ (loaded+unloaded)) are similar to the 45% assumption used for calculations, as shown in Table 5.4. These high values indicate that the dowels are initially able to transfer the majority of the load.

Figure 5.4 shows an example of the shear forces predicted and computed for the dowels in Load Case 1.

Table 5.4. Comparison of FEM-predicted and calculated shear forces for the critical dowels.

		FEM-Predicted				Calculated (Theory)					
						Load Transfer=45%, Eff. Dowel Distance=1.8/			Load Transfer=45%, Eff. Dowel Distance=1.5/		
Load Case	Critical Dowel	Shear Force kN	% Total Load[a]	Eff. Dowels[b] #	Load Transferred[c] %	Shear Force kN	Eff. Dowels #	% Diff	Shear Force kN	Eff. Dowels #	% Diff
1	1	33	34	4	45	28	3.9	17.6	33	3.5	0.8
2	1	39	46	3	46	33	3.4	19.2	38	2.9	2.4
3	1	38	22	5	47	37	5.1	3.9	39	4.7	1.8
4	1	43	33	5	47	39	5.6	12.4	41	4.8	5.3
5	10	33	27	6	47	35	6.3	7.0	38	5.6	13.5
6	10	43	26	5	47	39	5.6	10.8	41	4.8	3.8

[a] Percent of total load carried by critical dowel.

[b] Dowel carries 5% of total load.

[c] Load transferred by critical dowel.

5.6.3 Determination of bearing stresses

The shear forces acting on the dowels are transferred to the concrete surrounding the dowel through bearing, and these bearing stresses are proportional to the bending deflection of the dowel. The maximum compressive stresses predicted in both the dowel and the surrounding concrete at the joint face are presented in Table 5.5 for each load case. As might be expected, the locations of maximum compressive stress occurred in the concrete surrounding the critical dowels identified in Table 5.4. As suggested from theory, the critical dowel in all load cases was the dowel closest to pavement edge (Dowel 1 or Dowel 10) when a wheel was directly over the dowel. For reference, the dowel numbering convention is shown in Figure 5.2. From these results, Load Case 4 generated both the highest shear forces and highest bearing stresses in the concrete surrounding the critical dowel, with similar values for Load Case 6. Figure 5.5 shows the distribution of stresses surrounding the critical dowel. Figure 5.6 shows the stresses generated for all dowels for Load Case 4.

Table 5.5. FEM stresses for critical dowels and surrounding PCC.

Load Case	Critical Dowel	Max Dowel Compressive Stress		Max Concrete Stress (Bearing Stress)		Max Concrete Tensile Stress	
		MPa		MPa		MPa	
#	#	Loaded	Unloaded	Loaded	Unloaded	Loaded	Unloaded
1	1	40.3	33.3	33.6	29.0	2.6	3.7
2	1	47.5	41.1	34.4	32.7	3.6	2.7
3	1	46.8	41.1	37.4	36.9	2.5	3.4
4	1	52.7	46.6	37.9	35.5	3.6	3.5
5	10	50.9	45.4	36.1	32.8	3.3	3.6
6	10	52.0	45.8	35.7	32.8	3.5	3.4

Figure 5.4. Example of FEM-predicted and calculated (theory) shear forces.

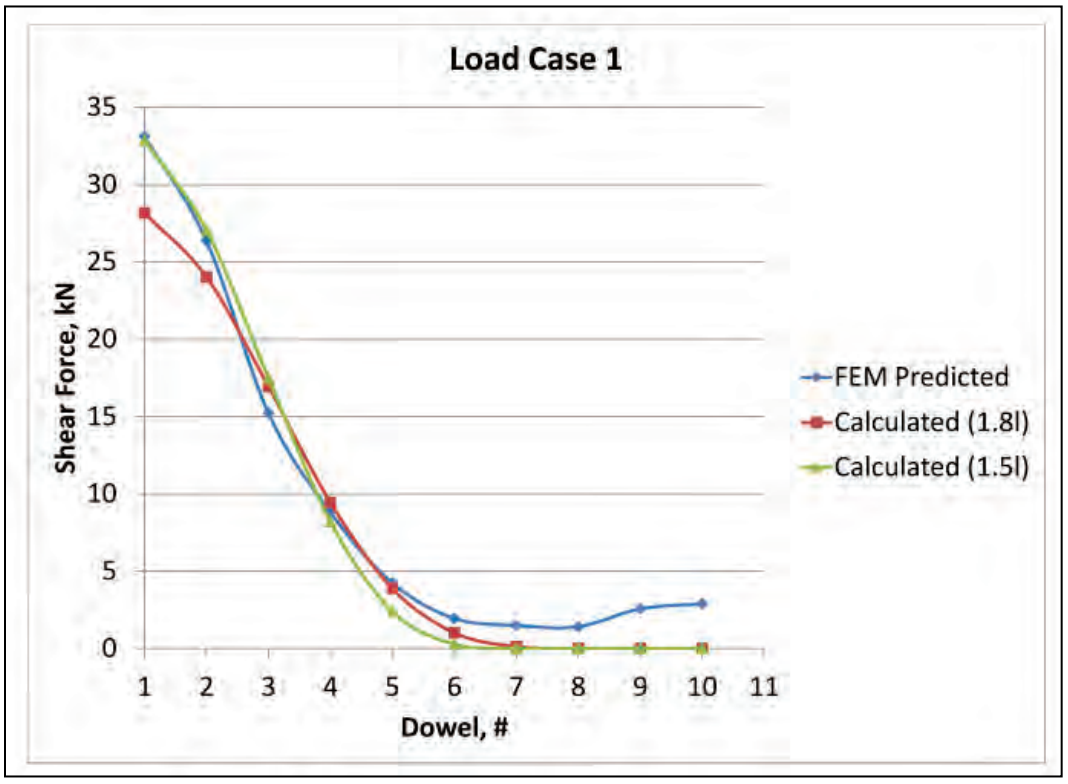

Figure 5.5. Distribution of compressive and tensile stresses around critical dowel for Load Case 4.

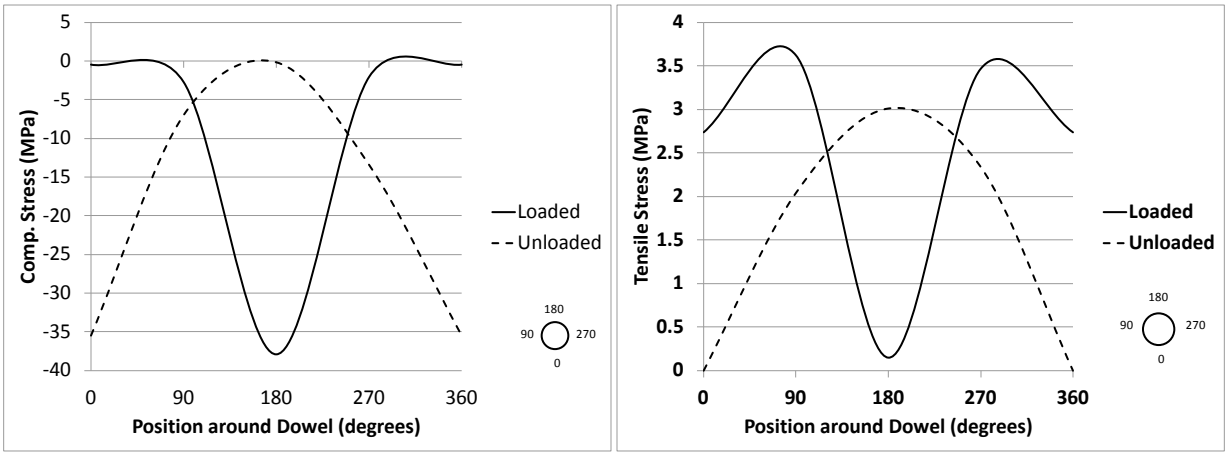

Figure 5.6. Comparison of stresses for all dowels (Load Case 4).

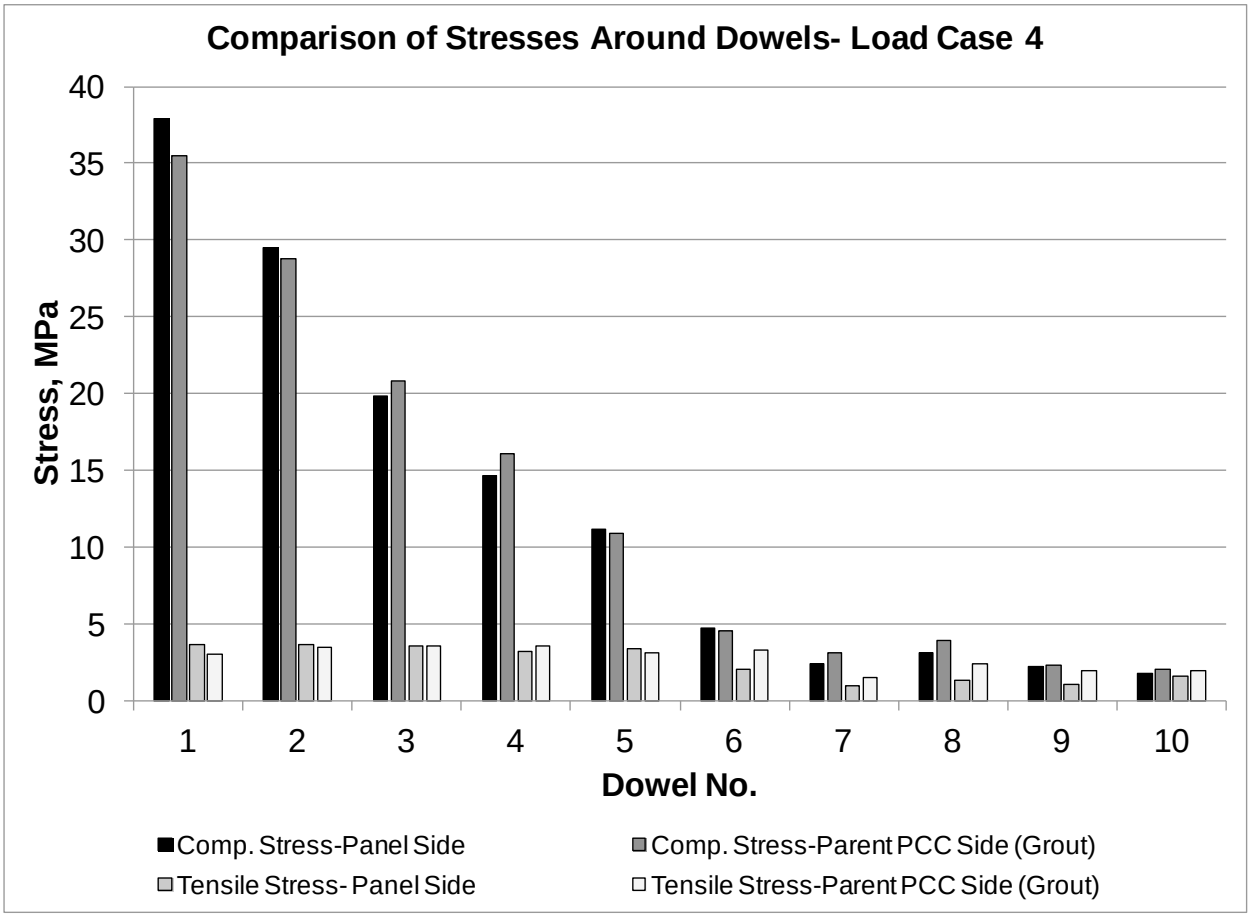

If the bearing stress exceeds the allowable bearing stress of the concrete after repeated applications of traffic, then cracking or crushing above or below the dowel will occur. The allowable compressive bearing stress in concrete is calculated using Equation 5.2 (Huang 2004).

$$f_b = \left(\frac{4-d}{3}\right) f_c' \tag{5.2}$$

where:

d = dowel diameter (25.4 mm in this case)
f_c' = concrete compressive strength

For the 25.4-mm-diam dowel, the allowable bearing stress, f_b, equaled the ultimate compressive strength for each concrete material presented previously in Table 5.2. As shown in Table 5.5, the bearing stresses for the critical dowels exceeded the dowel grout's ultimate compressive strength (34 MPa) in most load cases but not the parent PCC's (50 MPa) or the panel PCC's (39 MPa). These results indicate that compressive failure is a likely mode of failure for the repairs, with failure initiated by cracking and crushing of the dowel grout above or below the dowel closest to the panel's edge. The crushing results in gaps between the dowel and the surrounding concrete and will result in loss in dowel efficiency for transferring load, for the critical dowel. As a result, the next closest dowel will carry a greater portion of the load. The progressive crushing of material surrounding the dowels will ultimately lead to failure of the remaining dowel slots with repetitive loading.

As verification, a dowel gap was modeled beneath Dowel 1 in the dowel grout for Load Case 4. The gap was varied between 0.0025 and 1.02 mm, as suggested by Kim and Hjelmstad (2003). The dowel efficiency for each dowel was computed comparing maximum deflection of the concrete surrounding the dowels (dowel efficiency=$\delta_{unloaded}/\delta_{loaded}$). As anticipated, increasing the gap size caused reductions in Dowel 1's load transfer capabilities but with minimal reductions for the surrounding dowels, as shown in Figure 5.7. With a gap of 1.02 mm, the measured compressive stresses in both the grout and the panel around Dowel 1 decreased by almost 90% with increased compressive stresses for Dowels 2 through 4, as illustrated in Figure 5.7. These results confirm that if a gap forms in the concrete surrounding the critical dowel, it is not able to carry the load, forcing the nearest dowels to engage and carry the largest portions of the

Figure 5.7. Effects of dowel gaps on dowel efficiency: (a) dowel efficiency, (b) bearing stresses on panel side of joint, and(c) bearing stresses in grout.

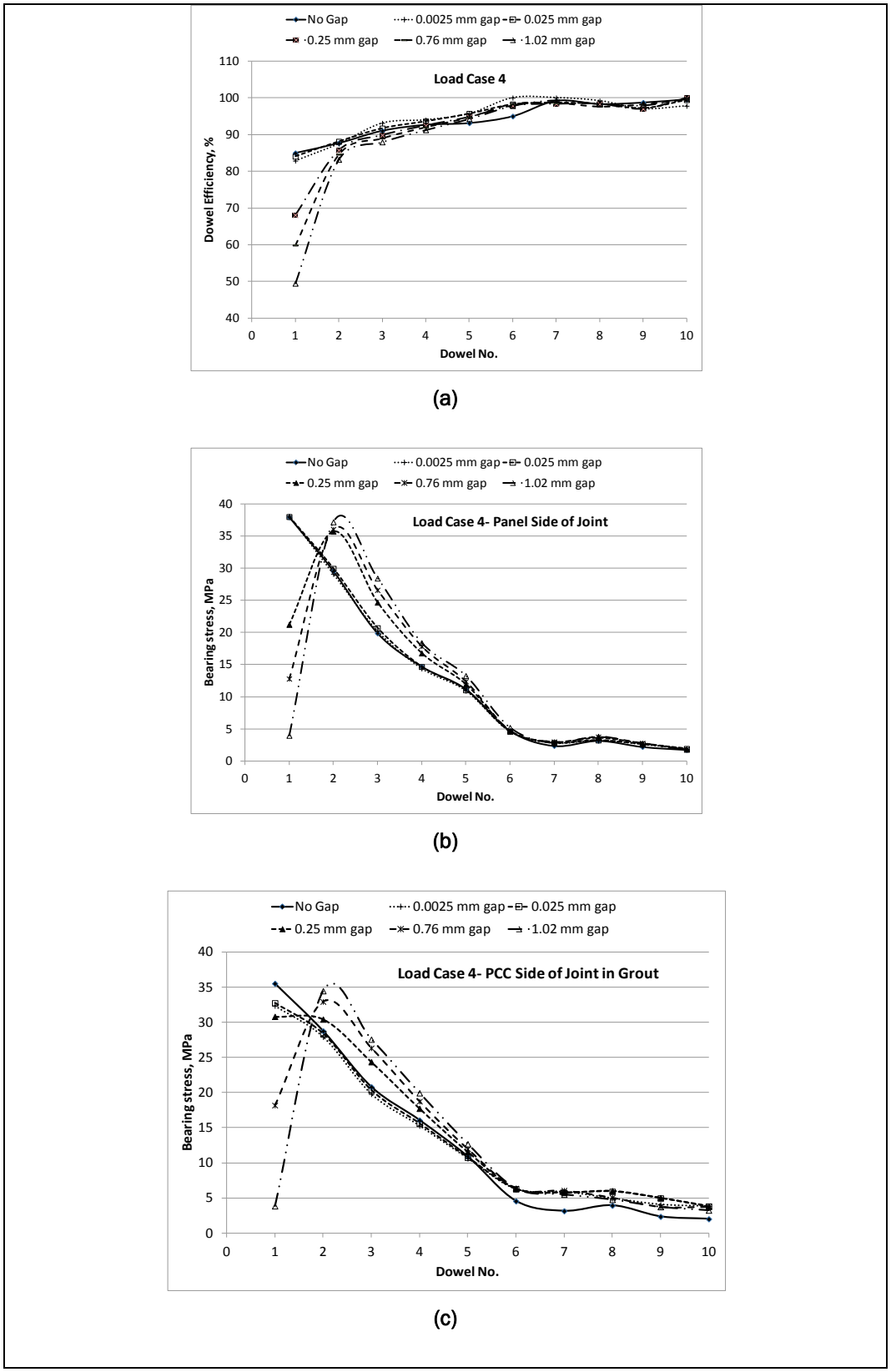

load. Also at this gap spacing, the compressive stress measured in the dowel grout surrounding Dowel 2 exceeded the ultimate compressive stress for the dowel grout. It was expected that the crushing of grout around the second dowel would cause similar losses in load transfer capabilities, and this progression of damage would continue from dowel to dowel as traffic progressed. Additional modeling efforts confirm similar behavior for the remaining dowels when additional dowel gaps are imposed.

5.6.4 Determination of tensile stresses

Tensile failure is also indicated by the model and field test results in the doweled region. If the tensile stresses in the dowel grout or surrounding concrete exceed the allowable tensile strength of the concrete, tensile cracks may occur in the concrete on the sides of the dowel under repeated applications of load and will be reflected to the edge of the dowel grout and propagated into the surrounding pavement. Additionally, tensile stresses measured under the panel and parent PCC must be minimized to limit tensile cracks in the concrete. Tensile stresses in the panel and parent PCC were also predicted using the FEM, but the predicted tensile strengths did not exceed the allowable tensile strength for the PCC portion of the parent slab or the precast panel concretes. In all cases, the maximum tensile stresses occurred in the dowel grout adjacent to the dowel, and the critical load case corresponded to that determined by compressive stresses (Load Case 4 as shown in Table 5.5). The maximum tensile stress predicted by the model was 3.5 MPa for Load Case 4, with similar results for Cases 5 and 6. The measured tensile stresses in the dowel grout approach or exceed its allowable tensile strength (3.4 MPa) for Load Cases 4 through 6.

5.7 Discussion

5.7.1 Behavior of doweled joint under critical load

The model and field test results indicated that the panel repairs failed due to excessive stresses in the dowel grout. Minimizing these stresses is therefore important to increase the repair life when using precast panels. This can be done by modifying the panel designs by increasing the panel thickness, decreasing the dowel spacing, or increasing the dowel diameter. Because the slab size and thickness of this military repair system are controlled by lifting capabilities available to military personnel (Bly et al. 2013) and therefore limit the panel weight, no increase in panel thickness could be applied. In addition, while it is generally accepted that smaller dowel spacings can

reduce the bearing stresses, increasing the number of dowels was not recommended because the time required to cut additional dowel slots in the parent PCC would hinder expedient repairs. Thus, the most logical approach for improving this repair technique was to increase the dowel diameter.

The benefit of increasing the dowel diameter was evaluated through FEM using Load Case 4. Three additional models were constructed with dowel diameters of 31.8, 38.1, and 50.8 mm to determine the reduction in stresses at the dowel-concrete interface by increasing the dowel diameter. For the 50.8-mm dowel, the depth of the dowel grout was increased by 12.7 mm to allow for at least 12.7 mm around the dowel for grout consolidation. The decreases in measured compressive and tensile stresses around Dowel 1 (the critical dowel) are presented in Table 5.6. As can be seen in the table, the 38.1-mm dowel reduces the bearing (compressive) stresses in the concrete around the dowel more than 25% compared to the 25.4-mm dowel. A 15% reduction in compressive stress in the concrete around the critical dowel may be achievable with a 31.8-mm dowel. Even greater reduction in stress may be achieved using a 50.8-mm-diam dowel; however, this size dowel may be too large for the thin panel. Also, the use of this size dowel requires a deeper dowel slot, which would require more costly rapid-setting grout to fill. As a result, it is recommended that the 31.8- and 38.1-mm dowels be considered for field-test analyses to determine if the repair life may be increased through their use.

Table 5.6. Dowel diameter variation results.

	Precast Side				Parent Slab (Grout)				
Dowel diameter	Peak Comp. Stress	Comp. Stress Reduction	Peak Tensile Stress	Tensile Stress Reduction	Peak Comp. Stress	Comp. Stress Reduction	Peak Tensile Stress	Tensile Stress Reduction	Dowel
mm	MPa	%	MPa	%	MPa	%	MPa	%	#
25.4	37.9	0	3.6	0	35.5	0	3.0	0	Dowel 1
31.8	31.6	17	3.6	1	30.0	16	3.0	2	Dowel 1
38.1	25.4	33	3.3	9	26.1	27	2.8	7	Dowel 1
50.8	21.7	43	3.1	14	19.5	45	3.0	0	Dowel 1

5.7.2 Benefit of modeling dowel grout

Previous modeling efforts of precast slabs and dowel retrofitting assumed that the dowel slots would not interfere with load transfer and that any differences in material properties between the dowel slots and the parent

slab were minimal. This study rejected these assumptions and modeled the parent slab and dowel-slot grout areas as separate parts. An additional model was used to compare the response of the repair joint under the critical load case if the dowel grout areas and parent PCC were not modeled as individual parts. Results of the model indicated that assuming the grouted area had the same properties as the parent PCC under-predicts the compressive stress surrounding the dowels on both sides of the joint. While the difference in measurements for the critical dowel is low (7%), the stresses measured in the remaining dowels increase with increasing distance from the load (up to 80%). These results indicate that differences in the material properties between the parent slab PCC and the dowel-slot grout do impact the FEM-predicted stresses surrounding the concrete dowels and should be considered to understand the state of stress in the doweled areas, particularly when complex aircraft-gear configurations are considered. Additional analyses are recommended to fully quantify the impacts of this assumption for traditional PCC pavements under a variety of aircraft-gear configurations.

5.8 Summary and recommendations

This paper presents the development and validation of a 3-D FEM for a precast panel repair joint using data collected during full-scale field testing of precast panel repairs and from theoretical calculations. Multiple load cases were examined to determine the most critical load case and the resulting responses of the dowel and surrounding concrete to static loads. Results of this study show that the compressive and tensile stresses measured in the concrete surrounding the dowels exceed the compressive and/or the tensile strengths for the dowel patching material. With repeated loading, it is expected that both compressive and tensile failure of the grout surrounding the dowel will occur.

Modeling results also show that increasing the dowel diameter reduces the stresses generated in the concrete at the dowel interface. By minimizing the compressive and tensile stresses around the dowels, the repair life may be extended beyond 5,000 passes. It is therefore recommended that additional field tests using larger diameter dowels be conducted to determine what increase in pavement repair life may be achieved. Additionally, because cracking of the dowel grout was the mode of failure for the repairs, a stronger dowel grout should be investigated to determine whether performance may be improved. Results of the modeling effort also showed that differences in the material properties between the parent

slab PCC and the dowel-slot grout impact the stresses surrounding the concrete dowels and should be considered to fully understand the state of stress in the doweled areas. Because the models used in this study focused on the joint and static load conditions, additional modeling is recommended to understand the mechanical response of full-sized single- and multiple-panel repairs under dynamic loading conditions.

5.9 Acknowledgements

Information described and presented herein, unless otherwise noted, was obtained from research sponsored by the U.S. Air Force Civil Engineer Center and performed at the U.S. Army Engineer Research and Development Center. Permission to publish this information was granted by the Director, Geotechnical and Structures Laboratory.

6 Development of Expedient Military Concrete Airfield Pavement Repairs

L.P. Priddy[1] and J.S. Tingle[2]

Reprinted by permission of ICE Publishing, August 2014.
Citation: Priddy, L.P. and Tingle, J.S. (2013). Development of Expedient Military Concrete Airfield Pavement Repairs. *Magazine of Concrete Research*, 66(1), 25–35, Institution of Civil Engineers (ICE), London, U.K.

Abstract: Recent military operations have highlighted the need for modernization of airfield damage repair capabilities. Damaged or distressed military airfield pavements, particularly PCC pavements, must be repaired using expedient methods and durable materials in order to minimize the time the pavement is removed from service and reduce or eliminate additional closure times for subsequent repairs. As a result of this need, extensive research was conducted to develop multiple concrete pavement repair techniques that could be applied across the full spectrum of military airfield repair operations. Developed methods included placing rapid-setting cementitious materials, foreign object debris covers, and precast concrete panels over various backfill materials. Newly developed backfill techniques included poured and injected polyurethane foams and dry-placed, rapid-setting flowable fill. The combination of these materials resulted in several new repair techniques that could return a damaged pavement to aircraft traffic within 4 to 6 hr after initiation of the repair. This paper summarizes the development of these repair technologies and describes their performances under accelerated pavement testing and aircraft validation tests. The paper also includes recommendations as to the suitability of each technique for specific operational scenarios, based on field evaluations.

[1] Research Civil Engineer, U.S. Army Engineer Research and Development Center, Vicksburg, MS 39180. Email:lucy.p.priddy@usace.army.mil.
[2] Research Civil Engineer, U.S. Army Engineer Research and Development Center, Vicksburg, MS 39180. Email:Jeb.S.Tingle@usace.army.mil.

6.1 Introduction

Since 2004, U.S. military researchers have been conducting research to develop new, expedient concrete pavement repair techniques in an effort to rapidly update repair guidance for military airfields. These pavements must be repaired with fast methods and durable materials to reduce the total time that the pavement is removed from service as well as to reduce the need to conduct subsequent repairs to maintain an operable pavement surface, especially during wartime scenarios.

In deployed locations, military aircraft may operate on damaged, abandoned, inadequately constructed, or minimally maintained airfields. To provide initial operational capability, temporary repairs, called expedient repairs, are first made by repair teams. Once operations have been established, the mission shifts into sustainment mode. Sustainment repairs, typically conducted with more durable materials than expedient repairs, are made to the airfield to allow continued aircraft missions. Permanent repairs, such as reconstruction or expansion of the airfield for longer operations, are then conducted. At a deployed location, the principal challenges are (1) completing repairs within a 4- to 6-hr timeframe and (2) having the repair resources available. All repair materials and equipment must be deployed with the repair teams for use with locally secured materials, if available. These challenges can result in hastily conducted repairs, such as compacted soil or aggregate with or without a foreign object debris (FOD) cover. These covers require frequent inspection to reduce the potential for damage to aircraft from FOD.

In non-deployed locations, airfield damage repair scenarios can also occur. If a permanent airfield is damaged due to munitions attack, the repair scenario is considered base recovery after attack. In this scenario, expedient repairs are used to re-establish operational capability. At a non-deployed location, the primary challenge is time (also 4 to 6 hr) because the airfield must be reopened quickly following an attack, but locally secured repair assets are readily available.

For either scenario, repairs must withstand numerous aircraft passes and ensure long-lasting repairs. The minimum acceptable pass levels defined for each operational scenario were 100 and 5,000 passes of the designated aircraft (either F-15 or C-17) for expedient and sustainment repairs,

respectively. For base recovery missions, a threshold of 3,700[1] passes with an objective of 5,000 passes was established. For permanent missions, the acceptable pass level depended on the mission requirements but was considered greater than 5,000 passes.

New materials have been developed that can be applied to overcome these pavement repair challenges at home bases or deployed locations. These materials were evaluated to determine suitability for incorporation into technical solutions that could be applied across the full spectrum of military operations while providing the safest, fastest, and longest-lasting pavement repairs.

6.2 Objective

The primary objective of this research was to identify the appropriate full-depth pavement repair technique(s) for military airfields. Each repair method was analyzed in terms of its performance, timing, and cost. This paper consists of a review of eight years of laboratory testing, accelerated pavement testing, and aircraft flight testing.

6.3 Materials

From 2004 to 2013, various materials were investigated to conduct full-depth repairs in airfield pavements. While the majority of this research was focused on repairing Portland cement concrete (PCC) pavements, the investigated methods showed versatility for PCC and asphalt concrete (AC) pavement surface types. The repair efforts focused on small repairs with damage expected to be less than 6.1 m (20 ft) in diameter but requiring full-depth repair, including removal and replacement of surface and sublayer materials. Replacement surface materials were called “capping” materials, and replacement sublayer materials were called “backfill” materials. Numerous materials were first investigated in laboratory and field investigations, and then the most promising repair materials and techniques were validated under aircraft flight testing. Brief descriptions of these investigations are provided in this section.

[1] This threshold has been reduced to 3,000 passes since the publication of this paper.

6.3.1 Capping materials

The capping materials investigated included rapid-setting proprietary materials, precast PCC panels, and FOD covers (also known as airfield mats). These materials were investigated to decrease total repair time and improve repair durability while reducing the logistical burden of transporting large quantities of materials to a deployed location. Brief descriptions are provided in this section.

6.3.1.1 Rapid-setting repair materials

Rapid-setting repair materials are generally categorized as cementitious or polymeric and provide short set times, high early strengths, and good durability. Since 2004, more than 70 proprietary rapid-setting repair materials have been evaluated for concrete airfield pavement repairs. Laboratory testing protocols (AFCESA 2008a, b) for selecting appropriate repair materials were developed as part of this research effort. Results of rapid-setting polymeric material testing (Mejias-Santiago et al. 2006) indicated that polymeric materials were best suited to small partial-depth repairs. Results of rapid-setting proprietary cementitious material investigations (Priddy and Rushing 2012), however, indicated that numerous repair products were applicable over a variety of repair sizes. Figure 6.1 presents the use of rapid-setting repair materials for full-scale field testing.

Figure 6.1. Placing rapid-setting cap.

6.3.1.2 Precast Portland cement concrete (PCC) panels

In 2011 and 2012, precast PCC panels were investigated to evaluate their performance when used for full-depth PCC pavement repairs. A reinforced precast panel repair system was designed to be used to conduct single- and multiple-panel repairs in concrete pavements. Each repair consisted of 27.9-cm-(11-in.-) thick precast panels doweled in the direction of traffic and placed over a layer of rapid-setting flowable fill (described later). Figure 6.2 presents completed precast panel repairs. As can be seen by the dark rectangular areas around the panels, dowel receptacles were saw cut in the surrounding pavement to re-establish load transfer. These areas were patched using a proprietary rapid-setting material.

6.3.1.3 Foreign object debris (FOD) covers

Deployable airfield mats (FOD covers) were investigated during 2006 and 2007 by Gartrell (2007). Unlike the previous materials presented, FOD covers typically provide minimal structural support for loading, as they simply cover a prepared aggregate backfill that supports the load. Covering the aggregate reduces the potential for FOD damage. Various matting systems have been investigated over the last 30 years but, in 2006, the U.S. military used two different FOD covers, folded fiberglass matting (FFM), and fiber-reinforced polyester matting (FRP). In 2006 and 2007, Gartrell (2007) concluded that a modified version of FRP matting with different anchoring systems for AC and PCC pavements provided the best FOD cover system for expedient repairs. Figure 6.3 shows an FRP repair.

6.3.2 Backfill materials

Traditional backfill materials for airfield repair include compacted aggregates or soils. Backfill research during this effort focused on alternative techniques to reduce repair time and eliminate the uncertainty in the quality of locally available backfill material at deployed locations. Various alternative backfill techniques have been investigated since 2006, including poured high-density polyurethane foam, injected high-density polyurethane foam, and rapid-setting flowable fill. Each technology is briefly described in this section.

Figure 6.2. Precast PCC panel repairs.

Figure 6.3. Modified FRP repair.

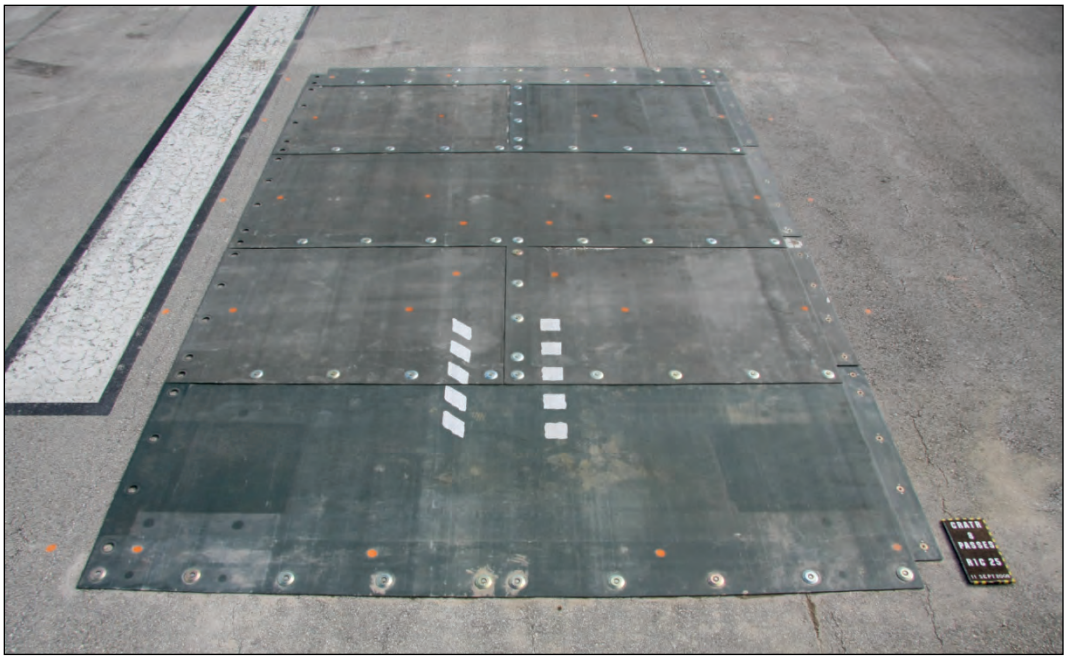

6.3.2.1 *Compacted aggregate*

From 2006 to 2008, compacted aggregate was investigated under rapid-setting caps (Priddy 2011) and FOD covers (Gartrell 2007). This concept of repair was to place and compact aggregate to reduce the required volume of rapid-setting concrete and to provide load-carrying capacity for FOD covers. Various aggregates were evaluated to identify performance differences with crushed angular stone providing the best performance. Results of field testing indicated that compacted aggregate backfill impeded rapid repair, particularly in deployed locations that may not have significant quantities of material or sufficient time to properly place and compact such material. As a result, new backfill methods were developed to determine if time savings could be gained through their use and whether or not the consequence of using a nontraditional backfill was acceptable for repair performance.

6.3.2.2 *Poured polyurethane foam*

During 2006 to 2010, pourable high-density polyurethane foams were investigated (Priddy et al. 2007a, 2010b; Priddy and Newman 2010) for use under a rapid-setting cap. The concept of this repair was to mix two-component foam and pour the material into a prepared repair area. The polyurethane foam precursor liquids could be shipped in relatively small containers, but the mixed material would expand to 4 to 10 times its liquid

volume. In deployed locations, expanding foam would eliminate the need for compacted aggregate while also reducing the volume of material that would have to be transported to complete the repair. Laboratory and field investigations indicated that the poured-foam materials were suitable for supporting a rapid-setting cap and aircraft traffic. The placement of foam and the hardened foam backfill are shown in Figures 6.4(a) and 6.4(b).

Figure 6.4. (a) Placing foam backfill and (b) hardened foam backfill after 15 min.

6.3.2.3 *Injected polyurethane foam*

In 2008 and 2009, high-density polyurethane foam was also investigated for an injection repair method (Priddy et al. 2010a) that allowed uncompacted pavement debris to be used as backfill. After placing a rapid-setting cap and allowing it to cure minimally, foam was injected through the surface layer into the backfill material to stabilize the debris and fill any voids. Like the poured polyurethane foam backfill, the expansive nature of the foam could be applied at a deployed location where quality backfill and/or time to compact aggregate may not be available.

6.3.2.4 *Dry-placed rapid-setting flowable fill*

From 2008 through 2011, rapid-setting flowable fill backfill materials were developed (Griffin et al. 2012) for use with rapid-setting caps. The concept of this repair was to place dry, preblended, proprietary rapid-setting flowable fill material into a prepared repair area requiring backfill. Researchers worked with rapid-setting repair-material vendors to develop airfield quality products for laboratory and field tests. This dry-placement method required adding water to the surface of the dry material, with no blending, to hydrate the cementitious materials within the mixture. The

backfill was placed and hydrated in thin layers of thicknesses no more than 50.8 to 76.2 cm (2 to 3 in.). The dry-placed flowable fill was paired with rapid-setting material caps for field testing. Figure 6.5 presents the steps involved in the dry-placement method.

Figure 6.5. (a) Prepared repair, (b) backfilling with flowable fill, (c) adding water, (d) cured backfill surface after 15 min.

6.4 Accelerated pavement testing and aircraft flight validation

Since 2006, more than 65 repairs conducted using the repair materials presented in the previous sections have been evaluated through full-scale field tests and repair demonstrations. The repair techniques were evaluated using accelerated pavement testing and aircraft flight validation tests. Load carts were used to simulate both C-17 and F-15 aircraft traffic. The multiple-wheel C-17 load cart used for these investigations matched the geometry and loading of one side of the main landing gear of a C-17, or a full set of six tires each inflated to 0.98 MPa (142 psi), supporting 102,512 kg (226,000 lb). The F-15 load cart was equipped with a single 2.2 MPa (325 psi) tire supporting approximately 16,023 kg (35,325 lb). Following accelerated traffic simulations, the most promising repair methods underwent flight validation testing using C-17 and F-15 aircraft. Figure 6.6 presents the load carts and aircraft used for these investigations.

Figure 6.6. (a) F-15 load cart, (b) C-17 load cart, (c) F-15 aircraft, and (d) C-17 aircraft.

6.4.1 Rapid-setting material cap over aggregate backfill

Twenty partial PCC slab replacements were conducted during 2006 and 2007 at the ERDC pavement testing facility in Vicksburg, MS. These repairs included dimensions of 1.5 by 1.5 by 0.46 m (5 by 5 by 1.5 ft), 2.4 by 2.4 by 0.91 m (8 by 8 by 3 ft), and 3 by 3 by 0.91 m (10 by 10 by 3 ft). Each repair was conducted with various proprietary rapid-setting materials placed over compacted aggregate backfills with California bearing ratio (CBR) values of at least 80% and was trafficked using an F-15 load cart within 2 to 3 hr after the proprietary caps were placed. The repairs were conducted in series with the best performing materials from the smallest repairs (12 materials) progressing to the next size repair (4 materials) and so on. The materials' performances varied under accelerated pavement testing. Results indicated that a 22.9-cm- (9-in.-) thick cap was capable of supporting more than 2,000 passes of simulated F-15 traffic without failing, and that a 25.4-cm- (10-in.-) thick cap over a compacted aggregate backfill of 80 CBR, or greater, was capable of supporting more than 5,000 passes of simulated F-15 traffic. Additional results of field testing are presented in Priddy (2011).

A single proprietary repair material was selected from this research for further testing.

Three additional partial PCC slab repairs were conducted in 2008 at the Silver Flag Training Facility, Tyndall Air Force Base, Panama City, FL. The repair sizes ranged from 2.4 to 4.0 m (8 to 13 ft) in length and 2.4 to 3.4 m (8 to 11 ft) in width. Each repair consisted of 61 cm (24 in.) of compacted crushed limestone backfill (80 to 100 CBR) and a 22.9- to 25.4-cm- (9- to 10-in.-) thick rapid-setting cap selected from the previous field testing. Each repair was trafficked with a combination of F-15 and C-17 simulated traffic, and test results indicated that the repairs were capable of supporting over 5,000 passes with only minor spalling produced along the repair edges during trafficking.

6.4.2 Rapid-setting material cap over poured-foam backfill

In 2008, the rapid-setting repair material selected from the previously described tests was tested as a cap over poured polyurethane foams in the same ERDC test area described previously. Four partial PCC slab replacements were conducted utilizing two sizes: 1.5 by 1.5 by 0.46 m (5 by 5 by 1.5 ft) and 2.4 by 2.4 by 0.91 m (8 by 8 by 3 ft) (2 repairs each). The tests indicated that the poured-foam backfill was suitable for supporting the rapid-setting materials, with repairs supporting over 1,000 passes of simulated F-15 traffic prior to failing. Additional results of field testing are presented in Priddy and Newman (2010).

An additional 15 poured-foam repairs were conducted during 2009 and 2010 at both the ERDC test area and the Silver Flag Training Facility. Repairs were conducted in both PCC (13 repairs) and AC (2 repairs) pavement sections and ranged from 1.5 to 5.8 m (5 to 19 ft) in width and length with the majority of the repairs having dimensions of approximately 3 by 3 by 0.91 m (10 by 10 by 3 ft). The cap thicknesses were 22.9 to 25.4 cm (9 to 10 in.) with 25.4 to 66.0 cm (10 to 26 in.) of foam backfill placed. Accelerated pavement testing during this time included both F-15 and C-17 traffic. Results of traffic testing indicated that the foam backfill paired with a 22.9- to 25.4-cm- (9- to 10-in.-) thick rapid-setting cap could support at least 1,000 passes of combined simulated F-15 and C-17 traffic prior to failing due to high-severity spalling and high FOD potential along the repair edges.

Based on these traffic results, the rapid-setting cap over poured-foam repair was recommended for validation under aircraft flight testing. In 2009, four poured-foam repairs were conducted in both PCC and AC pavements at Avon Park Air Force Auxiliary Field in Avon Park, FL. The four repairs varied from approximately 1.8 to 2.1 m (6 to 7 ft) in width and length and consisted of a 25.4-cm- (10-in.-) thick cap of proprietary rapid-setting material over 35.6 cm (14 in.) of poured foam. Results of the aircraft flight testing with both C-17 and F-15 aircraft indicated that this repair method was capable of supporting at least 169 combined aircraft passes with minimal distress. Additional aircraft testing was cost prohibitive.

6.4.3 Rapid-setting material cap over injected-foam backfill

In 2008, three partial PCC slab replacements using injected-foam backfill and the previously selected proprietary rapid-setting material cap were conducted at the ERDC test facility. The repair areas were 2.4 by 2.4 by 0.91 m (8 by 8 by 3 ft). The repairs were backfilled with a mixture of concrete rubble approximately 31 to 61 cm (12 to 24 in.) in diameter, aggregate, and soil debris generated from excavating the repair areas. The debris was placed into each repair area without any compaction, and 22.9-cm- (9-in.-) thick rapid-setting caps were immediately placed. Following a short cure time (1.5 hr), each repair was injected using high-density polyurethane foam and immediately trafficked. Results of F-15 load cart testing indicated that the injected repairs were capable of supporting between 1,500 and 2,000 passes prior to failure due to high-severity spalling and FOD production along repair edges. During field testing, it was determined that this repair technique relied upon sophisticated equipment and monitoring systems to minimize differential movement of the repair and surrounding pavement. If not monitored closely, cracking could occur in the repair and surrounding pavement. Additional details of this investigation are provided in Priddy et al. (2010a).

Based on the traffic results, the rapid-setting cap over injected-foam debris was further evaluated in 2008 at the Silver Flag Training Facility. Two repairs were conducted with sizes similar to those of the poured-foam repairs also conducted during this time. Results of simulated F-15 and C-17 traffic indicated that these repairs were capable of supporting at least 1,000 passes of combined aircraft traffic. This repair method was not included in the aircraft flight certification testing, but a separate flight experiment may be conducted in the future.

6.4.4 Rapid-setting material cap over dry-placed flowable fill backfill

In 2009, five repairs were conducted at the Silver Flag Training Facility. These repairs had geometries varying in length and width from 2.1 to 3.4 m (7 to 11 ft). Approximately 35.6 cm (14 in.) of flowable fill was placed using the dry-placement method, and the repair was capped with a 25.4-cm- (10-in.-) thick rapid-setting cap. The cap was the same used in the foam backfill placement studies. Results of simulated F-15 and C-17 traffic indicated that the dry-placed flowable fill backfill paired with a 25.4-cm- (10-in.-) thick cap could support more than 5,000 passes of combined simulated F-15 and C-17 traffic with only minor spalling along the repair edges noticed during testing. Additional details of this investigation are provided in Griffin et al. (2012).

Based on these traffic results, the rapid-setting cap over dry-placed flowable fill repair was recommended for validation under aircraft flight testing. In 2009, 12 repairs were conducted (5 in PCC and 7 in AC) at Avon Park, FL. The repairs varied from approximately 2.1 to 4.3 m (7 to 14 ft) in width and length and consisted of a 25.4-cm- (10-in.-) thick cap over 35.6 cm (14 in.) of flowable fill. Results of aircraft flight testing with both C-17 and F-15 aircraft indicated that this repair method was capable of supporting at least 169 combined aircraft passes with minimal distress. Additional aircraft testing was cost prohibitive.

6.4.5 Modified fiber-reinforced panels (FRP) over compacted aggregate backfill

In 2006, various FOD covers were investigated at the ERDC to evaluate the performance of different systems under simulated aircraft traffic. Results of this research (Gartrell 2007) indicated that the modified FRP system was the best mat for use with both C-17 and F-15 aircraft when placed over a compacted aggregate backfill with a CBR of 50 or more.

In 2008, four modified FRP repairs were conducted at the Silver Flag Training Facility in an AC pavement. Repairs were 3.7 to 4.0 m (12 to 13 ft) in length and 3.4 to 4.0 m (11 to 13 ft) in width, requiring 61 cm (24 in.) of crushed limestone backfill (CBR 80 to 100). Each repair was trafficked with an F-15 load cart for a minimum of 112 passes. At the end of trafficking, only minor rutting was noticed. Similar performance was expected in PCC pavement.

Based on these traffic results, the modified FRP method was recommended for validation under aircraft flight testing. In 2009, a single repair was conducted in an AC pavement at Avon Park, FL. The repair was approximately 5.8 m (19 ft) long and 4.9 m (16 ft) wide. The FRP was installed over 61 cm (24 in.) of compacted crushed aggregate. Results of the flight testing with both the C-17 and F-15 aircraft indicated that this repair method was capable of supporting at least 169 combined aircraft passes with a moderate level of repair distress. As with the previous repairs, additional aircraft testing was cost prohibitive.

6.4.6 Precast Portland cement concrete (PCC) panels over flowable fill backfill

In 2011 and 2012, precast PCC panels were investigated to evaluate their performance for full-depth PCC repairs. Repairs were conducted in a full-scale field test, including one single-panel and two multiple-panel repairs using precast panels designed in this research effort. Each repair consisted of 27.9-cm- (11-in.-) thick precast reinforced panels doweled in the direction of traffic and placed over flowable fill. A single-panel repair was used to replace a 3 by 3 m (10 by 10 ft) corner portion of a 6.1-m (20-ft) square slab, two 3- by 3-m (10- by 10-ft) panels were used to conduct a half-slab replacement, and four 3- by 3-m (10- by 10-ft) panels were used to conduct a connected full-slab replacement. Results of simulated C-17 trafficking indicated that these repairs were capable of supporting at least 5,000 passes of traffic and as many as 10,000 passes prior to failure. Aircraft validation testing was not conducted with this repair type, as it was developed after the aircraft testing in 2009. It is recommended that such testing be considered in the future.

6.5 Comparison of repair methods

In selecting an appropriate method for repairing a damaged or distressed airfield pavement, the repair performance, speed of return to traffic, and cost are the primary factors to consider. Each of these factors is explored in the following sections. Based on these analyses, decisions as to where these repair techniques may best be applied were made.

6.5.1 Performance

Based on the full-scale field testing, all repair methods could support at least 100 passes of aircraft traffic under accelerated testing. This indicates

that all five methods can meet the expedient repair pass criterion described earlier in this paper. Three of these repair methods were validated under aircraft flight testing as being able to withstand more than 100 passes of actual aircraft maneuvers. Although the injected repair method was not validated under aircraft flight testing, the accelerated testing indicated that it can withstand at least 1,000 passes. The precast panel repair type was developed after the flight testing and was thus not validated under actual aircraft. However, field testing indicated that the panels could support at least 5,000 passes of C-17 traffic.

Repairs conducted using a rapid-setting cap over compacted aggregate or flowable fill or a precast panel over flowable fill met the 3,700-pass criterion for base recovery operations and 5,000-pass sustainment pass criterion. A minimum of a 25.4-cm- (10-in.-) thick cap was recommended for the rapid-setting cap repair types. A minimum of a 27.9-cm- (11-in.-) thick precast panel was recommended for the precast repair method. The rapid-setting capped repairs after 5,000 passes showed only minor spalling along the repair edges, indicating that these repairs could withstand many more passes prior to failing. This suggests that use of the rapid-setting material over compacted aggregate or flowable fill could potentially be suitable for permanent repairs. For the precast panels, spalling along the loaded edges was noted particularly around the patched dowel receptacles when trafficked with the C-17 load cart. This repair type was capable of supporting between 5,000 and 10,000 passes of C-17 traffic; however, the condition of the repairs as a result of trafficking varied in field testing.

6.5.2 Speed of return to traffic

During field testing, the time required to complete each repair was recorded. The required time to complete a repair included the tasks of repair area preparation (removal of damaged pavement and excavation and removal of sublayer materials), backfilling, and capping the repair. Capping time also included a minimum 2-hr cure for the rapid-setting concrete prior to the return to aircraft traffic.

Repair times for a wide variety of repair sizes indicate that all methods except the FRP-crushed aggregate repair and the precast panel repairs could be conducted within a 4- to 6-hr repair window based on averages shown in Table 6.1. This table shows that the fastest repair method was the flowable fill backfilled repair (3.3 hr) with the injected- and poured-foam

repairs providing similar repair times (3.8 and 4.0 hr, respectively). These repairs were relatively small, with average lengths and widths of repairs around 3 m by 3 m (10 ft by 10 ft).

Table 6.1. Average repair time for field testing results for varying repair sizes.

Repair Type	Repairs, No.	Average Repair Volume, m^3 (ft^3)	Repair Area Prep, hr	Backfill, hr	Cap, hr	Total, hr
Rapid-Setting Cap/Compacted Aggregate	3	8.2 (291)	1.3	1.2	2.7	5.2
Rapid-Setting Cap/Poured Foam	19	5.9 (207)	0.6	0.5	2.9	4.0
Rapid-Setting Cap/Injected Foam	8	5.8 (206)	1.2	0.2	2.4	3.8
Rapid-Setting Cap/Rapid-Setting Flowable Fill	20	4.1 (144)	0.7	0.2	2.4	3.3
Precast Panel/Flowable Fill	3	7.7 (272)	3.4	0.3	3.8	7.5
FRP/Compacted Aggregate	3	8.7 (307)	2.5	2.2	2.9	7.6

The times to conduct precast panel repairs were 4.73 hr (1 panel), 7.47 hr (2 panels), and 10.15 hr (4 panels) with an average time of 7.5 hr. It is expected that efficiencies would be gained with an experienced field placement crew and through repair process refinements. Single-panel repairs are anticipated to require less than 5 hr to complete. Until such refinements are made, if large multiple-panel repairs are required, another repair method should be used.

Because the repair sizes and material volumes varied, an additional analysis was conducted to calculate the time required to complete a full-depth repair with average dimensions of 3 m by 3 m by 0.6 m (10 ft by 10 ft by 2 ft) with component thicknesses shown in Figure 6.7. Repair time was calculated by dividing the time to complete each repair task (area prep, backfilling, and capping) by the average volume prepared in each task as recorded during field testing. This number was then used to estimate the cost per repair task for the same-sized repair. The results are presented in Figure 6.8 and show similar repair preparation and rapid-setting capping times but show differences in backfilling times.

Figure 6.7. Repair schematics.

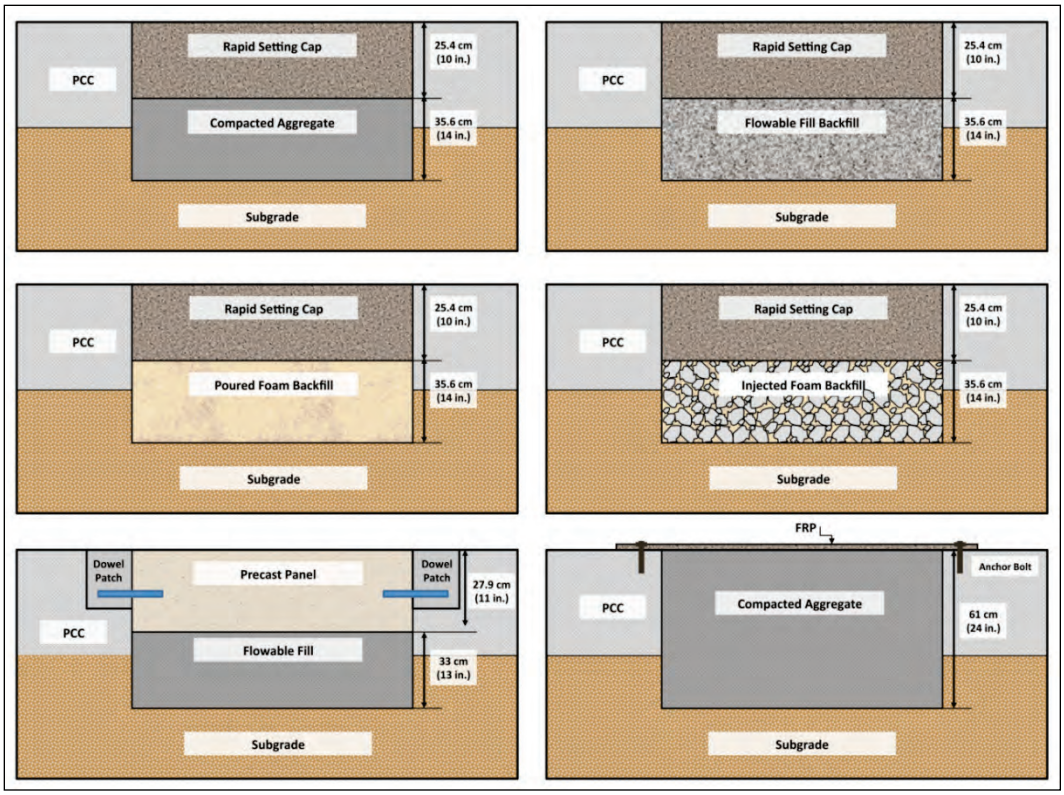

Figure 6.8. Comparison of time to complete steps to conduct a 3-m by 3-m by 0.6-m repair.

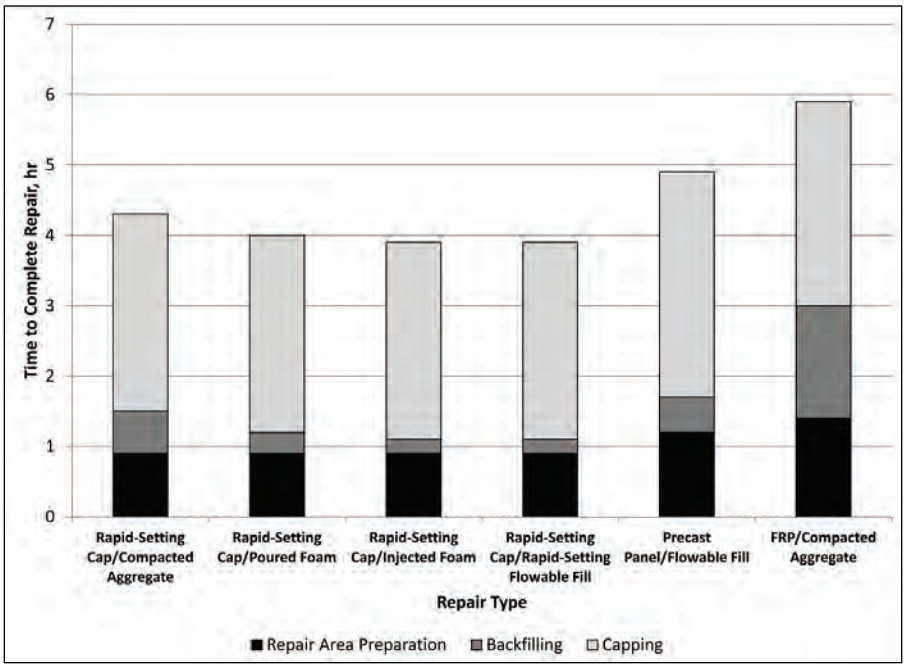

Area prep time was longer for the precast panels compared to the rapid-setting capped repairs due to the need to saw cut dowel receptacles in the parent PCC pavement. The FRP prep time was the largest due to need for careful excavation of the repair area. In contrast, the flowable fill and foam backfills required less careful excavation, as they did not rely on compacted aggregate for support. The need to place and cure rapid-setting repair material in the precast panel dowel receptacles accounted for the longer capping time for this repair compared to the rapid-setting capped repairs. The repair requiring the longest backfilling time was the FRP repair, which is not surprising because the FRP repair required backfilling a larger volume with careful compaction of the aggregate backfill for the structural support of the repair. Based on this analysis, all of the repair methods applied to small repairs could return the airfield to service within the 4- to 6-hr time window, indicating that they were all suitable for any of the operational repair scenarios.

6.5.3 Cost

The cost to conduct a 3-m by 3-m by 0.6-m (10-ft by 10-ft by 2-ft) repair with each repair method was calculated using material costs only. Material costs were based on 2011-2012 pricing for materials. Table 6.2 presents the estimated costs for the backfill and capping materials. The least expensive repair option for this repair size was the rapid-setting cap over aggregate followed by the precast panel over flowable fill. The cost of flowable fill for the precast panel was less than that for the dry-placed rapid-setting flowable fill paired with the rapid-setting cap, as it was locally available and not a proprietary rapid-setting blend. As shown in the table, the FRP repair was the most costly repair, and the price reflected in the table is roughly one-half the cost of an FRP kit, as only a portion of the kit options would be required; however, this kit is reusable. The poured-foam repair was also very costly compared to the flowable fill or aggregate backfilled options with the same rapid-setting cap cost. The injected-foam cost was also much higher compared to the compacted aggregate and flowable fill backfilled repairs with the rapid-setting cap but was lower than the poured-foam backfilled option, because debris was used to backfill the repairs at no cost and because the debris reduced the amount of foam needed to fill the volume. Thus, the cost of backfill was only the cost of foam required to be injected. It is important to note that specialized equipment was needed to inject the foam and to mix and place large volumes of pourable foam. Those costs were not included in these estimates.

Table 6.2. Estimated costs to conduct a 3-m by 3-m by 0.6-m (10-ft by 10-ft by 2-ft) repair.

Repair Type[a]	Backfill Cost	Capping Cost	Total Cost
Rapid-Setting Cap/Compacted Aggregate	$205	$1,360	$1,565
Rapid-Setting Cap/Rapid-Setting Flowable Fill	$1,900	$1,360	$3,260
Rapid-Setting Cap/Injected Foam	$4,700	$1,360	$6,060
Rapid-Setting Cap/Poured Foam	$4,735[b]	$1,360	$6,095
Precast Panel/Flowable Fill	$320	$2,260	$2,580
FRP/Compacted Aggregate	$355	$16,335[c]	$16,690

[a] See Figure 6.7 for repair schematics.

[b] Cost of 1/3 of a 500-gal foam kit

[c] Cost of 1/2 an FRP kit (FRP kit items are reusable.)

6.5.4 Repair summary

Table 6.3 compares the performance, speed, and estimated cost to repair a 3-m by 3-m by 0.6-m (10-ft by 10-ft by 2-ft) repair area. Repairs with the highest performance and fastest return to traffic were the rapid-setting cap with flowable fill followed by the rapid-setting cap with compacted aggregate. In terms of cost, the rapid-setting cap with compacted aggregate repair was the least expensive followed by the precast panel repair. The use of a rapid-setting cap with either compacted aggregate or flowable fill may be best suited for traditional airfield repairs where timing, speed, and cost are the key factors. For deployed airfield repairs, cost can be important, particularly when all materials and equipment to complete a repair must be brought to the airfield. However, in these instances, speed or material deployability (low logistical footprint) may control the decision making. In these cases, the use of either foam backfill method may be more suitable, particularly since the foam reduces the volume of material that must be brought to the site. The performance of both of these methods should exceed the current expedient repair pass criterion of 100 passes by a factor of 10. The use of FRP is also still applicable for expeditionary environments, particularly in cases where the airfield will be used for only very short periods of time or when it is logistically impossible to obtain materials for other repair methods. FRP also has a much smaller logistical footprint than foam and rapid-setting materials and is reusable. Therefore, it has been proposed that this method could be used to supplement other repair methods by applying those other repair methods to the most critical areas first, such as providing an initial operational capability, then using FRP where aircraft traffic applications will be limited. Recommended applications for each repair type are presented in Table 6.3.

Table 6.3. Comparison of repair methods.

Repair Type	Passes to Failure, #	Time to Complete Repair[a], hr	Estimated Material Cost	Recommended Application
Rapid-Setting Cap/ Compacted Aggregate	5,000+	4.3	$1,565	Base Recovery Sustainment Repairs Permanent Repairs
Rapid-Setting Cap/ Poured Foam	1,000	4.0	$6,095	Expedient Repairs
Rapid-Setting Cap/ Injected Foam	1,000	3.9	$6,060	Expedient Repairs
Rapid-Setting Cap/ Rapid-Setting Flowable Fill	5,000+	3.9	$3,260	Base Recovery Sustainment Repairs Permanent Repairs
Precast Panel/Flowable Fill	5,000+	4.9[b]	$2,580	Base Recovery Sustainment Repairs Permanent Repairs
FRP/Compacted Aggregate	100	5.4[b]	$16,690	Expedient Repairs Non-critical Repair Areas

[a] Time to complete a 3-m by 3-m by 0.6-m (10-ft by 10-ft by 2-ft) repair.

[b] Time to complete a larger repair is expected to take more than 6 hr.

6.6 Summary and conclusions

Extensive research to update the military's concrete airfield pavement repair methods has been conducted over the last eight years. The following achievements are noted:

- Six repair methods were developed that could be applied across the full spectrum of military airfield operations, including expedient repairs at deployed locations, sustainment repairs at forward operating bases, and base recovery after attack scenarios.
- Three repair methods using new repair materials were validated for aircraft compatibility under aircraft flight testing, and all repair methods were investigated under accelerated pavement testing.
- Selection criteria for proprietary rapid-setting repair materials were developed to help reduce the potential for selection of a faulty repair product.
- All repairs can be completed within 4 to 6 hr when conducting repair sizes up to 3 m by 3 m by 0.6 m (10 ft by 10 ft by 2 ft).
- Larger repairs will require up to 8 hr for the FRP repairs and up to 10 hr for a 6.1-m by 6.1-m (20 ft by 20- ft) precast panel repair.

- The least expensive repair method was the rapid-setting cap over compacted aggregate, and the most expensive repair was the FRP over aggregate.

6.7 Acknowledgments

The tests and the resulting data presented herein resulted from research sponsored by Headquarters, Air Combat Command; Headquarters, Department of the Navy, Office of Naval Research, Rapid Technology Transition Office; and the U.S. Air Force Civil Engineer Center. The tests, unless otherwise noted, were performed at the U.S. Army Engineer Research and Development Center, Vicksburg, MS, site. Permission to publish this information was granted by the Director, Geotechnical and Structures Laboratory.

6.8 Practical relevance and potential applications

Adequate airfield facilities are undeniably vital to the success of a military mission. Repairing substandard ones in critical locations can reduce the time and costs required to complete an operation. The technologies developed as a result of this research have provided tools to offer simpler, faster airfield repairs that can be applied across the full spectrum of military operations. While originally developed for military airfield pavements, these technologies are also applicable for non-military and non-airfield pavements, including highway pavements that have similar limitations in the time available to complete repairs.

7 Conclusions and Recommendations

7.1 Summary

This research explored the suitability of using precast panel technology to conduct expedient airfield pavement repairs. A single-panel repair precast system originally developed for the U.S. Air Force was identified as the most applicable technology for investigation, but it required modification to accommodate both single- and multiple-panel repairs and to support heavy aircraft traffic. Several panels were fabricated and were used to conduct single- and multiple-panel repairs in a full-scale airfield pavement test section. Timed tests were conducted to determine whether the modified panel system required additional adjustments to improve the efficiency of placement and/or the performance of the repairs. Accelerated pavement testing was conducted to understand the panel repairs' performances under simulated aircraft traffic and to determine whether the panels could support the threshold and objective pass levels of 3,000 and 5,000 passes, respectively.

Pavement responses, including deflections and stresses, were measured during field testing, using instrumentation and nondestructive testing procedures. Performance of the different repairs was reported in terms of the number of passes each withstood prior to failure and their mechanical responses to traffic loads. Distresses occurring during trafficking were recorded to show the progression of failure for the panels. The load transfer characteristics of the repair joints were also evaluated using nondestructive test methods to monitor joint effectiveness for the various repair joint types used for single- and multiple-panel repairs. A complementary FEM study was used to extrapolate field and laboratory experimental results to develop recommendations for improving the precast panel design. Based on the results of field testing and modeling efforts, recommendations are made to improve the panel repair performance through modifications to the design and placement procedures. Finally, the cost, speed, and performance of the precast repair method are compared to other expedient airfield pavement repair methods to identify the appropriate applications of the precast panel repair system.

7.2 Findings

The major findings of the research include the following:

- The airfield precast panel system was suitable for the intended temporary military repair application. Both single- and multiple-panel repairs could withstand the required aircraft passes and could be completed within 4 to 10 hr, depending on repair size.
- Accelerated testing of the repairs showed that joint spalling of the doweled transverse joints led to the failure of the panel repairs. While other distresses were identified during testing, the severe deterioration of the doweled joints presented the highest FOD potential. The development of these distresses indicated that the current panel design did not provide adequate load transfer. Additionally, the method of sealing the joints with the dowel-slot grout most likely contributed to the failure of the transverse joints. The absence of distresses along the longitudinal joints indicated that as long as traffic is applied only in the longitudinal direction, no load transfer devices are required for the longitudinal joints.
- Nondestructive test results were used to determine load transfer characteristics of each joint and thereby whether nondestructive testing could be used to monitor joint effectiveness and to predict joint deterioration. No criteria for load transfer effectiveness were applicable for predicting the joint deterioration, likely due to the current repair installation procedure; and additional tests are required to determine minimum thresholds. The use of differential deflections is promising, and a threshold of 5 mils may be appropriate for doweled transverse joints.
- Modeling efforts were used to identify the most critical load case for the transverse doweled joint and the resulting responses of the dowel and surrounding concrete to static simulated aircraft loads. Results of this study show that the compressive and tensile stresses measured in the concrete surrounding the dowels exceed the compressive and/or the tensile strengths for the dowel patching material for many of the load cases examined. With repeated loading, both compressive and tensile failure of the grout surrounding the dowel occurred. Modeling results show that increasing the dowel diameter will reduce the stresses generated in the concrete at the dowel interface. By minimizing the compressive and tensile stresses around the dowels, the repair life may be extended. Improvements to the panel design and placement procedures based on the full-scale field tests and modeling effort can

improve the panel performance and could result in longer-lasting pavement repairs.

- Finally, the precast panel repair system provides comparable performance to current expedient PCC repair methods using rapid-setting and high-early strength concretes. In terms of cost, the precast panel method was more expensive than rapid-setting and high-early strength PCC repairs; however costs may be reduced if the panels are produced in a precast facility or if a less expensive dowel grout is used. Finally, in terms of timing, small repairs made using precast panels may be completed in similar timeframes to other expedient repair methods, but larger repairs require up to 10 hr. Modification of the placement procedure and a more experienced repair team could improve repair timing.

7.3 Conclusions

This research shows that precast panel technology can successfully be applied for expedient airfield pavement repair efforts, and repairs conducted using this technology perform reasonably well under complex aircraft loads. Despite the limitations identified in the current precast panel system, the repair method provides an additional repair alternative to cast-in-place PCC. This repair method, in its current form, can be used for temporary repair of airfields and can be used to return an airfield to service within 4 to 10 hr from initiation of repair, depending on the number of panels required to complete the repair. In lieu of costly additional field tests, a complementary FEM study was used to extrapolate field and laboratory experimental results to develop recommendations for improving the precast panel design. Based on the results of field testing and modeling efforts, the panel performance can likely be enhanced by using a larger diameter dowel to reduce the stress states in the concrete surrounding the dowels.

7.4 Impact

This report provides a comprehensive analysis of precast panel technology for airfield pavement repair applications providing design, installation, timing, and performance data not available in the literature. Real data were analyzed from a full-scale airfield test section constructed specifically to determine the precast panel repair life under complex, heavy aircraft loadings. These data were used to develop a 3-D FEM that can be utilized to evaluate additional panel designs for future repair efforts. Though the precast panel repair method was developed for military airfield

pavements, this method shows potential for application at non-military airfields and for non-airfield pavement repairs, including highway pavements that have similar limitations in the time available to complete repairs. While the repair process and panel design can be enhanced through modifications, the general repair process and design show a step forward in providing an alternative to cast-in-place PCC.

7.5 Recommendations for future research

It is recommended that the precast panel technology presented in this report be further investigated in full-scale field tests and under actual aircraft loadings. Modifications to the panel repair method are recommended: increasing the dowel diameter, preventing dowel grout from entering the repair joints, and evaluating the use of different grout materials to determine whether their use might result in increased pavement repair life. Additional full-scale repairs are also recommended to determine the optimum team size, appropriate equipment requirements, and total time required for returning the airfield to service following both single- and multiple-panel repairs. Benefits from conducting multiple start-to-finish repairs will reveal the true time restrictions for a variety of repair sizes. A military repair team should also be used to conduct repairs using the modified system to identify any deficiencies in the design of the panels or their placement methods. Additionally, aircraft flight testing is recommended to validate this repair technique for military repair use.

Results of the modeling effort also show that differences in the material properties between the parent slab PCC and the dowel-slot grout impact the stresses surrounding the concrete dowels and should be considered to fully understand the state of stress in the doweled areas. Because the models used in this study focused on the joint and static load conditions, additional modeling is recommended to understand the mechanical response of full-sized single and multiple panel repairs under dynamic loading conditions.

Another area recommended for further investigation is commercial precast technology. Commercial technologies allow custom-built slabs and proprietary, precision equipment for both airfield repair and construction. Specific advantages of commercial technology include possible reduced cost and higher-quality panels constructed in a controlled environment. Despite these benefits, limitations on the use of precast technology for large slab replacements, such as difficulty in transporting large, thick

panels from the precasting facility to the construction site and the requirement for a large crane, could still exist. These limitations need to be considered and addressed so that versatile repair methods may be identified and verified as suitable for airfield repairs.

References

AASHTO. 1993. *AASHTO guide for design of pavement structures*. Washington, DC: American Association of State Highway and Transportation Officials.

ACI Committee 318. 2011. *Building code requirements for structural concrete and commentary*. ACI 318-11. Farmington Hills, MI: American Concrete Institute.

AFCESA. 2008a. *Testing protocol for rigid spall repair materials.* ETL 08-02. Tyndall Air Force Base, FL: Air Force Civil Engineer Support Agency.

_____. 2008b. *Testing protocol for polymeric spall repair materials*. ETL 08-04. Tyndall Air Force Base, FL: Air Force Civil Engineer Support Agency.

Ashish, W., Y. Mehta, D. Cleary, E. Guo, L. Musumeci, A. Zapata, and W. Kettleson. 2011. Load transfer efficiencies of rigid airfield pavement joints based on stresses and deflections. *Journal of Materials in Civil Engineering* 23(8): 1171–1180.

Ashtiani, R., C. Jackson, A. Saeed, and M. Hammons. 2010. *Precast concrete panels for contingency rigid airfield pavement repairs*. AFRL Technical Report AFRL-RX-TY-TR-2010-0095. Tyndall Air Force Base, FL: U.S. Air Force Research Laboratory.

Ashtiani, R., A. Saeed, and M. I. Hammons. 2011. Precast concrete panels for rapid repair of airfield rigid pavements. In *Transportation Research Board 90th Annual Meeting Compendium of Papers*. Washington, DC: Transportation Research Board of the National Academies.

Bayrak, M. B., and H. Ceylan. 2008. Neural network-based approach for analysis of rigid pavement systems using deflection data. *Transportation Research Record* 2068(1): 61–70.

Bhatti, M. A., I. Molinas-Vega, and J. W. Stoner. 1998. Nonlinear analysis of jointed concrete pavements. *Transportation Research Record* 1629(1): 50–57.

Bly, P. G., L. P. Priddy, C. J. Jackson, and Q. S. Mason. 2013. *Evaluation of precast panels for airfield pavement repair, Phase I: System optimization and test section construction*. ERDC/GSL TR-13-24. Vicksburg, MS: U.S. Army Engineer Research and Development Center.

Brabston, W. N. 1984. *Bomb damage repair: Precast slab design*. Accession Number ADA141687. Vicksburg, MS: U.S. Army Engineer Waterways Experiment Station.

Bradbury, R. D. 1938. *Reinforced concrete pavements*. Washington, DC: Wire Reinforcement Institute.

Brill, D. R. 1998. *Development of advanced computational models for airport pavement design*. FAA Technical Report DOT/FAA/AR-97/47. Washington, DC: Department of Transportation.

Buch, N., V. Barnhart, and R. Kowli. 2003. Pre-cast concrete slabs as full-depth repairs (FDR)-Michigan experience. In *Transportation Research Board 2003 Annual Meeting Compendium of Papers*. Washington, DC: Transportation Research Board of the National Academies.

Buch, N., A. H. Varma, and M. L. Prabhu. 2007. *Analytical investigation of the effects of aligned dowel bars coated with corrosive protective systems on initial dowel concrete bond stresses*. MDOT RC-1488. Lansing, MI: Michigan Department of Transportation.

Bull, J. W. 1986. An analytical solution to the design of precast concrete pavements. *International Journal for Numerical and Analytical Methods in Geomechanics* 10(2): 115–123.

Bull, J. W., and A. Singh. 1990. A comparison between the stresses computed for finite sized precast concrete pavement units using Westergaard's equations and a numerical design method. *Computers and Geotechnics* 9(4): 325–340.

Bull, J. W., and C. H. Woodford. 1997. Design of precast concrete pavement units for rapid maintenance of runways. *Computers & Structures* 64(1): 857–864.

Caliendo, C., and A. Parisi. 2010. Stress-prediction model for airport pavements with jointed concrete slabs. *Journal of Transportation Engineering* 136(7): 664–677.

Chen, Y. S., S. D. Murrell, and E. Larrazabal. 2003. Precast concrete (PC) pavement tests on Taxiway D-D at LaGuardia Airport. In *2003 Proceedings Airfield Pavements Specialty Conference, September 2003, Las Vegas, NV*.

Colley, B. E., and H. A. Humphrey. 1967. Aggregate interlock at joints in concrete pavements. *Highway Research Record* 189(1): 1–18.

Cook, R. D. 1995. *Finite element modeling for stress analysis*. New York, NY: Wiley.

Creech, M. F. 1975. Partial depth precast concrete patching. *Transportation Research Record* 554(1): 62–72.

Davids, W. G., G. M. Turkiyyah, and J. P. Mahoney. 1998. EVERFE rigid pavement three-dimensional finite element analysis tool. *Transportation Research Record* 1629(1): 41–49.

Davis, B. M. 2006. *Evaluation of prestress losses in an innovative prestressed precast pavement system*. MS thesis, University of Missouri–Columbia.

Embacher, R. A., and M. B. Snyder. 1999. Minne-ALF project overview and results of tests of PCC slab specimens containing retrofit dowels. In *Proceedings of the 1999 Accelerated Pavement Testing Conference, October 1999, Reno, NV*.

Farrington, R., W. C. Rovesti, D. Steiner, and W. J. Switzer. 2003. Overnight concrete pavement replacement using a precast panel and expanding polymer positioning technique - Washington Dulles International Airport case study. In *2003 Proceedings Airfield Pavements Specialty Conference, September 2003, Las Vegas, NV*.

FHWA. 2007. *Precast concrete panel systems for full depth pavement repairs field trials*. FHWA-HIF-07-019. Washington, DC: Federal Highway Administration.

Fort Miller Co. 2003. An overview of the super-slab system. www.superslab.com.

Foxworthy, P. T. 1985. *Concepts for the development of a nondestructive testing and evaluation system for rigid airfield pavements*. PhD diss., University of Illinois.

Frabizzio, M. A., and N. J. Buch. 1999. Performance of transverse cracking in jointed concrete pavements. *Journal of Performance of Constructed Facilities* 13(4): 172–180.

Friberg, B. F. 1940. Design of dowels in transverse joints of concrete pavements. *Transactions of the American Society of Civil Engineers* 105(1): 1076–1095.

Gartrell, C. A. 2007. *Investigations for airfield damage repair kit modifications and improvements*. ERDC/GSL TR-07-16. Vicksburg, MS: U.S. Army Engineer Research and Development Center.

Green Link. 2010. Removable urban pavement. http://green-link.info/post/removable-urban-pavement.

Griffin, J. R., L. P. Priddy, and D. W. Pittman. 2012. Properties of modern flowable fill incorporating rapid-setting cements. In *Commendation of Papers CD, International Society of Concrete Pavements 10th International Conference, July 2012, Quebec, Canada*.

Grimsley, R. F., and B. G. Morris. 1975. *An approach to concrete pavement replacement that minimizes disruption of traffic*. Special Report 153, 107–110. Washington, DC: Transportation Research Board of the National Academies.

Guo, E. H. 2003. Proof and comments on extensively used assumption in PCC pavement analysis and evaluation. *Journal of Transportation Engineering* 129(2): 219–220.

Guo, H., J. A. Sherwood, and M. B. Snyder. 1995. Component dowel–bar model for load–transfer systems in PCC pavements. *Journal of Transportation Engineering* 121(3): 289–298.

Hachiya, Y. 2001. Rapid repair with precast prestressed concrete slab pavements using compression joint system. In *Proceedings 7th International Conference on Concrete Pavements*. Orlando, FL: International Society for Concrete Pavements.

Hachiya, Y., F. Akamine, O. Takahashi, and Y. Miyaji. 2001. Rapid repair with precast prestressed concrete slab pavements using compression joint system. In *Proceedings, 7th International Conference on Concrete Pavements, (Vol. 2)*, 891–905. College Station, TX: International Society for Concrete Pavements.

Hammons, M. I. 1998. *Advanced pavement design: Finite element modeling for rigid pavement joints, Report II: Model development*. FAA Technical Report DOT/FAA/AR-97/7. Washington, DC: Department of Transportation.

Hammons, M. I., and A. M. Ioannides. 1997. *Advanced pavement design: Finite element modeling for rigid pavement joints. Report 1: Background Investigation*. FAA Technical Report DOT/FAA/AR-95/85. Washington, DC: U.S. Department of Transportation.

Hammons, M. I., and A. Saeed. 2010. Expedient spall repair methods and equipment for airfield pavements. *Transportation Research Record* 2155(1)*:* 63–70.

Hammons, M. I., D. W. Pittman, and D. D. Mathews. 1995. *Effectiveness of load transfer devices*. U.S. DOT/FAA/AR-95/80. Springfield, VA: Federal Aviation Administration.

Hiller, J. E., and N. Buch. 2004. Assessment of retrofit dowel benefits in cracked portland cement concrete pavements. *Journal of Performance of Constructed Facilities* 18(1): 29–35.

Hillerborg, A., M. Modeer, and P. E. Petersson. 1976. Analysis of crack formation and crack growth in concrete by means of fracture mechanics and finite elements. *Cement and Concrete Research* 6(1): 773–782.

Hoffman, M. S., and M. R. Thompson. 1981. *Mechanistic interpretation of nondestructive pavement testing deflections*. Transportation Engineering Series No. 32, Illinois Cooperative Highway and Transportation Research Program Series No. 190. Urbana, IL: University of Illinois.

Hossain, S., C. Ozyildirim, and T. R. Tate. 2006. *Evaluation of precast patches onU.S.60 near the New Kent and James City county line*. Charlottesville, VA: Virginia Research Council.

Houben, L. J. M., M. Huurman, and J. van der Kooij. 2004a. APT testing and 3D finite element analysis of 'Modieslab' modular pavement structures. In *Proceedings of the 2nd International Conference on Accelerated Pavement Testing, September 2004, Minneapolis, MN*.

Houben, L. J. M., S. Poot, M. Huurman, and J. van der Kooij. 2004b. Developments on the ModieSlab innovative concrete pavement concept. In *Proceedings of the 9th International Symposium on Concrete Roads, April 2004, Istanbul, Turkey*.

Huang, Y. H. 1985. A computer package for structural analysis of concrete pavements. In *Proceedings, 3rd International Conference on Concrete Pavement Design and Rehabilitation*. West Lafayette, IN: Purdue University.

_____. 2004. *Pavement analysis and design*. Englewood Cliffs, NJ: Prentice Hall.

Ioannides, A. M., and G. T. Korovesis. 1990. Aggregate interlock: a pure-shear load transfer mechanism. *Transportation Research Record* 1286(1): 14–24.

_____. 1992. Analysis and design of doweled slab-on-grade pavement system. *Journal of Transportation Engineering* 118(6): 745–768.

Khazanovich, L., K. Hoegh, and M. B. Snyder. 2009. *Guidelines for dowel alignment in concrete pavements*. NCHRP Report No. 637. Washington, DC: Transportation Research Board of the National Academies.

Kim, J., and K. D. Hjelmstad. 2003. Three-dimensional finite element analysis of doweled joints for airport pavements. *Transportation Research Record* 1853(1): 100–109.

Kim, Y. R. 2001. *Assessing pavement layer condition using deflection data*. National Cooperative Highway Research Program No. 254. Washington, DC: Transportation Research Board of the National Academies.

Kohler, L., L. du Plessis, J. Harvey, and L. Motumah. 2009. Comparison of precast and cast in-place concrete pavement responses under heavy vehicle simulator loads. In *Proceedings of the 8th International Conference on Bearing Capacity of Roads, Railways, and Airfields, June–July 2009*. Champaign, IL: University of Illinois at Urbana—Champaign.

Kohler, E., L. du Plessis, P. J. Smith, J. Harvey, and T. Pyle. 2007. Precast concrete pavements and results of accelerated traffic load test. In *Proceedings of the 2007 International Conference on Optimizing Paving Concrete Mixtures and Accelerated Concrete Pavement Construction and Rehabilitation, November 2007, Atlanta, GA.*

Korovesis, G. T. 1990. *Analysis of slab-on-grade pavement systems subjected to wheel and temperature loadings*. PhD diss., University of Illinois.

Kwik Slab. 2011. *Kwik Slab*. www.kwiklab.com.

Lee, J., and G. L. Fenves. 1998. Plastic-damage model for cyclic loading of concrete structures. *Journal of Engineering Mechanics* 124(8): 892–900.

Lee, Y. H., H. T. Wu, and S. T. Yen. 2004. Parameter studies and verifications on three-dimensional finite element analysis of rigid pavements. *Canadian Journal of Civil Engineering* 31(5): 782–796.

Liu, W., J. M. Ling, and H. D. Zhao. 2007. Analysis on mechanical responses of rigid airport pavement with load transfer of joints. *Journal of Highway and Transportation Research and Development* 12(5).

Lubliner, J., J. Oliver, S. Oller, and E. Onate. 1989. A plastic-damage model for concrete. *International Journal of Solids and Structures* 25(3): 299–326.

Mejias-Santiago, M., F. Del Valle, and L. P. Priddy. 2006. *Certification tests on cold patch asphalt repair materials for use in airfield pavements*. ERDC/GSL TR-10-06. Vicksburg, MS: U.S. Army Engineer Research and Development Center.

MnDOT Office of Construction and Innovative Contracting. 2005. *Installation of precast concrete pavement panels on TH62.* Minnesota Department of Transportation.

Nishizawa, T. 2008. *Japanese experience of precast concrete pavement.* Presentation at the Precast Concrete Pavement Forum, 9th International Conference on Concrete Pavements, International Society for Concrete Pavements. San Francisco, CA.

Olidis, C., D. J. Swan, A. Saeed, R. C. Mellerski, and M. I. Hammons. 2009. *Precast slab literature review report: Repair of rigid airfield pavements using precast concrete panels—a state of the art review*. AFRL-RX-TY-TR-2009-4588. Tyndall Air Force Base, FL: U.S. Air Force Research Laboratory.

Overacker, J. W. 1974. Thruway repairs concrete slabs overnight. *Public Works* 105(3): 63.

Prabhu, M., A. Varma, and N. Buch. 2009. Analytical investigation of the effects of dowel misalignment on concrete pavement joint opening behavior. *International Journal of Pavement Engineering* 10(1): 49–62.

Priddy, L. P. 2009. Foam backfill and foam stabilization for full-depth PCC repairs. In *Proceedings of the 2009 USACE Research and Development Conference, November 2009, Memphis, TN*.

Priddy, L. P. 2011. *Development of laboratory testing criteria for evaluating cementitious, rapid-setting pavement repair materials*. ERDC/GSL TR-11-13. Vicksburg, MS: U.S. Army Engineer Research and Development Center.

Priddy, L. P., and S. R. Jersey. 2009. Full-scale traffic tests and laboratory testing protocol using rapid-setting materials for expedient pavement repairs. *Transportation Research Record* 2113: 140–148.

Priddy, L. P., and J. K. Newman. 2010. Full-scale field testing for verification of mechanical properties of polyurethane foams for use as backfill in PCC repairs. *ASCE Journal of Materials in Civil Engineering* 22(3): 245–252.

Priddy, L. P., and T. W. Rushing. 2012. Development of a rapid-setting cementitious material laboratory testing protocol for airfield pavement repairs. *Transportation Research Record* 2290(1): 89–98.

Priddy, L. P, P. G. Bly, and G. W. Flintsch. 2013a. Review of precast portland cement concrete panel technologies for use in expedient portland cement concrete airfield pavement repairs. In *Transportation Research Board 92nd Annual Meeting Compendium of Papers.* Washington, DC: Transportation Research Board of the National Academies.

Priddy, L. P., P. G. Bly, C. J. Jackson, and T. N. Brogdon. 2013b. *Evaluation of precast panels for airfield pavement repair, Phase II: Results of accelerated pavement testing*. ERDC/GSL TR-13-24. Vicksburg, MS: U.S. Army Engineer Research and Development Center.

Priddy, L. P., S. R. Jersey, and C. M. Reese. 2010a. Full-scale field testing for injected foam stabilization of PCC repairs. *Transportation Research Record* 2155(1): 24–33.

Priddy, L. P., M. Mejias-Santiago, and J. F. Rowland. 2010b. *Evaluation of foam backfill technologies for crater repair*. ERDC/GSL TR-10-05. Vicksburg, MS: U.S. Army Engineer Research and Development Center.

Priddy, L. P., C. Moore, and E. Padilla. 2008. *Advanced airfield damage repair technologies-Phase I*. ERDC/GSL TR-08-27. Vicksburg, MS: U.S. Army Engineer Research and Development Center.

Priddy, L. P., D. W. Pittman, and G. W. Flintsch. 2014a. *Load transfer characteristics of precast portland cement concrete panels for airfield pavement repairs*. Transportation Research Record *(*in press). Washington, DC: Transportation Research Board of the National Academies.

Priddy, L. P., P. G. Bly, C. J. Jackson, and G. W. Flintsch. 2014b. Full-scale field testing of precast portland cement concrete (PCC) panel airfield pavement repairs. *International Journal of Pavement Engineering* 15(9-10): 840–853.

Priddy, L. P., R. Freeman, K. Newman, and M. Mejias. 2007a. Laboratory investigation of rigid polyurethane foams for repair of PCC pavements. *International Journal of Pavements* 6(1-3): 124–135.

Priddy, L. P., J. S. Tingle, T. J. McCaffrey, and R. S. Rollings. 2007b. *Laboratory and field investigations of small crater repair technologies*. ERDC/GSL TR-07-27. Vicksburg, MS: U.S. Army Engineer Research and Development Center.

Riad, M. Y. 2001. *Stress concentration around dowel bars in jointed rigid concrete pavements.* PhD diss., West Virginia University.

Rollings, R. S., and Y. T. Chou. 1981. *Precast concrete pavements*. Miscellaneous Paper GL 81-10. Vicksburg, MS: U.S. Army Engineer Waterways Experiment Station.

Roman Stone Construction Company. 2012. The Roman Stone Construction Company. www.romanstoneco.com.

Sapozhnikov, N., and R. Rollings. 2007. Soviet precast prestressed construction for airfields. In *Proceedings of the 2007 FAA Worldwide Airport Technology Transfer Conference, June 2007, Atlantic City, NJ*.

Sharma, A. K. 1990. Experimental rehabilitation of jointed portland cement concrete pavement. *Transportation Research Record* 1272(1): 27–34.

Simonsen, J. E. 1971. *Concrete pavement joint repair with precast slabs: Progress report*. Research Project 68 F-102, Research Report R-762. Lansing, MI: Michigan State Highway Commission.

_____. 1972. *Concrete pavement joint repair with pre-cast slabs: Construction report*. Research Project 68 F-102, Research Report R-804. Lansing, MI: Michigan State Highway Commission.

Simulia. 2011a. *ABAQUS 6.11 User's Manual.* Providence, RI: Simulia Corp.

_____. 2011b. *ABAQUS 6.11 Theory Manual.* Providence, RI: Simulia Corp.

Smits, F. 2004. ModieSlab, Innovative prefabricated modular concrete slab for concrete roads and airfields. In *Proceedings of 9th International Symposium on Concrete Roads, April 2004, Istanbul, Turkey*.

Swati, R. M., K. S. Reddy, and L. S. Ramachandra. 2009. Load transfer characteristics of dowel bar system in jointed concrete pavement. *Journal of Transportation Engineering* 135(11): 813–821.

Tabatabaie–Raissi, A. M. 1978. *Structural analysis of concrete pavement joints*. PhD diss., University of Illinois.

Tayabji, S., N. Buch, and E. Kohler. 2009. Precast concrete pavement for intermittent concrete pavement repair applications. In *Proceedings of the National Conference of Preservation, Repair, and Rehabilitation of Concrete Pavements, April 2009, St. Louis, MO*.

Tayabji, S., D. Ye, and N. Buch. 2013. *Precast concrete pavement technology*. Report S2-R05-RR-1, Strategic Highway Research Program 2. Washington, DC: Transportation Research Board of the National Academies.

Thomas, D. 2008. *Slab replacement using precast panels*. 2008 California Pavement Preservation Conference, April 2008, Newport Beach, CA.

Timoshenko, S., and J. M. Lessels. 1925. *Applied elasticity*. Pittsburg, PA: Westinghouse Technical Night School Press.

Tingle, J. S., P. S. McCaffrey, Jr., A. M. Ioannides, and R. S. Rollings. 2007. *Evaluation of prestressed precast slabs*. ERDC/GSL TR-11-x (Draft). Vicksburg, MS: U.S. Army Engineer Research and Development Center.

Tyau, J. S. 2009. *Finite element modeling of reinforced concrete using 3-dimensional solid elements with discrete rebar*. MS thesis, Brigham Young University.

Unified Facilities Criteria (UFC). 2001a. *Concrete repair*. UFC 03-270-04. Construction Criteria Base. Washington, DC: National Institute of Building Sciences.

_____. 2001b. *Pavement Design for Airfields*. UFC 03-260-02. Construction Criteria Base. Washington, DC: National Institute of Building Sciences.

_____. 2001c. *Airfield Pavement Evaluation*. UFC 3-260-03. Construction Criteria Base. Washington, DC: National Institute of Building Sciences.

van Dommelen, A. E., J. van der Kooij, L. J. M. Houben, and A. A. A. Molenaar. 2004. LinTrack APT research supports accelerated implementation of innovative pavement concepts in the Netherlands. In *Proceedings of the 2nd International Conference on Accelerated Pavement Testing*, September 2004, Minneapolis, MN.

Wadkar, A. 2011. *Study of load transfer efficiency of airfield rigid pavement joints based on stresses and deflections*. MS thesis, Rowan University.

Westergaard, H.M. 1925. Computation of stresses in concrete roads. *Highway Research Board* 5(1): 90–112.

Williams, B.A., L. P. Priddy, and P. G. Bly. 2011. *Field-prepared rapid-setting concretes: Phase 1, Laboratory testing*. ERDC/GSL TR-11-16. Vicksburg, MS: U.S. Army Engineer Research and Development Center.

Williams, B. A., L. P. Priddy, P. G. Bly, and J. S. Tingle. 2012. Developing mixture proportion guidance for field-prepared rapid-setting materials for emergency airfield repairs. In *Transportation Research Board 91th Annual Meeting Compendium of Papers.* Washington, DC: Transportation Research Board of the National Academies.

www.betterroads.com. 1974. Prefab pavement sections for PCC repairs slice time and cost for Caltrans. *Better Roads* 44(9):26-28.

Appendix A: Extended Literature Review

This appendix provides an extended literature review that is complementary to Chapter 2.

A.1 Background

Deployed military personnel require expedient methods for conducting full-depth repairs in damaged PCC airfield pavements. In contingency environments and other emergency situations, damaged areas must be replaced quickly to restore flight operations in the shortest time frames possible. The window for these repairs is often as short as 4 to 6 hr. Damage requiring a full-depth repair can result from traditional pavement distresses from repeated traffic, overloading from construction errors, environmental conditions, or explosive blasts. Traditional pavement damage or distresses include blowups, shattered slabs, corner breaks, durability cracking, deep spalling (past mid-slab depth), deteriorating patches, and utility cuts that have the potential to damage aircraft (rated as medium- and high-severity upon inspection) (UFC 2001a). Damage from explosive blasts includes deep spalls, craters, or camouflets. Regardless of the cause of damage or the repair environment, these distresses are normally repaired by removal and replacement of the damaged PCC and sublayers.

The most broadly used materials for repairing PCC pavements are conventional PCC, high early-strength concrete, and proprietary rapid-setting repair materials (Williams et al. 2011; 2012). Current military guidance for conducting full-slab replacement and full-depth repairs in PCC airfield pavements suggests using conventional PCC (UFC 2001a). Generally, conventional PCC provides the best results when conducting permanent repairs in PCC because the replaced material has similar mechanical properties to that of the parent pavement.

Disadvantages to using conventional cast-in-place PCC include long curing durations required to gain strength and the inability to place in all weather conditions (Ashtiani et al. 2011; Priddy and Rushing 2012). Additionally, over the past several years, the performance of proprietary rapid-setting rigid repair materials has improved, making their use acceptable for a

wide range of repair types including emergency, temporary, and permanent airfield repairs (Hammons and Saeed 2010; Priddy 2011).

Proprietary rapid-setting repair materials have been successfully used for partial- and full-slab replacements for contingency repairs; however, these materials are expensive and are a logistical burden to transport to remote locations (Priddy and Jersey 2009). Military repair teams in a contingency environment may have limited quantities of these materials; thus, alternative technologies that take advantage of local materials are desired.

High early-strength concrete has gained acceptance in the commercial and military airfield repair communities in recent years. The combination of high cement content and the use of accelerating admixtures yields repairs that can be reopened to traffic within 6 to 12 hr. High early-strength concrete typically costs more than traditional PCC but is usually less expensive than proprietary rapid-setting repair materials. In addition to cost, durability is a concern not only from the high cement contents required, but also from the questionable quality of materials often encountered in contingency environments (Williams et al. 2011). Furthermore, high early-strength concrete and proprietary repair materials have the same drawback as traditional PCC, as they cannot be placed in all weather conditions (Ashtiani et al. 2011).

A promising alternative repair method is the use of precast PCC panels for full-depth repairs. Precast PCC panels may provide a higher quality repair than that achieved using conventional, proprietary, or high early-strength concretes since the panels can be prepared with locally available conventional PCC and stockpiled for later use. More time would be available to fabricate each panel in advance of an emergency repair scenario, so the panel can be prepared in less haste than current emergency repair methods. Additionally, conventional PCC materials may be more economical than the expensive proprietary materials (Hossain et al. 2006).

A.2 Precast PCC panel usage

Modular or precast structural elements such as concrete columns, beams, piles, highway barriers, and railroad ties are used extensively in the building, highway, and bridge industries (FHWA 2007; Rollings and Chou 1981). Precasting and storing these elements away from the construction site can reduce congestion at the job site, and their mass production in a factory-like setting can result in improved quality control and minimized costs (Rollings

and Chou 1981). The use of precast concrete slabs or panels in conventional road and airfield pavements for either pavement construction or pavement repair is not a recent innovation; various studies have been conducted over the last 80 years. One reason usage of these panels has lagged behind other precast structural elements is that the precast panels used for pavements require more effort to place foundation or bedding materials in such a way as to maintain full and uniform underlying support for the panel (Kohler et al. 2009; Rollings and Chou 1981). Furthermore, the bedding material must be placed in such a manner to ensure panels match the elevation of the surrounding pavement. Careful base preparation is not only time consuming but also requires experienced field crews and heavy equipment. As a result, this repair method was not necessarily considered practical for contingency or emergency repair efforts.

Another reason reported in the literature that precast panel pavement repairs have lagged behind other repair techniques is the lack of documented design and construction practices for precast panels (Tayabji et al. 2013). While proprietary and non-proprietary panels exist and have been explored in recent years, pavement engineers have hesitated to use them on an extensive basis because of the lack of adequate documentation for their successful construction and long-term performance. Finally, the use of panels may be more expensive compared to other repair or construction techniques because of the need for heavy construction equipment, use of proprietary panel systems and equipment, and specially trained crews.

A.3 Early precast panel experiences

A review of the literature reveals usage of precast PCC slabs (or panels) for a variety of single- and multiple-panel repairs as well as rapid pavement construction in North America, Europe, the former Soviet Union, and Asia as early as the 1930s. Precast panels were used for airfield construction in the former Soviet Union as early as the 1930s and in Europe from 1947 through 1958 (Rollings and Chou 1981). Since this time, the majority of research in the U.S. using precast panel technologies has been for highway repairs. Summaries of early precast panel use are provided by Rollings and Chou (1981), Brabston (1984), Federal Highway Administration (FHWA 2007), Kohler et al. (2007), and Tayabji et al. (2009; 2013). Table A.1 summarizes the early international uses of precast panels; Table A.2 summarizes the U.S. precast panel efforts through the 1980s. As can be seen in these tables, panel designs, seating methods, load transfer mechanisms, and reinforcement types varied greatly among the reported efforts.

Table A.1. Early international highway and airfield efforts using precast panels.

Time Period	Location	Pavement Type	Dimensions	Comments	References
European and Asian Efforts					
1930s-1980s	Soviet Union (multiple locations)	Airfield construction and road construction	13-20 ft by 6 ft (airfield)	Multiple panel sizes used for both airfield and highway construction	Rollings and Chou (1981) Brabston (1984)
1947	Orly Airport, Paris, France	Airfield construction	3.3 ft by 3.3 ft by 6.3 in.		Rollings and Chou (1981) Brabston (1984)
1956	London, England	Airfield construction		Dimensions not reported	Brabston (1984)
1956	Finningley, England	Airfield construction	30 ft by 9 ft by 6 in.	Prestressed, precast slabs	Brabston (1984)
1958	Melsbroek, Belgium	Airfield	39 ft by 4.1 ft by 3 in.	Prestressed, precast slabs	Brabston (1984)
1980s	Germany	Airfield emergency repair	6.56 ft by 6.56 ft by 4.72-5.91 in.	Simulated munition blast repairs	Brabston (1984)
1970s	Japan	Airfields and container yards		Sizes not reported.	Kohler et al. (2007)
1981	Japan	Airfield	3.2 ft by 7.5 ft by 7.9 in.	Designed for DC-8 traffic.	Brabston (1984)
1991	Japan	Road	3.3-9.8 ft by 6.6 ft by 5.9 in.	No load transfer devices reported.	Brabston (1984) Kohler et al. (2007)

A.4 Recent U.S. precast panel experiences

As discussed in the previous section, infrequent precast panel investigations were conducted in the U.S. from 1970 to 2000; however, there has been a resurgence of investigations of this technology in the past 10 years (Tayabji et al. 2009; FHWA 2007). Until recently, the precast PCC panel systems were periodically studied for technical feasibility or as a "matter of technical curiosity" (Tayabji et al. 2009). Today, the major precast PCC panel focus is for highway or tollway repairs. Tayabji et al. (2009) provides a comprehensive summary of precast panel usage since 1995 that resulted in a resurgence of interest and investigations into precast panels for highway repairs. Major projects reported included those led by the FHWA, Michigan Department of Transportation (DOT), American Association of State Highway and Transportation Officials (AASHTO), Strategic Highway Research Program (SHRP2), and commercial efforts.

Table A.2. Early U.S. highway and airfield repair efforts using precast panels.

Time Period	Location	Pavement Type	Dimensions	Comments	References
U.S. Efforts					
1960s	South Dakota	Highway	24 ft by 6 ft by 4.5 in.	Panels were overlaid with 1.5 to 3.5 in. of AC. Panels were prestressed.	Rollings and Chou (1981)
1970s	Michigan	Highway	10-11 ft by 6-12 ft by 8-9 in.	Doweled and undoweled panels	Rollings and Chou (1981) Simonsen (1971, 1972)
	New York	Highway	20-30 ft by 12-13 ft by 9 in.	Pretensioned precast panels	Overacker (1974)
	Florida	Highway	20 ft by 12 ft by 8 in.	Panels raised into place using slab jacking. Used to conduct interstate repairs.	Grimsley and Morris (1975)
	California	Freeway	12.3-17.4 ft by 11.4 ft by 8 in.	Grout bedding and grout filled joints	*Prefab* (1974)
	Virginia	Highway	1-3 ft by 1-2 ft by 2 in.	Conducted 68 partial depth patches using precast panels seated on epoxy grout	Creech (1975)
	South Dakota	Highway	Unknown	Partial depth precast panels	Rollings and Chou (1981)
	New York	Airfield	30 ft by 12 ft by 9 in.		Overacker (1974)
1980s	Wisconsin	Highway	6 ft by 6 ft by 8.5 in.	Panels were placed on 0.5 in. of mortar grout.	Sharma (1990)
	California	Airfield		116 panels were replaced, and each panel was custom built to the slab requiring replacement. The panels were overlaid with 20.3 cm of AC.	Rollings and Chou (1981) Brabston (1984)
	Florida	Airfield	6 ft by 6 ft by 8-12 in.	Placed on grade and bonded with polymer concrete and/or covered with polymer concrete	Brabston (1984)
	Mississippi	Airfield	20-50 ft by 20-50 ft by 6-8 in.	Predicted repair times for continuous repairs to repair bomb craters.	Brabston (1984)

A.4.1 FWHA/Michigan DOT

In the late 1990s, the FHWA sponsored the Concrete Pavement Technology Program (CPTP) and provided the Michigan DOT with funding to investigate the use of precast PCC panel systems for full-depth PCC repairs. This work led to the Michigan Method of precast slab repair discussed later in this chapter. This method is one of the most common precast PCC panel repair methods used in the U.S. for highway repairs (Tayabji et al. 2009).

Buch et al. (2003) detailed the installation of 21 precast panels for full-depth patching efforts along two interstates in Michigan. The Michigan Method panels were fabricated by a vendor following specifications for slab thickness, dowel bar, and reinforcement placement. The panel dimensions were typically 12 ft by 12 ft by 10 in. with three 1.5-in.-diam dowel bars cast in the wheel paths to ensure load transfer across the joints.

This method uses precast panels seated on a layer of flowable fill. Dowel bars cast into the panels are connected to the surrounding pavement through dowel receptacles that are saw cut and excavated using a jackhammer. After the dowel slots (or receptacles) are prepared, the panels are lowered into place, leveled, and then the dowel receptacles are filled with high-early strength concrete or a rapid-setting proprietary material. Figure A.1 presents a cross-sectional view of the dowel placement. An alternative for leveling the panels is to use high-density polyurethane (HDP) foam instead of a grout. The foam is injected through either pre-formed or drilled holes in the panels. The final step in the process is to seal the joints. For the repair, the time-consuming activities included preparation of the dowel receptacles, removal of the existing PCC, and the adjustment of the panel elevation with respect to the surrounding slabs.

Figure A.1. Michigan Method cross section of dowel assembly (Buch et al. 2003).

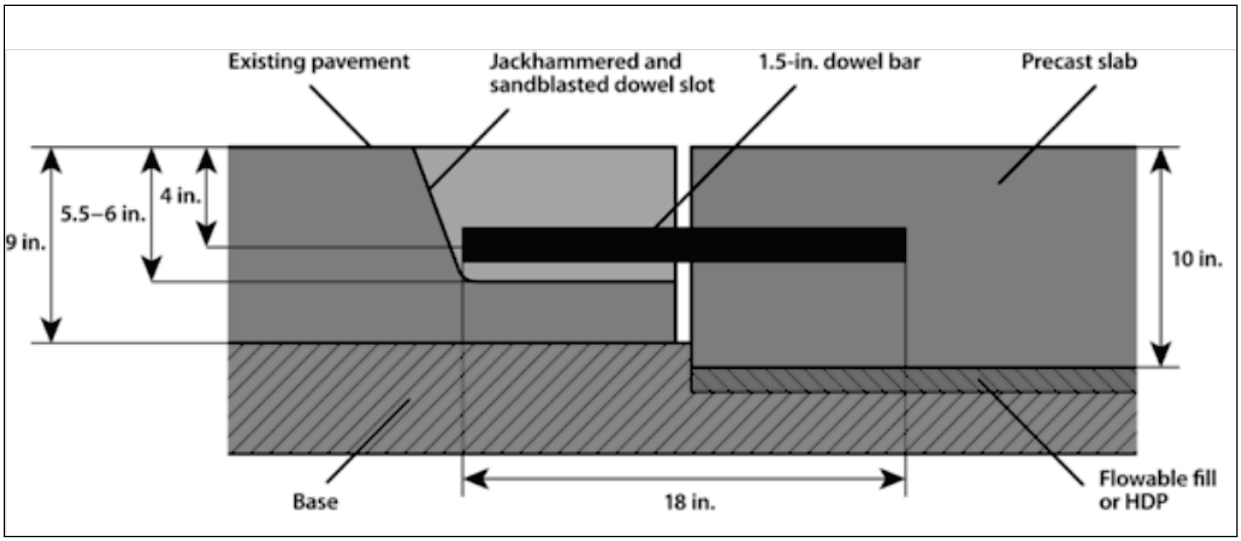

A.4.2 State highway

Numerous highway agencies— including the Illinois Tollway Authority, the New Jersey Turnpike, and the New York State Thruway Authority— have investigated the use of precast panels for pavement repair since 2000.

State DOTs included California, Iowa, New Jersey, New York, Colorado, Delaware, Florida, Hawaii, Indiana, Michigan, Minnesota, Missouri, Texas, and Virginia (Tayabji et al. 2009; Davis 2006). In 2006, the AASHTO promoted technology transfer activities related to precast PCC systems for a variety of highway paving and repair activities. In 2008, various documents were prepared and distributed regarding the use of this technology for roads. The documents provided specifications for precast PCC pavement panel systems' approval, guidance, and considerations for designing precast PCC panel systems for pavements, as well as generic specifications for fabricating and constructing the precast PCC pavement panels (Tayabji et al. 2009).

A.4.3 Recent airfield applications

A.4.3.1 International airports

While precast panels have been explored extensively for highway and tollway repairs in recent years, fewer research investigations have been focused exclusively on airfield pavement repairs. Some work was conducted between 2000 and 2003 at La Guardia International Airport in New York, St. Louis International Airport in Missouri, and Dulles International Airport in Washington, DC (Tayabji et al. 2013). Little information is available about the quality of these repairs or their performance under traffic. The repairs conducted at La Guardia were conducted in test sections to simulate primary taxiway repairs. The study investigated two types of precast panels, including 16-in.-thick reinforced panels and 12-in.-thick, two-way prestressed precast panels. The panel dimensions were both 12.5 ft by 25 ft and were used to construct two 200-ft-square test sections in 2002. These sections are continuing to be monitored under live aircraft loadings; and, according to Olidis et al. (2009), these sections are performing satisfactorily. Information about the performance of the precast panels at the St. Louis and Dulles airports is not readily available in the literature.

A.4.3.2 'Soviet-style' slabs

The U.S. encountered precast panel airfield pavements in countries formerly part of the Soviet Union during recent military operations in Afghanistan and Iraq (Figure A.2). Research was conducted in the U.S.by Tingle et al. (2007) to understand the load-carrying capacity of the panels and to predict damage caused by U.S. aircraft. A precast panel runway using

"Soviet-style" designed slabs was constructed in 2007, and a panel being placed over a sand bedding material is presented in Figure A.3. Sapozhnikov and Rollings (2007) conducted a complementary investigation to the Tingle et al. (2007) study to understand the Soviet precast panel manufacturing and design process to determine whether the technology could be applied for U.S. efforts. Only preliminary information was available on the Tingle et al. (2007) investigation at the time this document was written.

Figure A.2. (left) Stockpiled precast panels at a Soviet airfield and (right) precast concrete panel runway still in service.

Figure A.3. Placement of a precast panel.

A.4.3.3 Air Force method

Recently, the U.S. Air Force developed a prototype repair method using single precast panels referred to as the Air Force Method in the literature. The panels are designed such that deployed personnel can assemble pre-fabricated forms in the field and cast/stockpile panels on-site for future use. The precast panel dimensions are 9 ft 10.5 in. by 9 ft 10.5 in. by 11 in. Load transfer is provided by ten 1.0-in.-diam, 22-in.-long dowels precast into the slabs on both sides of the panel in the direction of traffic. Similar to the Michigan Method, dowel receptacles are saw cut and prepared in the surrounding PCC. Following the placement of each panel, the dowel receptacles are filled with rapid-setting cementitious repair material. Figure A.4 shows the installation of the precast panels and dowel receptacles.

Figure A.4. Air Force Method installation.

In a study conducted by the Air Force and described by Ashtiani et al. (2010), two single-panel repairs were conducted using foam injection for leveling, and a third single panel was seated on a layer of flowable fill backfill. Each repair was trafficked using an F-15 load cart for 1,508 passes. Load transfer was calculated for each repair before, during, and after trafficking, using deflection data obtained from heavy weight deflectometer (HWD) joint tests. The foam-injected repairs provided better load transfer, but the flowable fill backfill provided sufficient support for the design traffic and was deemed suitable for contingency repairs (Ashtiani et al. 2010).

A.4.4 Commercial precast panel systems in the U.S.

Currently, the most common methods of precast panel pavement repair in the U.S. are the Fort Miller Super-Slab Method, the Michigan Method, the Uretek Method, or some variation of these three methods. Additional com-

mercial systems have been developed recently, including the Kwik Slab System and the Roman Road System® by the Roman Stone Construction Company. Table A.3 presents the main characteristics of each repair method. The following sections summarize each method.

Table A.3 Main characteristics of precast panel repair methods.

Name of Repair Method	Application Type	Load Transfer	Base Support
Fort Miller Super-Slab®	Single- or multiple-panel repairs	Dowels inserted into the existing pavement	Manufactured sand and injected grout
Michigan	Single-panel repairs	Dowels cast into the precast panel and grouted in the existing pavement	Flowable fill or polyurethane foam
Uretek	Single- or multiple-panel repairs	Fiberglass ties inserted after the precast panel is placed	Grouting using injected polyurethane foam
Kwik Slab	Multiple-panel repairs/construction	Kwik Joint steel couplers	Grout pumped through grout holes and channels
Roman Road System®	Single- or multiple-panel repairs/ construction	Dowels either cast into the precast panel or inserted after precast pavement is placed	Grouting using injected polyurethane foam
Other	Single- or multiple-panel repairs	Dowels inserted after the precast panel is placed; other means	Any of the above

A.4.4.1 Fort Miller Super-Slab Method

The Fort Miller Super-Slab® Method is one of the most common proprietary precast panel methods used in the U.S. and Canada. The method consists of placing fabricated slabs on a carefully graded bedding material. Each panel is fabricated to exactly fit the area to be replaced. Panels are tied together through dowel receptacles that are formed in the bottom of the slabs to tie preinstalled dowels from the adjacent slabs (parent slabs). The dowel receptacles, also called slots or mouse holes, are grouted after placement with rapid-setting cementitious grout to embed the dowel bars through manufactured grout holes. The panels have additional grout holes that allow a bedding grout to be pumped under the panel through formed channels on the underside of the slab to fill any voids present and to level the panels (Fort Miller 2003). If precast panels are connected, then dowel bars are cast on one side of the precast panel with corresponding dowel receptacles formed on the opposite side, as shown in Figure A.5. Figure A.6 presents the dowel receptacles in the grouted and ungrouted conditions.

Figure A.5. Super-Slab® installation at a tollbooth (Ashtiani et al. 2010).

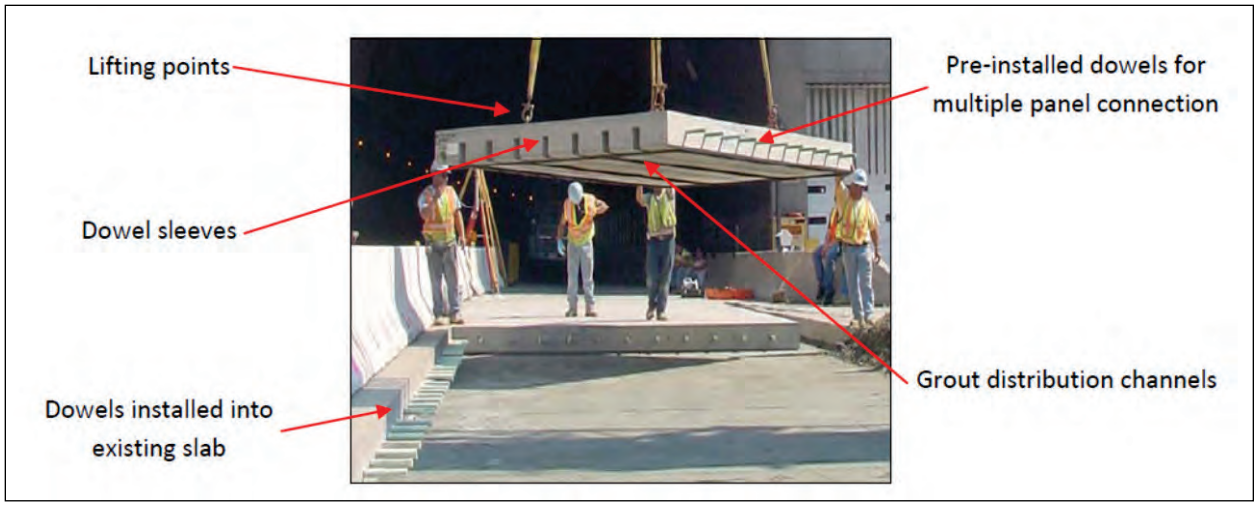

Figure A.6. (left) Dowel receptacles and grout holes; (right) grouted receptacle with dowel (Thomas 2008).

Since 2002, the Fort Miller Super-Slab® Method has been used by several agencies, as summarized in Table A.4 after Thomas (2008) and a recent SHRP2 investigation (Tayabji et al. 2013). Kohler et al. (2007) details a precast panel test section using the Super-Slab® system trafficked using a heavy vehicle simulator in San Bernardino County, CA. The test indicated that the Super-Slab System could support an estimated 140 to 240 million equivalent single-axle loads (ESALs), equivalent to more than 25 years of highway service. Failure was considered similar to jointed plain PCC with corner breaks resulting from loss of support. Tayabji et al. (2009) reports that repairs conducted using this method have lasted more than 7 years in highway applications with no issues.

Table A.4 Super-Slab® installations.

Project	Owner	Area (ft^2)	Work Window	Nature of Repair	Date of Installation
Tappan Zee Bridge Toll Plaza	New York State Thruway	158,000	Off-peak hour	Multiple panel	2002
Dulles Airport Taxiway	Metropolitan Washington Airport Authority	3,500	8 hr (night)	Single panel	2002
9A Ramp, Tarrytown, New York	New York State Thruway	15,750	Day and night	Multiple panel	2003
Lincoln Tunnel, New Jersey	Port Authority New Jersey	8,100	Weekend	Single panel	2003
Belt Parkway Ramps, Jamaica, New York	New York State DOT	16,030	Full closure (1 month)	Multiple panel	2003
Korean Veterans Parkway, Staten Island, New York	New York State DOT	8,850	8 hr (day)	Single panel	2003
Toronto, Ontario	Ministry of Transportation, Ontario, Canada	1,220	8 hr (night)	Single panel	2004
Port Jefferson, New York	New York State DOT	2,650	8 hr (night)	Cross walks	2005
I-90 - Albany, NY	New York State DOT	56,400	8 hr (night)	Single panel	2005
Fontana, California	CALTRANS	1,950	Off highway	Test section	2005
Minneapolis, Minnesota	Minnesota DOT	2,592	Full closure	Multiple panel	2005
Marine Parkway	Metropolitan Transit Authority (New York)	2,592	3 day full closure	Multiple panel	2005
Fordham Road, Bronx, New York	New York State DOT	3,852	8 hr (night)	Multiple panel	2006
Route 7 Cross Town, Schenectady, New York	New York State DOT	26,586	10 hr (night)	Intersection	2006
High Speed EZ Pass Slabs	New York State Thruway	576	8 hr (night)	Special	2006
Schuylerville, New York	New York State DOT	1,152	Off highway	Trial	2006
Southern State Parkway	New York State DOT	2,483	8 hr (day)	Single panel	2007
I-95, New Rochelle, NY	New York State Thruway	40,000	5 hr (night)	Single panel	2007
Chicago, Illinois	Illinois Tollway	768	Off highway	Trial	2007
I-295, Trenton, New Jersey	New Jersey DOT	2,300	8 hr (night)	Single panel	2007
I-88, Chicago, Illinois	Illinois Tollway	476	Not specified	Single panel	2007
I-294, Chicago, Illinois	Illinois Tollway	2,674	Not specified	Multiple panel	2007
1-88, Chicago, Illinois	Illinois Tollway	4.338	Not specified	Multiple panel	2008
I-295, Burlington County, New Jersey	New Jersey DOT	30,395	Not specified	Single panel	2007/2008
Route 21, Newark, New Jersey	New Jersey DOT	69,810	Not specified	Single and multiple panels	2008
I-280, Essex County, New Jersey	New Jersey DOT	38,000	Not specified	Single panel	2009
Route 42, Camden and Gloucester, New Jersey	New Jersey DOT	32,034	Not specified	Single and multiple panel	2009
Nassau and Suffolk Counties, New York	New York DOT	3,640	Not specified	Single panel	2009

Project	Owner	Area (ft²)	Work Window	Nature of Repair	Date of Installation
Memorial HWY and Division Street, New Rochelle, New York	New York DOT	3,041	Not specified	Multiple panel repairs	2008
Nassau Expressway, Queens, New York	New York DOT	85,000	Not specified	Multiple panel	2009
I-15, Utah	Utah DOT	28,800	Not specified	Single and multiple panel	2009
US 60 I-66 Ramp, Fairfax, VA	Virginia DOT	432	Not specified	Single and multiple panel	2009
I-15, Ontario, California	CALTRANS		Not specified	Multiple panel	2010

A.4.4.2 Uretek Method

Uretek USA, Inc., developed a repair method for leveling in-place slabs in the late 1990s. The method requires injecting HDP foam through holes drilled through the PCC surface into the sublayers to lift faulted slabs to match the surrounding pavement's elevation. This process is known as the Uretek Method. This method has also been applied to contingency airfield repairs using cast-in-place, rapid-setting material as a repair procedure developed by the U.S. Navy (Priddy et al. 2010a). Recently, the injection-leveling method has also been applied for precast panels for both the previously described Michigan and Air Force Methods.

For precast panels, the foam injection method may be combined with the Stitch-In-Time® Process also developed by Uretek. The Stitch-In-Time® Process is used to restore load transfer in jointed concrete pavements. For precast panel repairs, with little or no bedding preparation, a precast panel is lowered into the area where damaged pavement has been removed. The slab is then leveled by injecting the foam under the slab through either formed injection ports placed during panel construction or holes drilled after slab installation. Once the slabs are leveled, the Stitch-In-Time® Process is used to provide load transfer between the precast panel and the surrounding pavement (Tayabji et al. 2009; Ashtiani et al. 2010). The panels are "stitched" to the existing slab or to another panel using fiberglass ties that serve as load transfer mechanisms. The ties are inserted and grouted into receptacles that extend from the existing slab to the precast panel or from precast panel to precast panel. Figure A.7 shows the Uretek fiberglass tie installation procedure.

Figure A.7. Uretek fiberglass ties after Ashtiani et al. (2010).

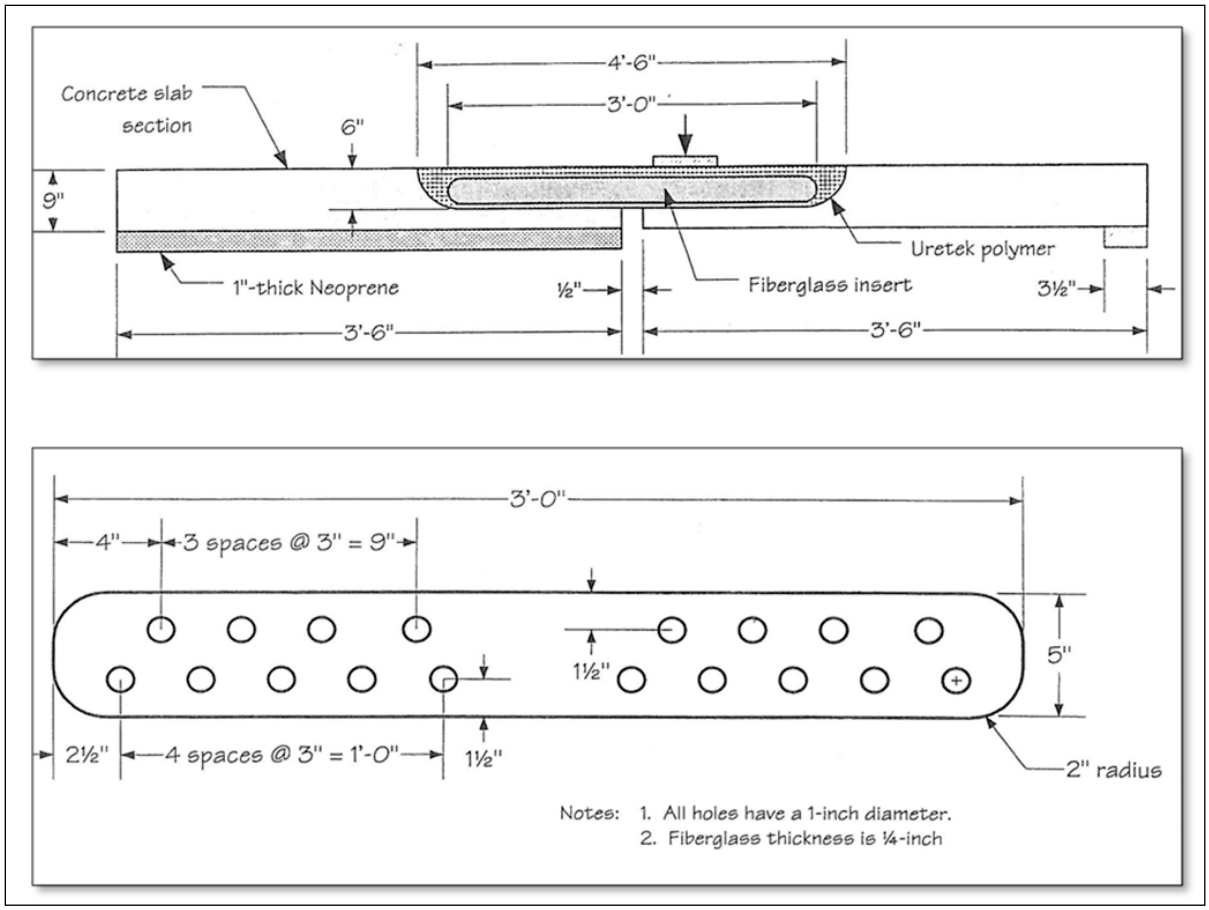

The U.S. Air Force evaluated the Uretek Method without the fiberglass ties for leveling precast panels in 2009. The Air Force prototype panels used dowels for load transfer in lieu of the fiberglass ties. However, the researchers did not recommend this procedure for expedient airfield repair applications because of the precision and training that would be required to properly use the foam injection system (Ashtiani et al. 2010).

A.4.4.3 Kwik Slab System

The Kwik Slab System is a newer precast panel repair system developed and marketed in Hawaii and Singapore. The system relies on the placement of precast panels that are connected using Kwik Joint steel couplers that are precast in one or more panel ends. The panels are leveled using the Uretek HDF injection, plastic leveling shims, or grout leveling pads (Kwik Slab 2011). The couplers are then grouted with a high-strength grout. The joint details are presented in Figure A.8. At the time of this report, little information was available about the performance of this system.

Figure A.8. (left) precast panel and (right) Kwik Joint connection (Kwik Slab 2011).

A.4.4.4 Roman Road System®

The Roman Road System® was developed by the Roman Stone Construction Company in 2009. Panels are placed in the prepared repair area then leveled using injected HDF in the same manner as the Uretek or Michigan seating methods. The HDF used is an Uretek product (Uretek 600). Load transfer is provided by saw cutting through both the parent PCC and the precast panel and installing load transfer devices following the leveling of the panel. The panels are typically thinner than the existing pavement by 1 in. (Tayabji et al. 2013; Roman Stone Construction 2012). The installation process is presented in Figure A.9. At the time of this report, little information was available about the performance of this system.

Figure A.9. (Left) installing Roman Road slab; (right) injecting polyurethane foam (Roman Stone Construction 2012).

A.5 Recent world experiences

In addition to the recent U.S. experiences, a resurgence of precast panel research has occurred around the world. Kohler et al. (2007) and Tayabji et al. (2013) present summaries of recent worldwide precast panel experiences.

A.5.1 Netherlands

Several pilot factory-produced modular road surface studies were conducted in the Netherlands during 2004-2006 (van Dommelen et al. 2004). One precast panel concept investigated was a modular pavement structure called ModieSlab. For this method, precast concrete panels are designed either to rest on concrete piles or be laid within existing pavement. The ModieSlab dimensions are 11.6 ft by 8.3 ft by 12.6 in. and do not use load transfer devices (Smits 2004). Houben et al. (2004a, b) and van Dommelen et al. (2004) detail a pilot study and accelerated pavement testing study using ModieSlab (among other technologies). In the pilot study, the ModieSlabs were constructed on a highway in the Netherlands. Problems encountered included smoothness, raveling, and polished aggregate.

A.5.2 France

Kohler et al. (2007) detailed a study conducted in France using hexagonal-shaped panels placed over a granular bed (Figure A.10). This precast panel research was part of a Removable Urban Pavements research project coordinated by the Laboratoire Central des Ponts et Chaussees in France. The method consisted of using small hexagonal panels that are connected to form the pavement so that when a panel is damaged, it can be removed and replaced with limited equipment and resources (“Removable Urban Pavement” 2010). Each slab was 8-in.-thick and had an equivalent diameter of 5 ft.

A.5.3 Indonesia

Tayabji et al. (2013) summarized a construction project in Indonesia in 2008 using precast concrete panels to construct a four-lane toll road across 22 miles of remote terrain. The panel dimensions were roughly 8.2 ft by 27 ft by 8 in. and were placed on 2 in. of a lean concrete base and required post-tensioning.

Figure A.10. Accelerated pavement testing of hexagonal slabs in France (Kohler et al. 2007).

A.5.4 Japan

Tayabji et al. (2013) also described the use of precast PCC pavements in Japan in recent years. For Japanese road applications, precast panels were placed on an asphalt layer to prevent pumping, and any gaps were filled with grout. Standard slab dimensions used were 18 ft by 4.9 ft by 8-10 in. The Japanese precast panels relied on a load transfer device called the "horn device" (Hachiya 2001). For airport applications, the panels were 47 ft by 8 ft by 10 in, prestressed, and some incorporated both the "horn device" and a compression joint for load transfer. The Japanese also developed an innovative sliding dowel bar for airport construction using precast panels. Details of the Japanese precast panels are provided by Hachiya (2001) and Nishizawa (2008).

A.5.5 SHRP 2 investigations

From 2008 through 2012, the Strategic Highway Research Program 2 (SHRP2) Project R05-Modular Pavement Technology was conducted to develop guidelines and to synthesize precast pavement information. The ultimate goal of the project was to encourage the adoption of precast repair and construction techniques by the paving industry. The study focused almost exclusively on precast panel technologies to develop guidance that would allow transportation agencies to design, construct, install, maintain, and evaluate modular pavement systems.

As part of this project, a number of in-service precast panel systems were investigated in the U.S. Preliminary results reported by Tayabji et al. (2013) indicated that as long as the panels were installed correctly (proper bedding, dowel alignment, etc.), they have the potential to provide long-term service for pavement repairs of 15 to 20 years for highway applications. Field-tested precast panel repairs were re-examined as part of this study. Results of inspections emphasized the need for good support under the repair and care when installing dowel-receptacle patching materials. The study also recommended using dowel bar caps to minimize failure of the dowel bar receptacle patches.

A.6 Precast panel installation process

In general, the precast panel installation process, regardless of pavement type (highway or airfield), can be summarized with the following activities or steps:

- Identify distresses requiring repair
- Establish and mark repair boundaries
- Select panel size(s)
- Fabricate panel(s)
- Saw cut panel boundaries and dowel receptacles (if required)
- Remove existing pavement and prepare dowel receptacles (if required)
- Clean dowel receptacles
- Prepare subbase
- Place leveling/bedding material
- Install panel
- Adjust panel elevation to match surrounding pavement/panels through reseating or through injecting foam/grout, depending on method
- Install load transfer if not precast in panels
- Grout dowel receptacles with high-early strength PCC or proprietary material
- Seal joints with joint sealant or grout
- Check installed panel for elevation differences

A.7 Advantages and disadvantages of precast paving technology

This section summarizes the general advantages and disadvantages of using precast PCC slabs for full-depth pavement repair as gleaned from the literature reviewed.

A.7.1 Advantages of using precast PCC slabs

- Improved quality of precast panels compared to hastily prepared cast-in-place patches
- Use of locally available materials
- Potentially less expensive than proprietary rapid-setting repair materials
- Reduced overall repair time. Little to no cure time required for cementitious materials
- Ability to place panels in most weather conditions

A.7.2 Disadvantages of using precast PCC slabs

- Potential for higher cost of repairs, especially for smaller projects
- Potential for slower field installation rate for multiple-panel repairs
- Experienced equipment operators and heavy equipment, such as cranes for installation, required
- Precast panel size restrictions because of lifting capabilities or transport dimensions
- Seating and leveling problems may require repeated placement and removal of precast panels and/or slab grinding
- Time and precision required for dowel receptacle cutting
- Time and precision required for panel insertion
- Warped panels required for non-planar subsurfaces
- Production of foreign object debris (FOD) from dowel receptacle or panel grouting
- Dowel alignment concerns
- Uncertain long-term performance

In addition to the advantages and disadvantages of precast panels, Tayabyi et al. (2009) provided additional technical and institutional challenges for precast PCC pavements:

- Lack of understanding of the load-carrying capacity of each system component, seating and support conditions, load transfer at joints between multiple panels and single panels and the existing pavements, and connectivity at joints;
- Lack of optimization for various system design features;
- Ensuring durability;
- Lack of adequate long-term performance history;
- Lack of component testing, such as joint connectivity;

- Availability of production/assembly plants for panel fabrication;
- Lack of well-developed QC procedures;
- Lack of well-developed QA procedures, including panel dimension tolerances, profile, load transfer effectiveness at joints, and initial faulting at joints;
- Lack of treatment procedures for early failures;
- Opening to traffic requirements;
- Maintaining safe riding surface;
- Maintaining vertical alignment of joints;
- Lack of best practices for design, construction, maintenance, and rehabilitation for precast systems;
- Lack of well-developed specifications for using precast systems; and
- General lack of support by precast concrete industry to support refinement of precast systems.

While these concerns were focused mainly on highway applications, there is a lack of understanding as to whether precast panels are capable of carrying heavy aircraft loads and whether currently available systems can be modified to suit temporary or permanent repairs of airfield pavements. Little information is available in the literature regarding the long-term performance of precast panels in an airfield setting. Some areas of particular concern are the opening to traffic requirements for emergency airfield repairs, joint connectivity, and load transfer for multi-panel repairs, and elevation differences that may exist between precast panels and the surrounding pavements. A final concern is the potential for increased FOD from panels requiring grouting or patching of dowel receptacles.

A.8 Summary

There has been resurgence in the use and study of precast PCC slabs for highway and airfield repairs in recent years. The majority of research in the U.S. has been focused on highway applications of precast PCC panels. This chapter summarized worldwide experiences using precast PCC slabs for pavement repairs. Since the 1930s, various procedures have been developed and investigated around the world, and these procedures are still evolving as more experience is gained through research and trial sections. Current systems vary based on slab size, reinforcement design, bedding materials, and load transfer mechanisms. The advantages of using precast pavement technology include higher quality concrete repairs through use of precision fabrication, minimal weather restrictions, and reduced delay in reopening a pavement to traffic. The main disadvantages

of precast panel repairs include lifting capabilities in the field, seating and leveling issues, and finally, the uncertainty of the long-term performance of the current systems. Continued research and trial sections of technologies will be required as methods are refined or new methods are developed to refine the current processes.

Appendix B: Precast Panel Construction

This appendix provides additional details of the precast panel construction process not fully covered in the main body of this report.

In 2011, the U.S. Air Force's precast repair system was modified by adding a second panel design that allowed the system to connect multiple panels to complete larger repairs. The original panel design, now referenced as the "standard" panel, was used (with modifications to thickness, size, and reinforcement) and was applied for both single- and multiple-panel repairs. This panel had load transfer dowels integrated mid-depth on both transverse edges. The dowels selected had 1-in. diam, were 22 in. long, and were epoxy coated. The dowels provided load transfer between the precast panel and the surrounding pavement and between the precast panel and another precast panel. The second panel, called a "terminal" panel, was designed for multiple-panel repairs only. Load transfer dowels were placed on only one transverse edge, while the other transverse edge had formed dowel receptacles for connecting to a standard panel to facilitate a larger repair.

Both panels were slightly smaller than 10 ft wide by 10 ft long to ensure fit and ease of placement within a 10-ft by 10-ft saw-cut repair area with a minimum 0.375-in.-wide joint around each panel. The panels each measured 9-ft 11-1/4 in. by 9-ft 11-1/4 in. by 11 in. and weighed approximately 13,600 lb. Panels were designed such that load transfer dowels were oriented parallel to the direction of traffic only; no load transfer dowels were installed perpendicular to the direction of traffic (on the longitudinal edges). Both panel types are shown in Figure B.1.

Details of reinforcement and panel dimensions are presented in Figures B.2 and B.3. The remaining sections describe the precast panel construction steps used in the investigation.

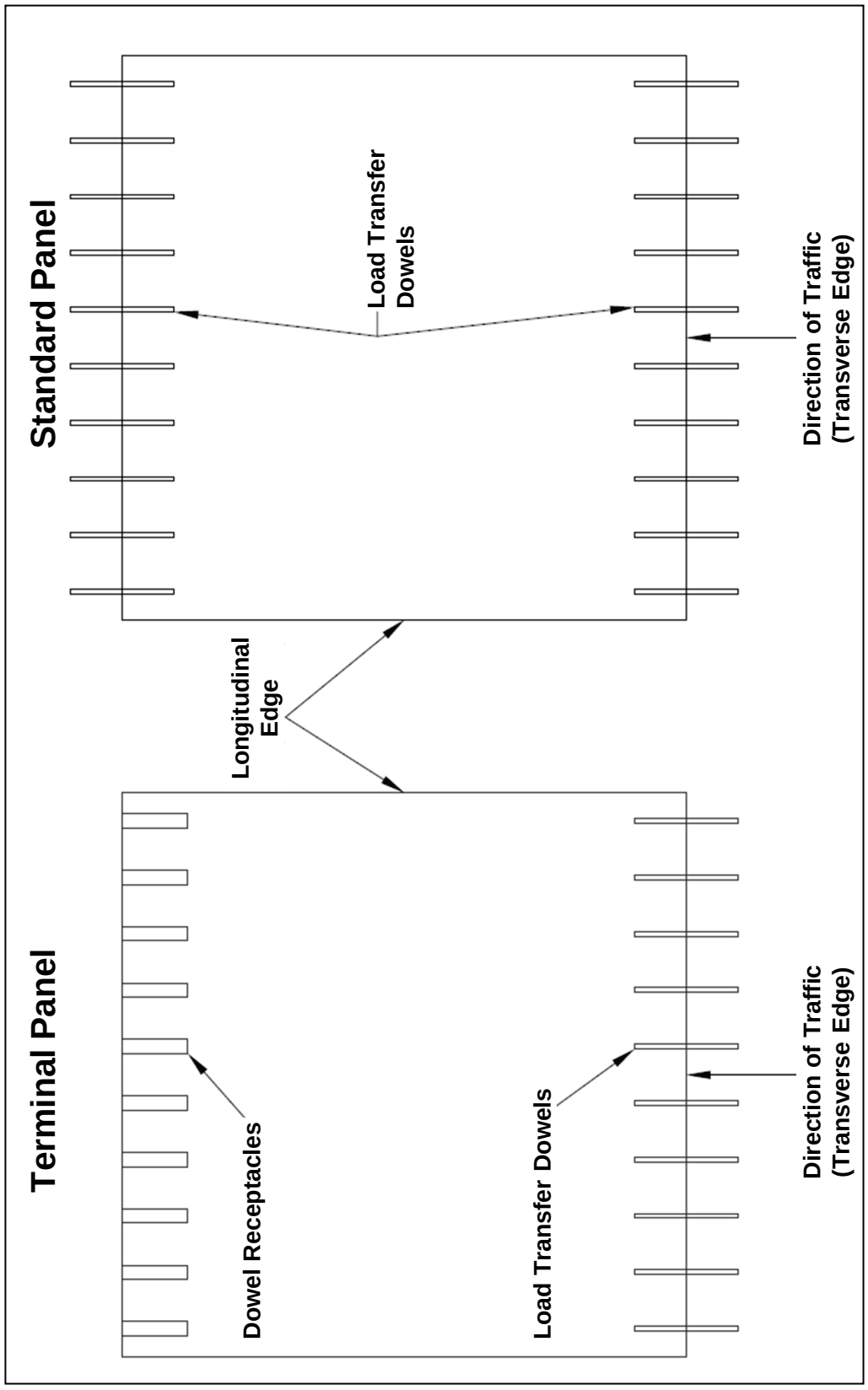

Figure B.1. Precast concrete panel types.

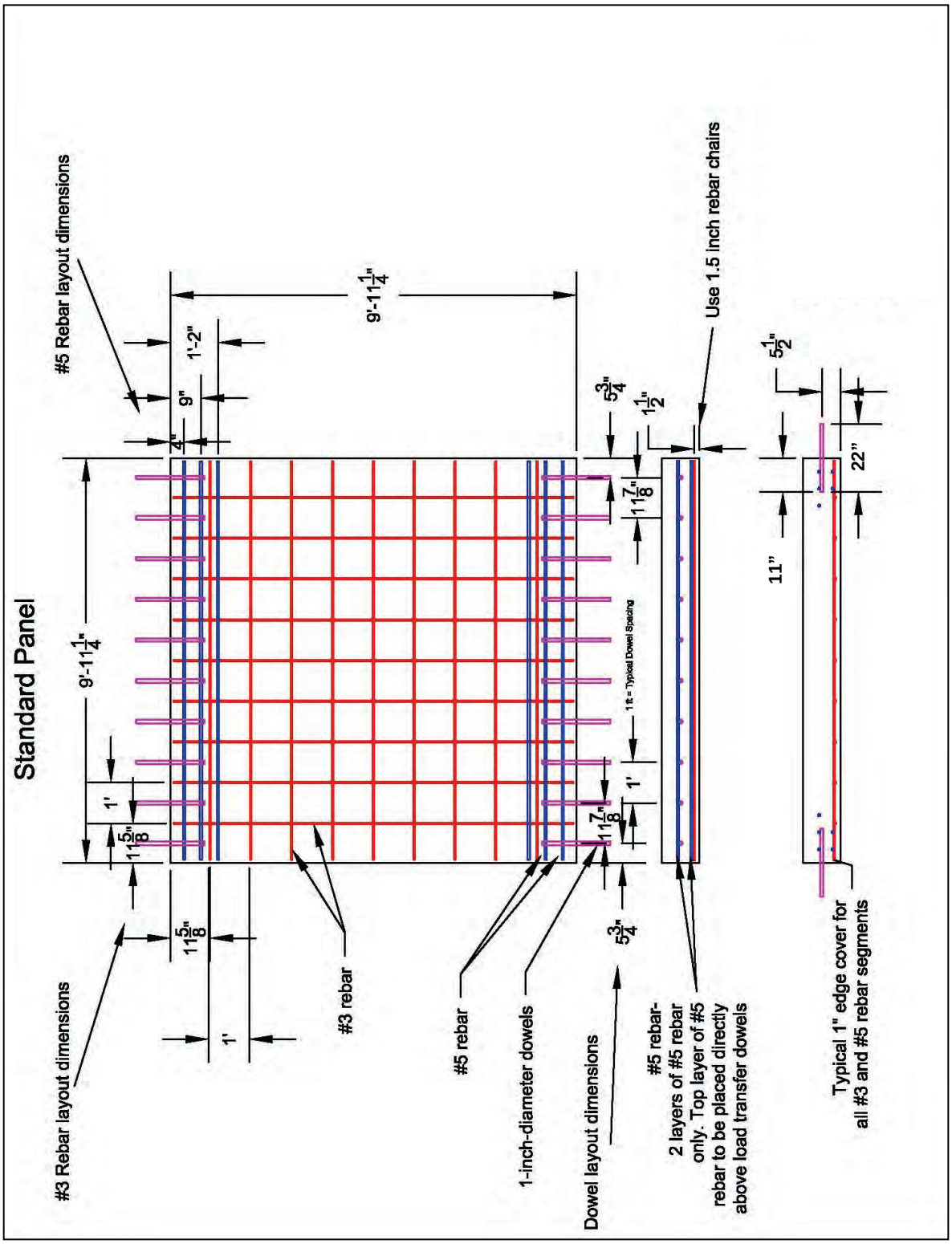

Figure B.2. Rebar layout for standard precast panel.

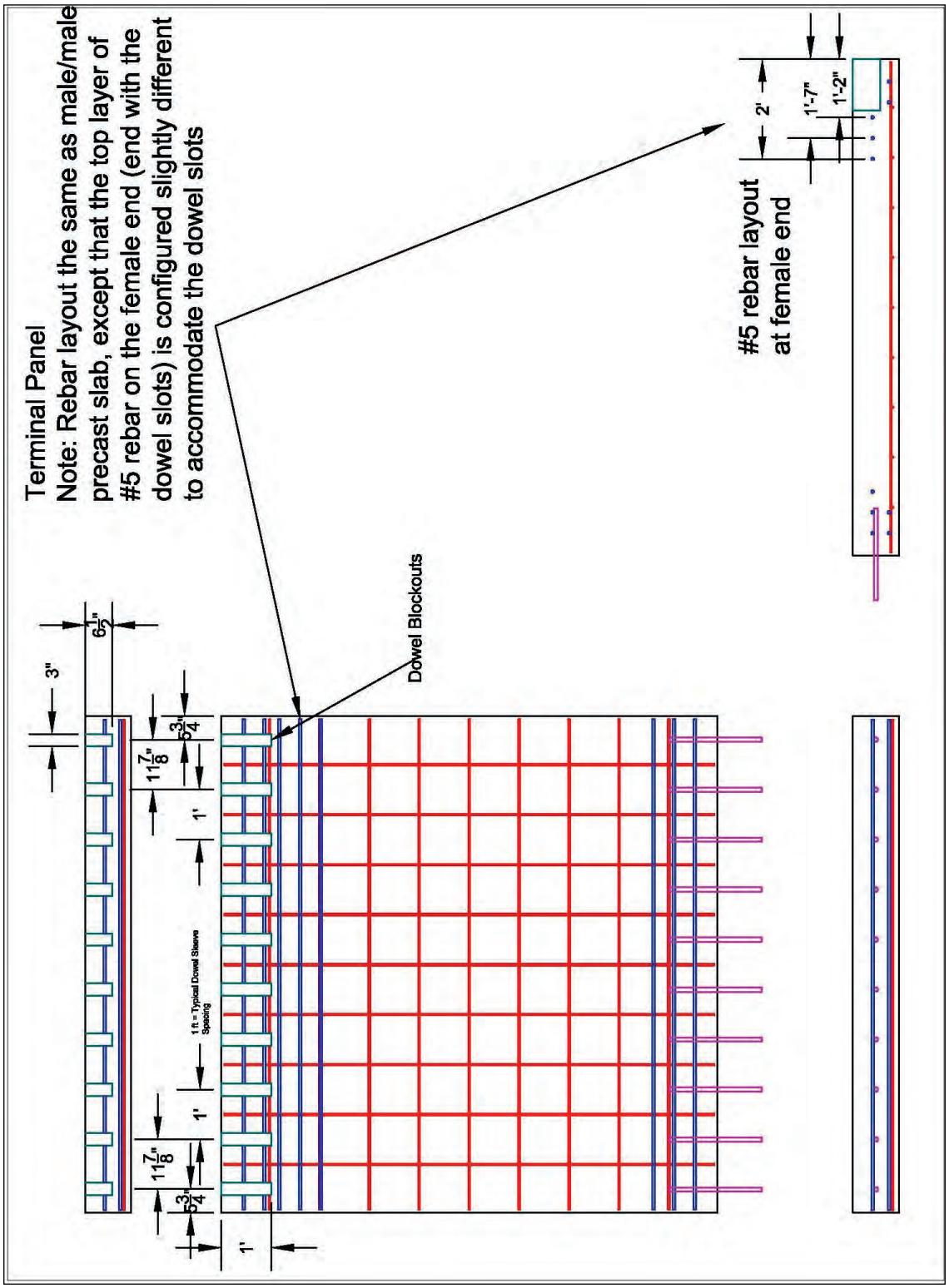

Figure B.3. Rebar layout for terminal precast panel.

B.1 Step 1: Secure construction and storage areas

Panels were prepared in an open-ended aircraft hangar, Hangar 4, located at the ERDC in Vicksburg, MS. This location provided a construction area with a smooth, level, hardened pavement surface with water and electrical hookups and had a sound pavement upon which to secure the panel formwork during placement of the PCC. Securing the forms to a hard surface such as a pavement is required to prevent movement of the forms to ensure panel dimensions meet required tolerances. The area was also large enough to construct all panels without removing the panels right away and had sufficient overhead clearance to operate the crane while still providing a shelter from the environment.

B.2 Step 2: Obtain equipment and materials for fabrication

All materials required for constructing the panels were gathered and moved to the preparation area. All debris was removed from a previously constructed 14-in.-thick PCC test section selected to be used for construction/fabrication of the panels.

Concrete was ordered from a local vendor, and the mixture design is provided in Figure B.4. Each panel required approximately 4 yd^3 of concrete, assuming 15% waste. Eight cubic yards of concrete was ordered to prepare two panels at a time. The average 28-day compressive results were 5,710 $lb/in.^2$, which is above the minimum 5,000 $lb/in.^2$ compressive strength at 28 days specified for airfield pavements and required for the precast panels. Table B.1 summarizes the strength test data for the PCC panels.

B.3 Step 3: Assemble formwork

The forms were organized according to the etched labels on each of the form pieces, allowing 20 ft between form setups to provide working space around the forms during fabrication and to allow room to remove the forms after the panels had cured. To assemble a form, the corners were aligned and connected using the key slots in the forms. Then, 0.75-in.-diam bolts were inserted into the holes on the form ends and were tightened using a hand ratchet. This process is shown in Figure B.5. The process resulted in a square form. Once assembled, the squareness of the forms was checked by measuring each diagonal, and the tops of the forms were checked for flushness.

Figure B.4. PCC mixture used for precast panels.

Material Properties and Source

Cementitious Material		Type		Source		Specific Gravity
Portland Cement		II		Holcim		3.15
Fly Ash		C		Headwaters		2.59
GGBFS (Slag)						

Admixtures		Name		Supplier		Dosage, Fl. Oz.
Type A		322 N		BASF		1-3 per cwt.
Type F		7500		BASF		4-8 per cwt
AE		MB90		BASF		3% - 6%
Note: Dosage rate will require adjustments for field and environmental conditions.						

Aggregate Size	Type	Supplier	Sp. Gr. SSD	Sp. Gr. OD	Absorption, %	F.M.
# 57	Stone	Vulcan	2.68	2.67	0.80	
Sand	Natural	Green Bro	2.60	2.58	0.66	2.65

Batch Quantities

Material	Quantities lb/yd^3 SSD	Absolute Volume ft^3
Cement, lb.	489	2.49
Fly Ash, lb	122	0.75
Mix Water, lb.	245	3.93
Slag, lb.		
Coarse Aggr., lb.	1850	11.06
Fine Aggr., lb.	1225	7.55
Air Content, %	4.5	1.22
Total Mass, lb.	3931	27.00

Water / cementitious material ratio: 0.40

Mix Design Information:

Mix Class 5000 psi. with Air
Comments: 650 Flex

Designed by: Andrew Lester
Title: Regional QA Manager

Organization: MMC Materials

Table B.1. PCC test data.

Panel No.	Specimen Number	Type of Specimen	Age in Days	Compressive Strength, lb/in.^{2}
1	1	4 by 8 cylinder	28	5,750
1	2	4 by 8 cylinder	28	5,700
Average				5,730
2	1	4 by 8 cylinder	28	6,040
2	2	4 by 8 cylinder	28	6,000
Average				6,020
3	1	4 by 8 cylinder	28	6,800
3	2	4 by 8 cylinder	28	6,630
Average				6,715
4	1	4 by 8 cylinder	28	6,200
4	2	4 by 8 cylinder	28	6,670

Panel No.	Specimen Number	Type of Specimen	Age in Days	Compressive Strength, lb/in.^{2}
Average				6,440
5	1	4 by 8 cylinder	28	6,010
5	2	4 by 8 cylinder	28	5,940
Average				5,980
6	1	4 by 8 cylinder	28	6,000
6	2	4 by 8 cylinder	28	6,000
Average				6,000
7	1	4 by 8 cylinder	28	5,530
7	2	4 by 8 cylinder	28	5,880
Average				5,710

Figure B.5. Connecting the formwork: (a) formwork label, (b) connecting lengths of formwork, (c) connected formwork; (d) bolted formwork.

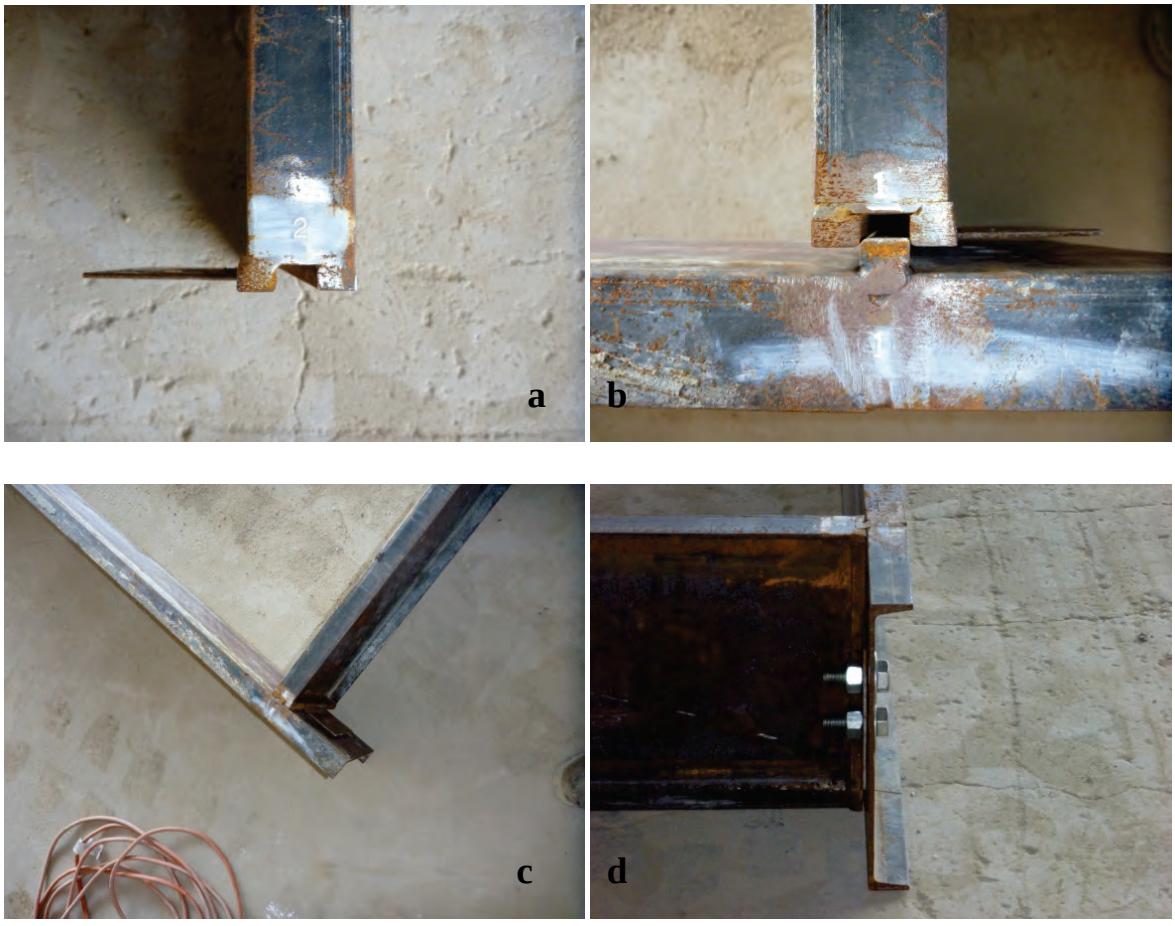

The next step was to secure the forms to the pavement (Figure B.6). Securing the forms to a sound pavement was necessary to prevent the forms from moving during concrete placement. Concrete anchors (0.5 in. diam

and 7 in. long) were used to secure the steel form to the pavement using specially designed anchor tabs, which were centered on the bottom edge of each segment of formwork. Anchor holes were drilled using a 0.5-in. masonry drill bit and hammer drill to a depth of 6 in. Concrete anchors were then installed and driven into the pavement using a steel mallet. After the installation of a single anchor, the forms were checked for squareness.

Figure B.6. Securing formwork to solid surface: (a) drilling anchor hole, (b-d) installing and activating the anchor.

Once all anchors were in place, the concrete anchors were tightened with an electric impact wrench. Debris caused by mortar removed during the drilling process was removed with a shovel or broom.

Following the assembly of the forms, they were sprayed with form-release oil to prevent bonding. During the spraying of release oil, all interior and exterior surfaces, including connection bolts, were also sprayed to facilitate clean up and prevent concrete build up (Figure B.7). A thin sheet of plastic was also inserted in the bottom of the form as a barrier between the fresh concrete and the underlying pavement.

Figure B.7. Spraying release agent on forms.

B.4 Step 4: Install reinforcement

Once the form was prepared, a steel reinforcement grid was installed. The reinforcement grid consisted of grade 60, 0.375-in.-diam rebar (#3), arranged in a 1-ft-square pattern shown in Figure B.8. Grade 60, 0.625-in. rebar (#5) was also utilized. A 1.5-in. concrete cover was maintained between the ends of the reinforcement bar and the side of the frame. The entire grid was placed on 1.5-in. rebar stands, providing a rebar depth of 7.5 in. from the top surface of the precast panel and a cover of 1.5 in. between the reinforcement and the bottom of the precast panels. The following paragraphs describe this process in more detail.

After positioning and securing the frame to a PCC surface, 18 #3-bars were used to prepare the reinforcement grid. For this project, the rebar was specially ordered precut to a length of 9 ft 7.5 in. ± 0.5 in. The rebar was measured to ensure that the materials were the proper length. Any pieces of rebar that were too long were trimmed, and any pieces of rebar that were too short were not used.

The rebar was marked with spray paint with the first mark 9.875 in. from the bars' ends and succeeding marks in 12-in. intervals. Nine of the bars were then spaced approximately 12 in. apart (on center) on a smooth flat surface and overlapped with the remaining nine bars in the opposite direction to layout the grid. Each piece of rebar was aligned so that the paint marks prepared earlier overlapped. Then 6-in. precut rebar ties were fastened with ratchet-tying tools to secure the rebar tightly together. All exterior connections were secured first, then interior connections were performed in a checkerboard pattern (i.e., not all connections in the interior portion of the grids were tied).

Figure B.8. Assembling #3 rebar grid: (a) spacing bottom layer of rebar, (b) spacing top layer of rebar, (c) tying rebar, (d) tightening ties, (e) tied grid, and (f) placing rebar grid in form.

Once the main reinforcement grid was complete, a layer of #5 reinforcement bars was attached to the existing #3 rebar grid. Four pieces of #5 rebar, each measuring approximately 9 ft 7.5 in. in length, were tied to the top of the existing #3 rebar grid (two #5 bars placed at each transverse end perpendicular to the load transfer dowels).

The entire reinforcement grid was then lifted and placed within the constructed formwork such that the #5 bars were oriented perpendicular to the load transfer dowels. The grid was centered within the formwork to allow a 1.5-in. gap between the ends of the reinforcement and the formwork. Then, approximately 25 1.5-in. metal bar chairs were placed under the lower #3 bar layer of the grid to hold the reinforcing grid at the correct elevation to allow the proper cover of the bottom of the panel to the reinforcement (1.5 in.) (Figure B.9). The chairs were spaced evenly to minimize any sagging and provide sufficient stability.

Figure B.9. Installation of rebar grid on chairs.

B.5 Step 5: Install load transfer dowels

The next step was to insert load transfer dowels into the forms (Figure B.10). The standard frame was designed with dowel openings on two sides of the frame. The terminal frame was designed with dowel openings on only one side of the frame. The dowels were centered 5.5 in. from the top surface of the panel. Each 1-in.-diam dowel was 22 in. long. This length allowed 11 in. for the precast panel, with an additional 11 in. remaining to tie into the parent slab. Dowel bars were spaced 1 ft apart with the first dowel situated 6 in. from the edge of the precast panel. Exterior dowel alignment forms were used to maintain proper alignment during concrete placement.

Figure B.10. Installation of the dowel bars.

Ensuring and maintaining proper alignment of each dowel was imperative. Misaligned dowels have the potential to prevent form removal, may possibly result in damage to the precast panel and/or the rigid form, and could negatively impact load transfer and/or cause premature pavement failure. The following paragraph describes the dowel installation process in greater detail.

Each dowel center was marked and taped with duct tape. The tape was necessary to help seal the void around the dowel openings in the frame. Each dowel was then lightly greased on one end and installed into the formwork by sliding the non-greased end from the interior of the formwork through the dowel receptacle. Inserting the dowels in this direction eliminated the loss of grease. Once all dowels were installed, the dowel holes were packed with grease to prevent concrete from flowing through the gap between the dowels and the edges of the dowel holes.

B.6 Step 6: Install blockouts (terminal panel only)

To cast dowel receptacles in the terminal panels, blockouts were installed on the side of the panel opposite the dowels. Prior to installation, all threaded holes and bolts were greased to ensure concrete did not flow around the threads. Additionally, form release oil was applied to all surfaces of the blockouts. The blockouts were then bolted to the form using individual bolts. For ease of installation, the top surface was stamped “TOP.” After ensuring that the top of each blockout was parallel and level with the top of the form, all bolts were tightened with an impact wrench.

B.7 Step 7: Install the upper #5 reinforcement bars

Following the installation of dowels on both forms and the installation of the blockouts on the terminal form, the next step was to install an upper layer of #5 reinforcement bars (shown in Figure B.11). Two groups of three bars were installed, and their installation location depended on the dowel bar arrangements on the side of the form.

Figure B.11. Locations of the #5 rebar.

For the dowel sides of forms:

Two of the #5 bars were positioned on top of the installed dowels, located at 5 and 10 in. on center from the edge of the formwork (vertically above and parallel to the #5 bar installed on reinforcement grid). A third bar was then placed with its center 15 in. from the edge of the formwork. This bar was held in place using three 6-in.-high reinforcing chairs to support the bar. The #5 bars were then tied to the dowels or chair. When tying to the dowels, 8-in.-long ties were used; otherwise 6-in.-long ties were used. Once tied, the ends of the #5 bars were checked to be flush with one another and the underlying #3 bars. (If correctly placed, the #5 reinforcement were perpendicular to the load transfer dowels.) Then 1-ft-long sections of #3 rebar were tied underneath the upper #5 bars. A total of three of these sections were equally spaced and centered between the original layers of #3 bars. Each was tied at the intersections.

For the terminal form:

Since there were no preinstalled dowels at this location, all bars were supported using 6-in.-high rebar chairs. Bars were installed 14, 19, and 24 in.

on center from the edge of the formwork. These distances were measured perpendicular to the exterior-most blockout. Each #5 bar was placed on 6-in.-high chairs to which they were tied.

B.8 Step 8: Place PCC

Following preparation of the forms, each was filled with PCC. The concrete was placed, consolidated, screeded, and finished following typical concrete placement techniques. A 1.5-in.-diam spud vibrator was used to consolidate the concrete. Particular care was taken to ensure good consolidation around the edges, in corners, and around blockouts and dowels. Each panel was slightly overfilled by 0.5 in. to provide enough material to fill in the surface while screeding. The panels were screeded using a vibratory concrete screed, and excess material was removed during screeding as needed to provide a PCC surface that was flush with the top of the forms. A 4-ft bull float and magnesium hand floats were then used to level and fill the slab surface. Care was taken not to over finish the surface. No water was used in finishing the panels, and finishing edgers were not used to round edges.

Following concrete placement, all materials used to place, consolidate, and finish the slabs were cleaned, and the dowel bar embedment depths were checked for each panel. If necessary, the dowels were adjusted.

B.9 Step 9: Install lifting anchors

Just prior to placing the PCC, the lifting anchors were prepared by assembling the anchor and attaching a rubber recess form (provided with the lifting anchor by the manufacturer) around the top (thicker) end of the anchor (Figure B.12). Then duct tape was used to completely seal the seams and surface of the rubber recess form to prevent mortar from entering during concrete placement.

After the PCC had been placed, lifting anchors were installed into the PCC approximately 30 to 60 min after finishing so that the anchor did not float in the concrete. A plywood template was used to aid in placing the anchors 2.5 ft from the corner of each panel. The anchor was inserted until approximately 0.25 in. of the rubber recess form was above the surface of the PCC (Figure B.13). Then a hand float was used to fill any holes around each anchor and to push the anchor into position where it was flush with the surface of the surrounding concrete.

Figure B.12. Anchor and rubber recess.

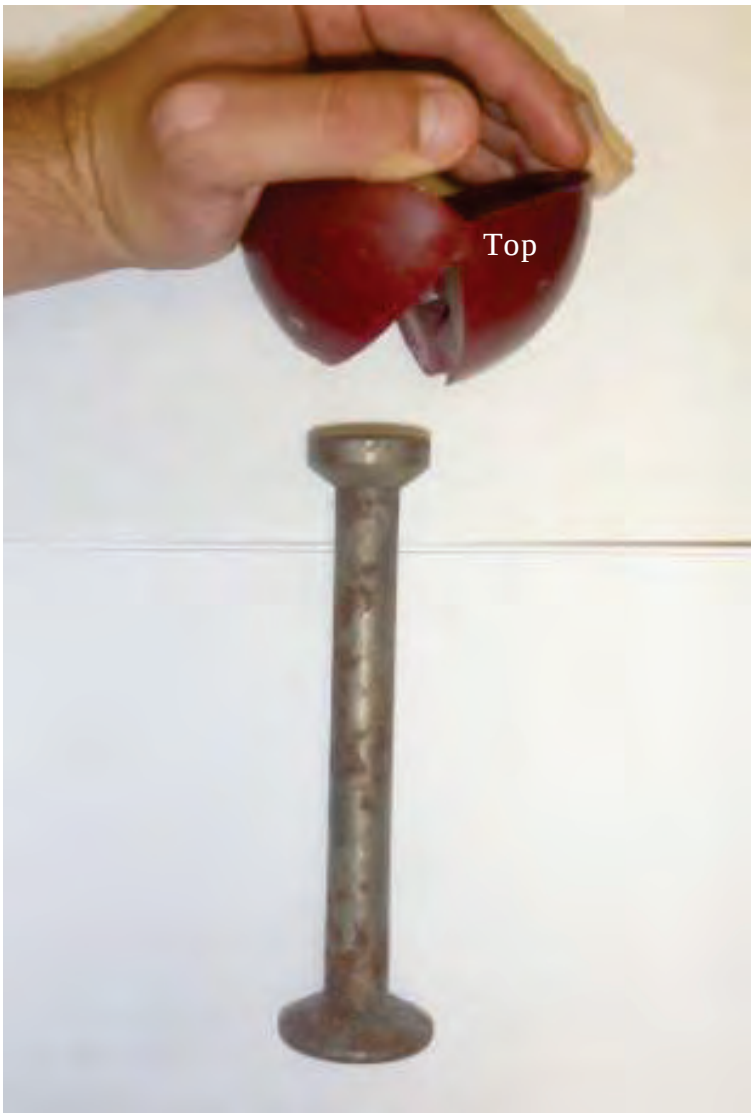

Figure B.13. Installing anchors.

B.10 Step 10: Final finish

After the lifting anchors had been installed and the concrete had stiffened sufficiently, final finishing techniques were applied with the bull float to remove any excess water and surface deformations caused from the smaller hand finishing tools. A broom finish was then applied to each panel. Panels were then coated with a double application of curing compound using a hand pump sprayer.

B.11 Step 11: Form removal

After approximately seven days, the concrete forms were removed from the panels. Figure B.14 shows the cured panel in the forms. The anchor bolts holding the forms to the underlying concrete pavement were first removed. Then, the connection bolts holding the forms together were removed. A mallet was used to remove the longitudinal form sections to break the bond between the PCC and the form by striking the ends of each corner of the form. Care was taken to remove the transverse form sections without damaging the dowels or the dowel blockouts. Lumber was used to pry the form segments away from the PCC. Using lumber mitigates potential damage to the precast slab (i.e., chipping, spalling).

Figure B.14. Cured panel in form.

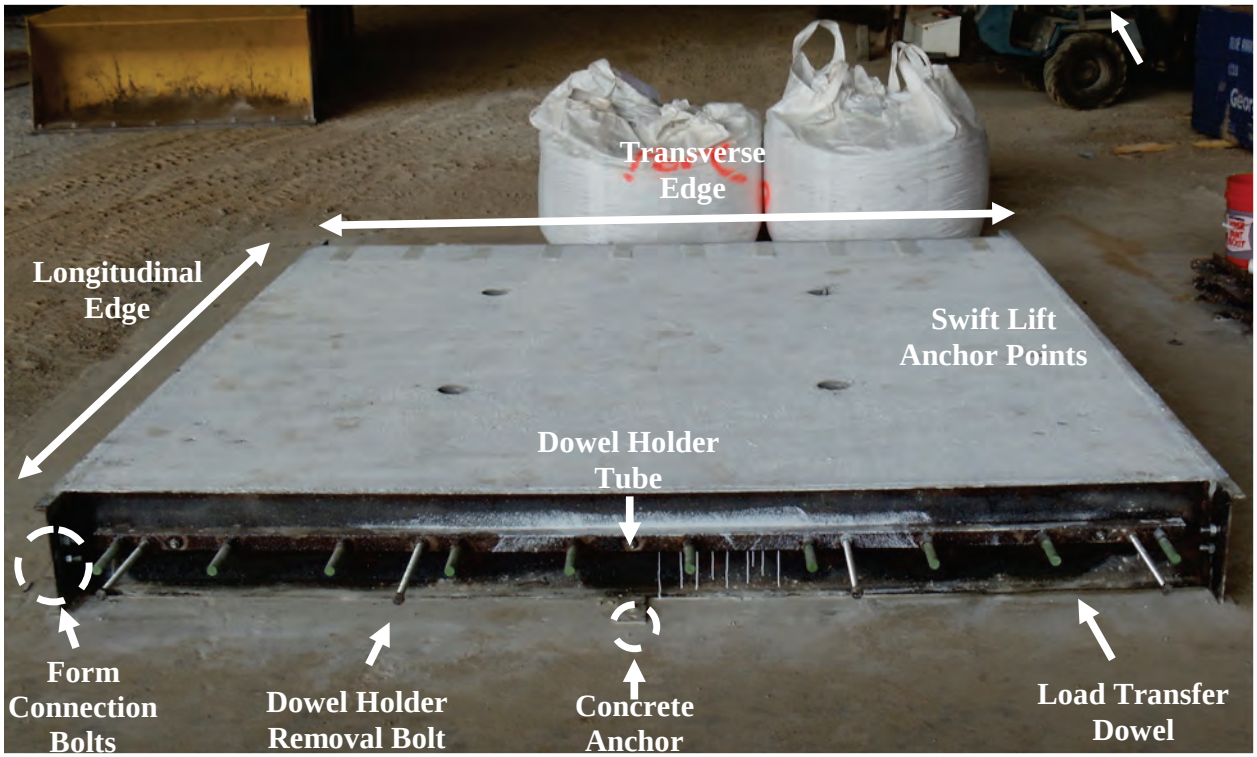

For forms using dowel blockouts, the bolts connecting the blockouts to the form were removed, and the blockouts remained in the PCC. The bolts were then reinserted into the blockouts to provide leverage to remove each blockout by lifting upwards. A hammer was used if needed to help in removal.

Once the forms were removed, the tape surrounding the tops of the lifting anchors was removed. All surfaces that had been covered by the forms were then sprayed with curing compound, and the forms were reassembled in a different location; all steps were repeated until an adequate number of panels had been prepared. Completed panels were allowed to cure in place for a total of 28 days.

Appendix C: Test Section Construction and Precast Panel Placement Procedure

This appendix provides details of the construction of the test section and the precast panel repair process not fully detailed in the main body of this report.

C.1 Test section construction

C.1.1 General design

A 60-ft-wide by 100-ft-long PCC test section was constructed at the ERDC in Vicksburg, MS, during the period April through July 2011. The test section was designed using the Pavement-Transportation Computer Assisted Structural Engineering (PCASE) software. Assumptions used as input to the software were (1) a PCC airfield surface with a flexural strength of 650 lb/in.^{2}, (2) no drainage layer, (3) an aggregate base thickness of 6 in., (4) a modulus of subgrade reaction of 150 lb/in.^{3}, and (5) a design life of 50,000 C-17 passes. Using the PCASE software and the above assumptions, a 14-in.-thick PCC layer was required. The software recommended a pavement joint spacing of 15 to 20 ft with dowel spacing of 15 in., dowel length of 20 in., and a dowel diameter of 1.00 to 1.25 in., based upon current DOD criteria for airfield pavements. Based on these results, the PCC test section was designed to consist of 15 20-ft-wide by 20-ft-long slabs, each 14 in. thick, as shown in Figure C.1. Dowel diameter was selected to be 1.00 in. with the required length of 20 in. and spacing of 15 in. also selected in accordance with rigid pavement design criteria for military airfield pavements.

Seven precast repair panels were fabricated as detailed in Appendix B and were installed in the test section as shown in Figure C.2 following its construction. This appendix describes the construction of the full-scale test section and the precast panel repair process.

C.1.2 Sublayer preparation

The subgrade of the test section was prepared by excavating all surface material to a depth ranging from 20 to 22 in. The natural soil consisted of low-plasticity clay with sand with a Unified Soil Classification of CL. The

Figure C.1. PCC test section original construction layout.

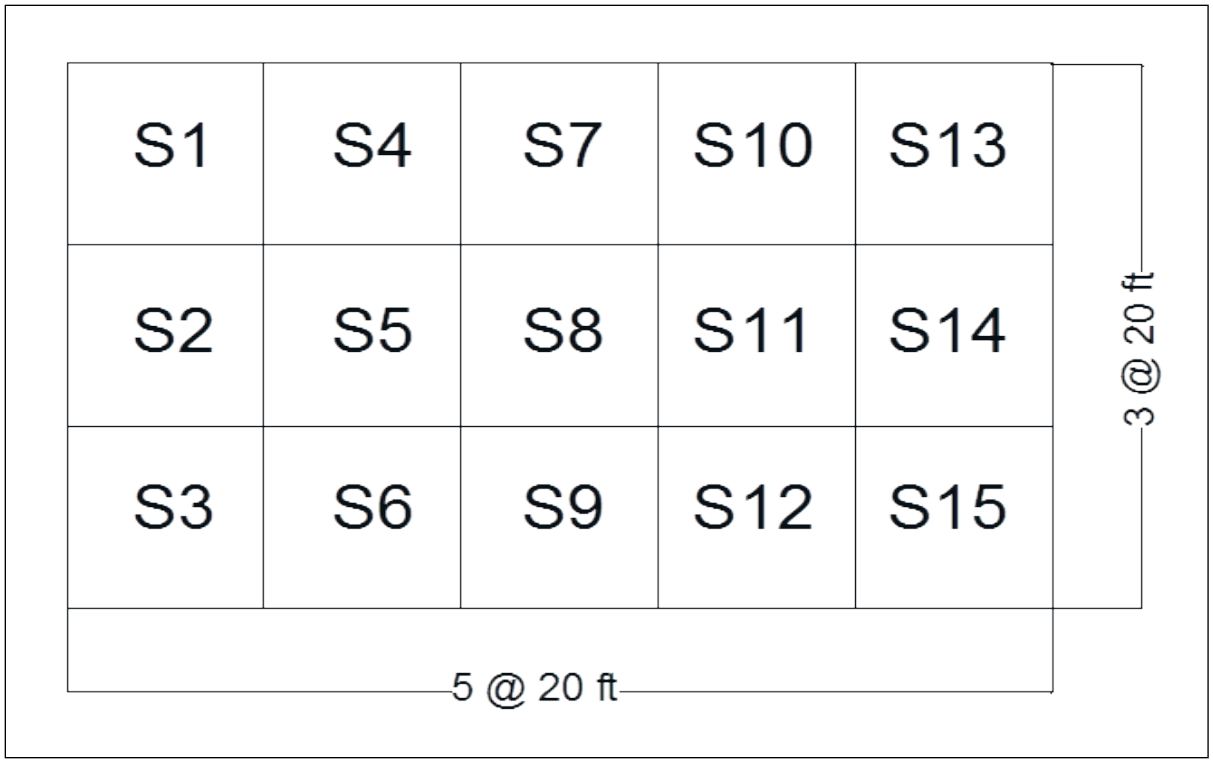

Figure C.2. PCC repair panel layout-plan view.

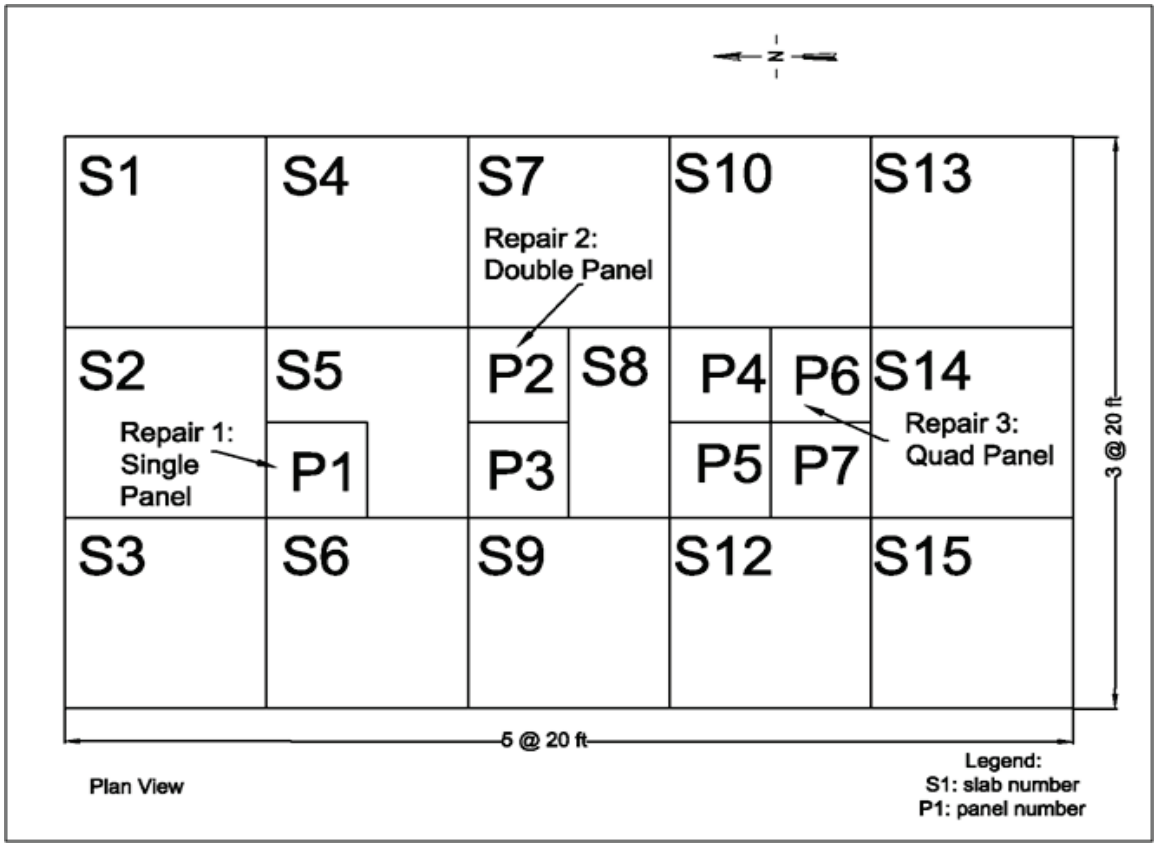

material had a liquid limit of 36 and a plasticity index of 14. The material consisted of 8.7% gravel, 11.5% sand, and 79.8% fines. Modified proctor testing resulted in a maximum dry density of 120.7 lb/ft^3 and an optimum moisture content of 12.1%. The CL was compacted with three passes of a 23,150-lb vibratory smooth drum compactor to create a firm working platform for placement of the upper foundation materials.

A 6-in.-thick base course was then constructed using crushed limestone with a classification of GW. The base was compacted with three passes of a 23,150-lb vibratory smooth drum compactor. Both the subgrade and base materials were placed on a 1% (1 ft) longitudinal slope and a 0.5% (0.3 ft) cross slope for drainage.

The foundation materials were further characterized by performing dynamic cone penetrometer (DCP), nuclear moisture-density, and modulus of subgrade reaction tests after compaction was completed. Table C.1 summarizes pertinent soils test data for the sublayers. As seen in the table, the DCP-estimated CBR under slab 1 was much stronger than that under the other test areas. The DCP test results indicated that the base layer under this slab was stronger than the other test points in the test section. This is because either the base layer was better compacted in this area or the DCP encountered a rock. Plate-load testing conducted on the surface of the base course resulted in an effective modulus of subgrade reaction (k) of 276 lb/in.^{2}/in.

Table C.1. Sublayer test data.

Corresponding Slab	Location	Moisture, %	Dry Density, lb/ft^3	CBR, %	Effective Modulus of Subgrade Reaction, lb/in.^{2}/in.
S1	Subgrade	10.3	116.4	31	276
S1	Base	2.1	127.5	95	
S3	Subgrade	11.6	108.5	25	
S3	Base	1.3	123.7	29	
S7	Subgrade	12.7	112.2	9	
S7	Base	2.7	126.3	15	
S9	Subgrade	9.0	115.7	6	
S9	Base	1.6	121.8	33	
S13	Subgrade	3.9	128.5	9	
S13	Base	4.9	124.2	27	
S15	Subgrade	12.6	113.8	6	
S15	Base	2.0	125.4	21	

C.1.3 PCC placement

Concrete construction work was completed in July 2011 by ERDC's Directorate of Public Works and APB personnel. The test section dimensions were 100 ft by 60 ft by 14 in. The joints were doweled using 1-in.-diam, 20-in.-long epoxy coated steel dowels, as shown in Figure C.3. Dowels were spaced 15 in. on center and placed mid-depth of the slab (7 in.). The section was constructed by placing concrete first in the outside slabs then in the interior slabs. A locally available 650-lb/in.^{2} flexural strength fixed-form paving concrete was used. Following placement, a light broom finish was applied to the section. A double coat of white-pigmented, membrane-forming curing compound was applied. The average 28-day compressive and flexural strength results were 7,240 lb/in.^{2} and 940 lb/in.^{2}, respectively. These average 28-day results are well above the minimum requirements of 5,000 lb/in.^{2} and 650 lb/in.^{2}, respectively. Table C.2 summarizes the strength test data for the PCC.

Figure C.3. Dowel locations.

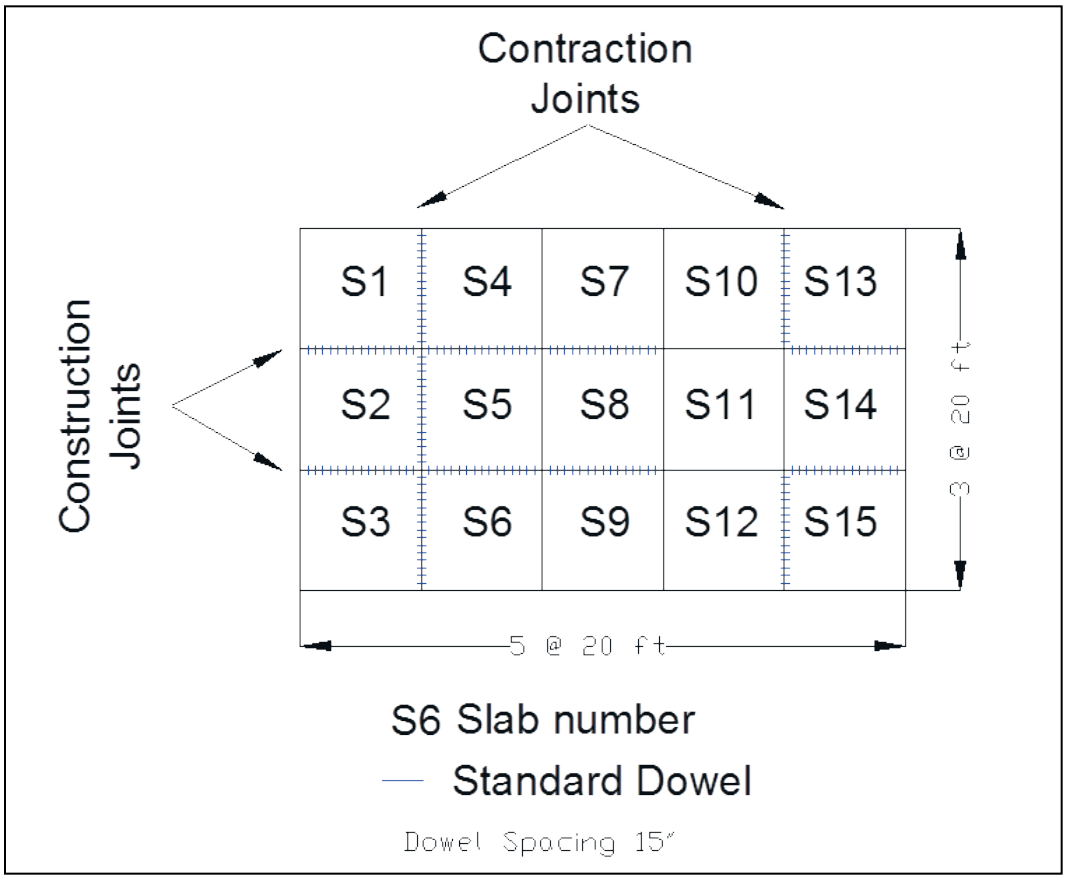

Table C.2. PCC test data.

Truck Number	Specimen Number	Type of Specimen	Age in Days	Compressive Strength, lb/in.^{2}	Flexural Strength, lb/in.^{2}
Lane 1 Truck 3	1	6 by 12 cylinder	28	6,950	--
	2	6 by 12 cylinder	28	7,200	--
	3	6 by 12 cylinder	28	6,870	--
	4	Flex beam	28	--	850
	5	Flex beam	28	--	840
	6	Flex beam	28	--	840
	Average			7,010	840
Lane 1 Truck 5	7	6 by 12 cylinder	28	5,840	--
	8	6 by 12 cylinder	28	6,340	--
	9	6 by 12 cylinder	28	6,280	--
	10	Flex beam	28	--	720
	11	Flex beam	28	--	770
	12	Flex beam	28	--	740
	Average			6,150	740
Lane 1 Truck 8	13	6 by 12 cylinder	28	6,250	--
	14	6 by 12 cylinder	28	6,590	--
	15	6 by 12 cylinder	28	6,190	--
	16	Flex beam	28	--	750
	17	Flex beam	28	--	760
	18	Flex beam	28	--	780
	Average			6,340	760
Lane 2 Truck 3	1	6 by 12 cylinder	28	7,930	--
	2	6 by 12 cylinder	28	6,670	--
	3	6 by 12 cylinder	28	6,630	--
	4	Flex beam	28	--	1,060
	5	Flex beam	28	--	980
	6	Flex beam	28	--	1,000
	Average			7,080	1,010
Lane 2 Truck 5	7	6 by 12 cylinder	28	8,390	--
	8	6 by 12 cylinder	28	7,930	--
	9	6 by 12 cylinder	28	8,890	--
	10	Flex beam	28	--	960
	11	Flex beam	28	--	930

Truck Number	Specimen Number	Type of Specimen	Age in Days	Compressive Strength, lb/in.²	Flexural Strength, lb/in.²
	12	Flex beam	28	--	1,060
	Average			8,400	980
Lane 2 Truck 5	13	6 by 12 cylinder	28	8,200	--
	14	6 by 12 cylinder	28	7,000	--
	15	6 by 12 cylinder	28	8,160	--
	16	Flex beam	28	--	1,110
	17	Flex beam	28	--	810
	18	Flex beam	28	--	1,030
	Average			7,790	980
Lane 3 Truck 8	1	6 by 12 cylinder	28	7,240	--
	2	6 by 12 cylinder	28	7,620	--
	3	6 by 12 cylinder	28	7,650	--
	4	Flex beam	28	--	1,040
	5	Flex beam	28	--	1,160
	6	Flex beam	28	--	1,310
	Average			7,500	1,170
Lane 3 Truck 6	7	6 by 12 cylinder	28	7,500	--
	8	6 by 12 cylinder	28	7,550	--
	9	6 by 12 cylinder	28	7,630	--
	10	Flex beam	28	--	1,040
	11	Flex beam	28	--	960
	12	Flex beam	28	--	980
	Average			7,560	990
Lane 3 Truck 12	13	6 by 12 cylinder	28	5930	--
	14	6 by 12 cylinder	28	8020	--
	15	6 by 12 cylinder	28	7960	--
	16	Flex beam	28	--	990
	17	Flex beam	28	--	990
	18	Flex beam	28	--	1,020
	Average			7,300	1,000
Average				7,240	940

After curing for 6 hr, joints were sawed to a depth of 4.5 in. A 0.5-in.-wide by 3/8-in.-deep back cut was made to create a joint sealant reservoir. The joints were sealed by first installing a layer of bond-breaking tape applied to the depth of the cut and a 1/4-in.-thick layer of field-molded joint sealant a few days after cutting the back cuts to allow the concrete to dry.

C.1.4 Field testing- precast panel repairs

Following curing for 28 days, three areas were marked in the test section to represent damaged pavement requiring repair, as shown in Figure C.2. Repair 1 simulated a partial slab replacement along two joints with a single-panel repair. This repair surface area was 10 ft by 10 ft. Repair 2 simulated a half-slab replacement along a joint requiring two panels to repair a surface area of 10 ft by 20 ft. Repair 3 simulated a full-slab replacement requiring four panels to repair a surface area 20 ft by 20 ft. The following sections describe the repair process for the three repair areas. Equipment and materials required to complete repairs are listed in Table C.3.

A team of 12 people was used for the installation, although not all of them were used for every repair step. Numerous activities were conducted simultaneously with subteams consisting of two to three people. One of the team members was a licensed crane operator needed to remove the damaged pavement and place the precast panels.

Table C.3. Equipment and materials required for placing precast panels.

	Activity							
Equipment/Supplies	Delivery	Distressed Area Prep	Distressed Area Removal	Bridge Plate Installation	Base Preparation	Panel Placement	Dowel Sleeve Sealing	Joint Sealing
4-ton Swift Lifting Eyes	x		x			x		
5-gal Plastic Buckets							x	
8-ft Synthetic Endless Round Slings	x		x			x		
Air Compressor			x	x			x	x
Dowel Receptacle Template		x						
Bolts, Washers etc.			x	x				
Bridge Plates (custom)				x		x		
Bridge Plate Template (custom)								
Bucket Opener (for dowel grout)							x	

Equipment/Supplies	Activity							
	Delivery	Distressed Area Prep	Distressed Area Removal	Bridge Plate Installation	Base Preparation	Panel Placement	Dowel Sleeve Sealing	Joint Sealing
Chalk Line Tools		x						
Concrete Anchor Drilling Jigs		x		x				
Concrete Expansion Anchors		x						
Concrete Floor Saw and Blades		x						
Concrete Sand						x		
Drilling Hammers		x		x				
Dunnage	x							
Expansion Joint Board							x	x
Extension Cords		x		x			x	x
Flatbed Truck	x							
Floor Brooms		x		x	x	x	x	x
Flowable Fill in Concrete Truck					x			
Flowable Fill Screed (custom)					x			
Generators		x		x			x	x
Grout Hand Mixers with Paddles							x	
Hand Elements- Shovels, Concrete Rakes, Pry Bars, Hammers, etc.			x	x	x	x		
Hand Floats							x	
Hand Grinder				x				
Heavy Duty Garden Hoses					x		x	
Impact Hammer		x						
Infrared Thermometer							x	x
Joint Sealant Gun								x
Knee Pads				x	x	x	x	
Lifting Eyes	x	x	x			x		
Marking Crayons/Paints		x		x	x			
Measuring Tapes		x		x	x	x		
Crane	x		x			x		
Pavement Breaker Chisels			x					
Pavement Breakers			x					
Pedestal (for 4-panel repair)						x		
Various Wrenches	x	x	x	x				
Plywood						x	x	
Portable Band Saw						x		

Equipment/Supplies	Activity							
	Delivery	Distressed Area Prep	Distressed Area Removal	Bridge Plate Installation	Base Preparation	Panel Placement	Dowel Sleeve Sealing	Joint Sealing
Personal Protective Equipment	x	x	x	x	x	x	x	x
Precast Panels	x					x		
Rapid-Setting Repair Mortar							x	
Silicon Joint Sealant								x
Shop Vacuum			x					
Swivel Hoist Rig	x		x			x		
Torque Wrenches		x						
Various Thickness Shims						x		
Vibratory Roller						x		

C.1.5 Repair 1 – single-panel repair

Repair 1 was conducted in early November 2011. The following sections detail the process and steps required for conducting this single-panel repair.

C.1.5.1 Distressed area removal

The process for removing the distressed area is presented in the following steps and in Figure C.4.

1. Mark area for removal

For Repair 1, a 10-ft by 10-ft section of Slab 5, as shown in Figure C.2, was selected for removal. A chalk-line tool was used to mark the area to be removed, and paint was applied to mark the saw-cut perimeters. The locations of dowel receptacles were then marked using a plywood template and spray paint. Dowel receptacles were marked on the transverse edges of the repair area perpendicular to the traffic direction.

Figure C.4. Preparation and removal of parent PCC: (a) saw cutting dowel receptacles and repair area, (b) drilling to install concrete lifting anchors, (c) installing lifting eyes, (d) connecting lifting eyes to crane rigging, (e) lifting "damaged" pavement, (f) preparing dowel receptacles using jackhammers, (g) close-up of dowel receptacles, and (h) prepared repair area.

2. Perform saw cutting

Once all locations for pavement removal and dowel receptacles were marked, saw-cutting operations were conducted with a concrete saw capable of cutting a depth of at least 18 in. The square repair area was saw cut first. The saw-cutting operations were completed using a series of four passes, with the depth of cut progressively increased approximately one-quarter of the total slab depth during each pass. Progressively larger saw blades were utilized to ensure precise, accurate cuts. The first and second passes were each made with a 24-in.-diameter blade. A 36-in.-diameter blade was used for the third and fourth (final) passes.

3. Once the 10-ft by 10-ft area was saw cut, the dowel receptacles in the parent concrete pavement were saw cut. Dowel receptacles were cut prior to extracting the damaged slab for safety purposes. Each marked dowel receptacle was 12 in. long and 3 in. wide and was designed to be 6.5 to 7 in. deep after excavation. Two 6.75-in. deep (approximate) vertical cuts were made for each dowel location. The saw operator used a 24-in.-diameter blade to cut the dowel receptacles. This step is shown in Figure C.4a.
4. Install expansion anchors

After saw cutting, expansion anchors were installed to remove the parent PCC in a single section. To install the anchors, each anchor location was marked 30 in. from each corner of the slab to be removed. Four anchors were required for balance and slab stability when lifting. A rotary hammer and a 1.25-in. concrete drill bit were then used to drill 12-in.-deep holes for the expansion anchors. This step is shown in Figure C.4b. Care was taken to ensure that the drill bit remained generally vertical. Once the holes were drilled, compressed air was used to remove debris from each hole, and then the expansion anchors were installed. The expansion anchors were checked to ensure that the base of the cone was flush with the threaded rod, and the assembly was tightened finger tight. The anchors were then placed into the holes cone-side down. An anchor-setting tool was placed through the threaded rod to drive the anchor into the pavement using a small sledgehammer. The anchor was finally driven into the pavement until the washer was flush with the pavement surface.

5. Remove damaged pavement section(s)

Once expansion anchors were installed, the nut and washer from each installed expansion anchor were removed, and a swivel hoist lifting point

and washer were inserted over the threaded anchor rod. The swivel hoist lifting points used were 8-ton Dayton Superior swift lifts. The nut and washer were then returned to the anchor, and an impact wrench was used to tighten the nut of the anchor. A torque wrench was then used to tighten the nut until 250 ft-lb of torque was reached. Any excess threaded rod was then removed using a portable band saw. This step is shown in Figure C.4c.

A crane was used to lift the 10-ft by 10-ft pavement section. For this project, four round slings were shackled together and installed on the hook of the crane. Each swivel lift point was connected with a sling. Care was taken to ensure that the nut and safety clip were installed prior to lifting. This step is shown in Figure C.4d. Once the lifting points were connected to the crane, the 10-ft by 10-ft section of pavement was slowly lifted from the test section and removed from the site (Figure C.4e).

6. Prepare dowel receptacles

Once the pavement section was removed, a 22-lb electric jackhammer with 1.5-in. chisel was initially used to remove the pavement between the parallel saw cuts performed previously, as shown in Figures C.4f and C.4g. The jackhammer was inserted at a slight angle at the back of the painted boundary. Care was taken to ensure that the receptacle was generally rectangular in shape with even dimensions across each side. Each receptacle was cleaned with compressed air, a steel brush, and a shop vacuum. The final prepared area is shown in Figure C.4h.

C.1.5.2 Installation of bridge-plate anchors and lifting points

The next step in the repair process was to install bridge-plate anchors that connected the precast panel (P1) to the parent slabs during seating. Figure C.5 shows the location of the bridge plates for all three repairs conducted. To reduce the total repair time, this step was conducted when the distressed area was being prepared. For single-panel repairs, four bridge plates were required. The bridge plates aided in installation of the precast panels by providing additional support during the seating of panels and prevented the panels from settling in the base material. An anchor template was used to mark the drilling locations for installing 1/2-in. concrete expansion anchors into the parent slabs to secure the bridge plate. A hammer drill with a 0.5-in. masonry drill bit was used to drill approximately 6-in.-deep holes that were then cleaned with compressed air.

Figure C.5. Bridge plate configurations for the repairs.

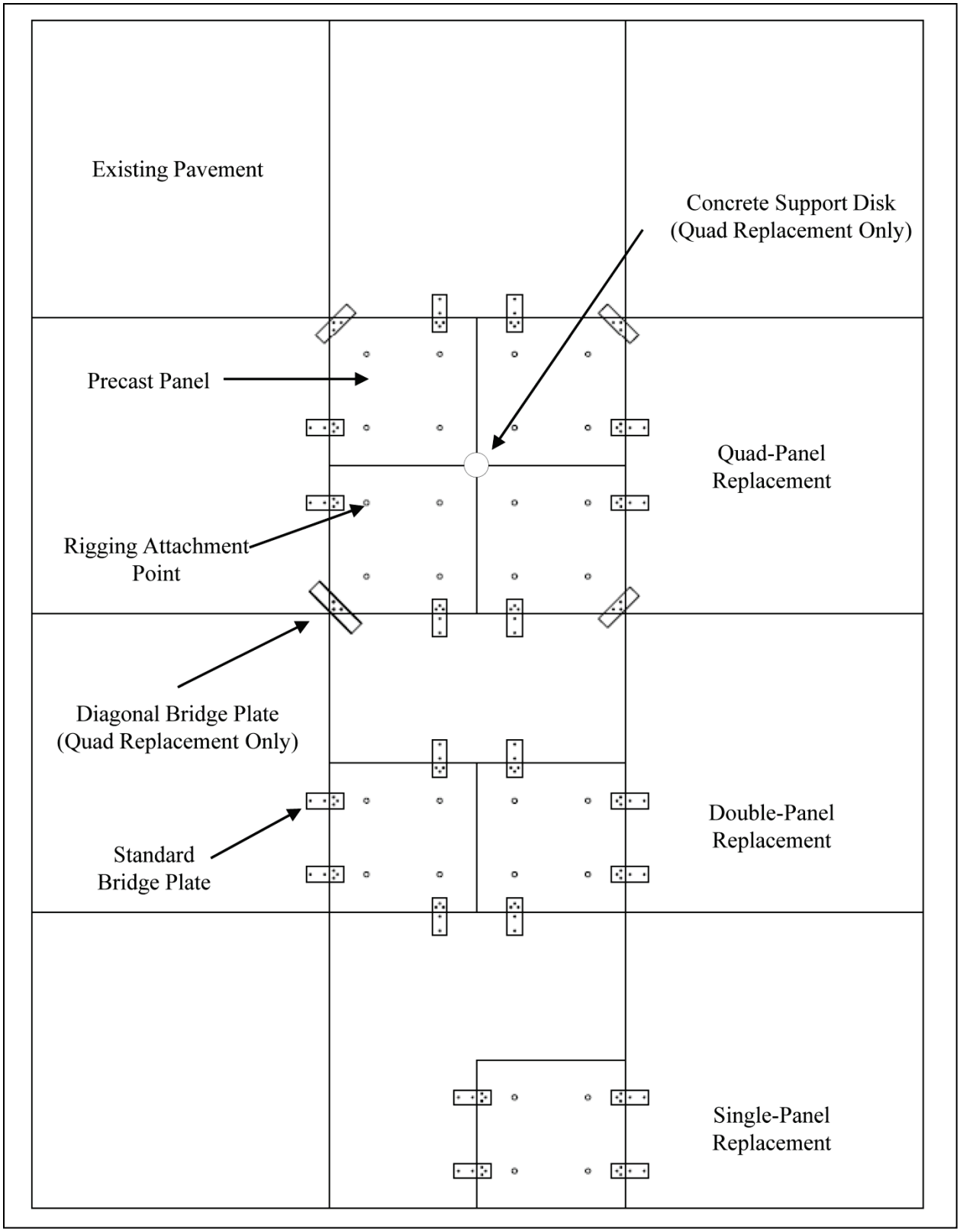

The concrete expansion anchors were inserted cone-side down without the nut and washer and were driven into the parent slabs with a small sledge-hammer. The bridge plates were then placed over the installed concrete anchors to ensure correct alignment. The bridge plates were removed, and the washer and nuts were returned to the anchors and tightened by hand. The nuts were then tightened with a torque wrench until 55 ft-lb of torque was reached. This process is shown in Figure C.6.

Figure C.6. Installation of bridge plates: clockwise from top left: using template to mark anchor locations, drilling holes for anchors, installing anchor, and completed bridge plate installation and lifting eyes.

C.1.5.3 Base preparation

Immediately following the removal of the damaged slab, the base layer was prepared. Because the parent slab was approximately 14 in. thick and the precast repair panels were only 11 in. thick, a new 3-in.-thick base course layer was needed for seating the precast panels.

Flowable fill was selected for the base layer due to the self-leveling nature of the material and because of its acceptable performance in previous

AFRL precast panel field tests. This material is a blend of Portland cement, fly ash, fine mineral aggregate, and water. The flowable fill was designed and delivered from a local ready-mix plant in a standard transit truck. The flowable fill mix design is presented in Table C.4. The base preparation is presented in Figure C.7.

Table C.4. Flowable fill mixture design.

Materials:	Supplier	Spec	Test Method
Cement	Suwannee Cement Company	Type I/II	ASTM C-150
Fly Ash	STI-Pro Ash Company	Class F	ASTM C-618
Coarse Agg.	NA	Grade # 67	ASTM C-33
Fine Agg.	Sikes Sand Company	Silica Sand	FDOT 901
Admixture #1	Euclid Chemical Co., WR	Type A/D	ASTM C-494
Admixture #2	NA	Type F/G	ASTM C-494
Admixture	Euclid Chemical Co., AEA928	Type F/G	ASTM C-494

Material per cu. yd	SSD Weights	Specific Gravity	Absolute Volumes
Cement, lbs	100	3.15	0.51 cubic ft
Fly Ash, lbs	500	2.44	3.28 cubic ft
Coarse Agg., lbs	0	2.6	0 cubic ft
Fine Agg., lbs	2260	2.63	13.77 cubic ft
Air Volume			4.05 cubic ft
Water, Gals.	40		
Water, lbs	333	1	5.34 cubic ft

Test Data	
Slump Range	NA
Air Range	15.00%
Unit Weight	118.47 lbs
W/C Ratio	0.56
Cememtitious	600 lbs

Figure C.7. Placement of precast panel: (a) screeding of flowable fill, (b) placing panel, (c) placed panel with plywood spacers, (d) close up of dowels in dowel receptacles, (e) using compactor to seat panel, and (f) panel prior to dowel receptacle grouting.

(a) (b)

(c) (d)

(e) (f)

Prior to placing the flowable fill, the sides of the repair area were marked around the perimeter of the hole 11 in. from the surface to provide a visual mark for the top of the base surface. The flowable fill was placed in the hole and was distributed using concrete rakes and flathead shovels. During placement, the flowable fill was extremely wet, indicating that the w/c ratio was higher than expected. The vendor was contacted to make adjustments to the mix for the subsequent repairs.

The flowable fill markings were overfilled by approximately 1/8 in. The material was then screeded using a simple metal screed that fit into a 10-ft-wide hole with a depth of approximately 11 in. (less the 1/8-in. overfill). Plywood was laid over the dowel receptacles to allow screeding; without the plywood, it was impossible to screed over the removed receptacle sections. The screed was used to level the surface of the flowable fill while still allowing adequate depth for the panel to be placed. During screeding, any excess material was removed. The flowable fill was screeded twice, using perpendicular screedings to ensure smoothness in both directions. Screeding is presented in Figure C.7a.

C.1.5.4 Placement of Panel 1

Prior to the placement of the flowable fill, Panel 1 (P1), a standard panel (with attached bridge plates), was secured to the crane using rigging hardware connected to each of the pre-installed swift-lift attachment points and was positioned next to the repair location. Immediately following placement and leveling of the flowable fill, as described in the previous section, the panel was placed using the crane (Figure C.7b). Various plywood spacing shims of thicknesses 0.125, 0.25, and 0.5- in. were placed in each corner of the prepared repair to maintain at least a 0.375-in.-wide joint between the precast panel and the existing slab and to protect the corners of the precast panel (Figure C.7c). Care was taken to prevent misalignment of the dowels within the dowel receptacles. Proper alignment is shown and presented in Figure C.7d. The installed panel did not completely compress the flowable fill layer, which had been slightly overfilled. A small vibratory roller compactor was rolled across the center of the panel to fully seat it (Figure C.7e). A full-sized plywood sheet was placed prior to roller operation to prevent damage to the precast panel. The final placed panel is shown in Figure C.7f.

C.1.5.5 Sealing the dowel receptacles and joints

The final installation procedure entailed filling the dowel receptacles and sealing the joints. A rapid-setting spall repair material, Pavemend 15.0, was used to fill the dowel receptacles. It was mixed following manufacturer guidance using drills and paddles. This rapid-setting grout was selected for use based on previous AFRL field testing of dowel grouting for precast panels. Once mixed, each bucket of material was emptied into the dowel receptacles. The grout flowed outside the edge of the parent pavement and into the joints surrounding the panel. The material was self-leveling and did not require surface finishing. The joints between the PCC slab and the precast panel were then shallowly saw cut and filled using silicone-based joint sealant. The placement of the grout is shown in Figure C.8. Additionally, the final completed repair is shown in this figure. After at least 2 hr of cure, the bridge plates were removed, and the anchors were cut and ground flush with the surface to reduce tire hazards.

Figure C.8. Left: placement of rapid-setting grout in dowel receptacles, and right: grouted and sealed panel.

C.1.6 Repair 2 – double-panel repair

Repair 2 was conducted during early November 2011 using a team of 12 people. The following sections detail the process and steps required for conducting a double-panel repair.

C.1.6.1 Distressed area removal

For this repair, two 10-ft by 10-ft sections of Slab 8 were removed. The process used to complete Repair 2 followed the steps detailed for Repair 1. First, the repair boundary and the locations of the dowel receptacles were marked. Then, a saw was used to cut two 10-ft by 10-ft square repair areas

along with all the dowel receptacle cuts. Eighty individual dowel receptacle cuts were required.

After performing the cutting procedures, concrete expansion anchors were installed in both concrete sections, swift-lift attachments were installed in one section, and the pavement was removed using the crane as detailed in the previous repair. The swift-lift attachments were then attached to the second pavement section, and that section was removed.

Once the pavement sections were removed, the dowel receptacles were prepared by removing the pavement between parallel saw cuts with a jackhammer and then cleaned as described for Repair 2.

C.1.6.2 Installation of bridge-plate anchors and lifting points

Bridge-plate anchors were then installed on both panels. As with Repair 1, four bridge plates each were attached to Panel 2 and Panel 3 (P2 and P3). These panels were standard panels (with attached bridge plates), and bridge plates were installed in the same manner as Repair 1 for both panels.

C.1.6.3 Base preparation

Following the removal of the distressed areas, a new base course layer was constructed using flowable fill following the process detailed for Repair 1. The material consistency of the flowable fill was deemed better than the previous repair's (less wet). The flowable fill was used to prepare enough base material for a single panel to be placed. Following the placement of one panel, the base for the second panel was prepared. This allowed any excess flowable fill on one side of the repair to flow under the panel to the unfilled side to prevent any excess flowable fill from having to be removed from the dowel receptacles.

C.1.6.4 Placement of Panels 2 and 3

Prior to the placement of the flowable fill, both panels were positioned next to the repair location. As detailed in the previous section, immediately following placement of the flowable fill for one-half the repair area (Figure C.9a), the surface was leveled (Figure C.9b), and Panel 3 was placed using a crane in a similar manner to Repair 1 (Figure C.9c). Following the placement of the first panel, the flowable fill was prepared for the remaining repair area (Figure C.9d); then Panel 2 was placed (Figure C.9e). As with Repair 1, a roller compactor was used to seat the panels (Figure C.9f). Any excess flowable fill around the dowels was then removed.

Figure C.9. Placement of two panels in Repair 2: (a) placing flowable fill and reading first panel, (b) screeding flowable fill for first panel, (c) placing first panel, (d) placed flowable fill for second panel, (e) placing second panel, and (f) seating panel using roller compactor.

C.1.7 Sealing the dowel receptacles and joints

As with Repair 1, the final installation procedure entailed filling the dowel receptacles and the joints following the same procedure detailed previously with the following exception: For the double- and quad-panel repairs, a 0.5-in.-wide construction joint was designed due to the panel and parent slab geometries.

During placement of Panels 2 and 3, the installation team allowed for an excessive construction joint during installation of the first panel, along the longitudinal edge between the existing PCC and the precast panel. This action decreased the available joint space between the precast panels and between the second installed panel and the existing PCC. The longitudinal joint between the precast panels was less than 0.125 in. after the second panel was placed. The two panels made contact with one another, resulting in minor spalling near the joint. This also necessitated using the walk-behind saw to saw cut an adequate longitudinal joint between the two installed precast panels. Following this remediation, the joints were sealed with joint sealant. Following at least 2 hr of cure, the bridge plates were removed from the panels.

C.1.8 Repair 3 – quad-panel repair

Repair 3 was conducted during early November 2011. The following sections detail the process and steps required for conducting a quad-panel repair.

C.1.8.1 Distressed area removal

For this repair, four 10-ft by 10-ft sections of Slab 11 were designated for removal. The process, used to complete Repair 3, followed the steps detailed for the previous repairs with a few differences. As with the previous repairs, the repair boundary and the locations of the dowel receptacles were marked. Then a saw was used to saw cut four 10-ft by 10-ft square repair areas in Slab 11, along with 80 individual cuts for the 40 dowels in this repair.

After performing the cutting procedures, concrete expansion anchors were installed in all four concrete sections to be removed, and swift-lift attachments were installed in one section. Then the pavement was removed using the crane as detailed in the previous repair. This process was repeated until all four sections were removed. Once the pavement

sections were removed, the dowel receptacles were prepared by removing the pavement between parallel saw cuts with a jackhammer and then cleaned as described for the previous two repairs.

C.1.8.2 Setting of the concrete pedestal

An additional step was required for the quad-panel repair. After the panels were removed, a 3-in.-thick concrete pedestal was installed in the center of the repair area to act as a support for the panel corners to prevent the inside corners from sinking into the flowable fill. The pedestal location is shown in Figure C.10a. The pedestal was placed by setting perpendicular string lines to identify and mark the intersection of the four interior panels. A 2-ft square by 1-in.-deep section of base course material, centered at the string line intersection, was excavated to allow the installation team to make fine-tuned adjustments to the pedestal elevation. A 1-in.-thick layer of concrete sand was placed in the excavated section, and the pedestal was placed on top of the concrete sand and twisted into place until the top of the pedestal was 11 in. below the string line.

C.1.8.3 Installation of bridge-plate anchors and lifting points

Bridge-plate anchors were then installed in all four panels. The placement of bridge plates varied from the previous two repairs. Bridge plates were installed in the outside corners of two sides of the panels, and a plate was installed across the outermost corner of each panel as shown in Figure C.5. No bridge plates were installed on the inner side of the panels because there was no parent PCC on which to rest the plate. The bridge plate set up is also shown in Figure C.10.

C.1.8.4 Base preparation and installation of Panels 4-7

Following the removal of the distressed areas, a new base course layer was constructed using flowable fill (Figure C.10a). The flowable fill was used to prepare enough base material for two panels to be placed (Panels 4 and 6). Panel 4 was a terminal panel, and Panel 6 was a standard panel. Following the placement of Panel 4 (Figure C.10b), Panels 4 and 6 were installed using the crane in the same manner as described for the previous two repairs (Figure C.10c). Care was taken when installing Panel 6 to align the dowels in the preformed dowel receptacles in Panel 4 and the dowel receptacles in the parent PCC. Following the placement of Panels 4 and 6, flowable fill was placed to provide base for installing the remaining panels (Figure C.10d). Panel 7 was installed followed by Panel 5 (Figures C.10e and C.10f).

Figure C.10. Installation of Repair 3 panels: (a) pedestal location, (b) placing first panel, (c) using shims to place second panel, (d) placing flowable fill for third and fourth panels, (e) placing third panel, and (f) placing fourth panel.

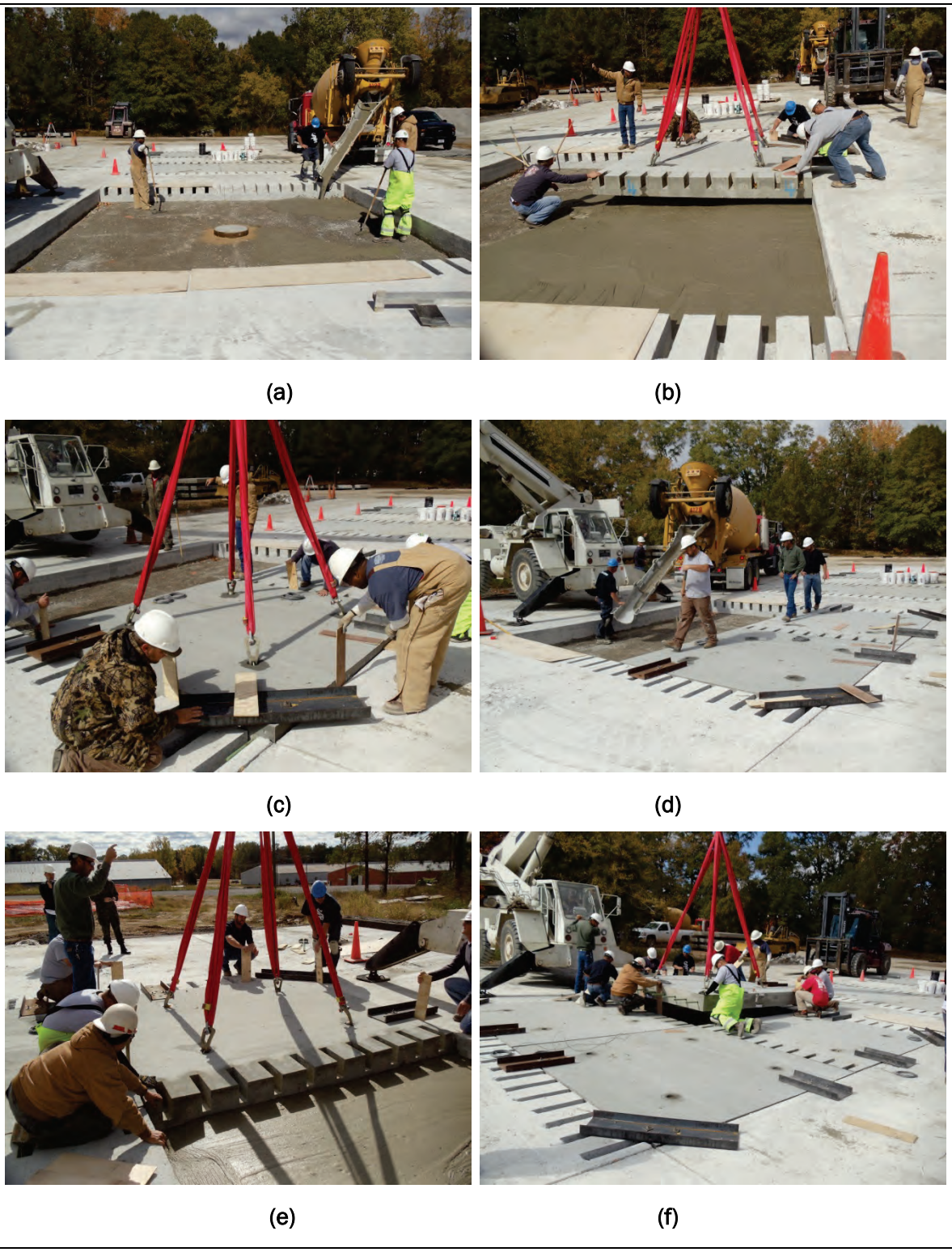

During the seating of Panel 5, the inside edge of Panel 4 was broken. This area required repair during the placement of the dowel receptacle grout, as shown in Figure C.11. There were no issues seating Panels 4, 6, and 7 because excess flowable fill material was able to flow into unoccupied quadrants of the repair section. The excess material migrated into the Panel 5 repair section, as it was the last panel placed. This section was screeded prior to panel placement, and an attempt was made to remove excess material. However, when Panel 5 was placed, there was still excess flowable fill material, and the panel was seated approximately 0.5 in. higher than the existing PCC and the previously installed precast slabs. A vibratory roller was utilized during the single- and double-panel repairs to fully seat the panels. The quad-panel repair bridge plate configuration was different from the previous repairs and did not allow adequate space for the vibratory roller to drive onto the panels. A smaller, portable vibratory roller was placed on the panels. This roller was only partially effective, and Panel 5 was ultimately seated approximately 0.25 in. higher than the existing PCC and precast panels.

Figure C.11. Left: broken corner of a panel, and right: repair of broken corner.

C.1.8.5 Sealing the dowel receptacles and joints

As with previous repairs, the final installation procedure entailed filling the dowel receptacles and the joints following the same procedure detailed previously. Unlike the previous repairs, additional dowel receptacles in the terminal panels also had to be sealed. In this step in the process, all dowel receptacles and the broken corner of Panel 4 were filled with rapid-setting repair material. Sealant was placed in the joint between Panels 4 and 5 and 6 and 7.

C.2 Installation timeline

This section summarizes the installation process timeline for the three precast panel repair operations. The timeline data were compiled during the precast concrete panel installation phase of this project using video footage and notes taken during the events. For rapid installation of panels, all equipment, personnel, and materials must be readily available on site prior to beginning installation. The time to move and set up for panel installation was not recorded, nor are these data included in the installation timeline. Additionally, while a task was being completed, materials and equipment were readied for the next task(s). This ensured the most rapid placement of the panels.

A minimum cure time of 2 hr was recommended for the dowel receptacle filling material to reach a minimum of 3,000 lb/in.^{2} unconfined compressive strength and the flowable fill to reach the required compressive strength based on projected aircraft (55 lb/in.^{2} for the F-15E and 85 lb/in.^{2} for the C-17). The time to remove the bridge plates was included in the curing time of the dowel receptacle fill and flowable fill. During this curing, cleanup and removal of equipment from the site was also conducted.

Following review of the installation timelines, recommendations were made to optimize the repair installation process by including simultaneous activities such as saw cutting of distressed areas and dowel receptacles, installing lifting anchors, excavating dowel sleeves, and sealing dowels and joints. Current and optimized timing for the installation process are included in Table C.5.

As can be seen in the table, none of the panel repairs could be conducted in less than 4 hr during the field testing. Through modification to the repair technique, the single-panel repair could possibly be conducted in less than 4 hr. Through optimization, the single-panel repair timing could be reduced by 1 hr, the double panel repair by slightly over 2 hr, and the quad-panel repair by almost 3 hr. If the repairs are to be conducted in 4 to 6 hr, then only the single- and double-panel repairs could meet this objective using the optimized repair approach. In the current form, none of the panel repairs would be applicable for emergency repairs. The quad-panel repair for a repair this size requires close to 10 hr to complete – outside the objective time frame of 4 to 6 hr. The timing of repairs using the optimized method is recommended to determine whether the estimated time savings can be obtained.

Table C.5. Current and proposed timing for completing repairs.

Task	Current Timing, min			Optimized Timing, min		
	Repair Type			Time (min)		
	Single Panel	Double Panel	Quad Panel	Single Panel	Double Panel	Quad Panel
Marking perimeter of distressed slab	10	15	20	10	15	20
Saw-cutting operations	15	35	60	7.5	17.5	30
Cutting dowel receptacles	25	50	50	12.5	25	25
Drilling anchors	15	30	60	5	10	20
Installing anchors	5	10	20	5	10	20
Attaching crane rigging hardware	1	2	4	1	2	4
Lifting distressed section	5	10	20	5	10	20
Excavating dowel sleeve (existing PCC slab)	30	60	60	15	30	30
Placing flowable fill	10	20	25	10	20	25
Placing precast panels	5	10	30	5	10	30
Compacting (if needed)	5	10	20	5	10	20
Removing flowable fill from dowel receptacles	3	6	10	3	6	10
Placing joint and dowel sealant	30	60	90	15	30	45
Finishing dowel receptacle	5	10	20	5	10	20
Curing	120	120	120	120	120	120
Total repair time, min	284	448	609	224	325.5	439
Total repair time, hr	4.73	7.47	10.15	3.73	5.43	7.32

Note: Optimized timing assumes doubling the manpower and equipment to perform saw cutting, dowel receptacle cutting, expansion anchor installation, and joint and dowel sealing efforts.

A potential solution to the timing issue is to divide the repair tasks into two separate periods (i.e., do a portion of the repair one night or during low traffic periods and complete the repair during the next available window). During the first repair period, the tasks of marking, saw cutting, and drilling locations for the lifting anchors could take place, still allowing aircraft operations when this repair period concludes. During the second repair period, the remaining tasks, including curing, would be completed.

Table C.6 presents the time for each phase of repair. As can be seen in the table, splitting the repair tasks into two phases reduces the operational downtime to conduct repair operations. The second phase of the repair process is the more time-consuming phase, due to curing of the dowel receptacle material. Despite this cure time, the second phase of repair for a quad-panel repair is less than 6 hr with the optimized repair procedure or

7 hr with the current procedure. Similar reductions in time are shown for the double- and single-panel repairs, but the biggest impact is seen for the quad-panel repair that cannot be completed using either the current or optimized procedure in less than 6 hr. If 7 to 11 hr are not available in a single repair window to complete this size repair, then this option may be a viable one.

Table C.6. Current and proposed timing for completing repairs during two separate repair phases.

Task	Current Timing, min			Optimized Timing, min		
	Repair Type			Repair Type		
	Single-Panel	Double-Panel	Quad-Panel	Single-Panel	Double-Panel	Quad-Panel
Phase 1						
Marking perimeter of distressed slab	10	15	20	10	15	20
Saw-cutting operations	15	35	60	7.5	17.5	30
Cutting dowel receptacles	25	50	50	12.5	25	25
Drilling anchors	15	30	60	5	10	20
Total phase 1 repair time, min.	65	130	190	35	67.5	95
Phase 2						
Installing anchor	5	10	20	5	10	20
Attaching crane rigging hardware	1	2	4	1	2	4
Lifting distressed section	5	10	20	5	10	20
Excavating dowel sleeves (existing PCC slab)	30	60	60	15	30	30
Placing flowable fill	10	20	25	10	20	25
Placing precast panels	5	10	30	5	10	30
Compacting (if needed)	5	10	20	5	10	20
Removing flowable fill from dowel receptacles	3	6	10	3	6	10
Placing joint and dowel sealant	30	60	90	15	30	45
Finishing dowel receptacle	5	10	20	5	10	20
Curing	120	120	120	120	120	120
Total phase 2 repair time, min	219	318	419	189	258	344

Note: Optimized timing assumes doubling the manpower and equipment to perform saw cutting, dowel receptacle cutting, expansion anchor installation, and joint and dowel sealing efforts.

Appendix D: Accelerated Pavement Testing

This appendix provides details of the accelerated pavement testing not fully described in the main body of this report.

During accelerated pavement testing, the precast panel repairs were trafficked with simulated C-17 aircraft loading using a load cart and an approximated normally distributed traffic pattern. The deterioration of each repair was monitored closely during traffic application. In addition to the load cart testing, nondestructive testing techniques and instrumentation were used to monitor changes in the repairs' load transfer efficiency, stiffness, and stresses and strains as a function of traffic applications. The collected data were used to perform analyses to understand the performance of the panels under aircraft traffic and also to assist in any future design work for precast panels. The remainder of this appendix details the trafficking procedure, data collection process, and failure criteria used.

D.1 Load cart description

A multiple-wheel C-17 load cart was used to simulate one-half the main gear of a C-17 fully loaded to its maximum gross ramp weight of 586,000 lb. Figure D.1 illustrates the geometrical arrangement of the C-17 landing gear. The multiple-wheel C-17 load cart (Figure D.2) simulates only one-half of the main gear with a test weight of 269,560 lb. Individual wheel loads were approximately 44,930 lb across two triple wheels in tandem gear (6 tires total). The gear used 50-in.-diam, 21-in.-wide, 20-ply tires maintained within normal inflation range (138 to 144 psi) during testing.

Simulated normally distributed traffic was applied across a 9-ft-wide traffic lane, as shown in Figure D.3. The pattern simulated the traffic distribution patterns, or wander width, typically seen when aircraft taxi to and from an active runway. The width of each lane corresponded to a contact width of 18 in. (not the overall published tire width of 21 in.) of the C-17 tires when fully loaded. The normally distributed traffic patterns were simplified for ease of use by the load cart operator. Traffic was applied by driving the load cart forward and then backward over the length of the test section and then shifting the path of the load cart laterally approximately one tire width (18 in.) on each forward pass. Tracking guides were attached to the load cart

to assist the driver in shifting the load cart the proper amount for each forward pass. This procedure was continued until one pattern of traffic was completed. One complete pattern consisted of 28 passes, which resulted in the application of a maximum of 25 coverages. Traffic was continued on each item in this manner until one pattern was applied to the test item, and the pattern was repeated for 10,000 passes or until failure occurred, whichever came first.

Figure D.1. Spatial layout of C-17 landing gear.

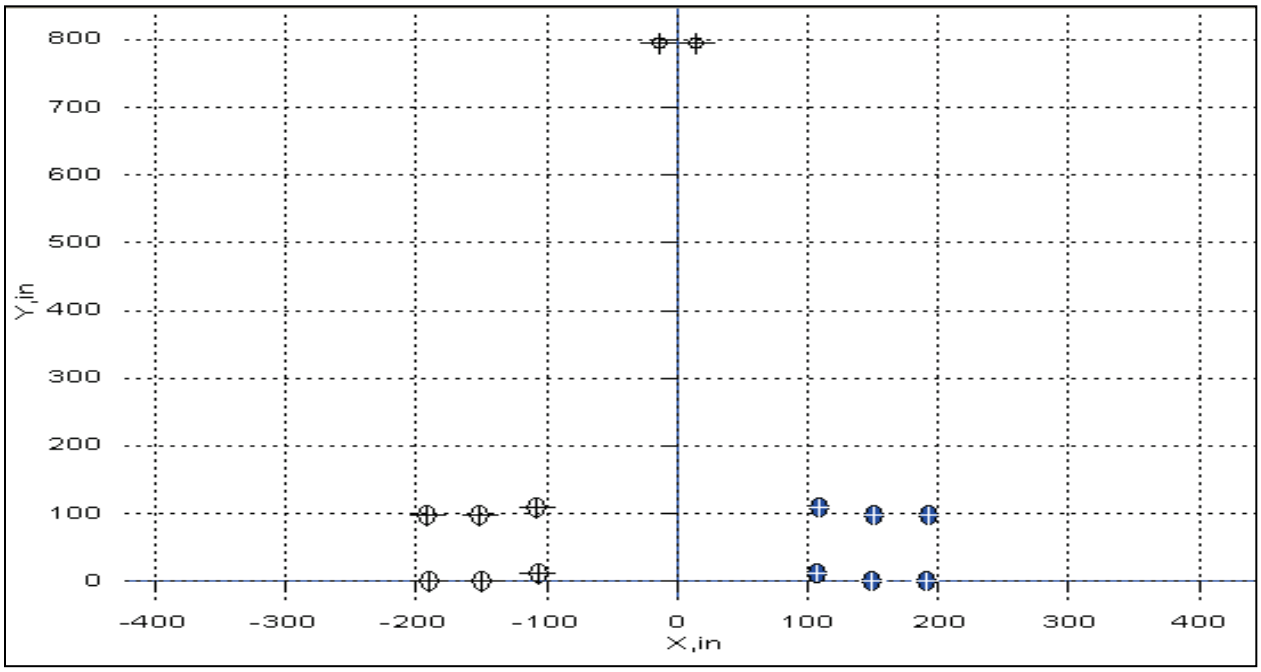

Figure D.2. C-17 load cart on test section.

Figure D.3. C-17 pattern on test section.

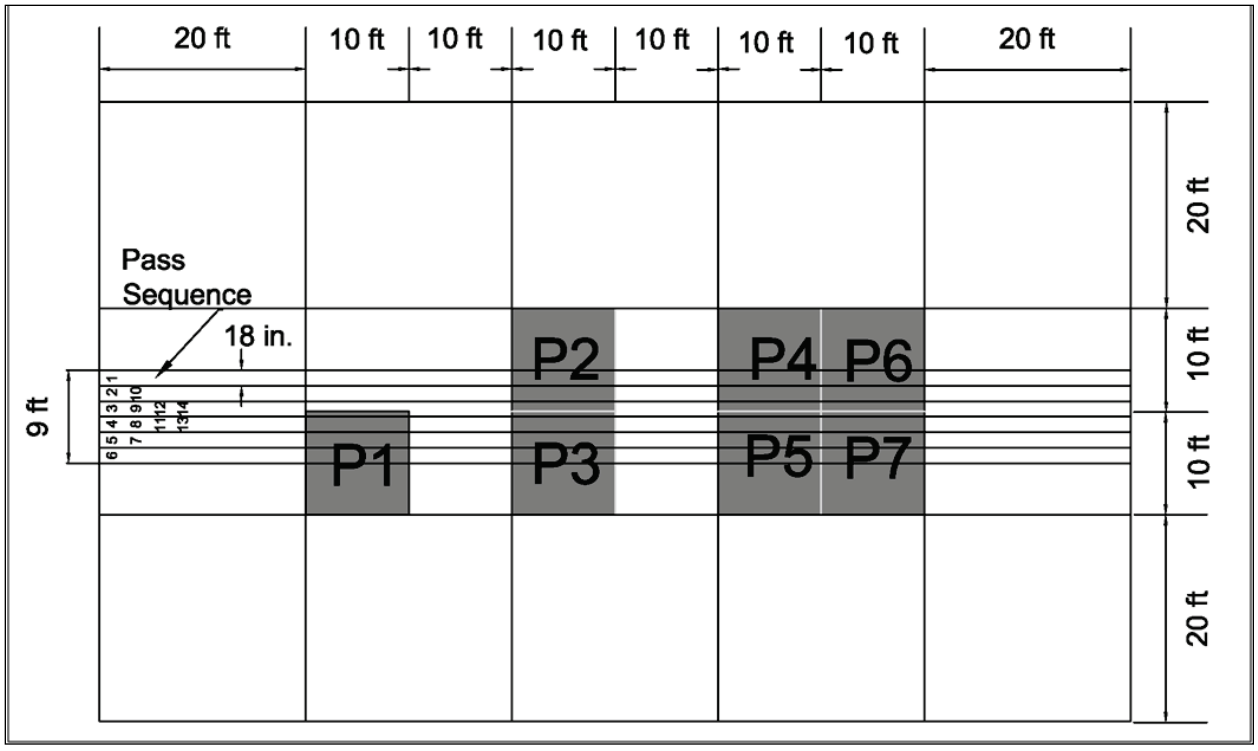

D.2 Data collection procedures

Data were collected periodically during trafficking, and the precast panels were inspected for damage during all trafficking intervals. Data collected included

- Pavement condition surveys of the parent slabs and precast panels during trafficking;
  - Photographs during trafficking showing damage over time and
  - Crack monitoring
- Heavy weight deflectometer (HWD) measurements;
  - Load transfer tests on existing slabs to establish baseline values,
  - Center plate measurements in the center of each slab and precast panel to measure changes in stiffness with traffic,
  - Load transfer tests on parent slab and at joints of connected panels in both the longitudinal and transverse directions, and
  - Corner deflection tests to monitor loss of support
- EPC data collection during trafficking in the centers of slabs, centers of precast panels, and corners and edges of panels to understand the stress distribution;

- Strain gauge data collection during trafficking to understand strains at the edges of panels; and
- Faulting and settlement measurements to determine changes in slab elevations.
- Test data were collected after a predetermined number of passes, as shown in Table D.1, until failure or 10,000 passes were completed. Results and analyses of the data collected are presented in the following sections.

Table D.1. Trafficking data collection intervals.

Static Data Collection Pass Level	Dynamic Data Collection Pass Interval
0	-
112	113-140
238	239-266
462	463-490
910	911-938
1,120	1,121-1,149
1,400	1,401-1,428
1,680	1,681-1,708
1,960	1,961-1,989
2,240	2,240-2,268
2,800	2,801-2,828
3,360	3,361-3,377
4,200	4,201-4,228
5,600	5,601-5,628
7,100	7,101-7,128
8,400	8,401-8,428
10,000	No data collected

D.3 Failure criteria

Pavement performance data were collected periodically during trafficking, and the panels and test section slabs were inspected for distresses. It was anticipated that the panels would fail as a result of surface deterioration from overloading the pavement (resulting in load-related surface distresses), loss of base support under the panels (resulting in faulting or settlement of the slabs), or from lack of load transfer at the joints (resulting in spalling, faulting, or settlement).

Visual inspections were performed at selected traffic intervals to identify specific distresses associated with high foreign object debris (FOD)

potential such as cracking, spalling, corner breaks, and shattered slabs. Cracking was considered minor unless development of associated spalls resulted in the accumulation of debris or cracks with widths greater than 1 in. Spalled materials have the potential to be sucked into jet engines or damage propellers and rotors of aircraft. Additionally, spalled concrete and wide cracks present a tire hazard because of the potential for the sharp edges to cut aircraft tires. When distresses posed high FOD potential or tire hazards were identified, the repair was considered failed.

The repairs were also monitored for failure due to high surface roughness. High surface roughness is associated with significant elevation changes, resulting from either settlement of the pavement from a weak foundation or significant abrupt surface deterioration. Elevation changes in excess of 3 in. are unacceptable for the C-17 aircraft because of the potential of damaging the landing gear. If elevation changes in excess of 3 in. occurred in this evaluation, the repair was considered failed. Other aircraft have different elevation change values and would need alternate consideration.

D.4 Surface deterioration results

The precast panel repairs and surrounding pavement were monitored using standard pavement condition survey procedures to identify common airfield pavement distresses and their severities. Changes to severity levels of distresses observed were monitored during trafficking. Using these distresses, the pavement condition index (PCI) for each panel was calculated during trafficking using pavement management software (PAVER). Because accelerated trafficking was completed, some climate and other related PCC distresses were not expected, since the test section would not be able to accumulate this type of damage in the short testing duration.

D.4.1 Pavement condition prior to traffic

A transverse cold joint was required in the center of Slab 2, after the final concrete delivery during test section construction was delayed for over 90 min. This joint was constructed approximately 8 ft from the N joint of Panel 1. The partially placed slab was cut back 2 ft from the face of the concrete to provide a smooth, vertical face. No tie bars were installed prior to the completion of the slab to maintain its structural integrity.

D.4.2 Repairs after installation

Before application of traffic, a small patch was conducted in Repair 3 in the NW corner of Panel 4. The thin piece of concrete that formed the exterior-most dowel receptacle wall was damaged (Figure D.4). Cracking was noticed before the panel's installation, but the concrete piece fully dislodged during the installation. The damage was sustained between the time in which the panel was constructed to after off-loading, when the panel was transported to the test section site; the source, however, is unknown. A rapid-setting cementitious repair material, Pavemend 15.0, was used to repair the damaged pavement after installation and was placed when the dowel receptacles were filled. Because of this distress, a slight decrease in condition occurred due to the patch with a calculated PCI of 90. The other repairs were in good condition with no visible distresses; thus, the repairs were considered in brand new condition (PCI=100).

Additionally, when the test section was saw cut to generate the repair areas, overcuts (kerfs) from the corners of the repairs extended approximately 12 to 15 in. into the parent PCC (Figure D.5). This overcutting was necessary to provide the full-depth cut using a round saw blade. During trafficking, cracks extended from these overcuts.

Figure D.4. Damaged and repaired dowel bar receptacle on panel 4.

Figure D.5. Saw cuts at corners of panels.

D.5 Pavement condition during traffic

Each of the three repair configurations constructed withstood different amounts of traffic before failing. Details of distresses noted during trafficking and their calculated PCI are presented in Table D.2. Intermediate distresses in the parent slabs are presented in Figure D.6. Figure D.7 presents photos of the distresses contributing to the failure of the repairs in both the panels and the parent slabs. The failure modes are detailed below:

Repair 1: A total of 5,600 C-17 passes was applied to Repair 1 prior to failure due to a high-severity shattered slab for the parent slab and the precast panel and due to spalling on the transverse doweled edges (high FOD potential).

Repair 2: A total of 10,000 passes was applied to Repair 2 prior to failure due to high-severity joint spalls and deterioration of the dowel receptacles in the parent slab (high FOD potential).

Repair 3: A total of 7,100 passes was applied to Repair 3 prior to failure due to a high-severity joint spalling along the south edge of the repair (high FOD potential).

Table D.2. Summary of repair performance.

Panel	Repair	Pass Level	Distress Description	PCI (%)
1	1	0	None	100
2	2		None	100
3			None	
4	3		During placement, the NW corner was broken at the outside dowel slot. A low-severity patch was noted for this repair in good condition.	90 - Pretraffic patch in one panel
5			None	
6			None	
7			None	
1	1	112	Low-severity cracking was noticed in the parent slab extending to the N joint of the panel.	86
2	2		A low-severity crack was noticed in the parent slab between Panel 1 and Panel 2 running from the saw cut in the parent slab.	100
3			None	
4	3		The low-severity patch in the NW corner was in good condition. A low-severity crack was noticed in the parent slab between Panels 2 and 3 and 4 and 5 extending to the saw cut.	90
5			None	
6			None	
7			None	
1	1	238	No change.	86
2	2		No change.	100
3			No change.	
4	3		Minor spalling was noticed on N joint and NW corner (not recorded as a distress following PCI procedures for minor spalls).	90
5			Minor spalling on N joint and SE corner was noticed (not recorded as a distress following PCI procedures for minor spalls).	
6			Minor spalling on S joint was noticed (not recorded as a distress following PCI procedures for minor spalls).	
7			Low-severity spalling on S joint of parent slab.	
1	1	462	No change.	86
2	2		Low-severity spalling noted on S joint.	89
3			Low-severity spalling noted on S joint.	
4	3		The patch in NW corner was in good condition.	87
5			No change.	
6			No change.	
7			Low severity joint spall noted on SE corner.	

Panel	Repair	Pass Level	Distress Description	PCI (%)
1	1	910	FOD developing in parent slab due to medium-severity corner crack in NE corner of the parent slab. A crack connects this distress to the panel. A low-severity spall is developing in the NE corner of the panel.	80
2	2		No change.	89
3			No change.	
4	3		No change.	78
5			A hairline crack was noticed in the NE corner.	
6			Cracks were noticed in the SE corner, creating a low-severity corner spall.	
7			A low-severity crack was noticed in the parent slab south of the panel between dowel slots.	
1	1	1,120	FOD noticed from saw overcut in parent slab NE of panel.	80
2	2		No change.	89
3			No change.	
4	3		No change.	65
5			No change.	
6			Low-severity crack noticed from S joint through parent slab to S edge of test section (longitudinal crack).	
7			Low-severity crack extended from S joint through parent slab to S edge of test section.	
1	1	1,400	No change.	80
2	2		Low-severity joint spall noticed on S joint in panel.	89
3			Low-severity joint spall noticed on S joint in panel.	
4	3		No change.	59
5			No change.	
6			Low-severity corner spall in SE corner producing small FOD. Low-severity spalling and cracking in dowel slots were noticed on the S edge.	
7			Low-severity corner spall in SE corner, producing small FOD. Low-severity spalling and cracking in dowel slots were noticed on the S edge.	
1	1	1,680	FOD produced NE of panel in parent slab.	80
2	2		No change.	89
3			No change.	
4	3		No change.	59
5			No change.	
6			Low-severity corner spall in SE corner, producing small FOD. Low-severity spalling and crack-	

Panel	Repair	Pass Level	Distress Description	PCI (%)
			ing in dowel slots were noticed on the S edge.	
7			Low-severity corner spall in SE corner, producing small FOD. Low-severity spalling and cracking in dowel slots were noticed on the S edge.	
1	1	1,960	No change.	80
2	2		Hairline cracks noticed in NW corner of panel.	84
3			No change.	
4	3		No change.	59
5			Low-severity spalling and cracking noticed in SE corner near repair.	
6			No change.	
7			No change.	
1	1	2,240	No change.	80
2	2		Low-severity corner spall noticed in NW corner.	84
3			No change.	
4	3		No change.	59
5			No change.	
6			No change.	
7			No change.	
	1	2,800	A low-severity corner spall approximately 6 in. long was noted in the NE corner of the panel. A 6-in.-long low-severity corner spall was also noted along the NE edge of the panel. A 3-ft-long transverse crack was noticed from the E edge of the panel progressing towards the panel center. A high-severity corner spall was noted in the NW corner of the panel. Additional distresses were noted in the parent slab N of the panel including a 5.5-ft-long medium-severity longitudinal crack and a medium-severity joint spall 4 ft long and 1.5 ft wide along the cold joint in the parent slab. A medium-severity diagonal crack approximately 8 ft long was noted extending from the saw overcut to the N edge of Repair 2 in the parent slab containing the panel. Another diagonal crack (low-severity) was noted running from the E edge of Panel 1 E towards the E joint of the parent slab.	72
2	2		A medium-severity joint spall approximately 3 in. long was noted on the SW edge of the panel. On the N panel joint, a 6-in.-long low-severity joint spall was noted. A low-severity corner spall approximately 1 ft long was noted in the NW corner of the panel.	62

Panel	Repair	Pass Level	Distress Description	PCI (%)
3			Medium-severity joint spall approximately 3.5 ft long was noted in the NE joint. A low-severity crack was noted approximately 1 ft long progressing towards the panel center from the NW joint. A low-severity longitudinal crack was noted that extended from the overcut from Panel 1 through the parent slab to Panel 3.	
4	3		A high-severity corner spall approximately 1 ft long was noted in the SE corner. This spall was located near the patch which was beginning to deteriorate and produce FOD.	25 - Although this repair was considered in serious condition, trafficking was continued. The repair was inspected more often to remove FOD and prevent damage to the tires.
5			A high-severity corner spall approximately 2.5 ft long was noted in the NE corner. A longitudinal crack was noted from the N joint in the center progressing approximately 7 ft towards the center of the panel. A 1.5-ft-long low-severity joint spall was noted on the NW edge, and a 1-ft-long low-severity joint spall was noted on the center of the west edge.	
6		2,800	A medium-severity joint spall approximately 1 ft long was noted on the E edge in the center, and a high-severity corner spall was noted on the SE corner. In the parent slab S of the panel, a 19-ft-long low-severity longitudinal crack was also noted along with a high-severity joint spall on the N edge of the parent slab.	25
7			A medium-severity joint spall approximately 6 in. long was noted on the central portion of the E edge. A high-severity corner spall approximately 1 ft in length was noted in the NE corner. A medium-severity corner spall approximately 6 in. long was noted on the N edge towards the NE corner.	
1	1	3,360	A low-severity transverse crack extended from the E edge of the pavement and was 5 ft long. A low-severity diagonal crack was noted extending from the center of the N edge towards the W edge of the panel.	59
2	2		The medium-severity joint spall on the SW edge of the panel produced additional FOD.	62
3			A low-severity joint spall approximately 4 in. long was noted along the center of the W edge of the panel.	
4	3		Additional FOD noted on SE edge from high-severity joint spall in the panel. A high-severity joint spall approximately 4 ft long was noted in the parent slab S of the panel.	25 - Although this repair was considered in serious condition, trafficking was continued. The repair was inspected more often to remove FOD and prevent damage to the tires.
5			The low-severity longitudinal crack extended towards the panel center. The joint spalling along the NW edge progressed, transforming into a low-severity corner spall.	

Panel	Repair	Pass Level	Distress Description	PCI (%)
6			A new low-severity joint spall was noted on the SW edge of the panel. Additional FOD from the dowel receptacles was produced along the S edge of the panel in the parent slab.	
7			New medium-severity joint spalls were noted on the NW and SW edges of the panel.	
1	1	4,200	The spalling along the NE corner included a medium-severity corner break. The panel was considered a low-severity shattered slab with the intersection of the longitudinal crack with a transverse crack.	0 - The PCI was calculated as 0 due to the low-severity shattered slab; however, the repair was not considered failed as the cracks were hairline. The distresses were low- and medium-severity. The panel required more frequent inspection to remove FOD.
2	2		No change.	62
3			No change.	
4	3		The patch in the SW corner continued to deteriorate.	7 - Although this repair was considered failed by traditional PCI procedures, trafficking was continued. The repair was inspected more often to remove FOD and prevent damage to the tires.
5			A low-severity longitudinal crack was noted in the center of the panel. A low-severity joint spall was noted near the NE corner on the E edge of the panel.	
6			A low-severity corner break was noted in the SW corner of the panel. FOD production continued on the S side of the panel in the parent slab.	
7			FOD production from the dowel receptacles continued on the S side of the panel in the parent slab.	
1	1	5,600	The panel was considered a high-severity shattered slab. FOD production on the NE corner was considered high. The panel was considered failed. The parent slab N of the repair was also considered failed due to cracking and spalling. Spalling in the parent slab where the panel was placed increased in severity to high as well.	0
2	2		A medium-severity corner break was noted on the SW corner. A high-severity joint spall was noted on the E edge. Spalling on the edges of the parent slabs and Repairs 2 and 3 continued to progress. The low-severity longitudinal crack between the repairs in the parent slab continued across the slab.	21- Although this repair was considered in serious condition, trafficking was continued. The repair was inspected more often to remove FOD and prevent damage to the tires.

Panel	Repair	Pass Level	Distress Description	PCI (%)
3			A low-severity joint spall was noted on the E edge of the panel. A medium-severity joint spall was noted on the W edge of the panel near the NW corner and a low-severity joint spall was noted towards the SW corner on the W edge.	21
4	3		A high-severity joint spall with high FOD production was noted on the SE corner of the panel.	0
5			A high-severity corner spall was noted on the NE corner of the panel. A medium-severity corner spall was noted on the NW corner of the panel.	
6			A medium-severity joint spall was noted on the E edge of the panel. A high-severity corner spall was noted in the SE corner of the panel, and a low-severity corner spall was noted in the SW corner of the panel. Spalling from the dowel receptacles continued in the parent slab south of the repair with high- and medium-severity joint spalls noted.	
7			A high-severity corner spall was noted in the NE and NW corners of the panel. A medium-severity spall was noted on the W edge of the panel.	
1	1	7,100	Panel considered failed. No additional data collected.	0
2	2		No change.	21 - Although this repair was considered in serious condition, trafficking was continued. The repair was inspected more often to remove FOD and prevent damage to the tires.
3			No change.	
4	3		Additional FOD produced by distresses. Repair considered failed.	0
5			Additional FOD produced by distresses. Repair considered failed.	
6			Additional FOD produced by distresses. Repair considered failed.	
7			Additional FOD produced by distresses. Repair considered failed.	
1	1	8,400	Panel considered failed. No additional data collected.	0
2	2		Additional FOD was noted in distresses.	21 - Although this repair was considered in serious condition, trafficking was continued. The repair was inspected more often to remove
3			Additional FOD was noted in distresses.	

Panel	Repair	Pass Level	Distress Description	PCI (%)
				FOD and prevent damage to the tires.
4	3		Panel considered failed. No additional data collected.	0
5			Panel considered failed. No additional data collected.	
6			Panel considered failed. No additional data collected.	
7			Panel considered failed. No additional data collected.	
1	1	10,000	Panel considered failed. No additional data collected.	0
2	2		FOD production continued. Repair considered failed due to condition of NW portion of the N joint with deterioration of the parent pavement and dowel slots.	0
3			FOD production continued. Repair considered failed.	
4	3		Panel considered failed. No additional data collected.	0
5			Panel considered failed. No additional data collected.	
6			Panel considered failed. No additional data collected.	
7			Panel considered failed. No additional data collected.	

Figure D.6. Parent slab distresses after 2,800 passes: (a) longitudinal crack in parent slab south of Repair 2 extending from saw overcut, (b) longitudinal crack in parent slab between Repairs 2 and 3 extending from saw overcut, (c) diagonal crack in parent slab extending from NE edge of Repair 1 from saw overcut, (d) diagonal crack in parent slab from SE edge of Repair 1 to Repair 2 extending from saw overcut and spalling and cracking between saw overcuts on SE corner of Repair 1, (e-f) spalling and cracking in parent slab north of Repair 1 near construction cold joint.

(a) (b)

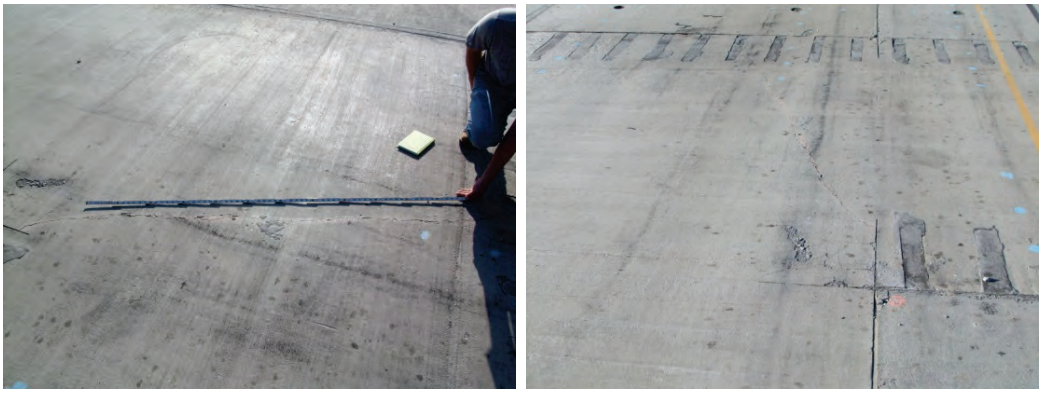

(c) (d)

(e) (f)

Figure D.7. Repair failure details: (a) Repair 1 (Panel 1): high-severity corner break/spall and shattered parent slab, (b) Repair 2: diagonal cracking in parent slab between Repairs 1 and 2 and cracking and spalling of Panel 2 due to the parent slab deterioration, (c) close-up of the cracking and deterioration in the parent slab and dowel slots and corner of Panel 2, and (d) Repair 3, Panels 6 and 7: high-severity spalling in corner of Panels 6, 7, and the parent slabs south of the repair.

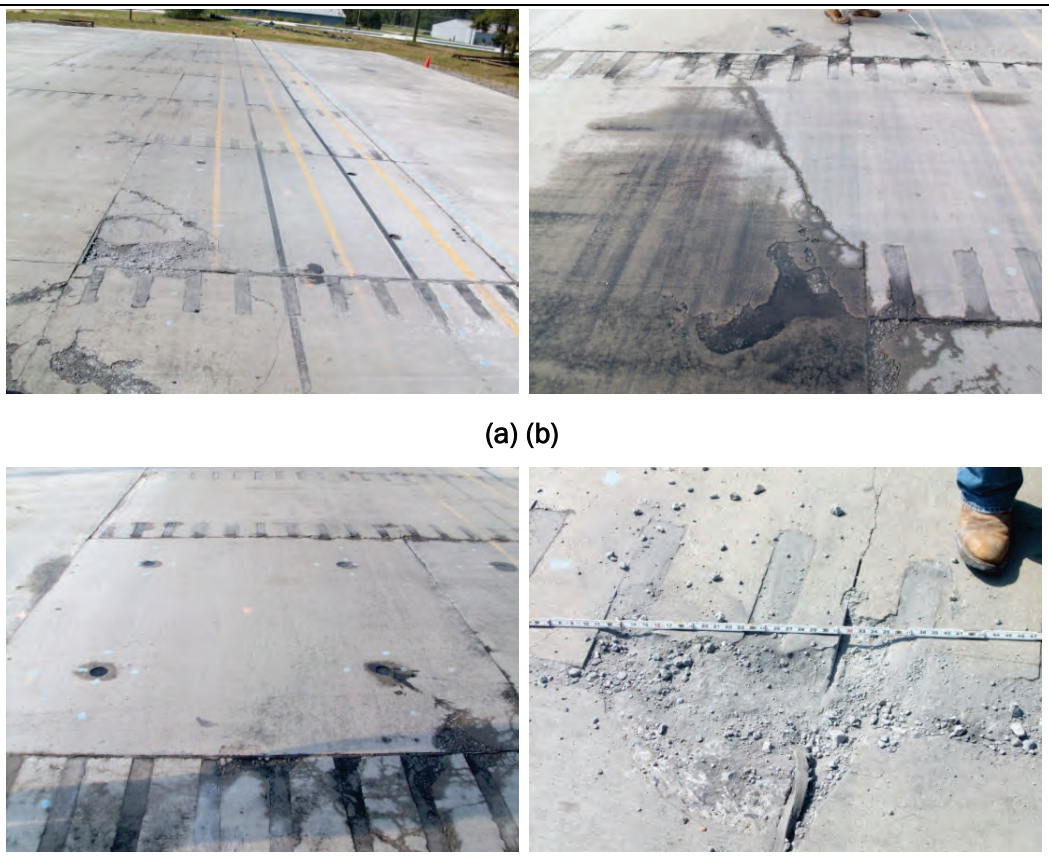

(a) (b)

(c) (d)

D.5.1 Settlement and faulting

In addition to the observed surface distresses, measurements were taken to monitor any elevation differences of the panels during trafficking. Faulting was considered an upward elevation change between slabs at a joint, and settlement was considered a negative elevation change at a joint. These distresses are commonly encountered in PCC pavements and are usually caused by upheaval (faulting), consolidation, or loss of support (settlement). Elevation differences are important measurements to determine whether aircraft can safely operate on the paved surface, since large differences can cause tire hazards and place large stresses on landing gear.

During trafficking, data were collected at selected pass intervals shown in Table D.1 to monitor the surface elevation of the repairs. Differences in

elevation were made using a 10-ft straightedge and hand ruler. The straightedge was placed at two locations across the joints on every edge of the panel (1 ft from the corners). A series of six measurements spaced at 12-in. intervals was made at preset marks on the surface of the test sections shown in Figure D.8 to monitor changes in the surface elevation and any rotation of the panel. The maximum measurement (elevation difference) was identified for each set of measurements.

The peak elevation differences for each set of measurements are presented in Table D.3. Negative differences represent changes in elevation due to settlement or loss of material. The data show the panels moved very little during trafficking. None of the repairs had settlement or faulting in excess of 3.0 in., and the differences in elevation were minimal.

D.5.1.1 Nondestructive testing

Nondestructive tests (NDT) were performed to determine the structural capacity of the repaired pavement. Response data were used to determine the structural capacity and the operational effectiveness of the precast panel repair methods in terms of stiffness and load transfer efficiency. These items are commonly used for monitoring the effectiveness of traditional PCC pavement repairs and were applied to precast panels for comparison purposes. Recent investigations into precast panels also recommend monitoring precast panel repairs using these NDT methods.

D.5.1.2 Equipment used

NDT were completed with a Dynatest model 8081 heavy weight deflectometer (HWD). The HWD uses heavy weights dropped onto a padded plate (11.8 in. diam) to measure the pavement's response to a dynamic load. The applied force and the pavement deflections, respectively, are measured with load cells and velocity transducers (geophones). The drop height of the weights can vary from 0 to 15.7 in. to produce a force from 0 to approximately 50,000 lb. The system is controlled with a laptop computer that also records the loading and pavement deflections. The HWD is shown in Figure D.9 during testing on a PCC test section.

Figure D.8. Locations of faulting and settlement measurements.

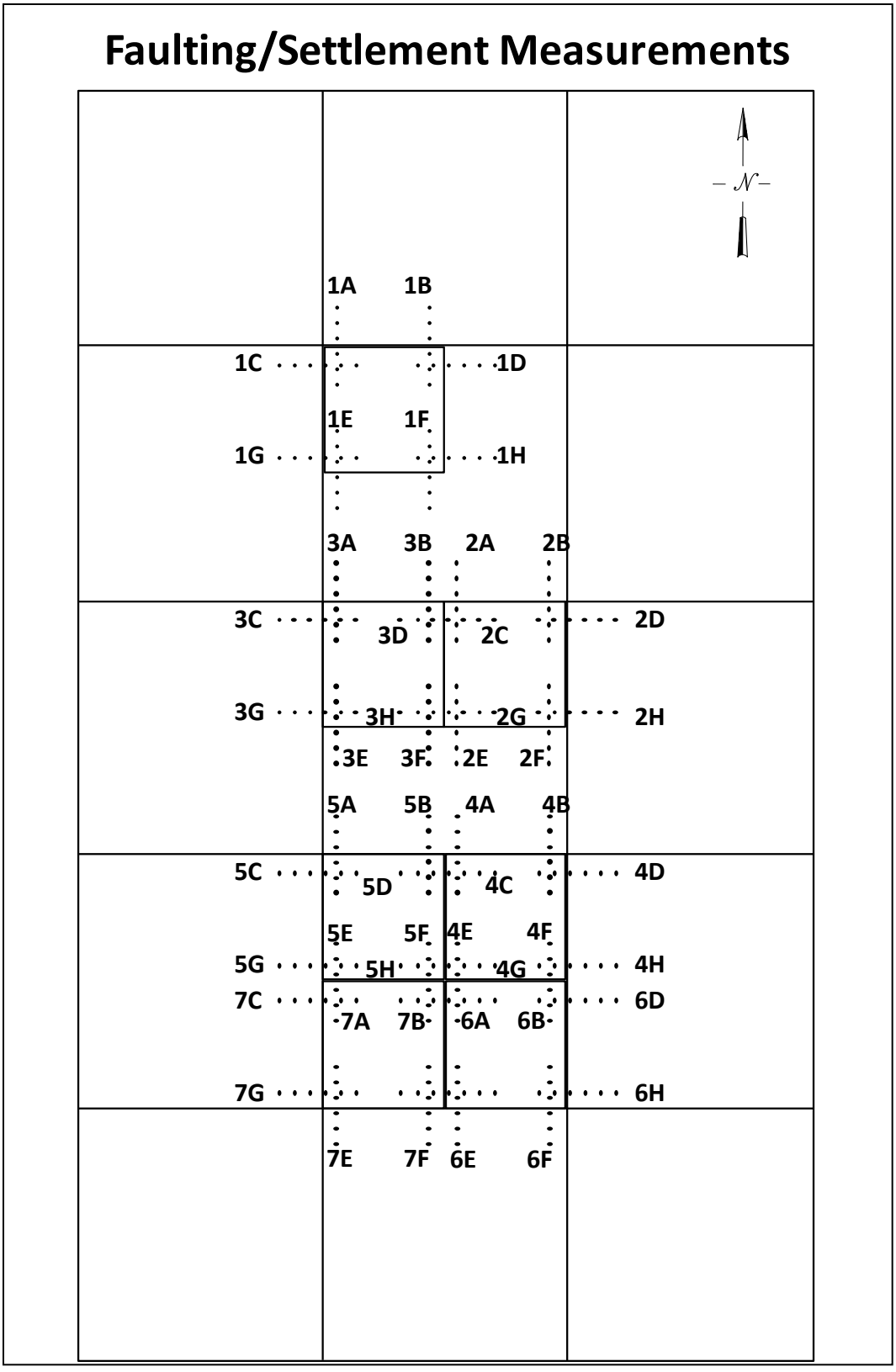

Table D.3. Elevation measurement intervals.

Repair	Test Location	Initial Installation Measurement, in.	Maximum Measurement, in.	Elevation Difference from Installation, in.
Repair 1	1a	0.375	0.375	0.000
	1b	0.1875	0.4375	-0.250
	1c	0.25	0.375	-0.125
	1d	0.25	0.625	-0.375
	1e	0.5	0.5	0.000
	1f	0.125	0.375	-0.250
	1g	0.3125	0.375	-0.063
	1h	0.5	0.5625	-0.063
Repair 2	2a	0.5	0.5625	-0.063
	2b	0.375	0.4375	-0.063
	2c	0.125	0.1875	-0.063
	2d	0.1875	0.25	-0.063
	2e	0.375	0.5	-0.125
	2f	0.3125	0.375	-0.063
	2g	0.125	0.1875	-0.063
	2h	0.375	0.375	0.000
	3a	0.25	0.3125	-0.063
	3b	0.4375	0.5	-0.063
	3c	0.1875	0.1875	0.000
	3d	0	0.0625	-0.063
	3e	0.3125	0.5	-0.188
	3f	0.1875	0.375	-0.188
	3g	0.5	0.5625	-0.063
	3h	0.0625	0.3125	-0.250
Repair 3	4a	0.125	0.1875	-0.063
	4b	0.125	0.1875	-0.063
	4c	0.125	0.1875	-0.063
	4d	0.25	0.625	-0.375
	4e	0.125	0.25	-0.125
Repair 3 (cont.)	4f	0.0625	0.125	-0.063
	4g	0.0625	0.1875	-0.125
	4h	0.125	0.1875	-0.063
	5a	0.125	0.375	-0.250
	5b	0.125	0.1875	-0.063
	5c	0.3125	0.3125	0.000

Repair	Test Location	Initial Installation Measurement, in.	Maximum Measurement, in.	Elevation Difference from Installation, in.
	5d	0.0625	0.125	-0.063
	5e	0	0.125	-0.125
	5f	0.0625	0.1875	-0.125
	5g	0.375	0.375	0.000
	5h	0.0625	0.125	-0.063
	6a	0.125	0.1875	-0.063
	6b	0.125	0.1875	-0.063
	6c	0.0625	0.125	-0.063
	6d	0.125	0.25	-0.125
	6e	0.125	0.1875	-0.063
	6f	0.1875	0.1875	0.000
	6g	0	0.0625	-0.063
	6h	0.0625	0.1875	-0.125
	7a	0.13	0.33	-0.21
	7b	0.13	0.19	-0.06
	7c	0.25	0.31	-0.06
	7d	0.13	0.17	-0.04
	7e	0.25	0.31	-0.06
	7f	0.06	0.19	-0.13
	7g	0.31	0.31	0.00
	7h	0.13	0.25	-0.13

Figure D.9. HWD test device.

D.5.1.3 Test locations

Prior to conducting repairs and following the completion of traffic testing, the HWD was used to obtain deflection basins for the parent PCC slabs. Locations of the HWD on the test section are provided in Figure D.10 (numbered from 1 to 15). Test 6 was not conducted because of the construction joint. In addition to backcalculating modulus values for pavement layers, the HWD was also used to measure the decay in stiffness with repeated applications of traffic. The stiffness properties of PCC significantly impact the distribution of aircraft loads between slabs and panels. Thus, the repair stiffness values were determined with traffic applications and compared to the parent PCC. Repair stiffness was monitored through center, corner, and joint deflection measurements. Deflection measurements were conducted in the center of each panel and at selected parent PCC locations (marked 1-10 in Figure D.11) at various traffic intervals (shown previously in Table D.1). Other deflection tests, including load transfer efficiency (LTE) and corner deflections, which will be detailed in the following sections, were conducted during the same traffic intervals.

Figure D.10. Locations of HWD tests pre-repair and posttest.

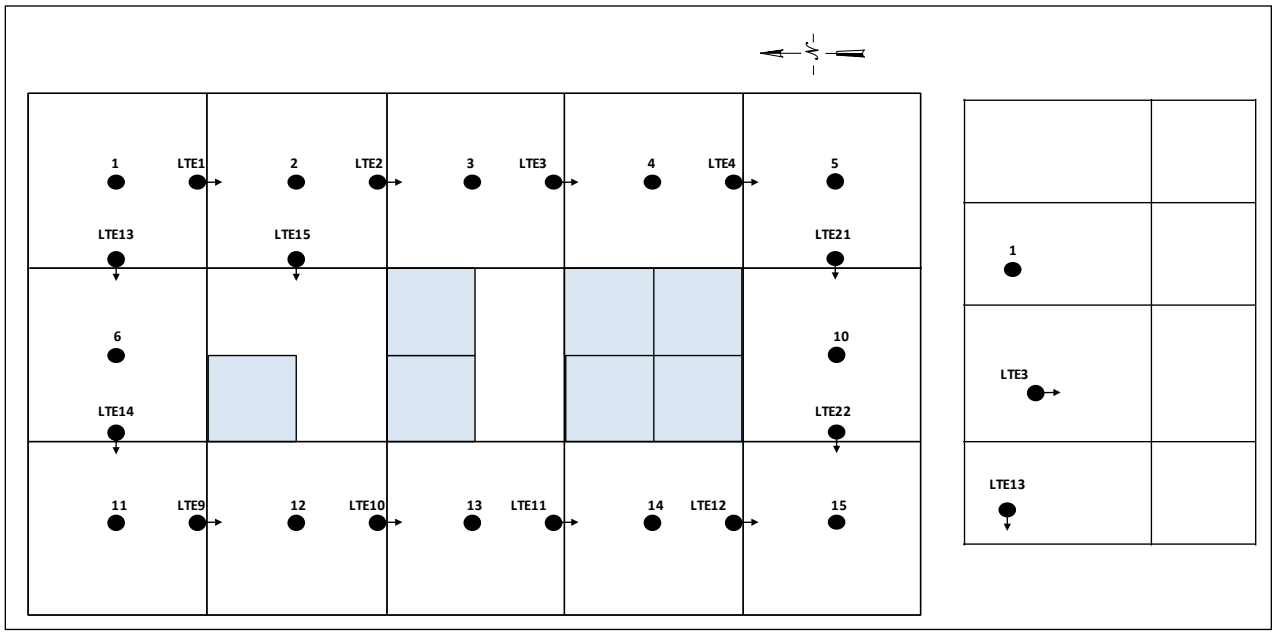

Figure D.11. Locations of ISM, corner deflection, and *LTE* HWD tests.

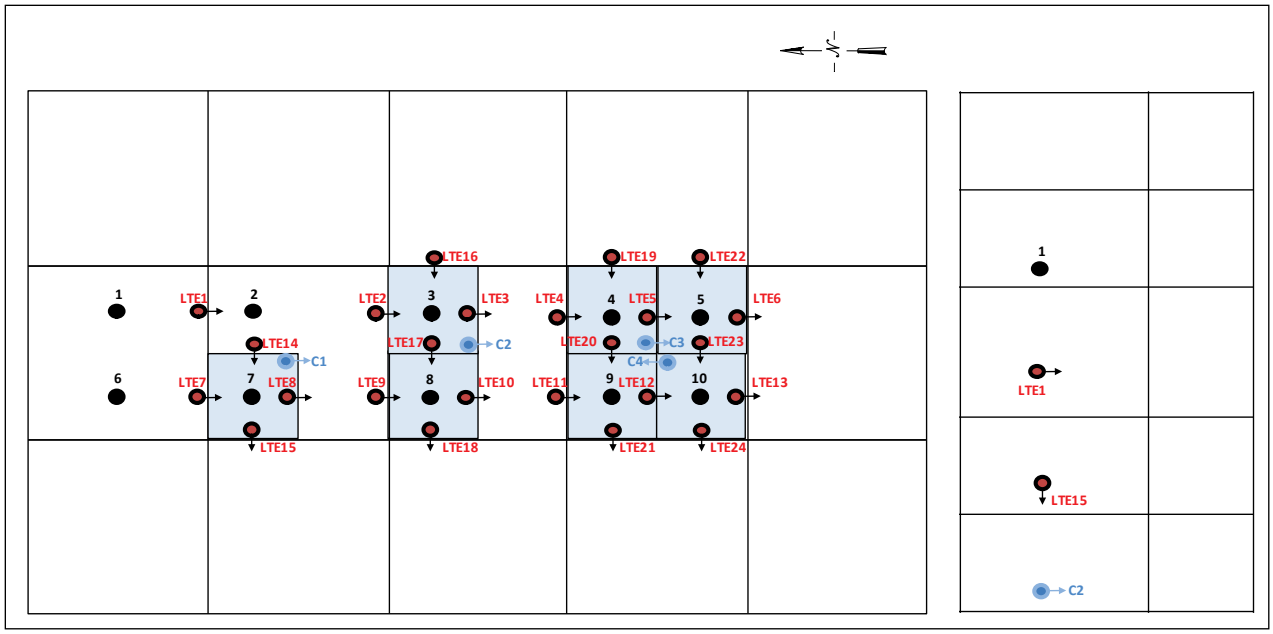

D.5.2 Backcalculation of moduli for the test section

The recorded HWD deflections and known pavement structure layer thicknesses were used to backcalculate the elastic modulus of each pavement layer for the parent PCC and for the precast panels. The backcalculated moduli before and after trafficking are presented in Table D.4. CBR values from dynamic cone penetrometer (DCP) tests prior to the construction of the PCC layer are provided for comparison against the backcalculated results for the parent slabs. The average DCP values (37% base and 14% subgrade) were converted into modulus values using the relationship presented in Equation D.1.

$$\text{DCP estimated modulus} = 1500 * \text{CBR}\ (\%) \quad \text{(D.1)}$$

The backcalculated base and subgrade moduli for the parent slabs are similar to the DCP-estimated values, with only a slight reduction to the respective values after traffic. This indicates that there was not a substantial loss in foundation support beneath the test section due to environmental factors that could contribute to early deterioration of the repairs. The backcalculated moduli for the precast panels show significant loss in strength during trafficking. This is attributed to the deterioration of the panels during trafficking.

Table D.4. Summary of modulus values.

Test	PCC Modulus, psi	Backcalculated HWD		DCP-Estimated	
		Base Modulus, psi	Subgrade Modulus, psi	Base Modulus, psi	Subgrade Modulus, psi
Pre-repair slabs	5,000,000	49,276	24,453	55,000	21,000
Post-traffic slabs	5,000,000	48,333	23,737	55,000	21,000
Pre-repair panels	6,248,706	54,892	24,453	n/a	n/a
Post-traffic panels	2,545,719	33,488	11,560	n/a	n/a

The equivalent PCC thickness of the panel system (panel plus the flowable fill) was calculated based on the HWD deflections using Ioannides and Korovesis' (1992) equivalent thickness solution for multi-layered pavements. This solution assumes that the equivalent PCC would have the same modulus of elasticity, Poisson's ratio, and modulus of subgrade reaction as the multi-layered system. The equivalent thickness calculated for the panel repair was 11.02 in., indicating that the contribution of the 3-in. flowable fill layer was negligible and that the reinforcement did not allow a reduction in panel thickness. The flowable fill provided base moduli (3 in. of flowable fill and 6 in. of compacted aggregate) similar to those of the compacted aggregate alone, as shown in Table D.4.

D.5.3 Center slab deflections and impulse stiffness modulus

Center slab deflections recorded at the maximum HWD load level (measured at the first sensor) are presented in Figure D.12. Deflections were normalized to a force of 50,000 lb to provide a comparison of the test data that varied in maximum force from approximately 39,000 to 57,500 lb. Normalized deflection values for each panel and pass level are also presented in Table D.5. Figure D.12 shows the general trend that as traffic applications increased, the deflections also increased for all repairs and adjacent pavement (parent PCC). This figure also shows that lower deflections were recorded for Panels 2 and 3 of Repair 2, slightly better than parent slab deflections. The highest deflections were recorded for Panel 1 of Repair 1 and Panels 4, 5, and 7 of Repair 3.

Figure D.12. Normalized deflections for panels with traffic passes.

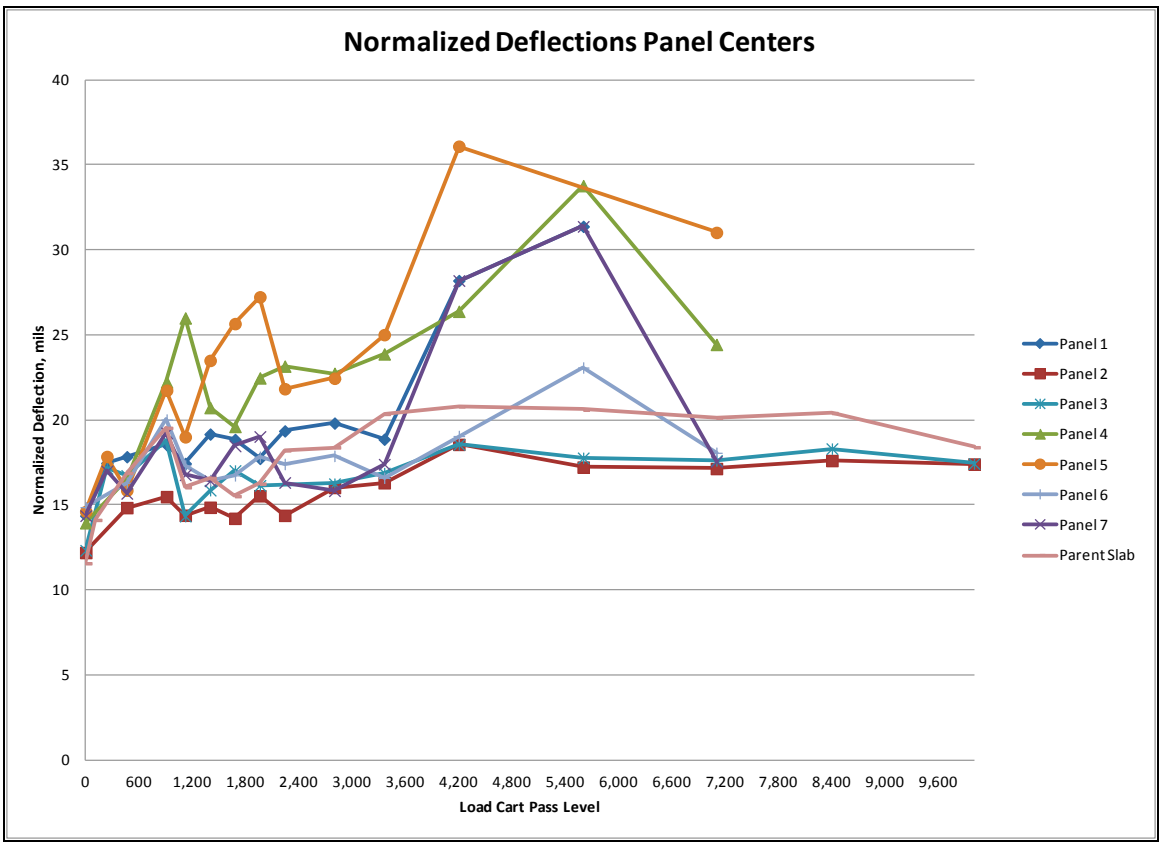

The impulse stiffness modulus (ISM) values were then computed by using the maximum force level, or load, divided by the deflection at the first sensor (center of the load plate) to provide a numerical indicator of the stiffness of the panel or slab being tested. The ISM was calculated at each interval to monitor the effect of repeated loading on the performance in the repaired areas as well as to compare this degradation to the non-repaired PCC response under repeated traffic applications. The deflection data used to calculate the ISM values were presented in Table D.5.

Figure D.13 shows the ISM values with increasing traffic levels for all panels and a parent PCC slab. The Figure shows that both the parent slab and the repairs lose strength over trafficking. This is expected, as fatigue damage increases as loadings are applied. The ISM values for Panels 2 and 3 indicated that Repair 2 was the strongest of all repairs. The ISM values indicated that the weakest panels were Panel 1 (Repair 1) and Panels 5 and 6 (Repair 3). This could signal that the flowable fill beneath these repairs was of lesser quality than that beneath Repair 2.

Table D.5. HWD deflection and ISM data.

Passes	Slab/Panel	ISM , kip/in.	Load, lb	Normalized D_0, mils	Deflection, mils						
					D_0	D_{12}	D_{24}	D_{36}	D_{48}	D_{60}	D_{72}
0	P1	3,478.33	55,375	14.37	15.92	14.30	12.68	11.11	9.69	8.62	7.48
238		2,861.51	39,031	17.47	13.64	12.55	11.18	9.81	8.64	7.58	6.78
462		2,802.54	55,210	17.84	19.70	17.71	15.79	13.84	12.17	10.73	9.41
910		2,695.28	54,202	18.55	20.11	18.00	15.92	14.00	12.11	10.75	9.31
1,120		2,866.03	55,429	17.45	19.34	17.39	15.35	13.19	11.33	9.78	8.54
1,400		2,608.09	54,170	19.17	20.77	18.83	16.50	14.15	12.26	10.52	9.22
1,680		2,651.77	55,528	18.86	20.94	19.06	16.74	14.46	12.41	10.60	9.31
1,960		2,818.56	56,174	17.74	19.93	17.93	15.91	13.60	11.80	9.94	8.75
2,240		2,582.92	52,614	19.36	20.37	18.28	16.22	13.94	12.21	10.69	9.48
2,800		2,523.05	51,672	19.82	20.48	18.44	16.13	13.81	12.08	10.61	9.37
3,360		2,649.92	52,866	18.87	19.95	18.11	15.86	13.56	11.76	10.12	8.89
4,200		1,773.13	50,357	28.20	28.40	24.49	20.51	16.65	13.50	10.58	9.24
5,600		1,593.28	52,658	31.38	33.05	27.89	22.89	18.00	13.88	10.25	8.97
0	P2	4,095.81	55,703	12.21	13.60	12.65	11.78	10.76	9.86	9.14	7.93
238		no data									
462		3,367.29	55,594	14.85	16.51	15.08	14.73	13.31	12.01	11.38	9.31
910		3,226.93	55,955	15.49	17.34	16.09	15.13	14.04	13.19	10.78	9.22
1,120		3,472.37	56,426	14.40	16.25	15.80	15.17	14.68	14.40	10.76	9.41
1,400		3,363.04	55,692	14.87	16.56	15.53	14.38	13.39	12.45	11.47	9.32
1,680		3,516.47	56,580	14.22	16.09	14.93	14.09	13.16	12.32	11.57	9.33
1,960		3,216.61	55,583	15.54	17.28	16.07	14.97	14.05	13.14	12.26	9.18
2,240		3,473.79	54,608	14.39	15.72	15.07	13.99	13.00	12.02	10.70	9.51
2,800		3,118.78	51,990	16.03	16.67	16.26	14.81	13.98	12.94	11.60	10.19
3,360		3,065.72	53,742	16.31	17.53	16.91	15.82	14.41	13.43	12.16	10.07

Passes	Slab/Panel	ISM , kip/in.	Load, lb	Normalized D_0, mils	Deflection, mils						
					D_0	D_{12}	D_{24}	D_{36}	D_{48}	D_{60}	D_{72}
4,200		2,693.14	50,631	18.57	18.80	18.48	17.69	16.81	16.23	11.94	10.58
5,600		2,901.87	54,323	17.23	18.72	18.18	17.90	17.38	17.01	10.59	9.42
7,100		2,916.13	54,969	17.15	18.85	18.64	18.48	17.72	17.09	16.40	9.65
8,400		2,838.35	54,695	17.62	19.27	18.99	18.75	18.28	18.13	11.81	10.39
10,000		2,871.74	55,999	17.41	19.50	17.46	15.70	13.92	12.30	11.02	7.95
0	P3	4,051.79	55,550	12.34	13.71	12.65	11.56	10.37	9.07	8.16	7.20
238		2,915.03	55,648	17.15	19.09	18.39	16.70	14.80	12.96	11.37	9.22
462		2,986.79	55,166	16.74	18.47	17.46	16.00	14.14	12.47	10.86	9.45
910		2,661.78	55,791	18.78	20.96	19.91	18.62	17.07	15.78	12.44	10.44
1,120		3,484.78	54,049	14.35	15.51	17.41	16.11	14.74	13.76	10.94	9.50
1,400		3,149.62	54,520	15.87	17.31	16.56	15.27	13.78	12.65	11.05	9.60
1,680		2,935.98	52,877	17.03	18.01	17.24	15.99	14.53	13.52	12.60	10.10
1,960		3,094.36	55,451	16.16	17.92	17.43	16.29	14.80	13.88	13.20	10.15
2,240		no data									
2,800		3076.02	52,077	16.25	16.93	16.62	15.42	14.15	12.91	11.63	10.18
3,360		2962.64	52,735	16.88	17.80	17.35	16.20	14.86	13.49	12.00	10.33
4,200		2693.14	50,631	18.57	18.80	18.48	17.69	16.81	16.23	11.94	10.58
5,600		2,813.13	52,296	17.77	18.59	18.51	17.65	16.77	16.17	11.93	10.40
7,100		2,837.43	52,691	17.62	18.57	17.88	17.02	15.81	15.01	12.42	10.96
8,400		2,729.80	52,767	18.32	19.33	18.85	17.93	16.84	16.07	15.27	10.23
10,000		2,867.69	55,375	17.44	19.31	17.58	15.77	13.68	11.53	10.91	8.74
0	P4	3,582.48	54,991	13.96	15.35	14.25	12.89	11.44	10.11	9.31	7.77
238		no data									
462		3,034.58	56,777	16.48	18.71	17.59	15.93	14.15	12.40	10.73	9.17
910		2,248.64	55,429	22.24	24.65	22.71	20.31	18.33	16.52	14.16	12.20

Passes	Slab/Panel	ISM , kip/in.	Load, lb	Normalized D_0, mils	Deflection, mils						
					D_0	D_{12}	D_{24}	D_{36}	D_{48}	D_{60}	D_{72}
1,120		1,923.11	44,847	26.00	23.32	21.34	18.24	14.83	13.46	9.90	7.17
1,400		2,412.06	55,791	20.73	23.13	20.94	18.11	15.70	13.65	12.26	10.41
1,680		2,548.54	55,813	19.62	21.90	21.35	18.49	15.86	14.09	12.68	10.97
1,960		2,224.85	56,667	22.47	25.47	22.90	19.94	17.56	16.00	14.54	12.54
2,240		2,158.24	52,877	23.17	24.50	22.25	19.03	15.77	13.24	11.33	9.97
2,800		2,198.31	51,990	22.74	23.65	20.94	17.62	14.47	12.06	10.17	8.93
3,360		2,093.45	52,713	23.88	25.18	23.85	19.96	16.19	13.46	11.52	9.99
4,200		1,894.68	53,392	26.39	28.18	25.34	21.47	18.06	15.48	13.07	11.47
5,600		1,480.31	54,520	33.78	36.83	31.69	27.02	22.52	19.12	15.40	13.48
7,100		2,045.72	54,498	24.44	26.64	27.38	23.16	18.98	15.72	13.08	11.27
0	P5	3,419.07	55,594	14.62	16.26	14.92	13.47	11.86	10.27	8.84	7.46
238		2,800.51	55,254	17.85	19.73	18.90	17.58	16.17	14.72	13.55	10.57
462		3,150.63	55,199	15.87	17.52	16.40	15.00	13.40	11.79	10.38	8.75
910		2,299.04	54,947	21.75	23.90	22.48	20.49	18.44	16.57	15.22	11.20
1,120		2,630.42	55,002	19.01	20.91	20.13	18.42	16.44	14.95	13.86	10.70
1,400		2,127.43	52,888	23.50	24.86	22.59	19.52	16.87	15.07	13.87	10.42
1,680		1,948.14	54,509	25.67	27.98	26.36	22.95	19.70	17.33	15.98	11.88
1,960		1,835.60	55,068	27.24	30.00	28.24	24.70	21.24	18.38	16.32	12.22
2,240		2,289.78	52,001	21.84	22.71	21.45	17.79	14.29	11.37	9.71	8.56
2,800		2,226.91	50,818	22.45	22.82	20.91	17.31	13.74	10.98	9.41	8.13
3,360		1,998.65	51,825	25.02	25.93	24.50	20.43	16.56	13.75	11.97	9.17
4,200		1,385.26	49,634	36.09	35.83	31.61	27.20	23.01	19.36	16.96	12.14
5,600		no data									
7,100		1,611.55	53,874	31.03	33.43	30.23	25.33	20.92	17.98	16.44	11.28
0	P6	3,361.60	53,315	14.87	15.86	14.20	12.88	11.67	10.59	9.26	8.15

Passes	Slab/Panel	ISM , kip/in.	Load, lb	Normalized D_0, mils	Deflection, mils						
					D_0	D_{12}	D_{24}	D_{36}	D_{48}	D_{60}	D_{72}
238		no data									
462		3,065.57	55,824	16.31	18.21	16.97	15.43	13.48	11.88	10.84	8.78
910		2,496.77	55,703	20.03	22.31	21.63	20.55	19.33	18.04	10.80	9.27
1,120		2,885.66	56,963	17.33	19.74	19.65	18.94	18.11	17.48	11.20	9.82
1,400		3,036.51	56,054	16.47	18.46	17.90	16.99	15.80	14.95	14.21	9.35
1,680		2,985.98	57,062	16.74	19.11	18.80	17.96	17.10	16.28	11.22	9.87
1,960		2,802.81	56,897	17.84	20.30	20.05	19.29	18.59	18.09	12.22	10.77
2,240		2,871.29	53,808	17.41	18.74	17.89	16.38	14.80	13.48	11.72	10.31
2,800		2,794.57	53,041	17.89	18.98	18.42	16.80	15.20	13.82	11.99	10.53
3,360		3,011.84	54,936	16.60	18.24	17.47	15.96	14.63	13.38	11.31	9.96
4,200		2,623.75	53,918	19.06	20.55	20.58	19.85	18.85	18.04	13.41	11.29
5,600		2,165.91	56,032	23.09	25.87	26.28	25.98	25.17	24.71	13.83	12.11
7,100		2,766.75	55,999	18.07	20.24	19.76	19.19	18.25	17.50	11.33	9.59
0	P7	3,478.33	55,375	14.37	15.92	14.30	12.68	11.11	9.69	8.62	7.48
238		2,941.77	54,717	17.00	18.60	17.67	16.47	15.27	13.96	12.85	7.07
462		3,187.69	55,944	15.69	17.55	16.43	15.02	13.59	12.20	10.47	8.93
910		2,598.79	55,900	19.24	21.51	20.80	19.90	18.93	17.87	16.92	8.76
1,120		2,979.76	54,619	16.78	18.33	18.62	17.96	17.20	16.67	8.48	7.04
1,400		3,044.11	55,068	16.43	18.09	18.26	17.56	16.69	16.04	15.32	7.32
1,680		2,705.71	55,440	18.48	20.49	20.91	20.12	19.34	18.56	17.80	8.67
1,960		2,627.44	56,306	19.03	21.43	21.07	20.48	19.82	18.94	18.15	8.91
2,240		3,062.59	53,381	16.33	17.43	16.57	15.09	13.39	11.95	10.19	8.67
2,800		3,156.97	51,869	15.84	16.43	16.16	14.57	12.91	11.49	10.13	8.49
3,360		2,873.52	52,844	17.40	18.39	17.50	16.22	14.74	13.59	10.69	7.93
4,200		1,773.13	50,357	28.20	28.40	24.49	20.51	16.65	13.50	10.58	9.24

Passes	Slab/Panel	ISM , kip/in.	Load, lb	Normalized D_0, mils	Deflection, mils						
					D_0	D_{12}	D_{24}	D_{36}	D_{48}	D_{60}	D_{72}
5,600		1,593.28	52,658	31.38	33.05	27.89	22.89	18.00	13.88	10.25	8.97
7,100		2,847.55	43,653	17.56	15.33	15.00	14.73	14.19	13.82	7.18	6.12
0	Slab	4,318.71	57,007	11.58	13.20	12.47	11.69	10.76	9.87	8.81	7.62
112		3,539.72	56,317	14.13	15.91	15.54	14.66	13.51	12.35	11.01	9.77
238		No data									
462		2,961.01	55,134	16.89	18.62	17.60	16.50	15.19	13.71	12.32	10.93
910		2,559.35	56,229	19.54	21.97	20.59	19.10	17.24	15.55	13.89	12.13
1,120		3,116.25	55,407	16.04	17.78	16.19	15.72	14.36	12.94	11.44	10.03
1,400		3,013.23	55,112	16.59	18.29	17.28	16.21	14.85	13.56	12.15	10.91
1,680		3,221.23	44,453	15.52	13.80	14.35	13.33	12.27	11.17	10.08	9.02
1,960		3,075.09	57,412	16.26	18.67	18.14	16.95	15.53	14.64	13.43	12.39
2,240		2,745.23	54,630	18.21	19.90	19.40	18.60	17.56	16.52	15.35	13.55
2,800		2,719.18	42,963	18.39	15.80	15.56	15.08	14.29	13.58	12.72	10.90
3,360		2,456.20	53,447	20.36	21.76	21.24	20.55	19.57	18.69	17.07	14.44
4,200		2,403.91	52,910	20.80	22.01	20.87	19.60	17.97	16.46	14.93	13.33
5,600		2,425.64	55,353	20.61	22.82	21.85	20.96	19.17	17.96	16.12	14.52
7,100		2,483.45	55,977	20.13	22.54	21.45	20.23	18.99	17.77	16.37	14.79
8,400		2,449.94	56,667	20.41	23.13	22.22	21.52	20.10	18.85	16.63	14.74
10,000		2,717.45	45,789	18.40	16.85	15.95	14.46	12.90	11.66	10.11	8.94

Figure D.13. ISM versus load cart passes.

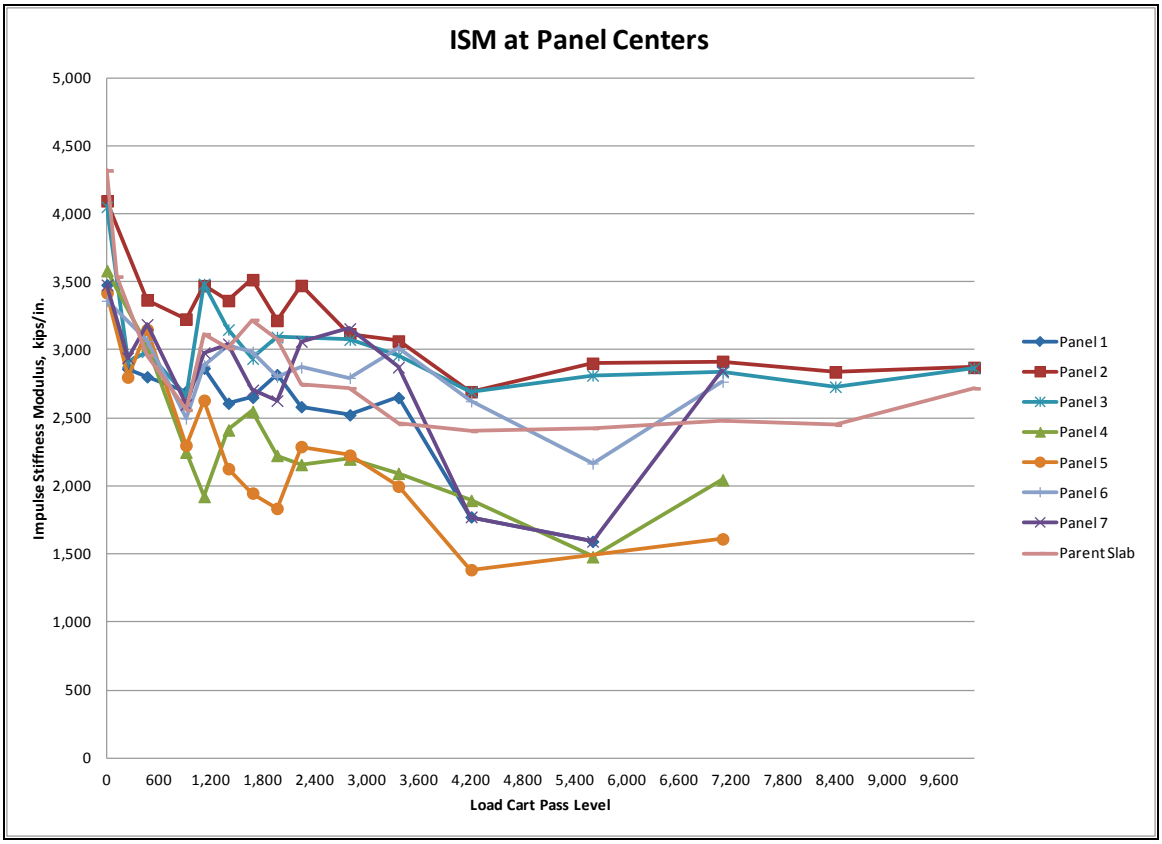

D.5.4 Load transfer efficiency (LTE)

Using the HWD, load transfer (joint) testing was conducted on the longitudinal and transverse joints of precast panels and surrounding PCC slabs. In PCC pavements, dowel bars, aggregate interlock, and foundation characteristics all contribute to distributing the load of aircraft between slabs at the joints. How well these mechanisms transfer the load, or the load transfer efficiency (LTE) of the joints, is commonly measured during evaluation of PCC airfield pavements. Decreased load transfer will result in high stresses at the slab edges and corners and may cause distresses such as faulting, corner breaks, and spalling along the joint.

LTE can vary over the life of the pavement because of changes in temperature causing the joint to open or close due to expansion or contraction of the PCC, number of repetitions of load, foundation support, aggregate particle angularity/interlock, and the quality of the load transfer devices. To reduce temperature-related LTE variations, measurements were taken at the same time each day of testing (early morning) to minimize temperature effects.

The three most common methods of calculating LTE— deflection-based (LTE_δ), stress-based (LTE_σ), or strain-based (LTE_ε) — can be calculated using the following formulas:

$$LTE_\delta = \delta_u / \delta_l \quad \text{(D.2)}$$

$$LTE_\sigma = \sigma_u / \sigma_l \quad \text{(D.3)}$$

$$LTE_\varepsilon = \varepsilon_u / \varepsilon_l \quad \text{(D.4)}$$

where:

δ_u = deflection of the unloaded side of the joint
δ_l = deflection of the loaded side of the joint
σ_u = bending stress in the unloaded slab
σ_l = bending stress in the loaded slab
ε_u = bending strain in the loaded slab edge at the joint
ε_l = bending strain in the unloaded slab edge at the joint

Equation D.2 is the most widely used due to the availability and acceptance of NDT equipment such as the HWD for pavement evaluation, which can measure slab edge deflections. Equations D.3 and D.4 rely on accurate measurements of the stress and strains through instrumentation or theoretical modeling. Stress or change in stress can be estimated from these calculated or measured strains.

For this investigation, LTE_δ was calculated based on the HWD deflection data. Stress- and strain-based load transfer calculations were intended to be conducted using data collected by strain gauges. Unfortunately, the gauges were destroyed during the initial passes of the load cart, and the data could not be collected.

In order to calculate LTE_δ, the HWD was used to conduct joint tests during the same data collection intervals described previously for calculating ISM. In the joint test, the HWD load was applied at one side of a joint close to the edge of a slab (or panel), and the deflections were measured by seven geophones located at a spacing of 12 in. on the adjacent slab or panel. The deflections at the maximum drop load were used to calculate LTE_δ. These measurements were used to produce deflection basins like those shown in Figures D.14 and D.15. Good LTE_δ results in an almost no slope between Sensors 1 and 2. Poor LTE_δ results in large differences between deflections measured at Sensors 1 and 2 and a steep slope.

Figure D.14. Deflection basin example good LTE_{δ}.

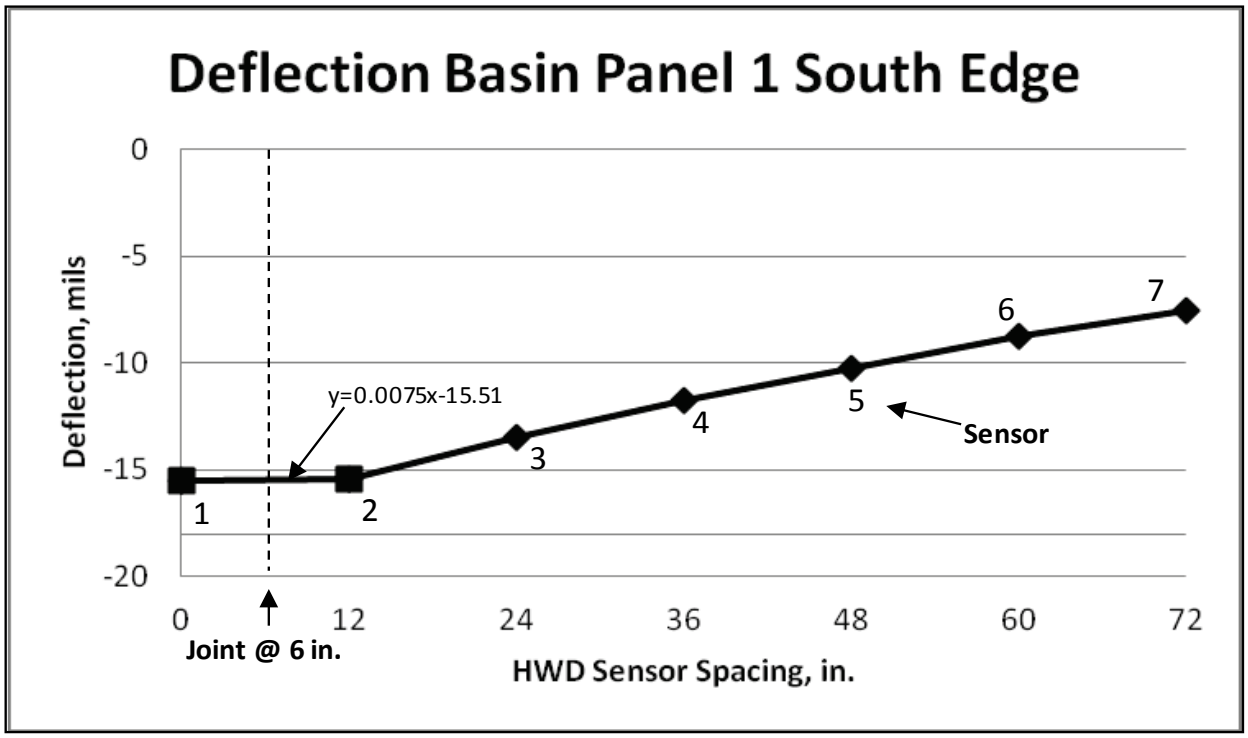

Figure D.15. Deflection basin example poor LTE_{δ}.

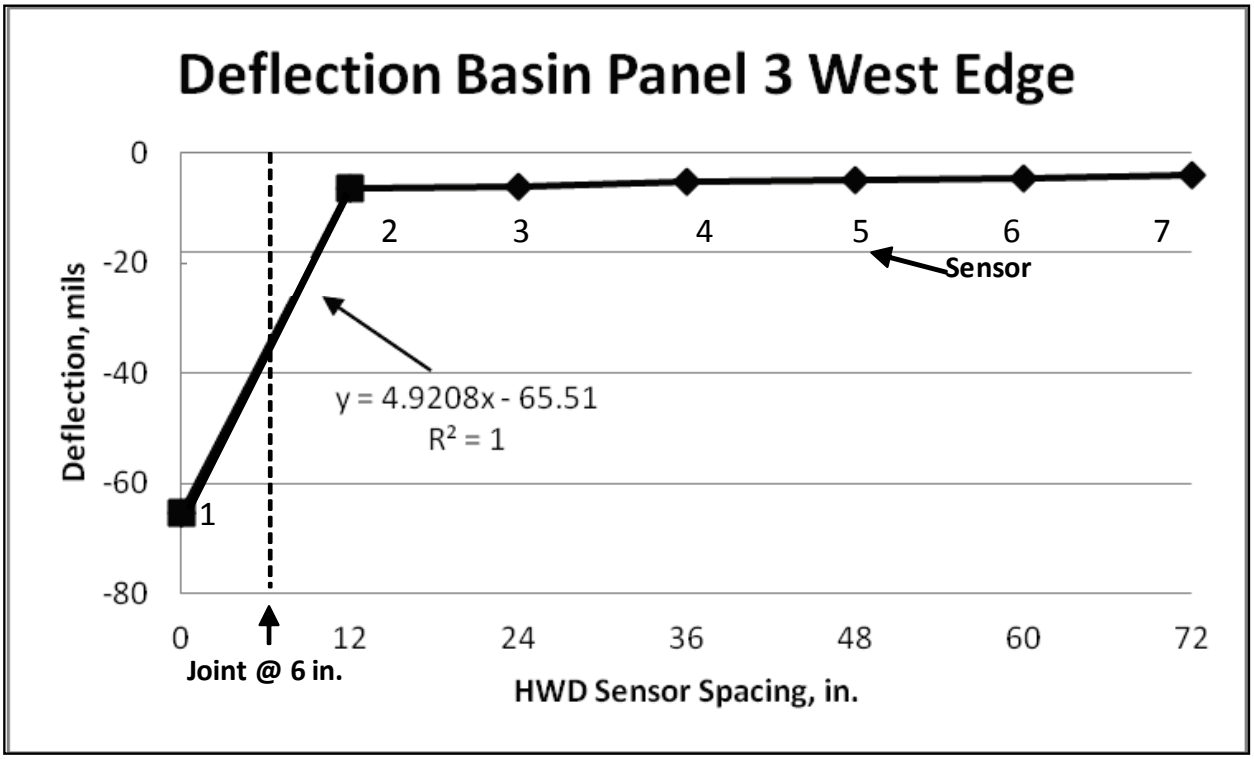

D.5.5 Load transfer mechanisms

In general, in PCC pavements there are two main mechanisms used for load transfer. The first is aggregate interlock. Joints constructed in PCC pavements use shallow cuts to initiate a crack from the surface to the bottom of the pavement. Beneath this cut, a full-depth crack propagates, separating the pavement into two slabs, each with rough vertical faces. These rough vertical faces, in contact, produce aggregate interlock through friction. If the spacing is large or the surfaces of the faces are smooth, then aggregate interlock contributes less to transferring load, and the LTE_{δ} is reduced. The second mechanism for providing load transfer is the installation of dowel bars. These devices allow transfer of load across a joint through bending of the dowel bars and allow the pavement to expand and contract. If the joint opening is not large, then both aggregate interlock and dowel bar mechanisms can contribute to load transfer. In addition to these two mechanisms, the base and foundation can contribute to load transfer of the PCC. If the base material is strong, then the foundation material may contribute by resisting shear and vertical deformations under the slab.

For this investigation, load transfer was provided by dowels precast in the panels on the transverse joints. No dowels were provided along the longitudinal joints. For the transverse joints, it was thought that the primary load transfer mechanism would be through the dowels with lesser effects attributed to aggregate interlock or foundation support. For the precast slabs, the spacing between the panels and the surrounding pavement was 0.375 to 0.5 in., and both the PCC panel and the parent PCC had relatively smooth surfaces. Thus, it was thought that aggregate interlock would contribute minimally to load transfer, unless the two faces were in close contact, causing the faces to roughen through contact and loading repetitions and contribute more shearing resistance.

Along the longitudinal joints, no load transfer dowels were installed, and it was assumed that load transfer would be poorer unless panels and the parent PCC slabs were in close contact. It was also assumed that there would be less joint shear face roughness for aggregate interlock effects between panels and the surrounding PCC and the panels to each other to allow good LTE. Thus, the LTE_{δ} was expected to be lower along the longitudinal joints due to the lack of aggregate interlock and the lack of dowels.

D.5.6 LTE_{δ} calculation

The changes in LTE_{δ} with increasing traffic levels for Repairs 1, 2, and 3 are presented in Figures D.16 through D.19. As shown in the figures, the LTE_{δ} generally decreased gradually with increasing traffic, and the LTE_{δ} was better for the doweled joints (N and S joints) compared to the undoweled joints (E and W joints). Some measurements were encountered in which the LTE_{δ} increased temporarily before decreasing again. This is due to changes in the slab temperatures during testing, causing the joints to close during warmer temperatures. For comparison, the LTE_{δ} for the parent slabs was calculated prior to traffic and after 10,000 passes and is shown in Table D.6.

D.5.7 Corner deflections

Corner deflection tests were conducted on selected panel corners for each repair. Tests were conducted for Repair 1 in Panel 1, Repair 2 in Panel 2, and Repair 3 in Panels 4 and 7. The HWD was used to conduct this test with the load plate placed near the corner of the slab in the direction of traffic. Corner deflections were monitored, as deflections in the corners of the panels were expected to be higher than those measured in the center of the panel based on traditional pavement design concepts. Deflections were normalized to 50,000 lb to show comparisons between the numerous load applications and measured deflections.

Figure D.20 shows the deflections for the panels. As can be seen, the deflections at the corners increased with increasing traffic application as a general trend. For comparison, Figure D.21 presents the center deflections, and Figure D.22 presents the edge deflections.

Figure D.16. Load transfer efficiency for Repair 1 (Panel 1) with traffic.

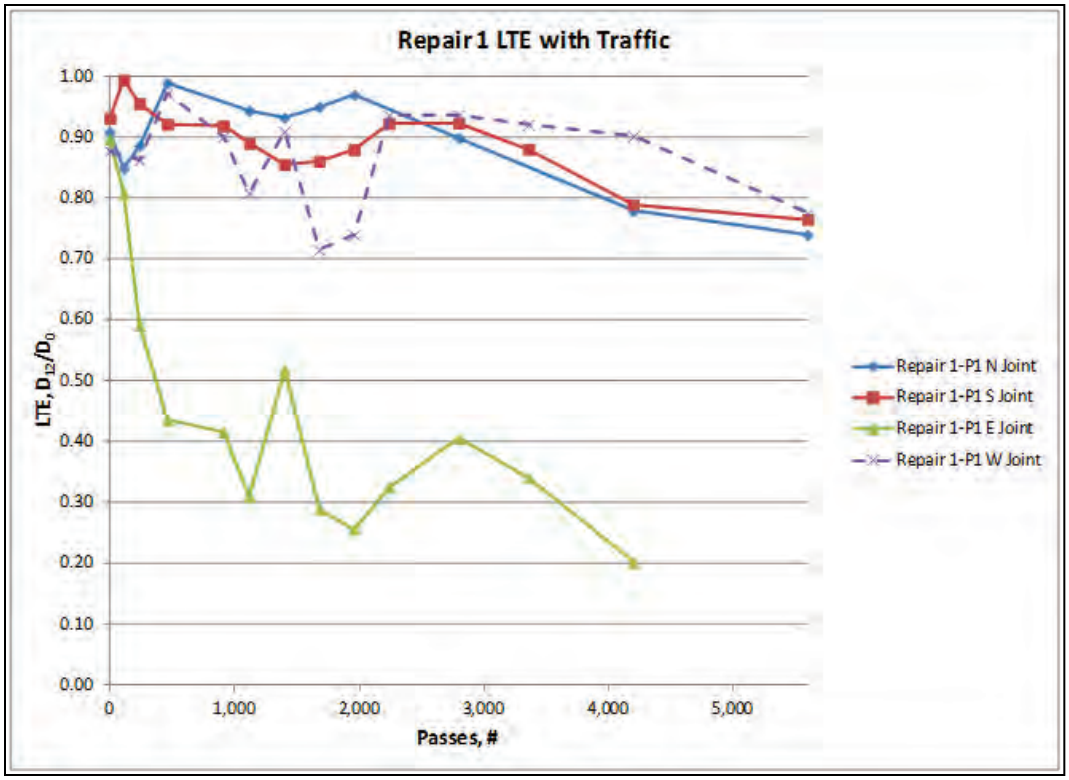

Figure D.17. Load transfer efficiency for Repair 2 (Panels 2-3) with traffic.

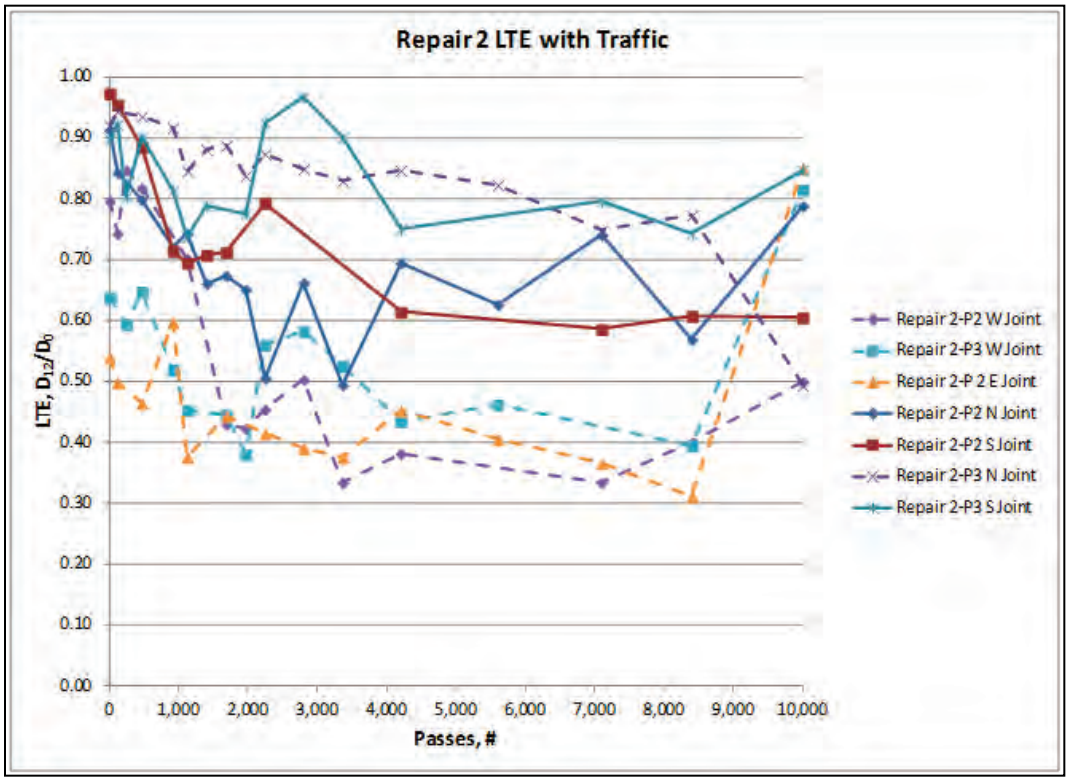

Figure D.18. Load transfer efficiency for Repair 3 (Panels 4-5) with traffic.

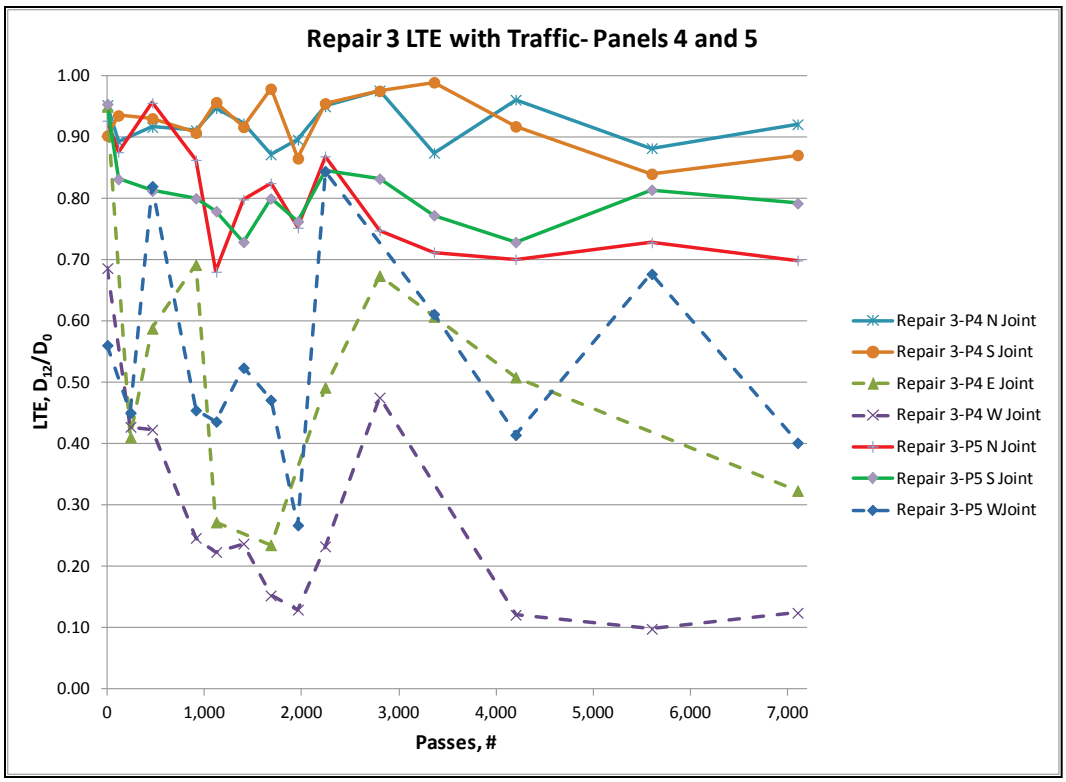

Figure D.19. Load transfer efficiency for Repair 3 (Panels 4-5) with traffic.

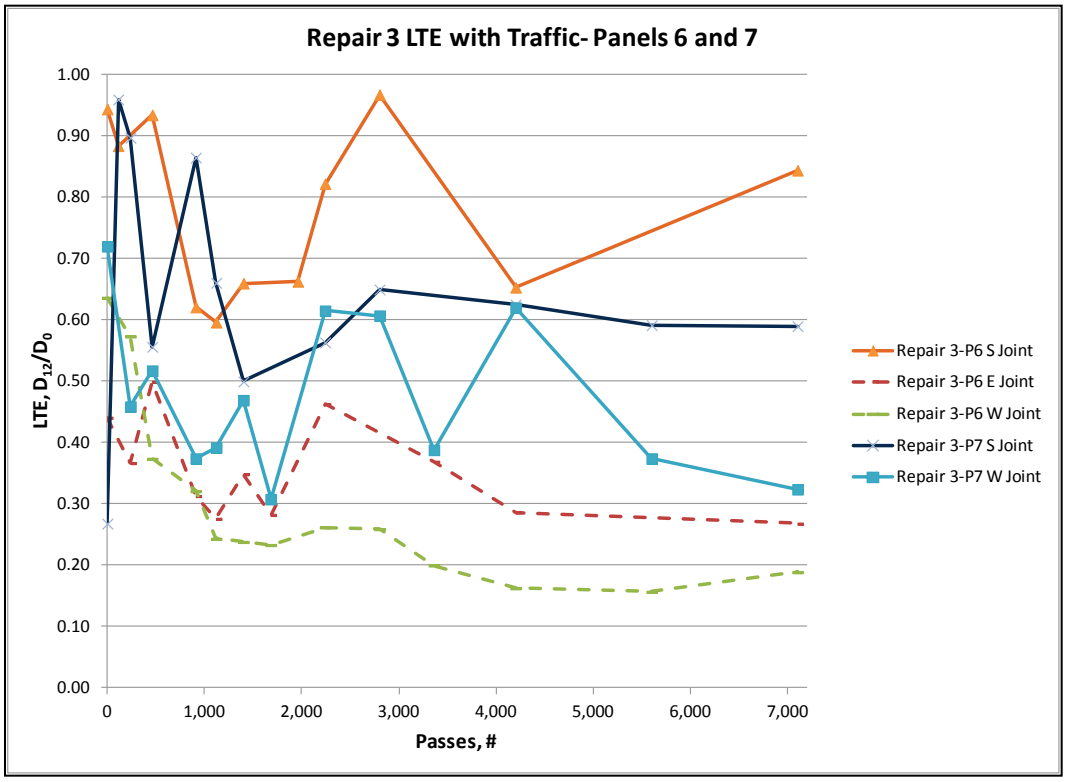

Table D.6. Load transfer FWD test data parent PCC slabs prior to repair.

Passes	HWD Reference Number	Direction	LTE_δ D_{12}/D_0	Load, lb	Normalized D_0 mils	Deflection, mils D_0	Deflection, mils D_{12}
0	2	N-S	0.90	55,846	22.69	25.35	22.75
0	3	N-S	0.19	53,852	38.28	41.23	7.89
0	4	N-S	0.90	55,670	20.40	22.72	20.38
0	9	N-S	0.98	54,608	18.86	20.60	20.14
0	10	N-S	0.29	54,772	30.30	33.20	9.70
0	11	N-S	0.23	54,235	31.02	33.65	7.69
0	12	S-N	0.95	55,210	18.19	20.09	19.17
0	13	E-W	0.78	53,556	31.88	34.15	26.80
0	14	E-W	0.86	54,542	23.02	25.11	21.63
0	15	E-W	0.86	55,035	20.41	22.46	19.42
0	21	W-E	0.98	54,991	18.48	20.32	19.90
0	22	W-E	0.84	54,750	20.48	22.43	18.90
10,000	2	N-S	0.95	54,520	20.41	22.25	21.18
10,000	3	N-S	0.22	53,742	35.82	38.50	8.56
10,000	4	N-S	0.96	56,163	17.86	20.06	19.30
10,000	9	N-S	0.96	55,670	19.14	21.31	20.43
10,000	10	N-S	0.53	55,561	24.18	26.87	14.36
10,000	11	N-S	0.25	53,458	31.87	34.07	8.50
10,000	12	S-N	0.96	56,481	15.57	17.59	16.91
10,000	13	E-W	No Data				
10,000	14	E-W	0.80	53,852	25.96	27.96	22.29
10,000	15	E-W	No Data				
10,000	21	W-E	0.91	53,786	20.79	22.36	20.33
10,000	22	W-E	0.33	52,691	44.69	47.09	15.33

Figure D.20. Corner deflections for selected panels.

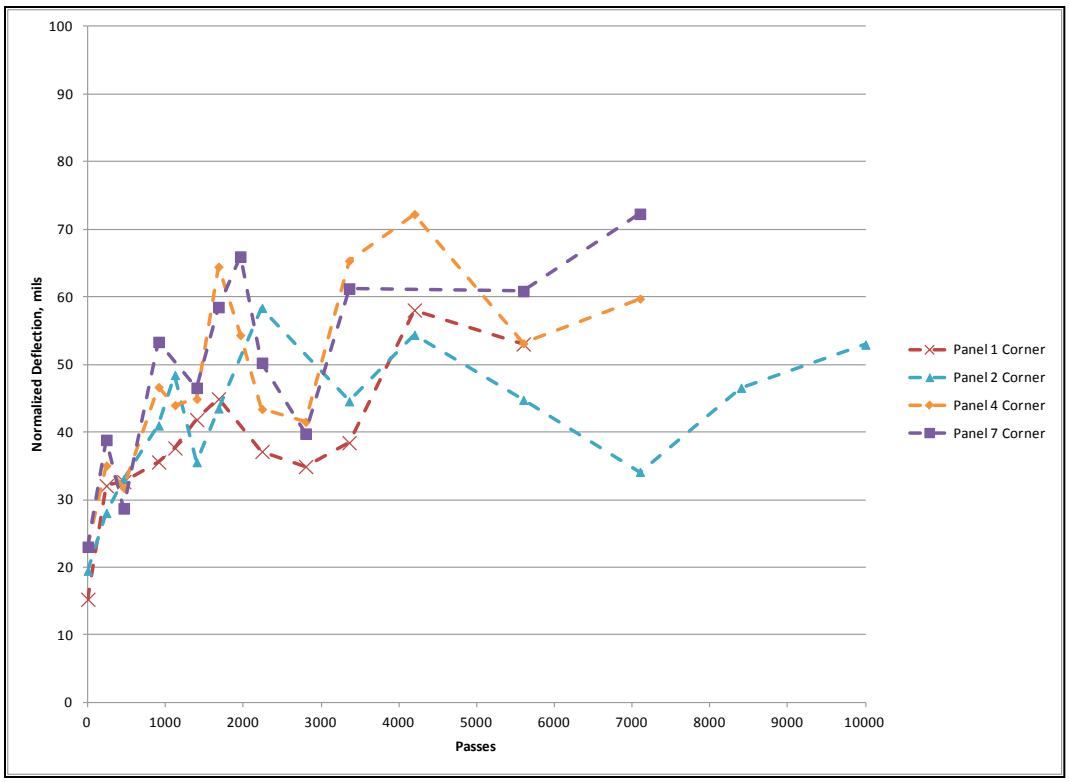

Figure D.21. Center deflections.

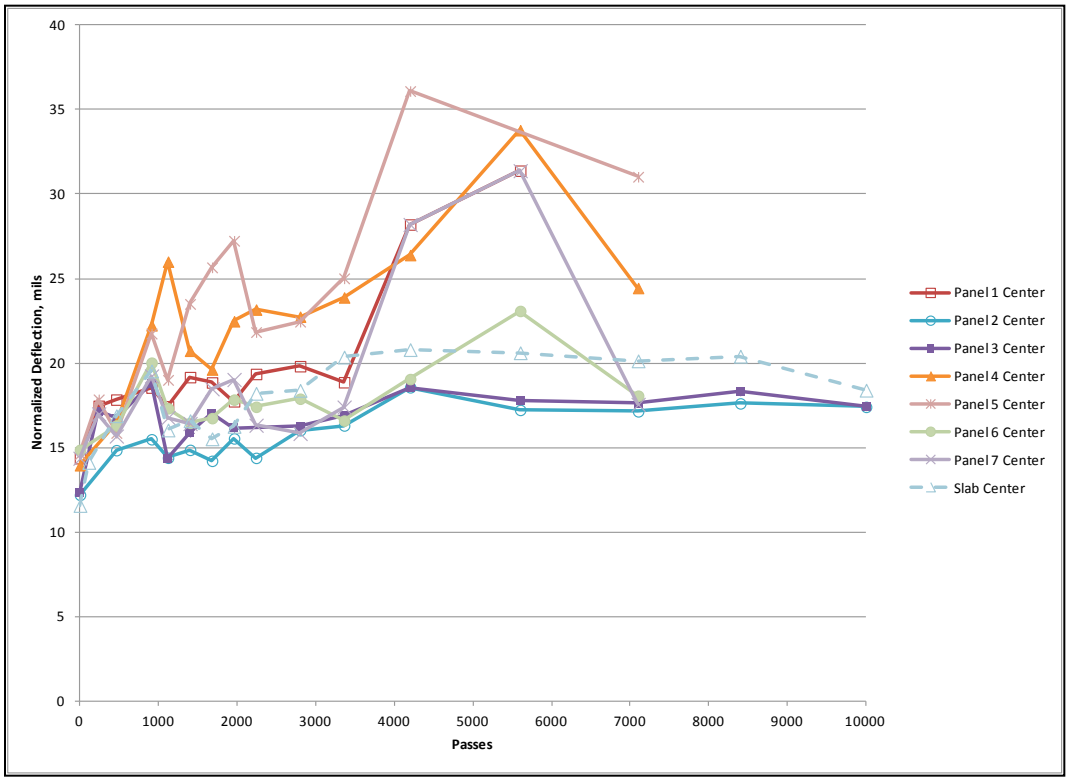

Figure D.22. Edge deflections.

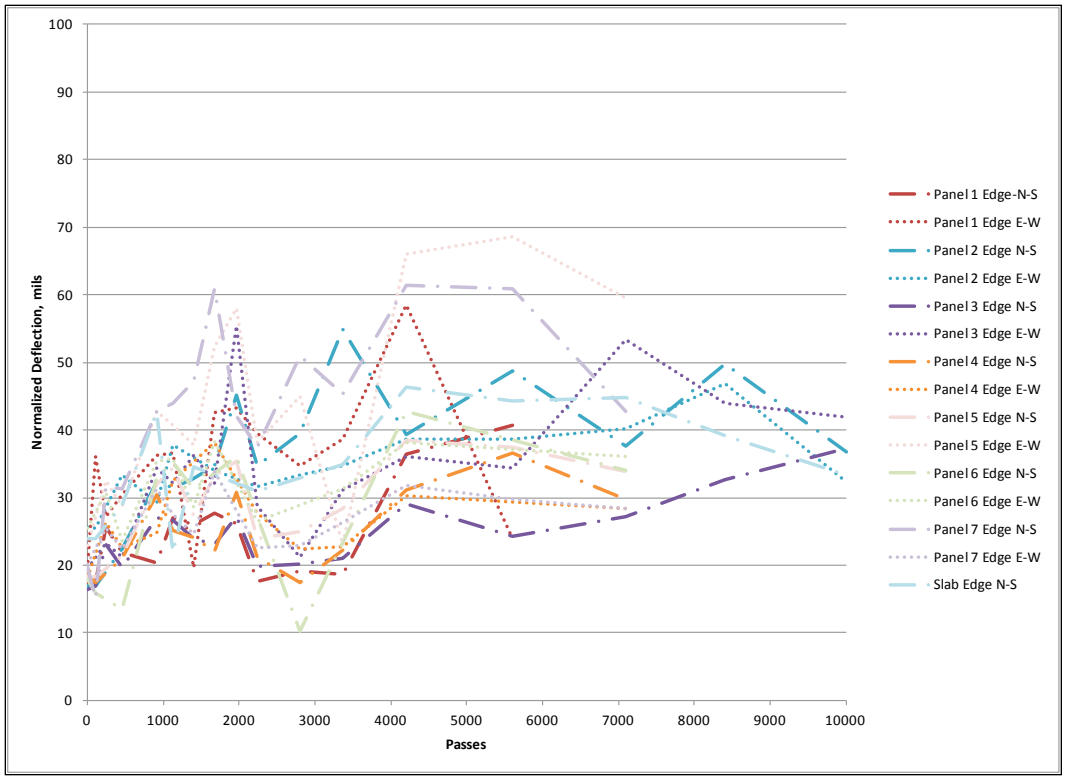

Appendix E: Finite Element Modeling

This appendix provides details regarding the development of the model, additional figures and data results from the finite element modeling efforts, and calculations of shear forces carried by dowels and bearing pressures not fully presented in the body of this report.

E.1 Development of the finite element model

E.1.1 Selection of the software and elements

As discussed in Chapter 5, 3-D finite element modeling (FEM) was conducted to determine the state of stress surrounding the dowels in the transverse repair joint. In recent decades, many software programs have been used, including PCC-specific FEM programs such as ILLI-SLAB, WESLIQID, J-SLAB, EverFE, WESLAYER, and ISLAB2000 and general-purpose FEM software such as ABAQUS, ANSYS, and DYNA-3D. Based on the review of the literature, ABAQUS was selected for this study due to its widespread use for modeling PCC pavements and built-in concrete damage models. Additionally, while a number of PCC joint modeling approaches have been used, 3-D continuum solid elements for concrete and dowels and frictional contact interactions were used because this method can provide detailed stress distributions at the dowel-concrete interface rather than simplification methods using spring elements. Three-dimensional first order reduced integration continuum elements were used to model all parts, including the concrete parts and steel dowel bars. C3D8R solid elements (8-node bricks) available in the ABAQUS software were selected because they were suitable for both linear and nonlinear analysis and for frictional contact interactions.

E.1.2 Selection of the material models

Elastic models are generally used to model the response of sublayer materials and concrete dowel bars. However, elastic models alone are not adequate to model the non-elastic behavior of concrete. ABAQUS has three built-in concrete models that can be used to model both plain and reinforced concrete. The models are the smeared crack model, the concrete damaged plasticity model, and the brittle cracking model. These models are used to predict the two main concrete failure mechanisms in concrete: cracking under tension and crushing under compression. The brittle

cracking model was excluded from consideration because it is intended for applications in which tensile cracking, not compressive failure, is the dominant mode of failure. Of the remaining models, the concrete damaged plasticity model was selected over the smeared crack model based on its versatility to be used for predicting concrete material behavior undergoing static, dynamic, or cyclic loading and implementation by other researchers for PCC pavement investigations. The concrete damaged plasticity model takes into account degradation caused by reductions in elastic stiffness caused, in turn, by plastic straining in both tension and compression. This model combines concepts of damaged elasticity and tensile and compressive plasticity to model the inelastic behavior of concrete (Simulia 2011a, b). The following sections summarize the concrete damaged plasticity model described by (Simulia 2011a, b).

E.1.3 Mechanical behavior of concrete

The behavior of concrete is complex due to its composition of coarse and fine aggregates and cement paste. When a concrete material undergoes loading, it initially exhibits elastic behavior, and the deformation is completely recoverable; however, if the load exceeds a certain limit (the yield load), then deformation is no longer recoverable (strain is no longer reversible). Plasticity theory is used to model this nonrecoverable behavior. The fundamental concepts of plasticity theory have been applied to concrete material models; and in general, these models are defined using the yield surface, the flow rule, and evolution laws defining hardening. For reference, the yield surface is used to determine whether a material responds elastically to a stress state; after the yield load has been exceeded, the material response is inelastic. In plasticity models, the flow rule defines the inelastic deformation after elastic response has ended; and hardening is the change in the yield or the flow definitions in response to inelastic deformation (change in loading surface and change in material hardening properties undergoing plastic flow).

E.1.3.1 Yield surface

The plastic damage model used in the concrete damaged plasticity model is based on models proposed by Lubliner et al. (1989), modified by Lee and Fenves (1998) and the yield function proposed by these researchers. In this model, the yield surface is controlled by two hardening variables: the tensile $\tilde{\varepsilon}_t^{pl}$ and compressive $\tilde{\varepsilon}_c^{pl}$ equivalent plastic strains generated under tension and compression loading. The yield function is defined in

terms of effective stresses as follows, and the yield surface is shown in Figures E.1 and E.2:

$$F(\bar{\sigma},\tilde{\varepsilon}^{pl}) = \frac{1}{1-\alpha}\left(\bar{q} - 3\alpha\bar{p} + \beta(\tilde{\varepsilon}^{pl})\left\langle\hat{\bar{\sigma}}_{max}\right\rangle - \gamma\left\langle-\hat{\bar{\sigma}}_{max}\right\rangle\right) - \bar{\sigma}_c(\tilde{\varepsilon}_c^{pl}) \le 0 \quad \text{(E.1)}$$

with

$$\alpha = \frac{\left(\frac{\sigma_{b0}}{\sigma_{c0}}\right) - 1}{2\left(\frac{\sigma_{b0}}{\sigma_{c0}}\right) - 1}; 0 \le \alpha \le 0.5 \quad \text{(E.2)}$$

$$\beta = \frac{\bar{\sigma}_c(\tilde{\varepsilon}_c^{pl})}{\bar{\sigma}_t(\tilde{\varepsilon}_t^{pl})}(1-\alpha) - (1+\alpha) \quad \text{(E.3)}$$

$$\gamma = \frac{3(1-K_c)}{2K_c - 1} \quad \text{(E.4)}$$

Figure E.1. Yield surfaces in the deviatoric plane, corresponding to different values of K_c (Simulia 2011a).

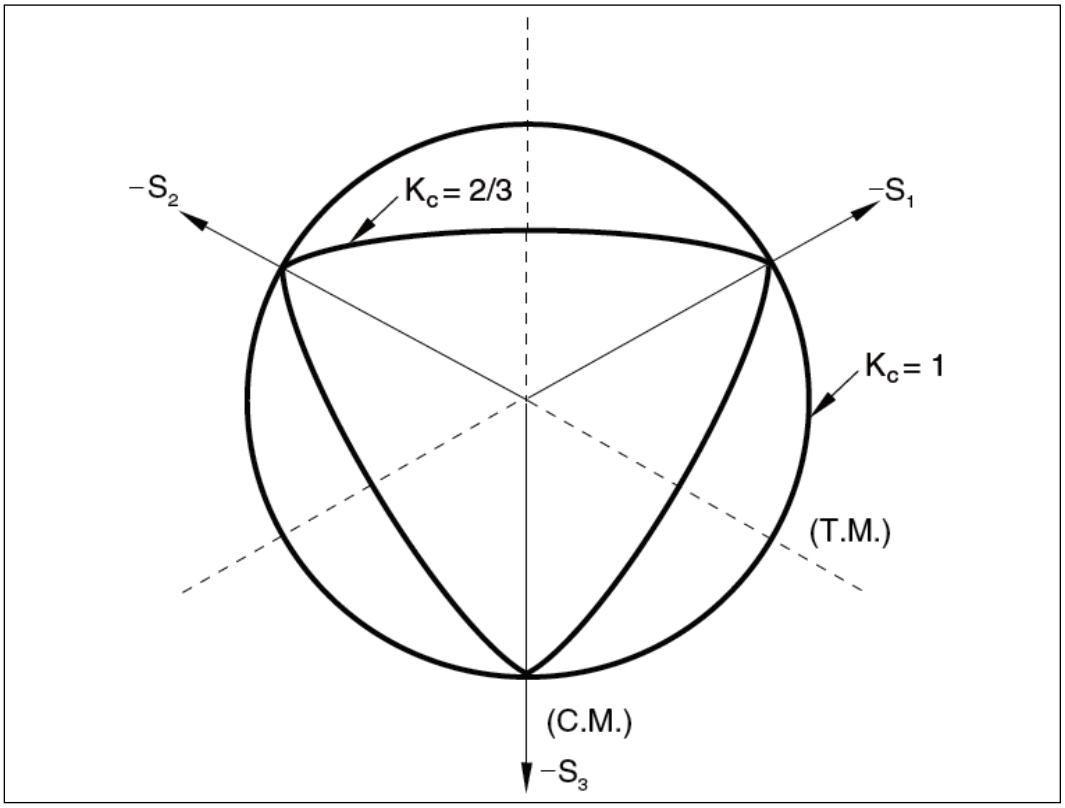

Figure E.2. Yield surface in plane stress (Simulia 2011a).

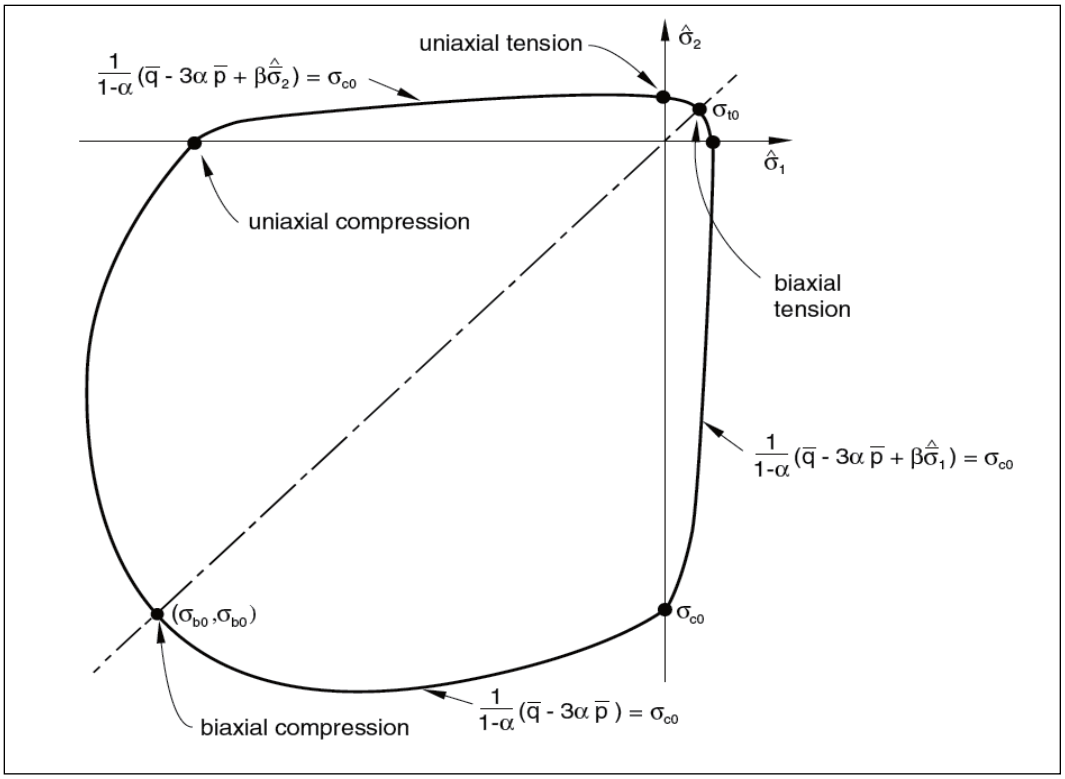

In this form:

$\hat{\bar{\sigma}}_{max}$ = maximum principal effective stress

$\frac{\sigma_{b0}}{\sigma_{c0}}$ = ratio of the initial equibiaxial compressive yield stress to initial uniaxial compressive yield stress (ABAQUS default is 1.16)

K_c = ratio of the second stress invariant on the tensile meridian to that on the compressive meridian at initial yield for any given value of pressure invariant p (ABAQUS default 2/3)

$\bar{\sigma}_t(\tilde{\varepsilon}_t^{pl})$ = the effective tensile cohesive stress

$\bar{\sigma}_c(\tilde{\varepsilon}_c^{pl})$ = the effective compressive cohesive stress

and

$\bar{q} = \sqrt{\frac{3}{2}\bar{\mathbf{S}}:\bar{\mathbf{S}}}$ ($\bar{q}$ is the Mises equivalent effective stress)

$\bar{p} = \frac{1}{3}\bar{\boldsymbol{\sigma}} : \mathbf{I}$ ($\bar{p}$ is the effective hydrostatic pressure)

$\bar{\mathbf{S}} = \bar{p}\mathbf{I} + \bar{\boldsymbol{\sigma}}$ ($\bar{\mathbf{S}}$ is the deviatoric part of the effective stress tensor $\bar{\boldsymbol{\sigma}}$)

E.1.3.2 Flow rule

The flow rule defines the inelastic deformation after elastic response has ended, and the concrete damaged plasticity model assumes nonassociated potential plastic flow. The flow potential, *G*, used is the Drucker-Prager hyperbolic function:

$$G = \sqrt{(\varepsilon \sigma_{t0} tan\psi)^2 + \bar{q}^2} - \bar{p} tan\psi \quad \text{(E.5)}$$

where:

ψ = the dilation angle (ABAQUS default 30°)
σ_{t0} = the uniaxial tensile stress at failure
ε = the eccentricity parameter (ABAQUS default is 0.1)

E.1.3.3 Uniaxial tension and compressive stress behavior

In this model, uniaxial tensile and compressive responses are characterized by damaged plasticity theory. When concrete is placed in uniaxial tension, initially, the stress-strain response is linear elastic until the ultimate tensile strength, σ_{t0} (failure stress) is reached. At this point, microcracking in the concrete material occurs with a tension softening response. When concrete is placed in uniaxial compression, initially, the stress-strain response is also linear elastic (the elastic response) until the point of initial yield is reached, σ_{c0}. After this point, stiffness is lost due to bond failure between the aggregates in the concrete and the cement paste, and the behavior becomes non-linear (the plastic response). Stress hardening occurs until the ultimate stress, $\sigma_{cu,}$ is reached. Beyond this point, strain softening occurs. The response of concrete to uniaxial loading in both tension and compression is shown in Figure E.3.

In the inelastic portions of the stress-strain curves, the elastic stiffness (modulus of elasticity) is reduced or damaged/degraded. The reduction in stiffness can be calculated using two damage variables, d_t and d_c, which are a function of the plastic strains and other variables. The damage variables have values between 0 and 1 where 0 is no damage to the material and 1 is complete loss of strength. In these Figures, E_0 is the modulus of elasticity (undamaged).

Figure E.3. Uniaxial loading response in (a) tension and (b) compression (Simulia 2011a).

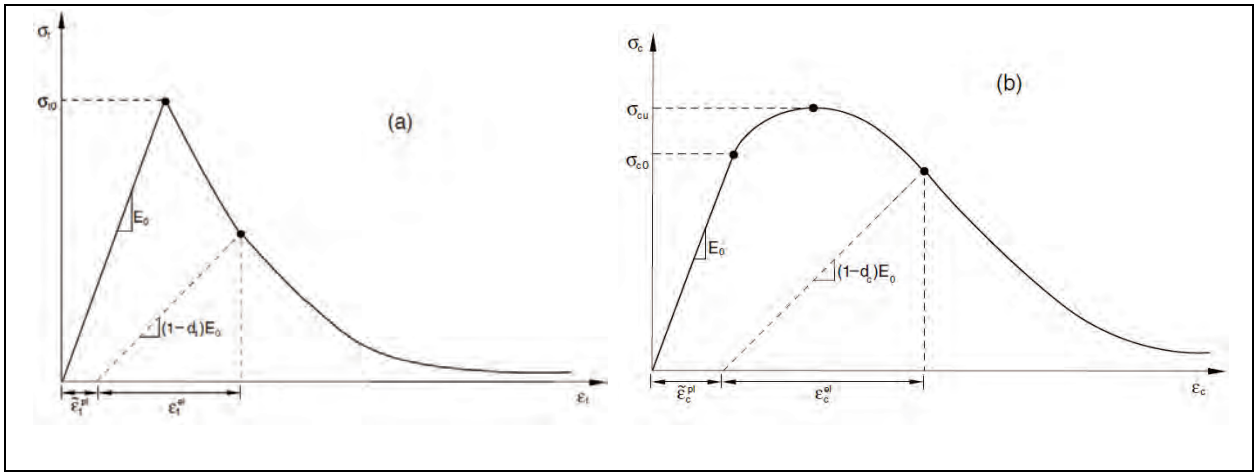

Using these curves, the stress-strain relationships under uniaxial tension and compression may be expressed as

$$\sigma_t = \left(1 - d_t\right) E_0 \left(\varepsilon_t - \tilde{\varepsilon}_t^{pl}\right) \tag{E.6}$$

$$\sigma_c = \left(1 - d_c\right) E_0 \left(\varepsilon_c - \tilde{\varepsilon}_c^{pl}\right). \tag{E.7}$$

To define the size of the yield (failure) surface, the effective tensile and compressive stresses are computed as

$$\bar{\sigma}_t = \frac{\sigma_t}{\left(1 - d_t\right)} E_0 \left(\varepsilon_t - \tilde{\varepsilon}_t^{pl}\right) \tag{E.8}$$

$$\bar{\sigma}_c = \frac{\sigma_c}{\left(1 - d_c\right)} E_0 \left(\varepsilon_c - \tilde{\varepsilon}_c^{pl}\right) \tag{E.9}$$

E.1.4 Required concrete damaged plasticity model properties

To use the concrete damaged plasticity model in ABAQUS, a number of material properties and inputs are required. The concrete damaged plasticity model input parameters include the (1) uniaxial compression stress-strain curve, (2) the uniaxial tension stiffening stress-strain curve, (3) ψ, (4) $\frac{\sigma_{b0}}{\sigma_{c0}}$, and (5) K.

In this study, the uniaxial compressive stress-strain curve was defined using laboratory test data for the concrete materials, including σ_{cu} and E, using a stress-strain model. The uniaxial compressive stress-strain curves defined for the concrete parts in the model are presented in Figures E.4 through E.6. The data were entered into ABAQUS in tabular form with compressive stress data as a function of the inelastic strain. The compressive inelastic strain is defined as the total strain minus the elastic strain corresponding to the undamaged material (corresponding to the strain measured at approximately 0.7 σ_{cu}).

The tension stiffening stress-strain curve required in ABAQUS was developed using the fracture energy criterion described by Simulia (2011a). When large amounts of steel reinforcement are not used, stress-strain response is usually not used. Instead, fracture energy criterion to model the post failure response can be used following the Hillerborg et al. (1976) approach. This characterizes the brittle nature of the concrete using stress-displacement response in lieu of stress-strain response. The energy required to open a unit area of crack, G_f, is required to generate this curve along with the failure stress in tension for concrete, σ_{t0}. The model assumes a linear loss of strength after cracking (to zero). Typical values for this parameter are 0.22 lb/in. for concrete of approximately 2,850 psi and 0.67 lb/in. for high-strength concrete of approximately 5,700 psi. This study used 0.67 lb/in., as the compressive strengths were higher than 5,000 psi for all materials modeled. Tensile stress (σ_{t0}) values are obtained from compressive laboratory test data for each concrete material modeled using the direct tensile strength relationship $\sigma_{t0} = 1.7\left(f_{c0}\right)^{2/3}$.

E.1.5 Other model properties

In addition to the concrete damaged plasticity parameters, elastic material properties including density, Young's modulus, and Poisson's ratio were entered into ABAQUS for all materials. Only elastic response was considered for the steel dowels, flowable fill, base, and subgrade following traditional pavement modeling practices. These and the concrete damaged plasticity input parameters used for finite element modeling are provided in Table E.1.

Figure E.4. Compressive stress-strain curve for parent slab concrete.

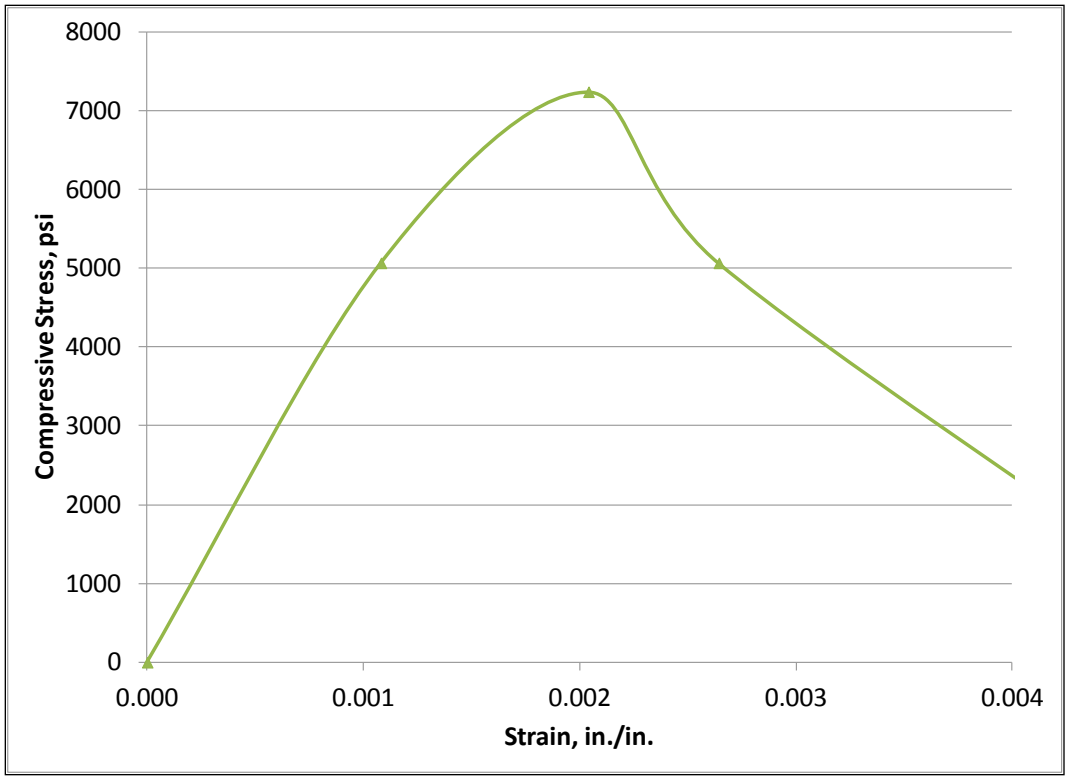

Figure E.5. Compressive stress-strain curve for precast panel concrete.

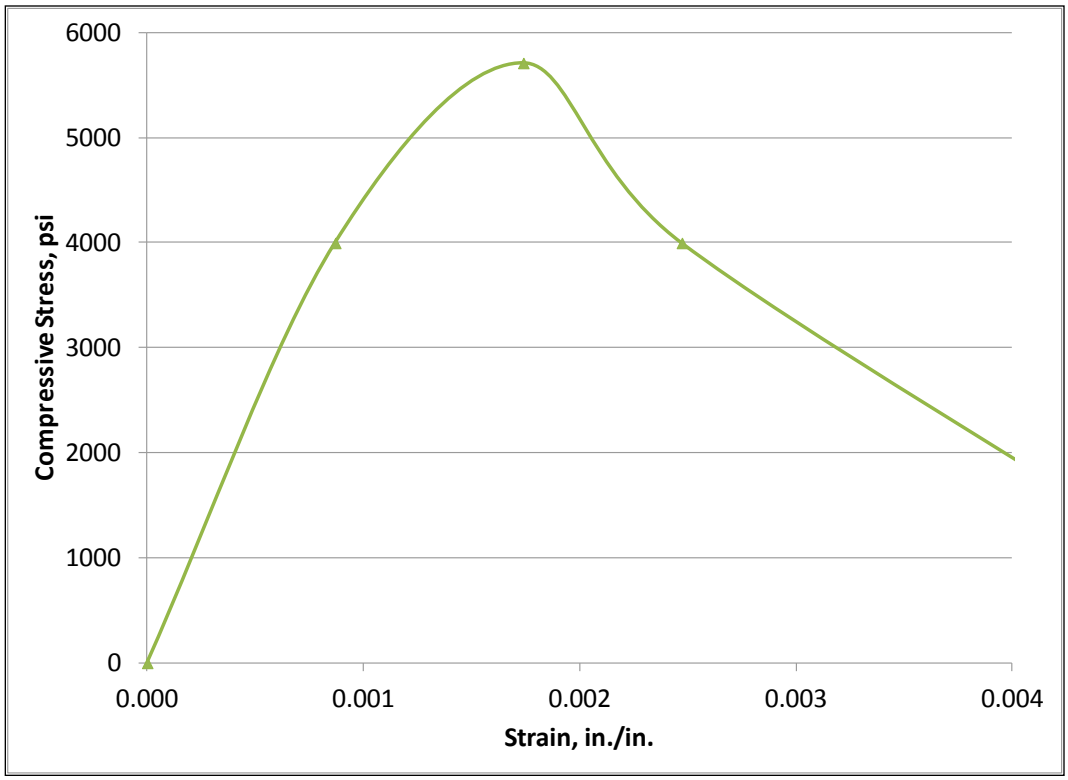

Figure E.6. Compressive stress-strain curve for dowel grout.

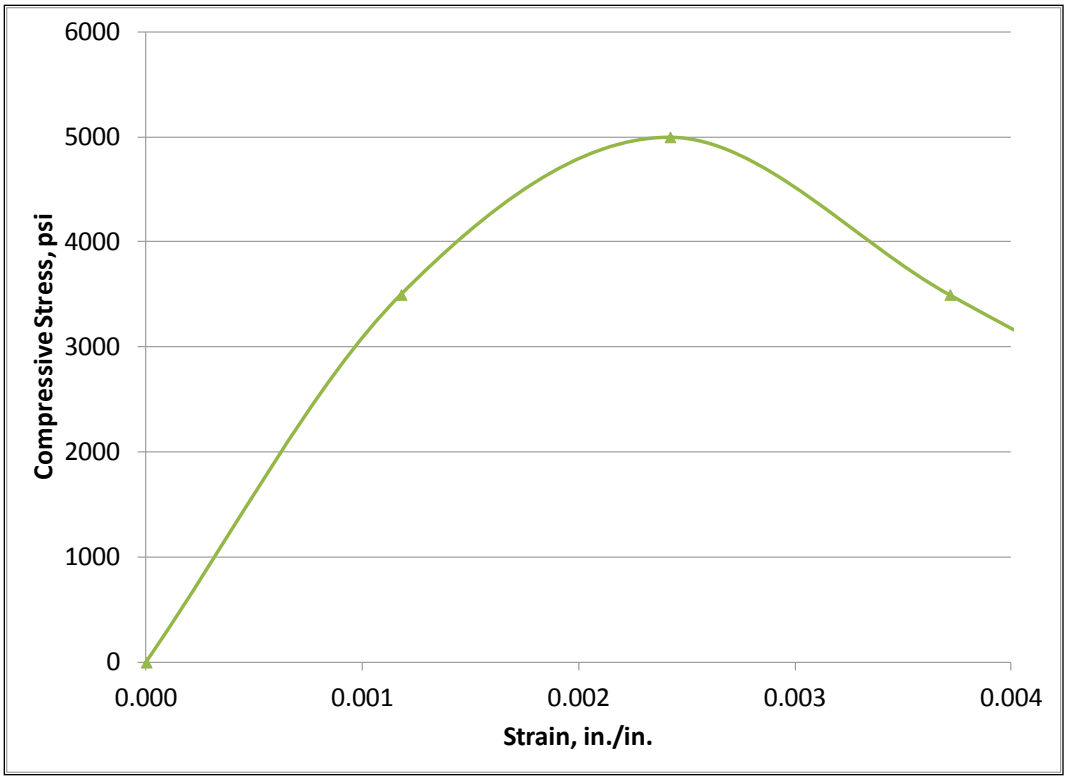

Table E.1. Input parameters for the finite element model.

Material Property	Parent Slab	Panel	Dowel Grout	Steel Dowel	Base	Flowable Fill	Subgrade
Mass Density, kg/m^3	2.32E+03	2.32E+03	1.84E+03	7.80E+03	2.00E+03	1.91E+03	1.84E+03
Young's Modulus, E, MPa	33 440	33 440	22 063	199 948	379	276	145
Poisson's Ratio, v	0.2	0.2	0.2	0.3	0.4	0.2	0.4
Ultimate Stress, σ_{cu}, MPa	49.9	39.4	34.5				
Failure Stress, σ_{t0}, MPa	4.4	3.7	3.4				
Dilation Angle, ψ	30	30	30				
Flow Potential Eccentricity, ε	0.1	0.1	0.1				
Initial Biaxial/Uniaxial Ratio, σ_{b0}/σ_{c0}	1.16	1.16	1.16				
Ratio of the Second Stress Invariant on the Tensile to Compressive Meridian, K_c	0.667	0.667	0.667				
Viscosity Parameter, μ	0	0	0				
Fracture Energy, G_F	0.67	0.67	0.67				

Note: Blanks indicate that the value was not required as input.

E.1.6 Model parts, load configurations, and results

Models were constructed as discussed in Chapter 5. This section provides additional schematics of the model parts, the loading configurations for the C-17 aircraft, and results of the modeling.

- Figures E.7 through E.10 show the various parts used to construct the model.
- Figure E.11 shows the completed model used for this study.
- Figures E.12 through E.18 show the configuration of the C-17 wheels on the model for the seven load cases.
- Figures E.19 through E.25 show the deformations caused by the seven load cases.
- Figures E.26 through E.29 show the distribution of compressive and tensile stresses under Load Case 4.
- Table E.2 presents the model-predicted maximum compressive and tensile stresses generated around the dowels for both sides of the joint.

Figure E.7. Dowel grout part.

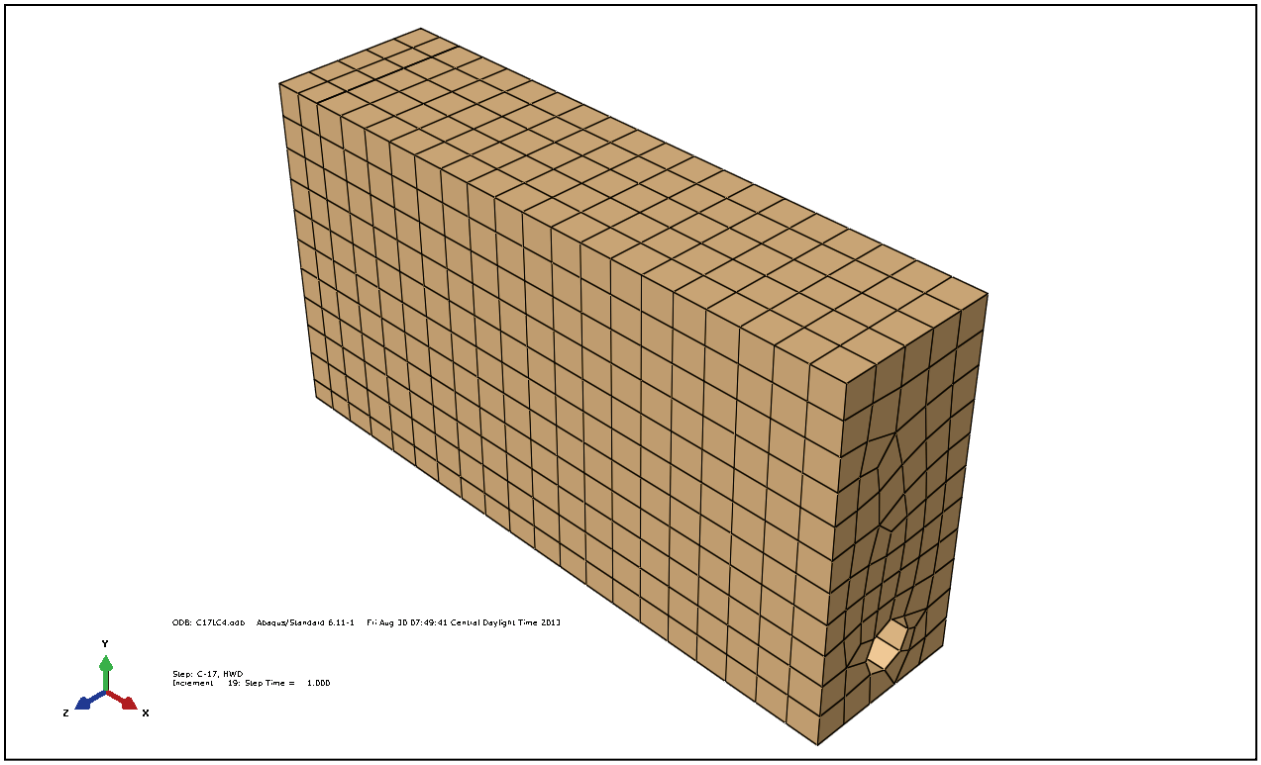

Figure E.8. Dowel part.

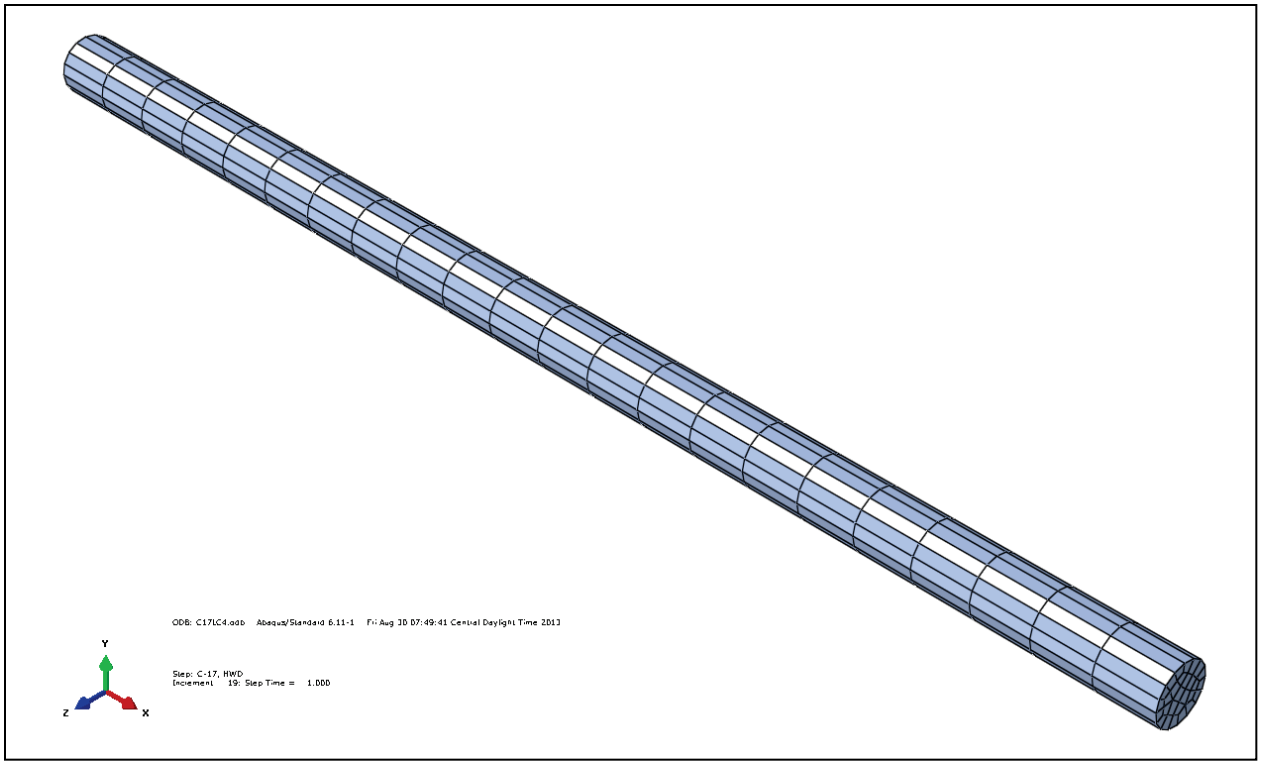

Figure E.9. Precast panel with dowels.

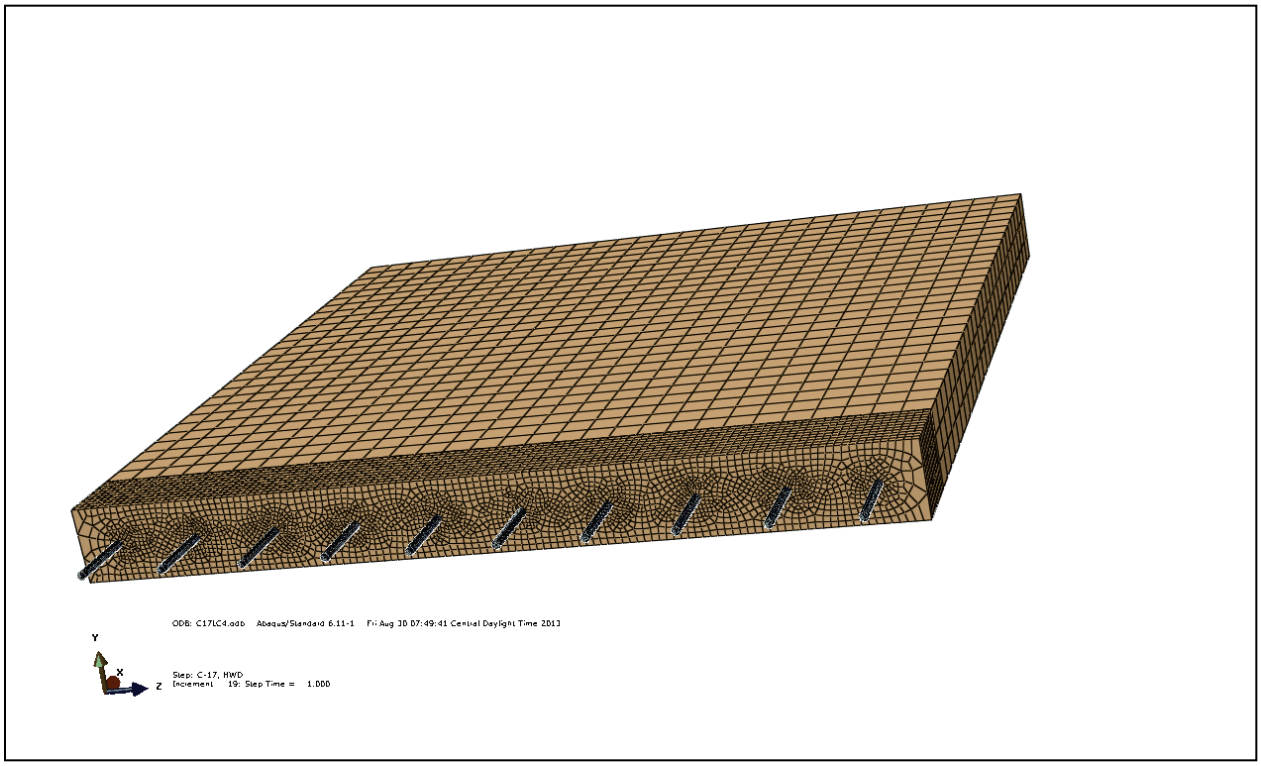

Figure E.10. Parent slab with dowel grout and dowels.

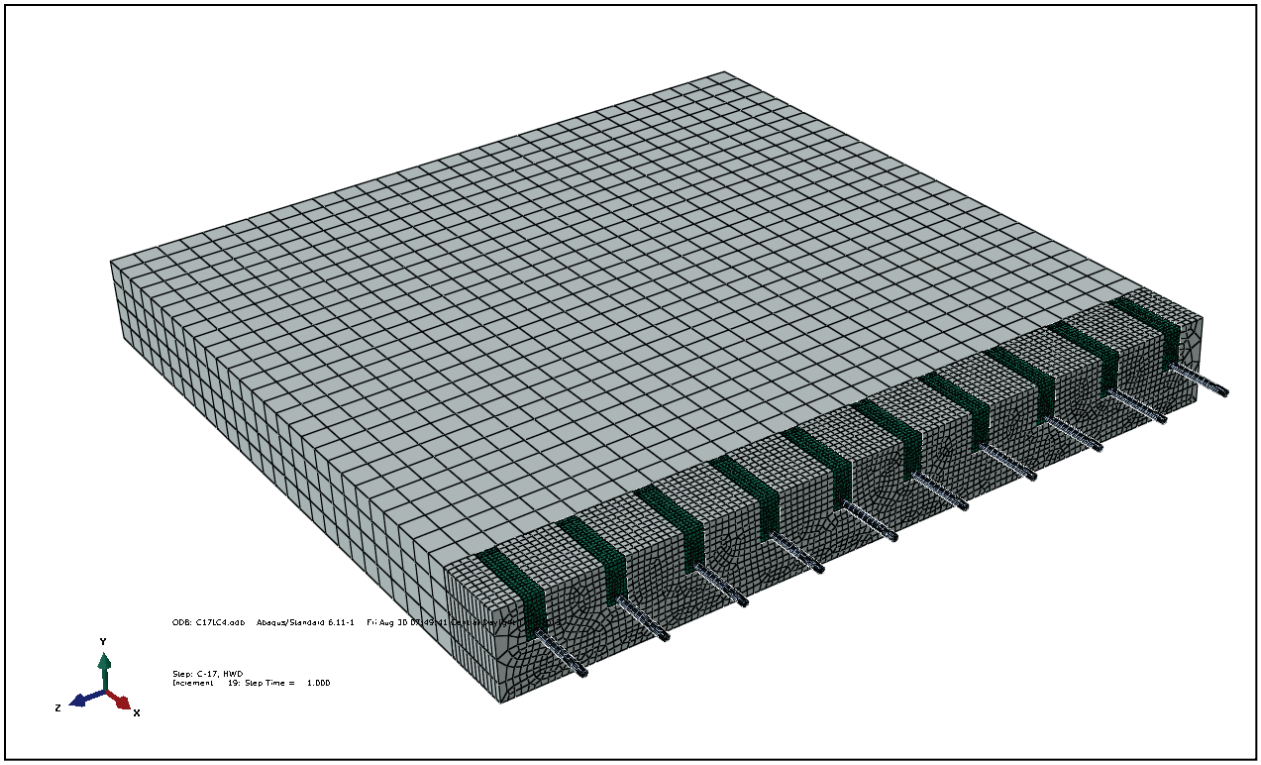

Figure E.11. Precast panel joint model.

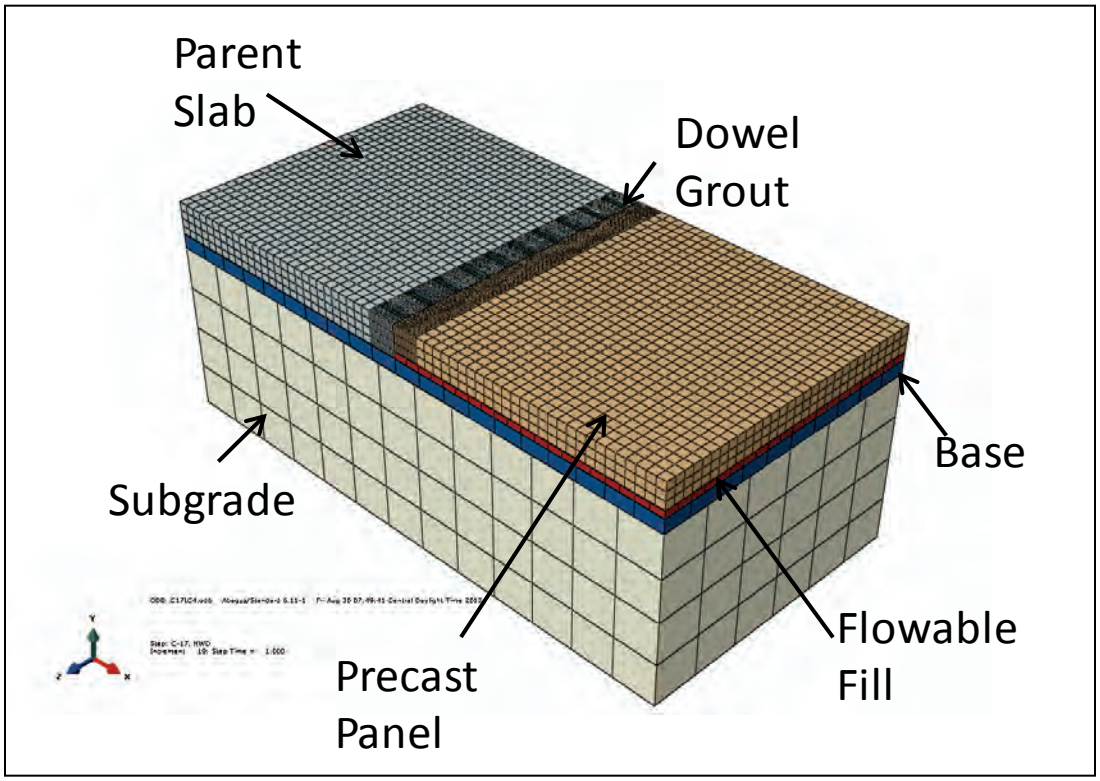

Figure E.12. Model schematic- Load Case 1.

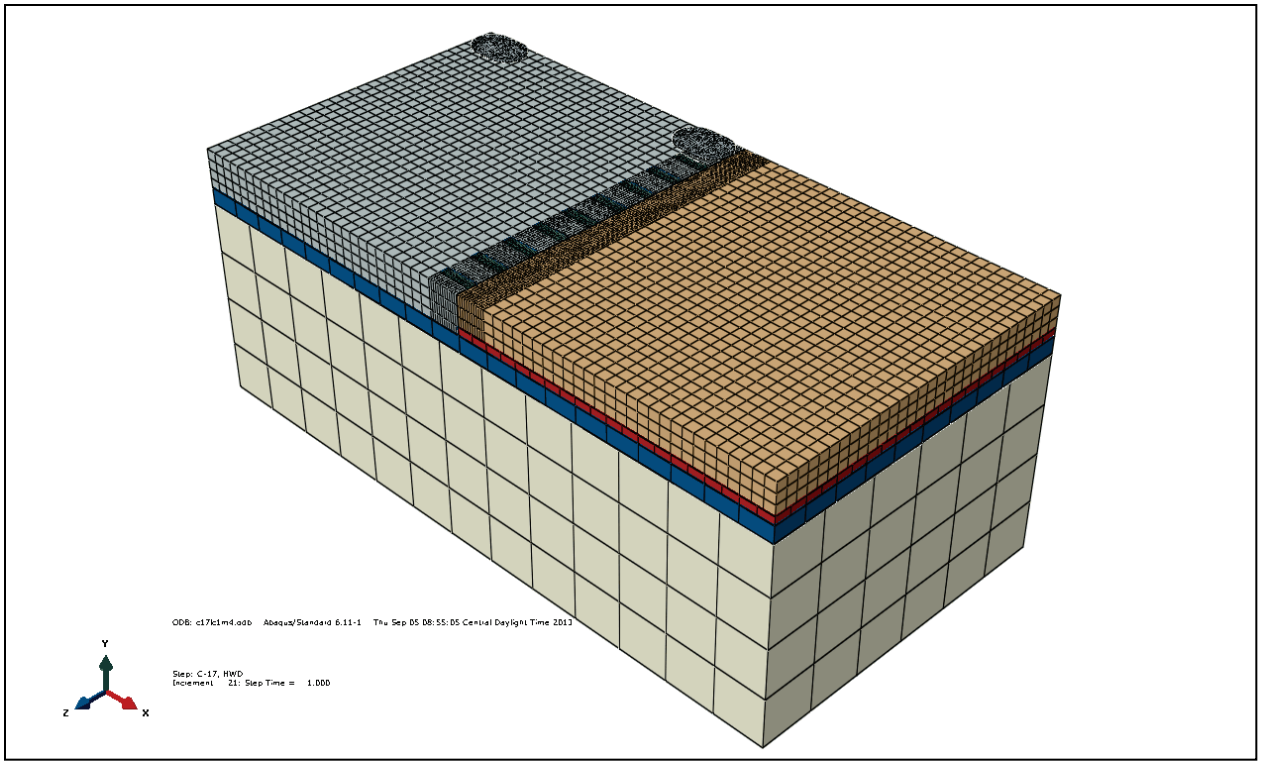

Figure E.13. Model schematic- Load Case 2.

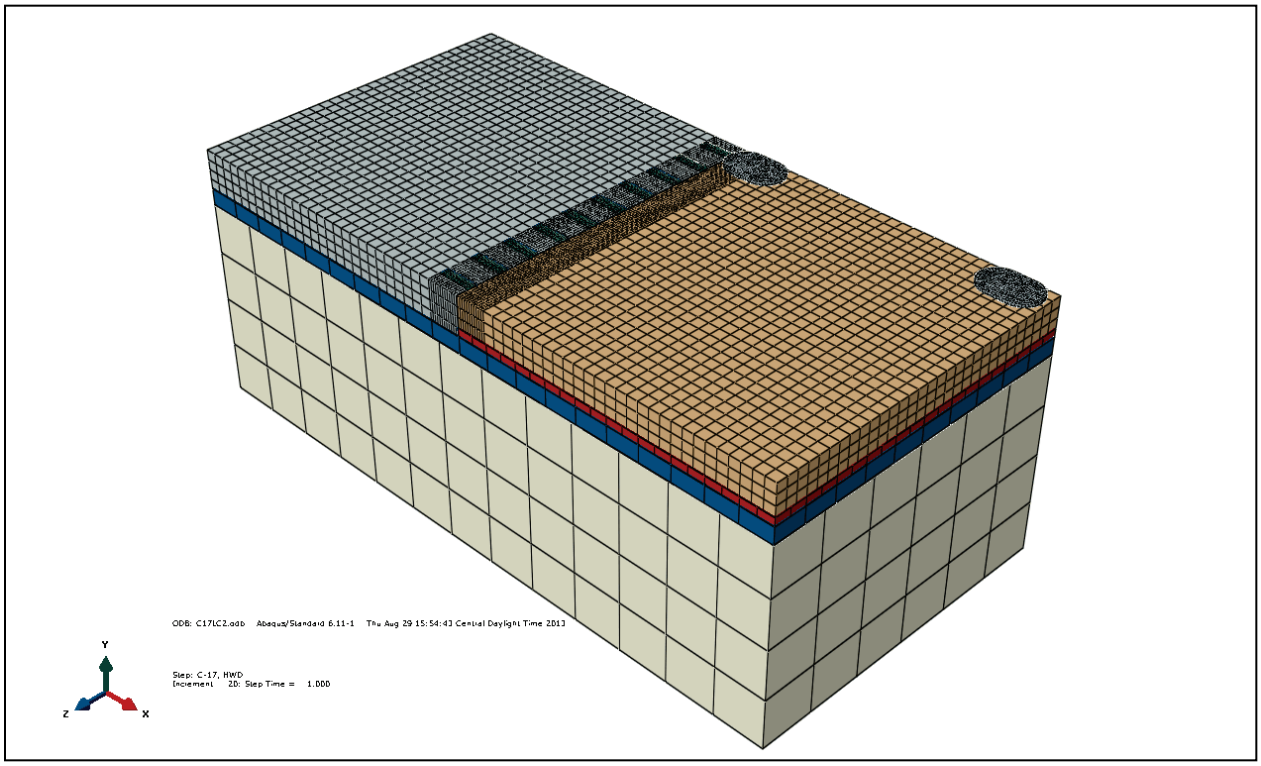

Figure E.14. Model schematic- Load Case 3.

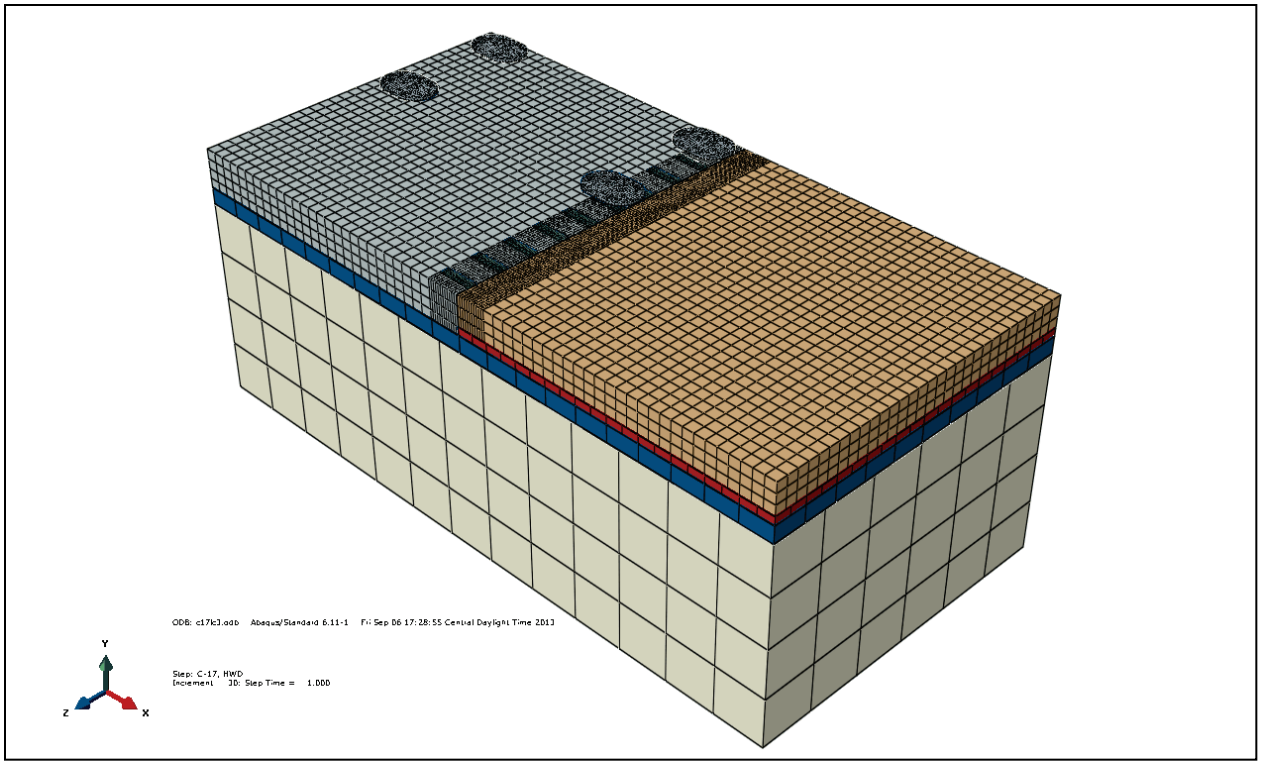

Figure E.15. Model schematic- Load Case 4.

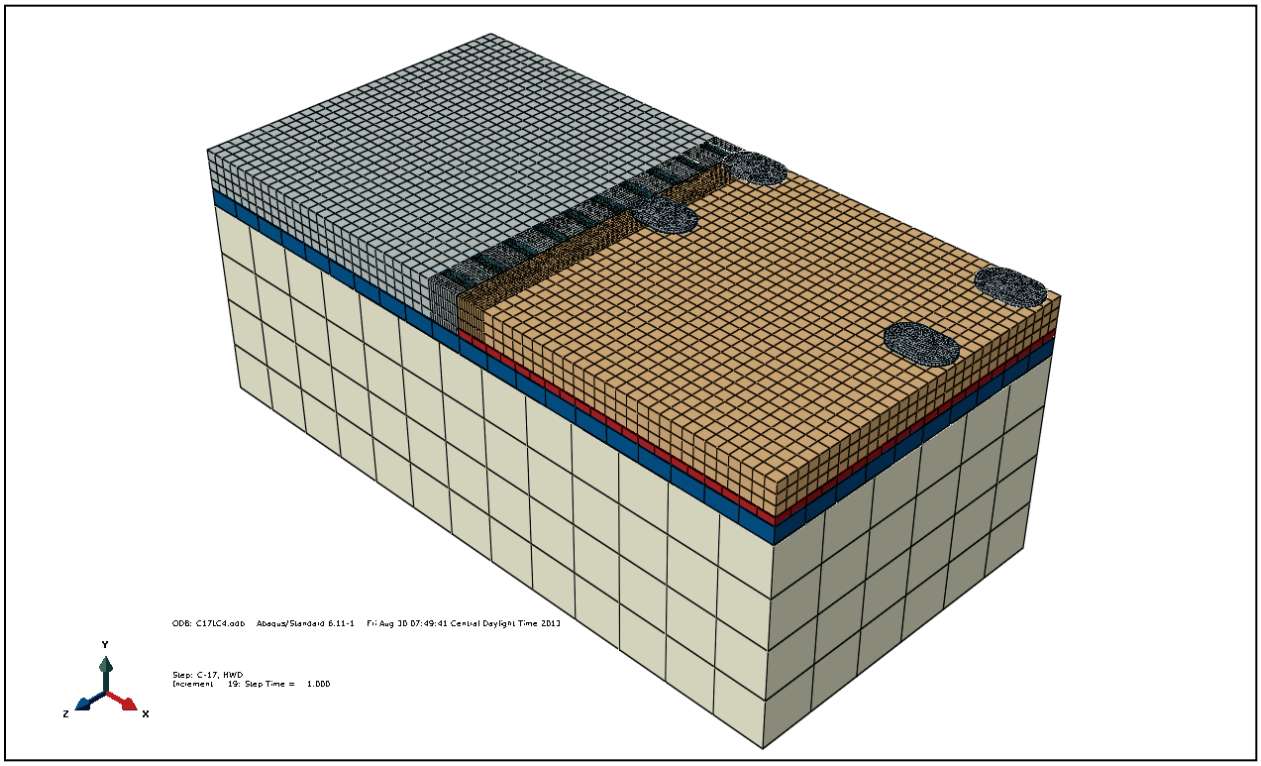

Figure E.16. Model schematic- Load Case 5.

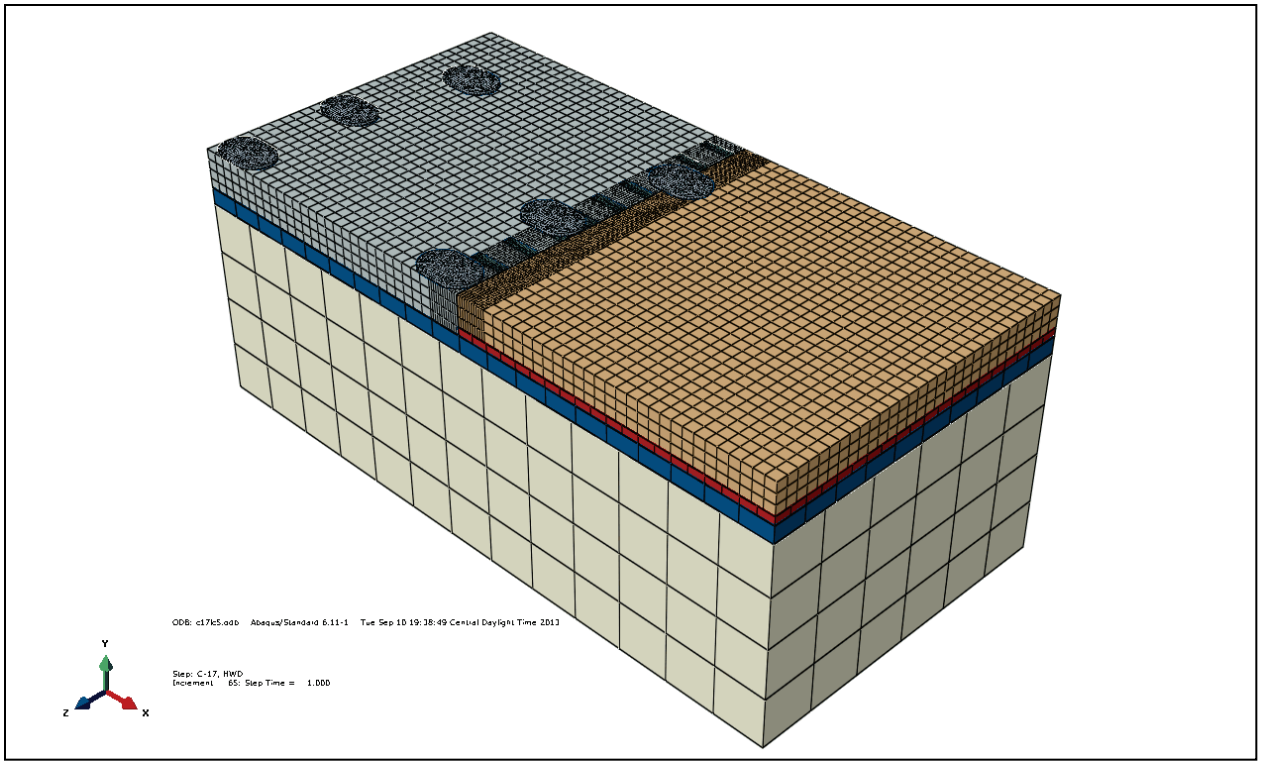

Figure E.17. Model schematic- Load Case 6.

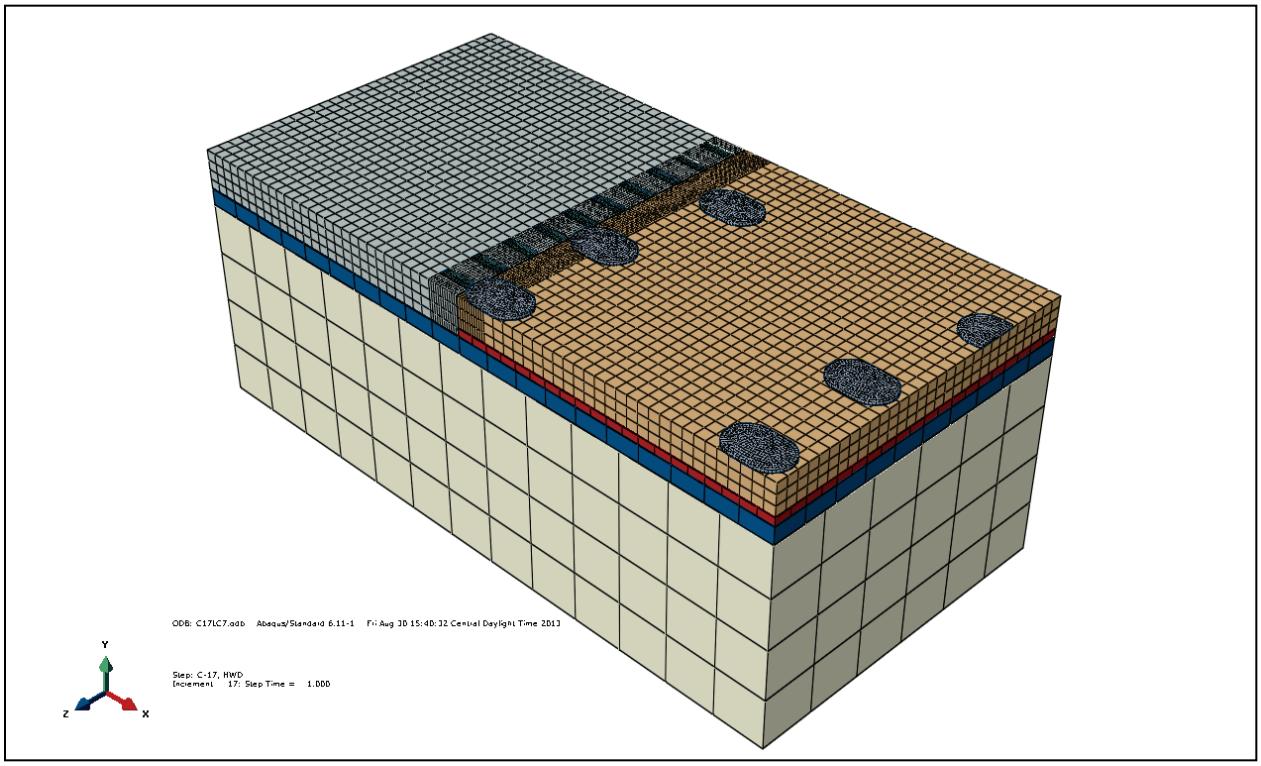

Figure E.18. Model schematic- Load Case 7.

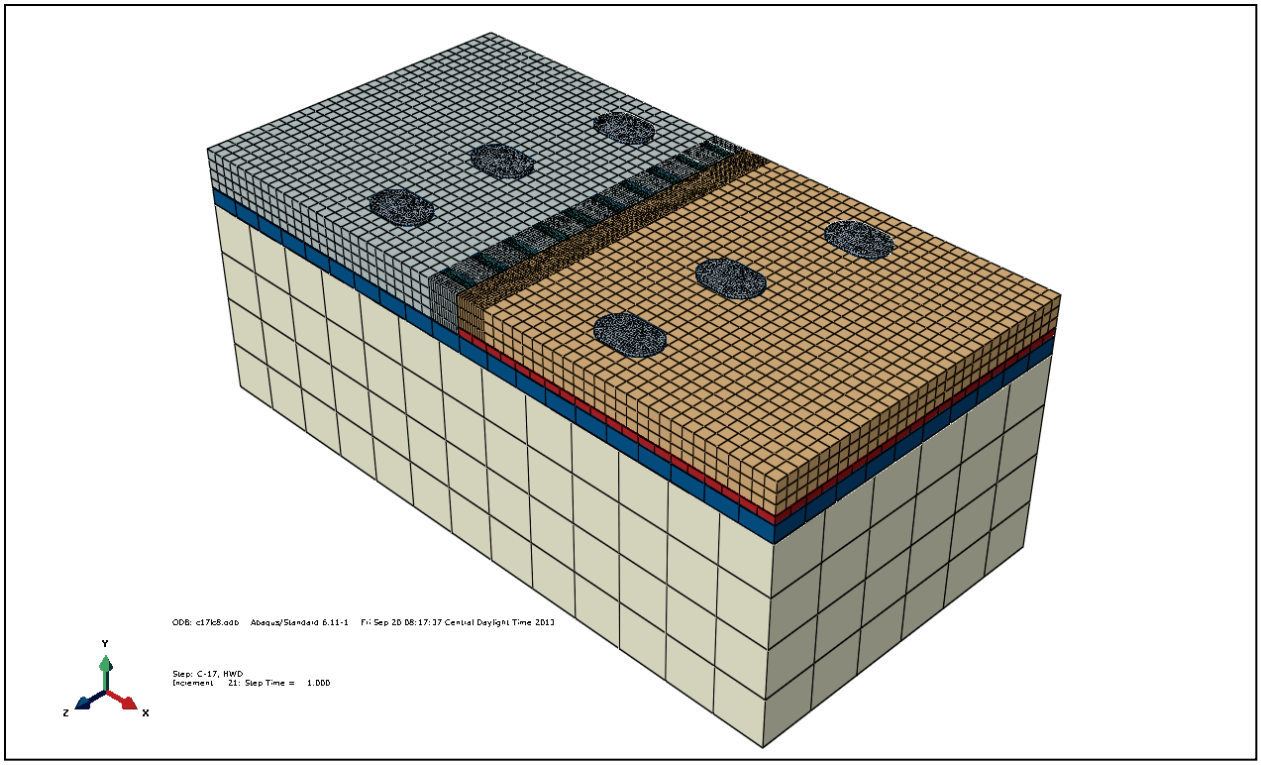

Figure E.19. Deflections - Load Case 1.

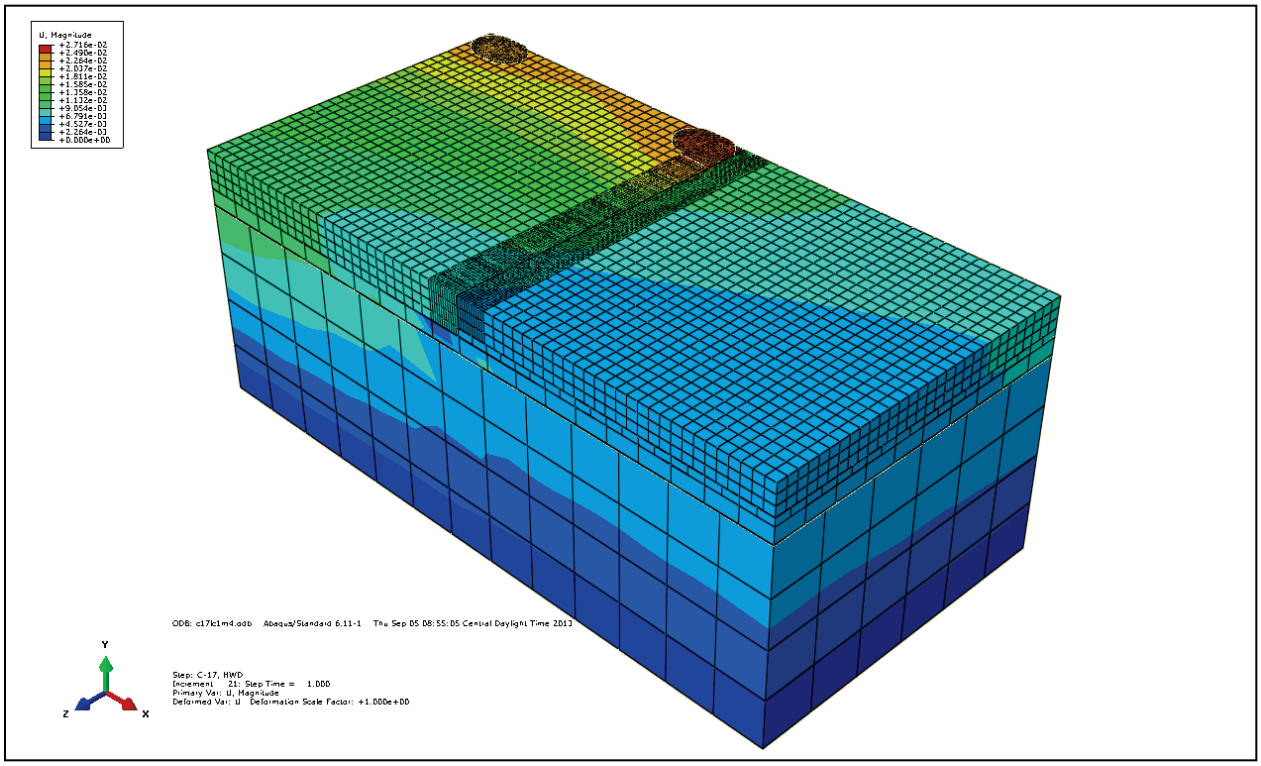

Figure E.20. Deflections - Load Case 2.

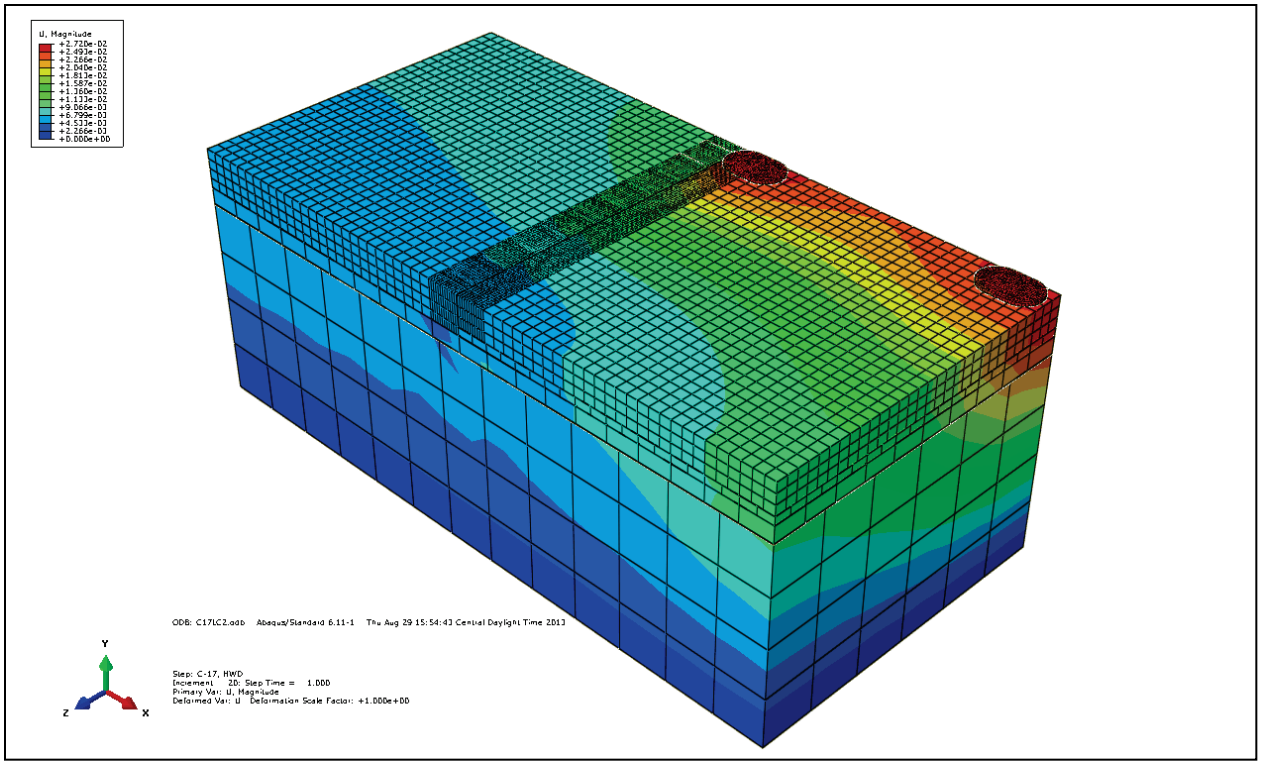

Figure E.21. Deflections - Load Case 3.

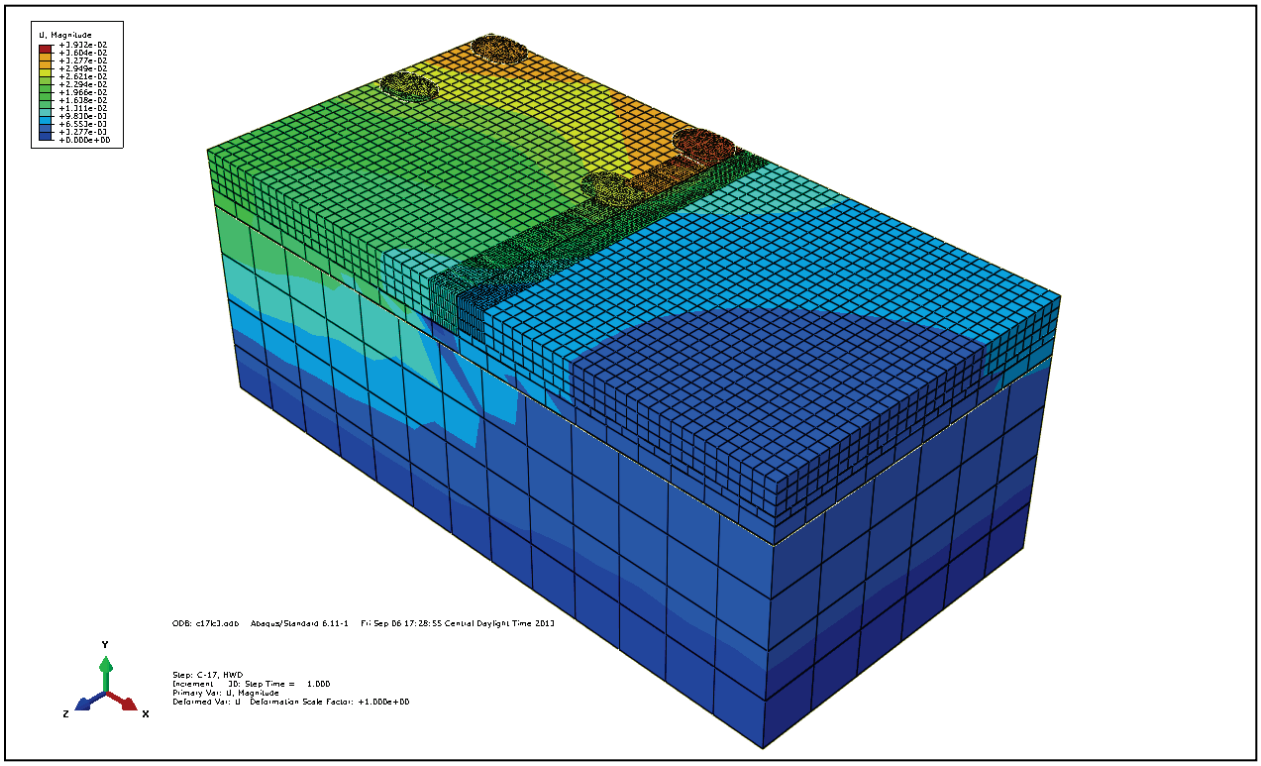

Figure E.22. Deflections - Load Case 4.

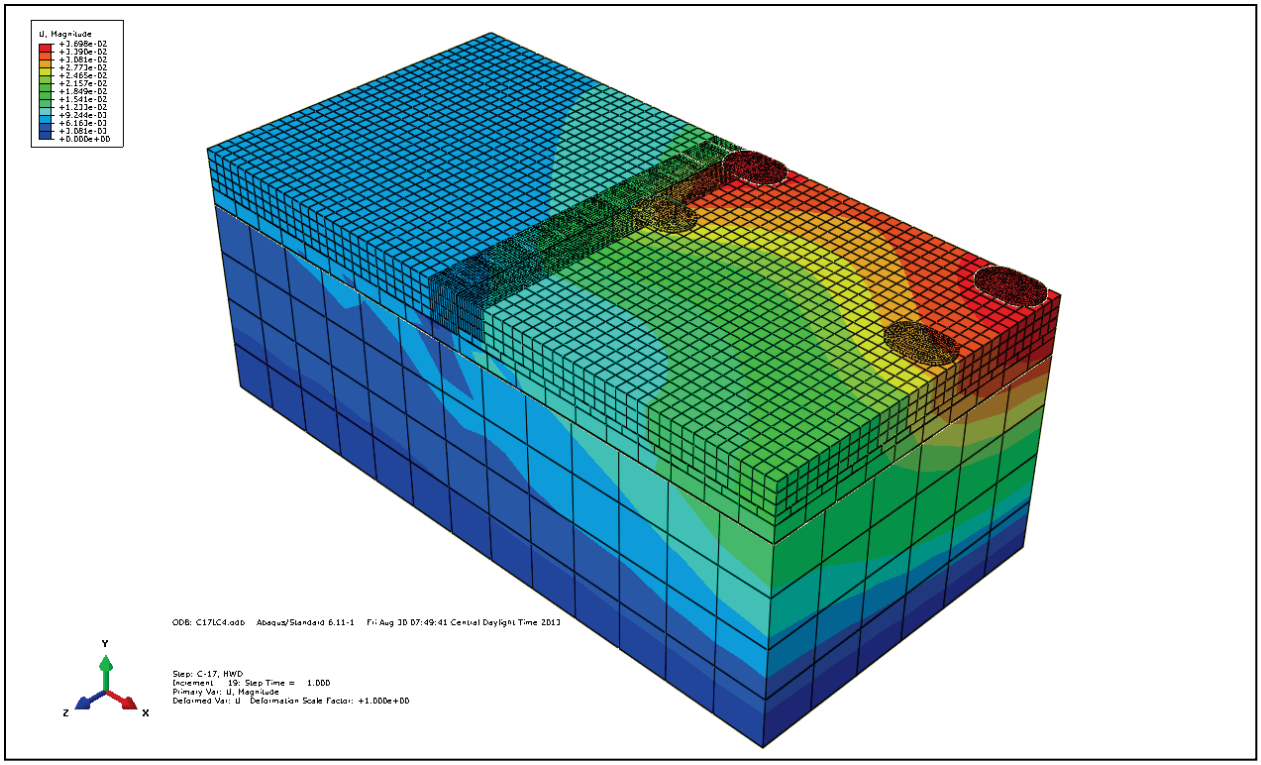

Figure E.23. Deflections - Load Case 5.

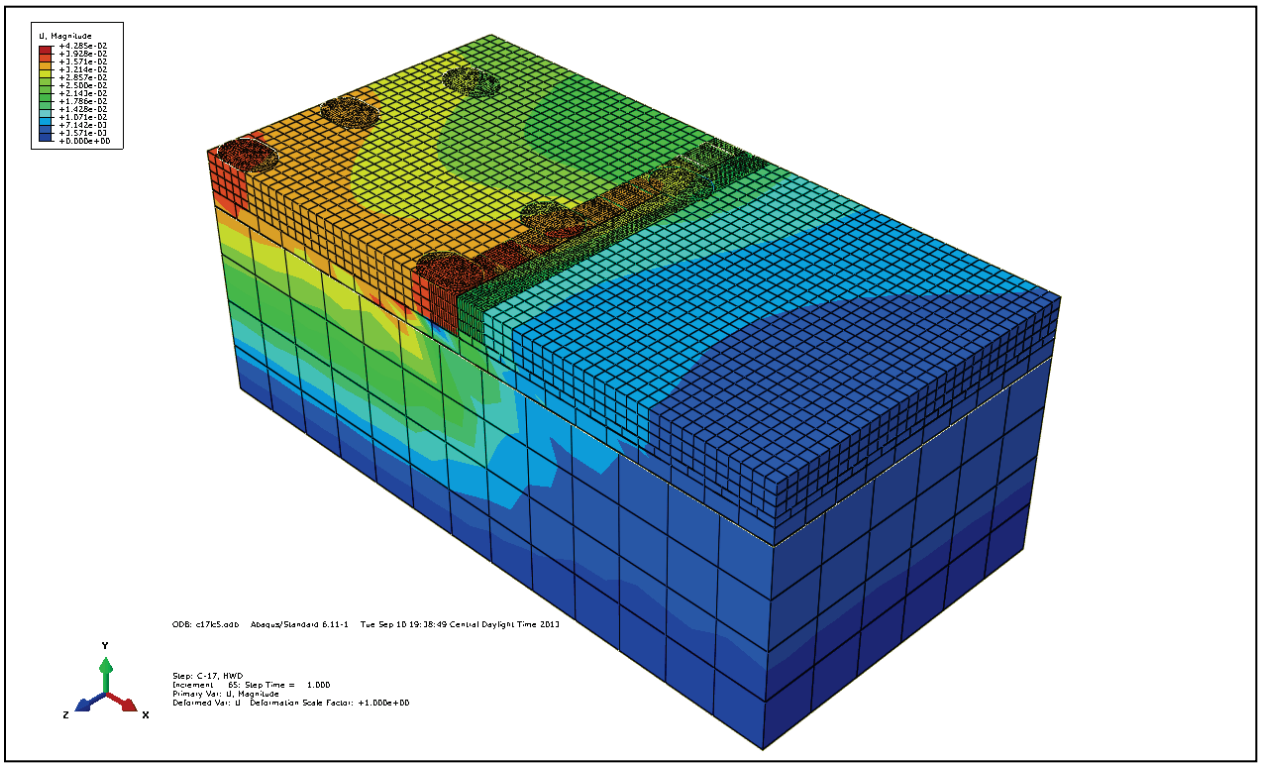

Figure E.24. Deflections - Load Case 6.

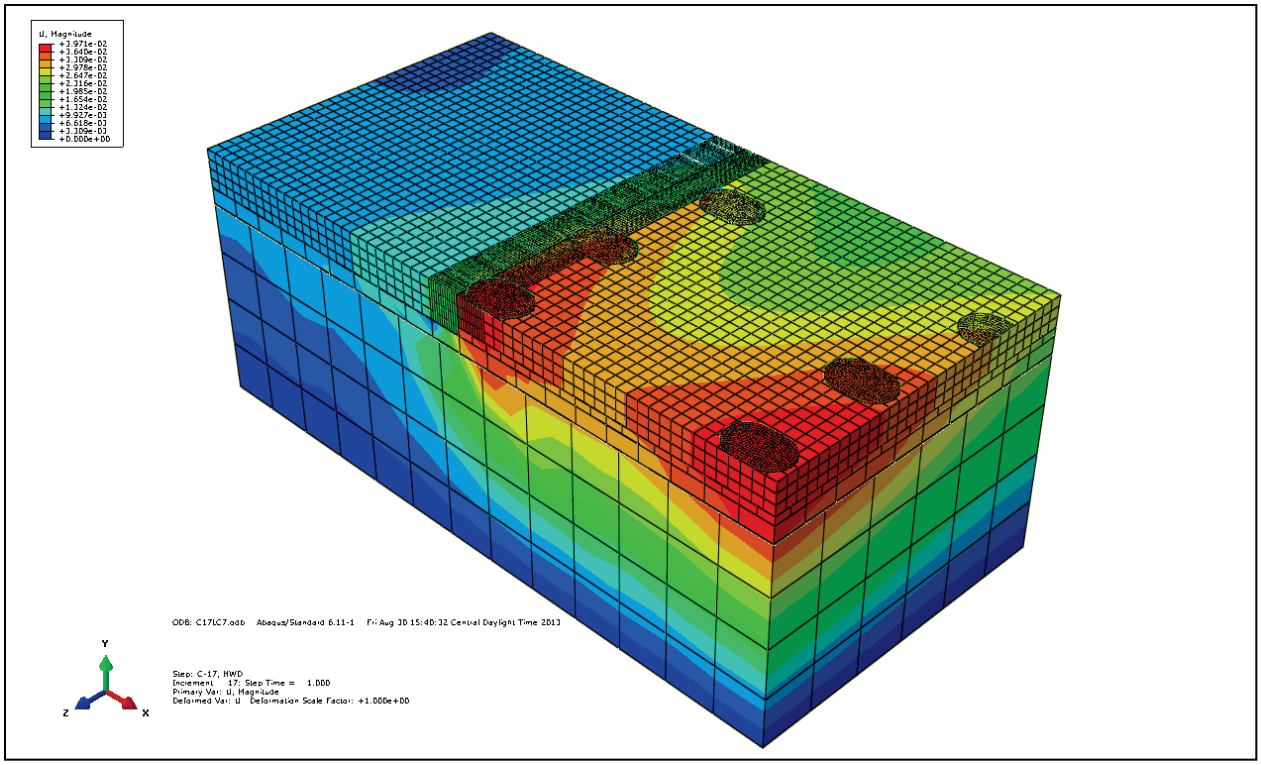

Figure E.25. Deflections - Load Case 7.

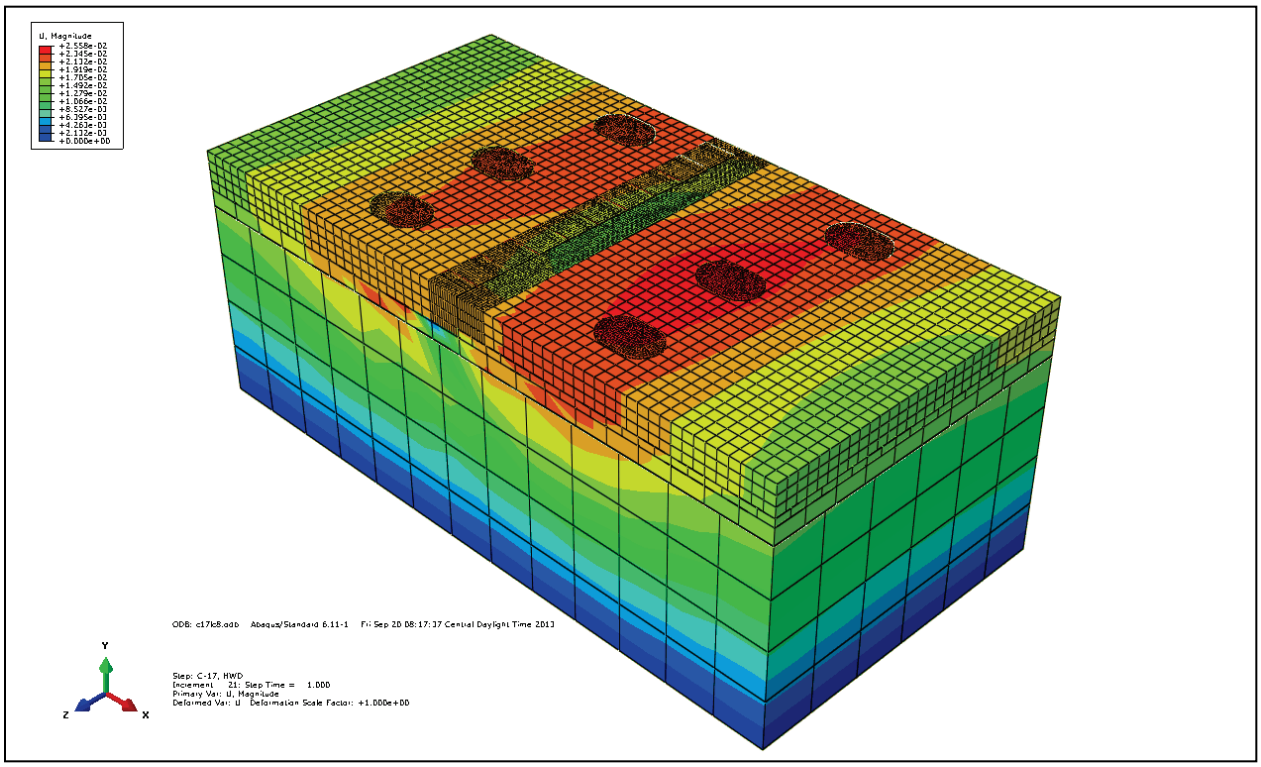

Figure E.26. Compressive stresses- Load Case 4, precast panel side of the joint.

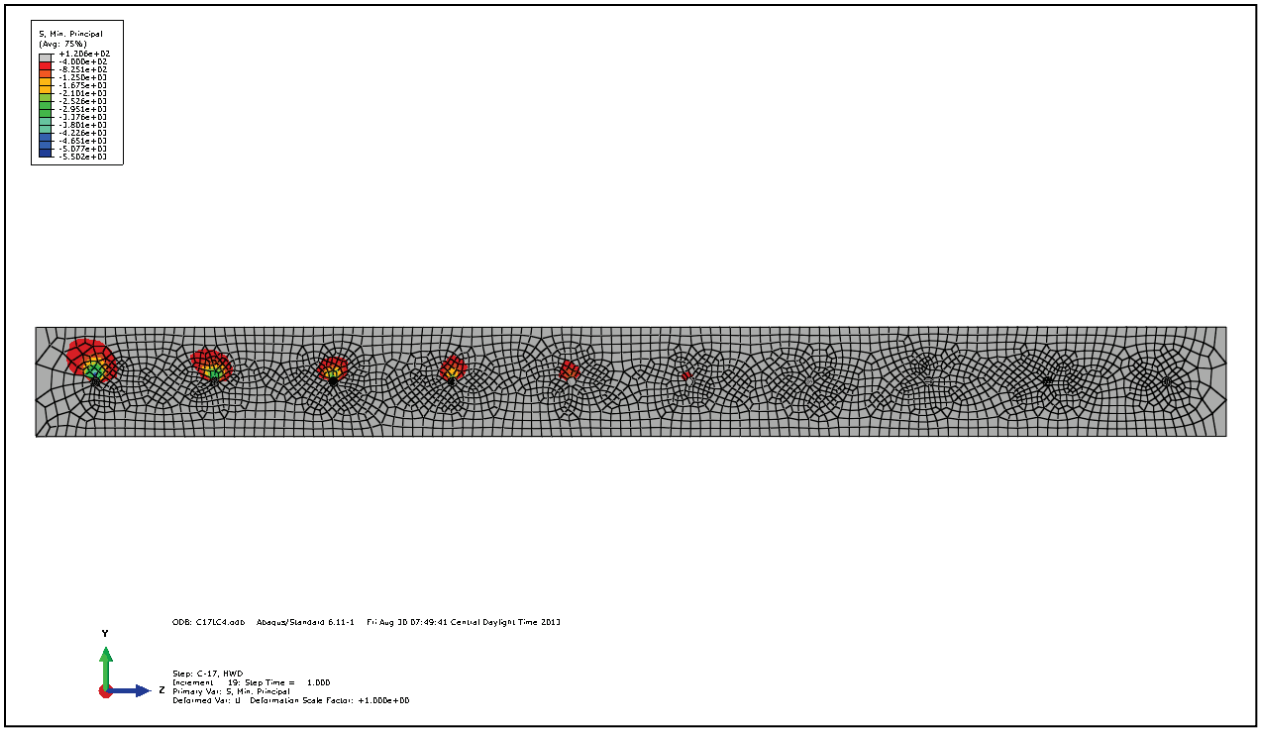

Figure E.27. Compressive stresses- Load Case 4, parent slab side of the joint.

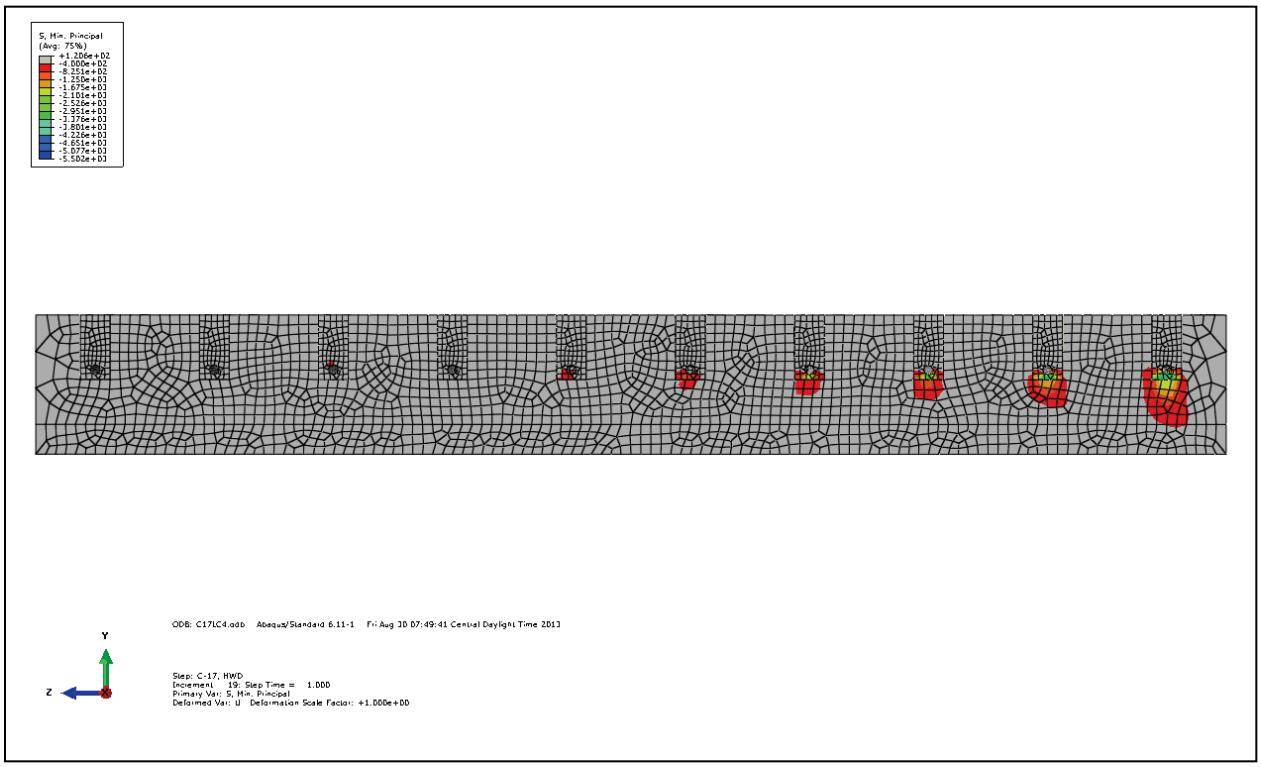

Figure E.28. Tensile stresses- Load Case 4, parent slab side of the joint.

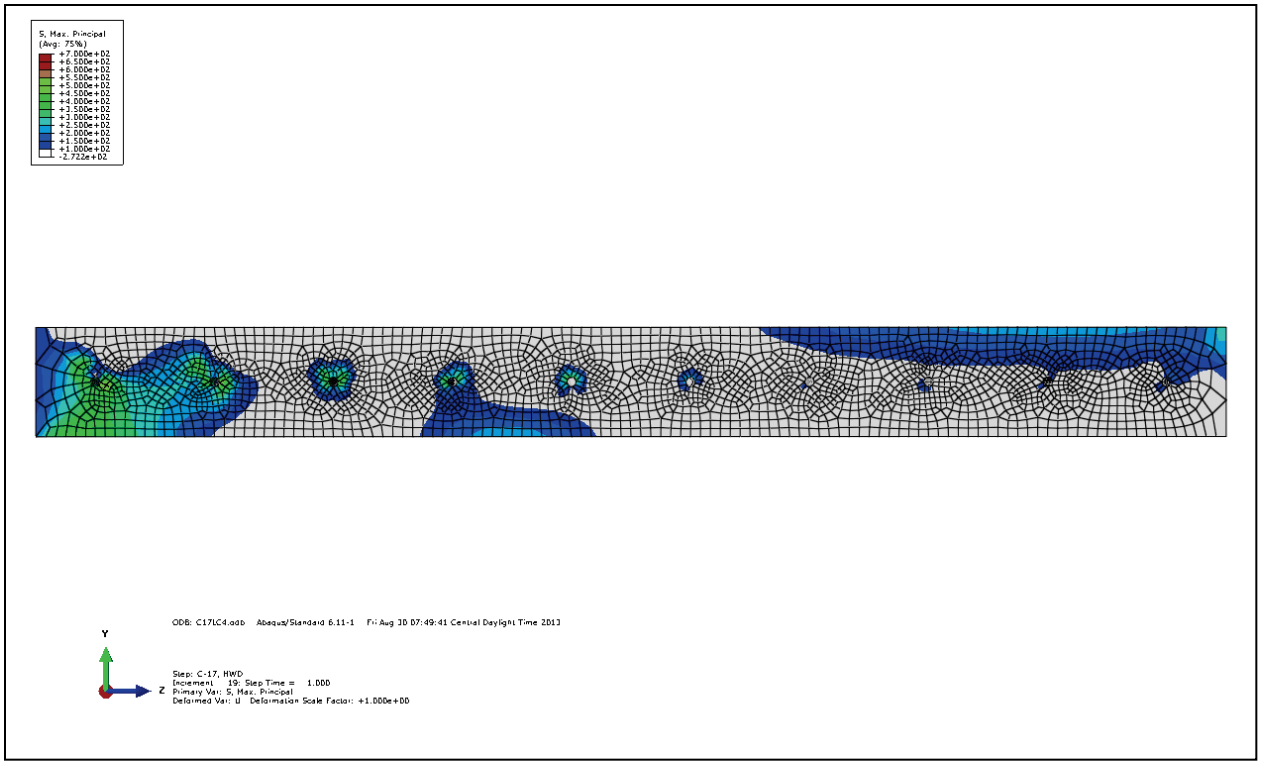

Figure E.29. Tensile stresses- Load Case 4, parent slab side of the joint.

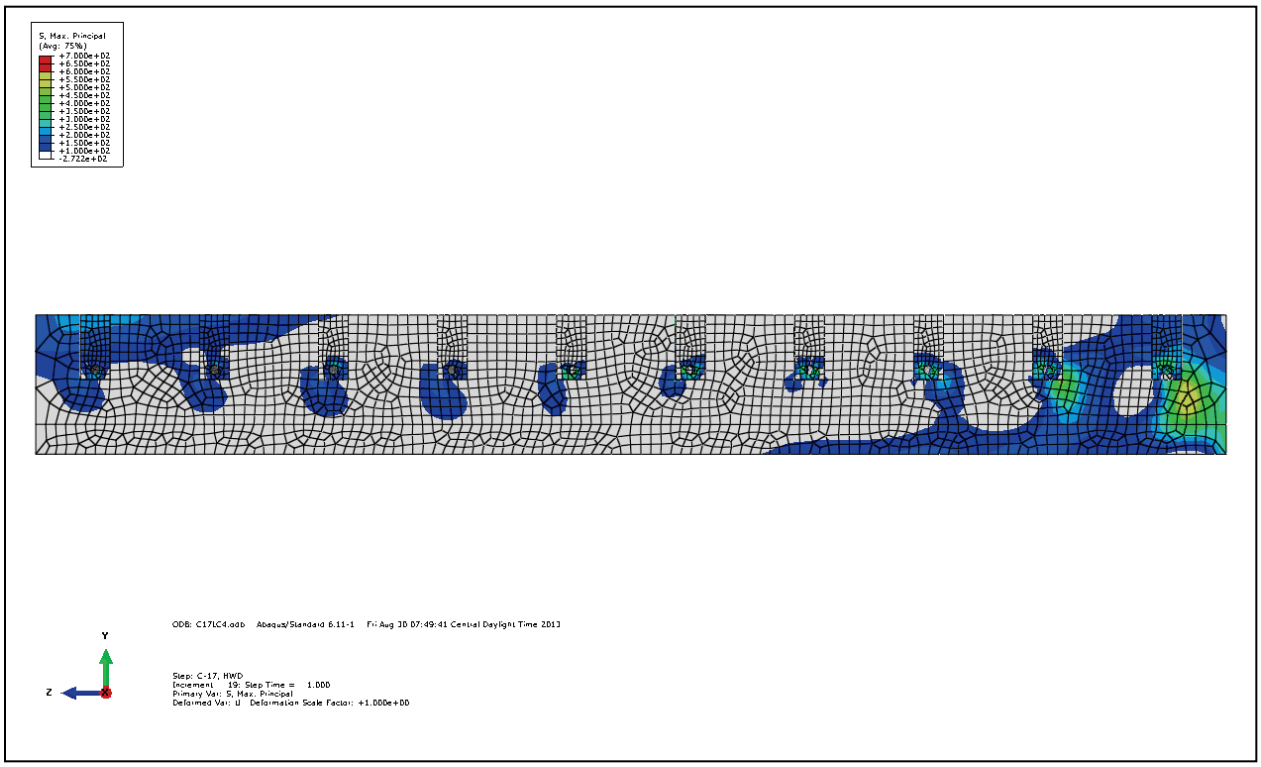

Table E.2. Model predicted maximum stresses around dowels for edge load cases.

Load Cart Position No.	Dowel No.	Panel Side of Joint		Parent Slab Side of Joint	
		Max. Compressive Stress, psi	Max. Tensile Stress, psi	Max. Compressive Stress, psi	Max. Tensile Stress, psi
1	1	4,205.53	530.25	4,877.51	379.83
	2	3,046.33	540.75	3,735.95	394.42
	3	1,966.62	506.41	2,440.34	454.52
	4	1,039.20	459.29	1,536.21	494.80
	5	510.15	252.67	842.42	377.85
	6	294.11	175.35	447.15	211.37
	7	163.23	113.27	315.47	154.33
	8	214.10	124.32	318.81	152.41
	9	295.22	161.03	448.18	199.31
	10	497.74	243.31	727.92	415.57
2	1	4,994.33	520.45	4,745.25	395.25
	2	3,492.40	537.76	3,548.83	518.03
	3	1,635.34	491.24	1,708.79	459.84
	4	348.60	154.64	341.02	317.14
	5	349.88	185.48	478.15	261.89
	6	627.80	258.90	724.28	367.06
	7	499.37	233.58	671.63	322.87
	8	425.28	166.09	516.55	254.50
	9	252.87	115.48	345.00	185.89
	10	150.41	79.73	191.45	125.39
3	1	5,345.44	498.85	5,418.64	366.92
	2	4,094.02	527.00	4,717.04	376.32
	3	3,214.21	538.59	3,894.66	398.59
	4	2,671.81	486.38	3,462.61	436.92
	5	1,996.07	529.40	2,823.90	454.20
	6	1,406.07	499.96	1,915.89	484.07
	7	791.84	419.00	1,377.60	497.62
	8	822.60	434.53	1,188.26	498.17
	9	873.05	473.77	1,414.41	491.21
	10	1,360.00	494.28	1,885.19	476.82
4	1	5,501.72	525.25	5,149.86	436.62
	2	4,285.00	526.76	4,169.28	508.41
	3	2,883.59	515.86	3,015.85	519.18
	4	2,976.26	462.78	2,328.92	520.08
	5	2,132.66	486.27	1,576.91	453.47
	6	1,624.08	293.95	659.97	482.08

Load Cart Position No.	Dowel No.	Panel Side of Joint		Parent Slab Side of Joint	
		Max. Compressive Stress, psi	Max. Tensile Stress, psi	Max. Compressive Stress, psi	Max. Tensile Stress, psi
	7	343.30	148.64	455.78	222.75
	8	458.35	197.55	570.03	344.80
	9	320.41	154.55	340.55	284.71
	10	253.16	232.36	291.40	280.54
5	1	1,340.72	523.43	1,840.92	476.24
	2	653.59	510.67	1,219.28	487.00
	3	251.69	211.87	646.81	399.06
	4	422.13	150.50	1,188.80	494.64
	5	922.08	399.80	1,993.32	472.46
	6	2,041.53	484.42	2,848.68	475.74
	7	2,047.65	417.62	3,573.74	444.53
	8	3,016.36	494.26	3,731.67	392.29
	9	3,543.34	469.64	4,395.41	377.75
	10	4,764.32	466.88	5,241.14	369.18
6	1	2,199.66	534.86	2,462.69	509.28
	2	1,256.32	507.25	1,372.87	493.13
	3	342.96	279.19	754.09	415.18
	4	233.33	183.13	696.21	360.45
	5	852.54	329.27	1,004.37	433.84
	6	1,700.28	501.96	1,842.85	455.67
	7	2,131.13	464.28	2,428.66	520.66
	8	2,803.12	534.62	2,932.29	519.90
	9	4,585.66	523.83	3,976.32	508.95
	10	5,182.97	503.04	4,753.89	493.31

E.2 Calculation of stresses in dowel bars

As mentioned in Chapter 5, stress in dowel bars and bearing stresses in the concrete surrounding the dowel bars were computed using mathematical analyses of dowel design using equations presented by Bradbury (1938) and Friberg (1940) based on principles presented by Timoshenko and Lessels (1925). These calculations were conducted for each joint load case presented in Chapter 5 to validate the FEM. The calculations were conducted using the equations and concepts presented in this section.

When examining a PCC joint, if a load is applied to one side of a doweled joint, the dowel portion in that side deflects downward and exerts pressure

on the concrete beneath it. On the opposite side of the joint, the dowel bar will exert pressure from the top of the dowel on the concrete above it. At some distance, the dowel will exert pressure again from the bottom of the dowel bar (see Figure E.30). According to Timoshenko and Lessels (1925), the deflection of the dowel bar loaded on one end results in a wave curve with decreasing deflection with increasing distance from the load.

Figure E.30. Timoshenko and Lessels (1925) and Friberg (1940) analysis of dowel bar support.

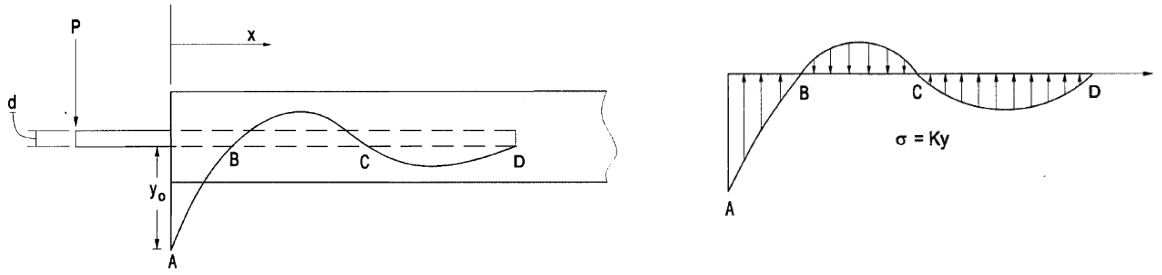

(a) Deflection diagram (b) Stress diagram

The deflection (y) of the bar resulting from the load (P_t) on the dowel is calculated using the equation

$$y = \frac{e^{-\beta x}}{2\beta^2 EI}[P_t \cos\beta x - \beta M_0(\cos\beta x - \sin\beta x)] \quad \text{(E.10)}$$

where:

x = the distance along the dowel from the face of the concrete
M_0 = bending moment on the dowel at the face of the concrete
P_t = the transferred load or transferred shear force by the dowel (assumed to be 0.45 to 0.5 of the total applied load or design load because a portion of the load is transferred)
β = is the relative stiffness of the dowel bar embedded in the concrete calculated as

$$\beta = \left(\frac{Kd}{4E_d I_d}\right)^{0.25} \quad \text{(E.11)}$$

where:

K = modulus of dowel support
d = diameter of the dowel
E_d = modulus of elasticity of the dowel
I_d = moment of inertia of the dowel

Friberg (1940) expanded the formula presented by Timoshenko and Lessels (1925) to determine the bending moment and shear in the dowel using the following equations:

$$-EI\frac{d^2y}{dx^2} = M = -\frac{e^{-\beta x}}{\beta}\left[P_t \sin\beta x - \beta M_0(\sin\beta x + \cos\beta x)\right] \quad \text{(E.12)}$$

$$\frac{dM}{dx} = V = -e^{-\beta x}\left[(2\beta M_0 - P_t)\sin\beta x + P_t \cos\beta x\right]. \quad \text{(E.13)}$$

Setting the joint width equal to z, the moment at the dowel-concrete interface is calculated using the equation

$$M_0 = \frac{P_t z}{2} \ . \quad \text{(E.14)}$$

To calculate the deflection at the face of the joint (x=0) where the maximum deflection will occur, and using the previous equation for moment at the concrete dowel interface, the deflection of the dowel at the joint face can be calculated using the following equation:

$$y_0 = \frac{P_t(2+\beta z)}{4\beta^3 EI} \ . \quad \text{(E.15)}$$

The bearing pressure or stress on the concrete at the concrete joint face is calculated using the equation

$$\sigma = Ky_0 = \frac{KP_t}{4\beta^3 EI}(2+\beta z) \ . \quad \text{(E.16)}$$

Friberg (1940) found that the maximum negative moment for interior and edge loadings occurs at a distance of 1.8l from the load, where l is the

radius of relative stiffness calculated using the equation (Westergaard 1925)

$$l = \left[\frac{Eh^3}{12\left(1 - \nu^2\right)k} \right]^{0.25} \tag{E.17}$$

where:

ν = the Poisson's ratio for the slab,
h = the thickness of the slab,
E = modulus of elasticity of the PCC, and
k = the modulus of subgrade reaction.

The maximum moment occurs when the shear force is equal to zero. The shear in each dowel decreases inversely with the distance of the dowel from the point of loading where the maximum shear would occur under the load (critical dowel) or closest to the point of loading and decrease to zero at a distance of 1.8l. Also, the location of maximum shear would result in the maximum bearing stress in the concrete at the critical dowel. The dowels within this distance that carry a portion of the load are considered the effective dowels (N_{eff}). The shear force (P_c) that is applied to the critical dowel is calculated by dividing the shear load by the number of effective dowels or

$$P_c = P_t \; / \; N_{eff} \tag{E.18}$$

The modulus of dowel support (K) is the reaction per unit area causing a deflection equal to one. K is generally assumed to be between 200,000 and 1,500,000 psi; however, there is a general lack of experimental or theoretical procedures in the literature to determine the value of K. A value of 250,000 psi was used for this investigation.

The following example shows the calculation of the dowel shear loads and bearing stresses for Load Case 1:

Assumptions:

Wheel load 44,930 lb (single C-17 wheel placed on the parent slab side of joint)

Transferred load, P_t	44,930/2 = 22,465 lb assuming 100% LTE for the dowel
Dowel Spacing	12 in.
Dowel diameter, d	1.0 in.
Slab thickness, h	14 in.
k	276 psi/in. (measured in field testing)
E_{pcc}	4,850,000 psi (PCC)
E_d	29,000,000 psi (steel dowel)
ν	0.2
K	250,000 psi
I_d	0.05 in.^{4} for a round 1.0-in. dowel using $I = \frac{1}{64}\pi d^4$
β	$\beta = \left(\frac{Kd}{4E_d I_d}\right)^{0.25} = \left(\frac{250{,}000 * 1.0}{4 * 29e6 * 0.05}\right)^{0.25} = 0.457$
z	Joint width of 0.375 in.

Assuming shear goes to zero at 1.8l, the effective number of dowels may be calculated. First,

$$1.8l = 1.8\left[\frac{Eh^3}{12\left(1-\nu^2\right)k}\right]^{0.25} = 1.8\left[\frac{4.85e6 * 14^3}{12\left(1-0.2^2\right)276}\right]^{0.25} = 1.8 * 45.23 = 81.4 \text{ in.} \quad \text{(E.19)}$$

The calculation of effective dowels (N_{eff}) using similar triangles and the effective load-carrying distance for the dowels is shown in Figure E.31.

Figure E.31. Sample calculation of individual shear load proportions for dowels.

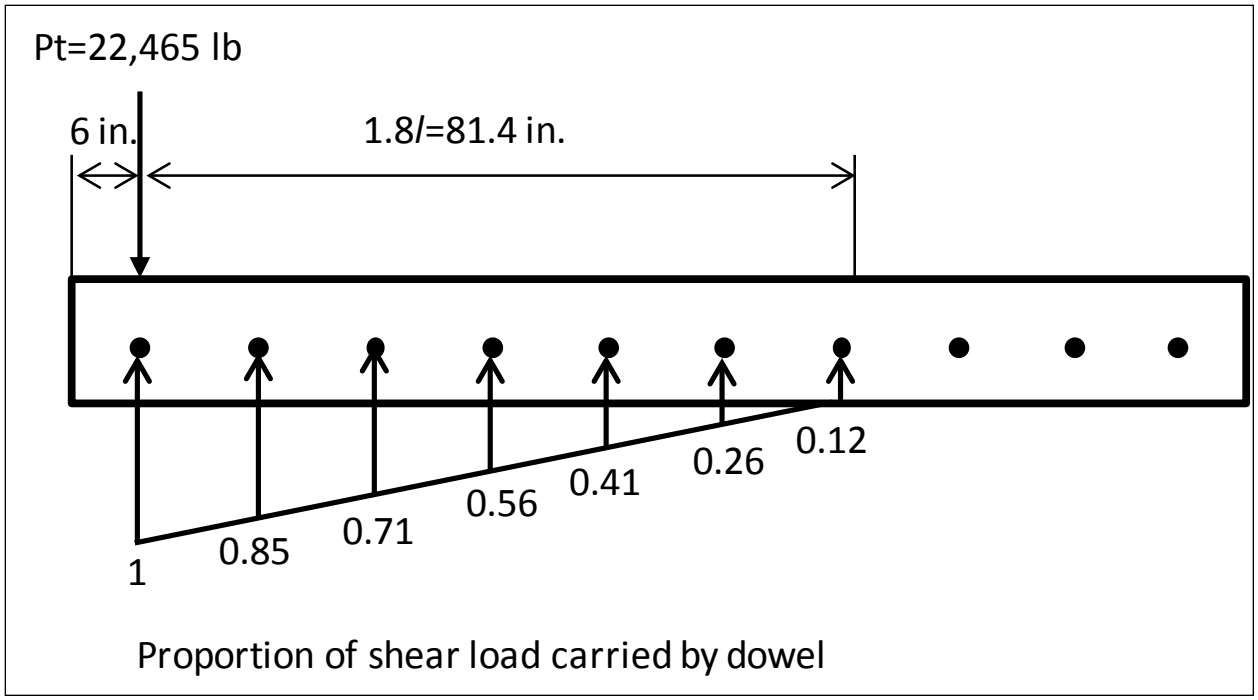

Dowel directly under load:	(81.4-0)/81.4 =	1.0 effective dowels
Dowel 12 in. from load:	(81.4 in.-12 in.)/81.4 in. =	0.85 effective dowels
Dowel 24 in. from load:	(81.4 in.-24 in.)/81.4 in. =	0.71 effective dowels
Dowel 36 in. from load:	(81.4 in.-36 in.)/81.4 in. =	0.56 effective dowels
Dowel 48 in. from load:	(81.4 in.-48 in.)/81.4 in. =	0.41 effective dowels
Dowel 60 in. from load:	(81.4 in.-60 in.)/81.4 in. =	0.26 effective dowels
Dowel 72 in. from load:	(81.4 in.-72 in.)/81.4 in. =	0.11 effective dowels
Sum of effective dowels, N_{eff} dowels		3.9 total effective dowels

The shear force (P_c) that is applied to the critical dowel is then calculated by dividing the shear load by the number of effective dowels or

$$P_c = P_t \ / \ N_{eff} \qquad \text{(E.20)}$$

Shear force in critical dowel (Pt): 22,465 lb/3.9 = 5,760 lb

The remaining dowels carry a portion of this shear force by the proportions calculated previously:

Shear force in dowel 12 in. from load: 0.85*5760 = 4,911 lb

Shear force in dowel 24 in. from load: 0.71*5760 = 4,062 lb

Shear force in dowel 36 in. from load: 0.56*5760 = 3,213 lb

Shear force in dowel 48 in. from load: 0.41*5760 = 2,364 lb

Shear force in dowel 60 in. from load: 0.26*5760 = 1,515 lb

Shear force in dowel 72 in. from load: 0.11*5760 = 273 lb

Remaining dowels are assumed to carry no load.

Calculating the bearing stress on the critical dowel (dowel directly under load):

$$\sigma = Ky_0 = \frac{KP_t}{4\beta^3 EI}(2+\beta z) = \frac{250{,}000 * 5760}{4 * 0.457^3 * 29e6 * 0.05}(2 + 0.05 * 0.375) = 5251\,\text{psi} \quad \text{(E.21)}$$

Similar calculations may be conducted for the remaining dowels using the shear loads carried by each dowel. This process was used to calculate the bearing stresses for the critical dowels for each edge load case so that comparisons to the FEM-estimated values presented in Chapter 5 could be made.

REPORT DOCUMENTATION PAGE

Form Approved
OMB No. 0704-0188

1. REPORT DATE *(DD-MM-YYYY)*	2. REPORT TYPE	3. DATES COVERED *(From - To)*
May 2015	Final	

4. TITLE AND SUBTITLE

Evaluation of Precast Portland Cement Concrete Panels for Airfield Pavement Repairs

5a. CONTRACT NUMBER

5b. GRANT NUMBER

5c. PROGRAM ELEMENT NUMBER

6. AUTHOR(S)

Lucy P. Priddy

5d. PROJECT NUMBER

5e. TASK NUMBER

5f. WORK UNIT NUMBER

7. PERFORMING ORGANIZATION NAME(S) AND ADDRESS(ES)

Geotechnical and Structures Laboratory
US Army Engineer Research and Development Center
3909 Halls Ferry Road
Vicksburg, MS 39180-6199

8. PERFORMING ORGANIZATION REPORT NUMBER

ERDC/GSL TR-15-10

9. SPONSORING / MONITORING AGENCY NAME(S) AND ADDRESS(ES)

Headquarters, Air Force Civil Engineer Center
Tyndall Air Force Base, FL 32403-5319

10. SPONSOR/MONITOR'S ACRONYM(S)

HQ-AFCEC

11. SPONSOR/MONITOR'S REPORT NUMBER(S)

12. DISTRIBUTION / AVAILABILITY STATEMENT

Approved for public release; distribution is unlimited.

13. SUPPLEMENTARY NOTES

14. ABSTRACT

During the period November 2011 through August 2013, research was conducted to develop a precast panel repair system suitable for airfield pavement repairs. This investigation included the selection and refinement of a precast panel system, fabrication of precast panels, timed repair activities, and accelerated pavement testing. Simulated C-17 traffic was applied to three repair surfaces of various sizes to determine whether the precast panel repairs were suitable for emergency or contingency airfield operations. This report presents the description of the process for selection and modification of a precast system, results of accelerated pavement testing including the passes-to-failure, surface deterioration, load transfer efficiencies, deflections, stress-strain measurements during trafficking, and three-dimensional finite element analyses. Results indicated that the repairs were capable of supporting anticipated contingency pass levels defined by the U.S. Air Force, but the precast panel system's dowel diameter should be increased to reduce stresses, decrease foreign object damage potential, and improve repair performance. Finally, the precast repair technology was compared to other expedient repair techniques in terms of repair speed, performance, and cost. Compared to other methods, the precast panel repair alternative provided similar return-to-service timelines and traffic performance at a slightly higher cost. Modifications to the system design and placement procedures are also recommended to improve the field performance of the panels.

15. SUBJECT TERMS

Airfield
PCC
Pavements
Airfield Damage Repair
Full-Scale Field Testing
Test Section
Finite Element Modeling

16. SECURITY CLASSIFICATION OF:			17. LIMITATION OF ABSTRACT	18. NUMBER OF PAGES	19a. NAME OF RESPONSIBLE PERSON
a. REPORT	b. ABSTRACT	c. THIS PAGE			19b. TELEPHONE NUMBER *(include area code)*
Unclassified	Unclassified	Unclassified		284	